

Main Group Metal Coordination Polymers

Scrivener Publishing

100 Cummings Center, Suite 541J
Beverly, MA 01915-6106

Publishers at Scrivener

Martin Scrivener (martin@scrivenerpublishing.com)
Phillip Carmical (pcarmical@scrivenerpublishing.com)

Main Group Metal Coordination Polymers

Structures and Nanostructures

Ali Morsali and Lida Hashemi

*Department of Chemistry, Tarbiat Modares University,
Tehran, Islamic Republic of Iran*



WILEY

This edition first published 2017 by John Wiley & Sons, Inc., 111 River Street, Hoboken, NJ 07030, USA and Scrivener Publishing LLC, 100 Cummings Center, Suite 541J, Beverly, MA 01915, USA
© 2017 Scrivener Publishing LLC

For more information about Scrivener publications please visit www.scrivenerpublishing.com.

All rights reserved. No part of this publication may be reproduced, stored in a retrieval system, or transmitted, in any form or by any means, electronic, mechanical, photocopying, recording, or otherwise, except as permitted by law. Advice on how to obtain permission to reuse material from this title is available at <http://www.wiley.com/go/permissions>.

Wiley Global Headquarters

111 River Street, Hoboken, NJ 07030, USA

For details of our global editorial offices, customer services, and more information about Wiley products visit us at www.wiley.com.

Limit of Liability/Disclaimer of Warranty

While the publisher and authors have used their best efforts in preparing this work, they make no representations or warranties with respect to the accuracy or completeness of the contents of this work and specifically disclaim all warranties, including without limitation any implied warranties of merchantability or fitness for a particular purpose. No warranty may be created or extended by sales representatives, written sales materials, or promotional statements for this work. The fact that an organization, website, or product is referred to in this work as a citation and/or potential source of further information does not mean that the publisher and authors endorse the information or services the organization, website, or product may provide or recommendations it may make. This work is sold with the understanding that the publisher is not engaged in rendering professional services. The advice and strategies contained herein may not be suitable for your situation. You should consult with a specialist where appropriate. Neither the publisher nor authors shall be liable for any loss of profit or any other commercial damages, including but not limited to special, incidental, consequential, or other damages. Further, readers should be aware that websites listed in this work may have changed or disappeared between when this work was written and when it is read.

Library of Congress Cataloging-in-Publication Data

Names: Hashemi, Lida. | Morsali, Ali.

Title: Main group metal coordination polymers : structures and nanostructures
/ Lida Hashemi and Ali Morsali.

Description: Hoboken, New Jersey : John Wiley & Sons, Inc., [2017] | Includes bibliographical references and index.

Identifiers: LCCN 2016052371 | ISBN 9781119370239 (cloth) | ISBN 9781119370765 (epub)

Subjects: LCSH: Coordination polymers. | Polymers. | Metal complexes.

Classification: LCC QD382.C67 H37 2017 | DDC 547.7--dc23

LC record available at <https://lcn.loc.gov/2016052371>

Cover image: Russell Richardson

Cover design by Russell Richardson

Set in size of 12pt and Minion Pro by Exeter Premedia Services Private Ltd., Chennai, India

Printed in

10 9 8 7 6 5 4 3 2 1

Contents

Preface	xi
Abbreviations	xiii
1 Introduction to Coordination Polymers	1
1.1 Coordination Space	1
1.2 Coordination Polymer	2
1.3 Development of Coordination Polymer	5
1.4 Synthetic Methods	7
1.5 Design of Coordination Polymer	10
References	13
2 Application of Coordination Polymers	17
2.1 Introduction	17
2.2 Gas Storage	17
2.3 Catalysis	19
2.4 Luminescence	20
2.5 Redox Activity	21
2.6 Magnetism	21
2.6.1 Long-Range Magnetic Ordering	22
2.6.1.1 Molecule-Based Magnets	23
2.6.1.2 Single-Chain Magnets	24
2.6.2 Spin Crossover	24
2.7 Acentric and Chiral Networks	25
References	28
3 Zinc(II) Coordination Polymers	31
3.1 Introduction to Zinc(II) Coordination Polymers	31
3.1.1 Coordination Polymers Constructed from Rigid Two-Connecting Ligands	33
3.1.1.1 Rod-Type Ligands	33
3.1.1.2 Angular, Rigid Two-Connectors	36

3.1.2	Coordination Polymers Constructed from Rigid, Trigonal Three-Connectors	38
3.1.3	Coordination Polymers Constructed from Carboxylates, Pyridine Carboxylates and Pyrazine Carboxylates	40
3.1.4	Coordination Polymers Constructed from Secondary Building Blocks (SBUs)	41
3.1.5	Coordination Polymers Constructed from Conformational Flexible Ligands	43
3.1.6	Coordination Polymers Constructed from Phosphate and Phosphonate Ligands	46
3.2	Nano Zinc(II) Coordination Polymers	46
3.3	Conclusion	52
	References	52
4	Cadmium(II) Coordination Polymers	59
4.1	Introduction to Cadmium (II) Coordination Polymers	59
4.1.1	One-dimensional Coordination Polymers	60
4.1.2	Two-dimensional Coordination Polymers	63
4.1.3	Three-dimensional Coordination Polymers	67
4.2	Nano Cadmium(II) Coordination Polymers	70
4.3	Conclusion	74
	References	75
5	Mercury(II) Coordination Polymers	83
5.1	Introduction Mercury(II) Coordination Polymers	83
5.1.1	One-dimensional Coordination Polymers	84
5.1.2	Two-dimensional Coordination Polymers	89
5.1.3	Three-dimensional Coordination Polymers	91
5.2	Nano Mercury(II) Coordination Polymers	93
5.3	Conclusion	97
	References	97
6	Lead(II) Coordination Polymers	101
6.1	Introduction	101
6.2	Mono-donor Coordination Mode	102
6.2.1	Discrete Complexes	102
6.2.2	One-Dimensional Coordination Polymers	104
6.2.3	Two-Dimensional Coordination Polymers	105
6.2.4	Three-Dimensional Coordination Polymers	105
6.3	Bi-donor Coordination Polymers	106

6.3.1	Bridging ($\mu^2-\mu^1;\mu^1$) Mode	106
6.3.1.1	Discrete Complexes	106
6.3.1.2	One-Dimensional Coordination Polymers	106
6.3.1.3	Two-Dimensional Coordination Polymers	107
6.3.1.4	Three-Dimensional Coordination Polymers	108
6.4	Tri-donor Coordination Polymers	109
6.4.1	Bridging ($\mu^3-\mu^1;\mu^2$) Mode	109
6.4.1.1	Two-Dimensional Coordination Polymer	109
6.4.1.2	Three-Dimensional Coordination Polymers	110
6.5	Tetra-donor Coordination	111
6.5.1	Chelating, Bridging ($\mu^3-\mu^1; \mu^2; \mu^1$) Mode	111
6.5.1.1	One-Dimensional Coordination Polymers	111
6.5.1.2	Two-Dimensional Coordination Polymers	112
6.5.1.3	Three-Dimensional Coordination Polymers	113
6.6	Nano Lead(II) Coordination Polymers	113
6.7	Conclusion	122
	References	123
7	Thallium(I) Coordination Polymers	131
7.1	Introduction to Thallium(I) Coordination Polymers	131
7.2	Thallium(I) Coordination Polymers	133
7.2.1	One-Dimensional Coordination Polymers with Secondary Interactions in Tl^I Coordination Sphere	136
7.2.2	One-Dimensional Coordination Polymers without Secondary Interactions in Tl^I Coordination Sphere	138
7.2.3	Two-Dimensional Coordination Polymers with Secondary Interactions in Tl^I Coordination Sphere	138
7.2.4	Two-Dimensional Coordination Polymers without Secondary Interactions in Tl^I Coordination Sphere	140

7.2.5	Three-Dimensional Coordination Polymers with Secondary Interactions in Tl^I Coordination Sphere	141
7.2.6	Three-Dimensional Coordination Polymers without Secondary Interactions in Tl^I Coordination Sphere	142
7.3	Nano Thallium(I) Coordination Polymers	143
7.4	Conclusion	147
	References	147
8	Bismuth(III) Coordination Polymers	153
8.1	Introduction to Bismuth Coordination Polymers	153
8.2	Bismuth(III) Complexes with Monoaminopoly Carboxylate	156
8.2.1	Bi(III) Complexes with Iminodiacetate Ligands	156
8.2.2	Bi(III) Complexes with Nitrilotriacetate	156
8.2.3	Bi(III) Complexes with 2-hydroxyethyliminodiacetate	157
8.2.4	Bi(III) complexes with Pyridinedicarboxylate Ligands	159
8.3	Bismuth(III) Complexes with Diaminopolycarboxylate Ligands	160
8.3.1	Bi(III) Complexes with Ethylenediaminetetraacetate	160
8.3.1.1	Protonated Bi(III) Ethylenediaminetetraacetate Complexes	160
8.3.1.2	Bi(III) Ethylenediaminetetraacetate Complexes with Alkali Metal and Ammonium Cations	161
8.3.1.3	Bi(III) Ethylenediaminetetraacetate Complexes with Divalent Metal Cations	162
8.3.1.4	Bi(III) Ethylenediaminetetraacetate Complexes with Protonated Organic Base Cations	163
8.3.1.5	Bi(III) Ethylenediaminetetraacetates with Metal Complex Cations	164

8.3.1.6	Mixed-Ligand Bi(III) Ethylenediaminetetraacetate Complexes	165
8.3.2	Bi(III) Complexes with other than edta ⁴⁻ diaminopolycarboxylate Ligands	166
8.4	Bismuth Complexes with Polyaminopolycarboxylate Ligands	167
8.4.1	Bi(III) Complexes with Diethylenetriaminepentaacetate Ligands and its Analogues	167
8.4.2	Bi(III) Complexes with Triethylenetetraaminehexaacetate Ligands	168
8.4.3	Bi(III) Complexes with Macrocyclic Polyaminopolycarboxylate Ligands	169
8.5	Applications	170
8.6	Nano Bismuth(III) Coordination Polymers	170
8.7	Conclusion	175
	References	176
9	Main Group Metal Coordination Chemistry	183
9.1	Introduction	183
9.2	Group 12	185
9.3	Group 13	185
9.3.1	Boron	185
9.3.2	Aluminium	186
9.3.3	Gallium	188
9.3.4	Indium	190
9.3.5	Thallium	191
9.4	Group 14	191
9.4.1	Silicon	191
9.4.2	Germanium	192
9.4.3	Tin	194
9.4.4	Lead	195
9.5	Group 15	195
9.5.1	Phosphorus	195
9.5.2	Arsenic	195
9.5.3	Antimony	196
9.5.4	Bismuth	197
9.6	Group 16	198
	References	199

10 S-block Coordination Polymers (Group1)	205
10.1 Introduction	205
10.2 Group 1(Alkali) Metal Coordination Polymers	206
10.2.1 Neutral Oxygen Donor Ligands	206
10.2.2 Anionic Oxygen Donor Ligands	208
10.2.2.1 Alkoxides and Aryloxides	208
10.2.2.2 Carboxylates	208
10.2.2.3 Sulfonates and Nitro-derivatives	209
10.2.2.4 Amino Acids	210
10.2.2.5 Mixed O- and N-donors	210
10.2.3 N-donor Ligands	211
10.2.4 Carbon Donor Ligands	211
10.2.5 Sulfur Donor Ligands	213
10.3 Conclusion	214
References	214
11 S-block Coordination Polymers (Group2)	219
11.1 Introduction	219
11.2 Group 2(Alkaline Earth) Metal Coordination Polymers	220
11.2.1 Neutral Oxygen Donor Ligands	221
11.2.2 Anionic Oxygen Donor Ligands	222
11.2.2.1 Beta-diketonates	222
11.2.2.2 Alkoxides	222
11.2.2.3 Carboxylates	223
11.2.2.4 Phosphonates	224
11.2.2.5 Sulfonates	225
11.2.3 Mixed N- and O-donors	225
11.2.4 N-donor Ligands	225
11.2.5 Carbon Donor Ligands	226
11.2.6 Sulfur Donor Ligands	227
11.3 Conclusion	228
References	229
Glossary	233
Index	239

Preface

Coordination polymer is a general term used to indicate an infinite array composed of metal ions which are bridged by certain ligands among them. This is a general term that incorporates a wide range of architectures including simple one-dimensional chains with small ligands to large mesoporous frameworks. The coordination chemistry of main group's metal compounds with organic ligands in the widest sense has been, until relatively recently, largely unknown compared to transition metal coordination networks. This is true despite the fact that many s-block metal-organic compounds are already of commercial importance. Thus, pharmaceuticals, dyes, and pigments typically use alkali and/or alkaline earth metal cations in preference to transition or lanthanide metal ions because most of them have the advantage of being nontoxic, cheap and soluble in aqueous media. Indeed, s-block cations should not be ignored as simple "spectator" ions when it comes to properties which depend on the solid-state structure and the intermolecular interactions. Therefore, understanding the changes of material properties caused by changing the s-block metal ion is based on consideration of the fundamental properties such as charge, size, and electronegativity of these cations and their influence on the nature of the resultant solid-state structure. Furthermore, the chemistry of main group metal ions is not limited to the classical ionic behavior as known from aqueous media, but may exhibit a more covalent character similar to transition metal compounds when polar organic solvents are used. In this book we explain the main group metal coordination polymer in bulk and nano size with some of their applications, synthesis method etc.,. We hope

this book will help graduate and upper-level undergraduate students to get an understanding of metal coordination polymer in bulk and nano dimension and their applications.

Ali Morsali and Lida Hashemi
Tehran, Islamic Republic of Iran
December 2016

Abbreviations

Abdc	2-amino-1,4-benzenedicarboxylate
Adc	acetylenedicarboxylate
Amtz	5-aminotetrazole
Atb	adamantanetetrabenzoate
Atc	adamantanetetracarboxylate
Amoimy	1-(9-anthracenylmethyl)-3-octylimidazol-2-ylidene
Ampa	aminomethylphosphonic acid
Azpy	<i>trans</i> -4,4'-azobis(pyridine)
Azobpy	3,3'-azobispyridine
4,4'-azpy	4,4'-azopyridine
Bbdc	4,4'-bibenzenedicarboxylate
Bbi	1,1'-(1,4-butanediyl)bis(imidazole)
Bbimms	1,3-bis(benzimidazol-1-ylmethyl)-2,4,6-trimethylbenzene
Bcsar	1,8-bis(carboxymethylamino)sarcophagine
bdaipH	2,6-bis{ <i>N</i> -[2-(dimethylamino)ethyl]iminomethyl}-4-methylphenol
1,2-bdc	1,2-benzenedicarboxylate
1,3-bdc	1,3-benzenedicarboxylate
1,4-bdc	1,4-benzenedicarboxylate
BX ₄ ⁻	tetrakis(imidazolyl)borate
BY ₄ ⁻	tetrakis-(4-methylimidazolyl)borate
Bbsb	1,4-bis(benzylsulfanyl)butane
Bbsp	1,5-bis(benzylsulfanyl)pentane
4-bedpef	9,9-bis-ethyl-2,7-di-(4-pyridyl)ethynylfluorene
Besb	1,4-bis(ethylsulfanyl)butane (C ₄ H ₉ S)
Besp	1,3-bis(ethylsulfanyl)propane
Bib	1-bromo-3,5-bis(imidazol-1-ylmethyl)benzene

Bidtp	bis(isopropyl)dithiophosphate $\{S_2P(OPri)_2\}$
Bin	1,5-bis(isonicotinamido)naphthalene
2,2'-bipy	2,2'-bipyridine
4,4'-bipy	4,4'-bipyridine
BipyP2	tetraethyl 2,2'-bipyridyl-4,4'-diphosphonate
2-bmps	bis(2-methylpyridyl) sulfide
Bnbap	binaphthyl-bis(amidopyridyl)
Bddo	1,8-bis(3,5-dimethyl-1-pyrazolyl)-3,6-dithiaoctane
Bepb	1,2-bis(4-ethynylpyridyl)benzene
Bepf	2,5-bis(4-ethynylpyridyl)furan
Bimb	4,4'-bis(imidazole-1-ylmethyl)biphenyl
Bmptc	1,2-bis[2-methyl-5-(4-pyridyl)-3-thienyl]perfluoro cyclopentene
Bna	2,2'-bi-1,6-naphthyridine
Bpb	1,4-bis(4-pyridyl)butane
Bpbb	biphenylenebis(phosphonate)
Bpce	<i>N,N'</i> -bis(3-pyridinecarboxamide)-1,2-ethane
Bpdc	4,4'-biphenyldicarboxylate
Bpa	1,2-bis(4-pyridyl)ethane;
Bpba	<i>N,N'</i> -bis(4-pyridyl)-1,4-benzenedicarboxamide
2-bpdb	1,4-bis(2-pyridyl)-2,3-diaza-1,3-butadiene
3-bpdb	1,4-bis(3-pyridyl)-2,3-diaza-1,3-butadiene
4-bpdb	1,4-bis(4-pyridyl)-2,3-diaza-1,3-butadiene
2-bpdh	2,5-bis(2-pyridyl)-3,4-diaza-2,4-hexadiene
3-bpdh	2,5-bis(3-pyridyl)-3,4-diaza-2,4-hexadiene
4-bpdh	2,5-bis(4-pyridyl)-3,4-diaza-2,4-hexadiene
Bpe	1,2-bis(4-pyridyl)ethane
Bpen	1,2-bis(4-pyridyl)ethylenediamine
4-bpet	2,2'-bis-(4-pyridylethynyl)tolane
Bpfb	<i>N,N'</i> -bis(4-pyridylformamide)-1,4-benzene
Bpfp	<i>N,N'</i> -bis(3-pyridylformyl)piperazine
Bpeb	4- [2-(4-pyridyl)ethenyl]benzoate
Bpen	<i>trans</i> -1,2-bis(4-pyridyl)ethylene
Bpethy	1,2-bis(4-pyridyl)ethyne
Bph	1,7-bis(4-pyridyl)heptanes
Bpp	1,3-bis(4-pyridyl)propane
Bptz	3,6-bis(pyridin-3-yl)-1,2,4,5-tetrazine
4,4'-bpyO	4,4'-bipyridine <i>N,N'</i> -dioxide

Btb	benzenetribenzoate
Btc	1,3,5-benzenetricarboxylate
1,4-cbdc	2,3-cyclobutyl-1,4-benzenedicarboxylate
Citr	citraconate
Crot	crotonate
Ctc	<i>cis,cis</i> -1,3,5-cyclohexanetricarboxylate
Caf	caffeine
Cht	cyclohexanethiolate
3,5-Cl ₂ py	3,5-dichloropyridine
2-cpa	(2-chlorophenoxy)acetate
Crypt and 5	1,13-bis(8-chinolyl)-1,4,7,10,13-pentaoxatridecane
Cy	cyclohexyl
Dbco	diazabicyclo[2.2.2]octane
Dbcoac	1,4-diazoniabicyclo[2.2.2]octane-1,4-diacetate
Dbcop	1,4-diazoniabicyclo[2.2.2]octane-1,4-dipropionate
Dcmb	3,6-dichloro-2-methoxybenzoate
Def	diethylformamide
Detp	<i>O,O'</i> -diethyldithiophosphate
Dhbtb	dihydrobis(tetrazolyl)borate
Dma	dimethylacetamide
Dme	1,2-dimethoxyethane
Dmpz	3,5-dimethylpyrazolate
Dpe	<i>P,P</i> -diphenyl-2-{3,5-dimethylpyrazol-1-yl}- ethylp-hosphinate
Dpk	di-2-pyridyl ketone; dpt, 2,4-bis(4-pyridyl)-1,3,5-triazine
Dptf	1,1'-(4-dipyridinethio)ferrocene
Eda	ethylenediaminium
EbpH ₂	ethylenebis(phosphonic) acid
En	ethylenediamine
Eob	<i>o</i> -ethoxybenzoate
Fa	fumarate
Facac	1,1,1,5,5,5-hexafluoroacetylacetonate
FcaH	1-ferrocenylbutane-1,3-dione
Ferd	1,1'- ferrocenedicarboxylate
HaaiEt	1-ethyl-2-(phenylazo)imidazole
HAm4DH	2-pyridineformamide Tthiosemicarbazone
H4bpb	N,N'-bis(3-pyridylmethyl)-1,4-benzenedimethylamine

Hmt	hexamethylenetetramine
2-Hoz	2-oxazolidone (1,3-oxazolidin-2-one, C ₃ H ₅ NO ₂)
3-Hpapap	2-[3-(pyridylamino)-phenylazo]pyridine)
HpicOH	3-hydroxypicolinic acid
Hpyta	4-pyridylthioacetic acid
Htrz	1,2,4-triazole
Htma	hexamethylenetetramine
Htzb	hydrotris(1,2,4-triazolyl)borate
HytH ₂	hydrochlorothiazid
IacH	imidazole-4-acetic acid
Im	imidazole
Ini	isonicotinate
Iva	isovalinate
Lac	lactate
Limb	1-(1-imidazolyl)-4-(imidazol-1-ylmethyl)benzene
LBA	d-lactobionates
Mal	malonate
Male	maleate
MbppH	4-methyl- 2,6-bis(pyrazole-1-ylmethyl)phenol
MB	methylene blue
Mbpa	meso-2,5-bis(pyridinio)adipate
Mim	2-methylimidazole
Mppz	3(5)-methyl-5(3)-phenylpyrazole
3-mpy	3-methylpyridine
4-mpy	4-methylpyridine
Mtb	methanetetra benzoate
Mtmta	2-(1-methyl-1H-tetrazol-5-yl)-2-(2'-methyl-2'H-tetrazol-5'-yl)acetonitrile
1,4-ndc	1,4-naphthalenedicarboxylate
2,6-ndc	2,6-naphthalenedicarboxylate
Nic	nicotinate
4,4'-oba	4,4'-oxybis(benzoate)
Ox	oxalate
Pbp	phenylenebis(phosphonate)
2,3-pdc	pyridine-2,3-dicarboxylate
2,4-pdc	pyridine-2,4-dicarboxylate
Peb	4-2-(3-pyridyl)ethenylbenzoate

Pemc	<i>N</i> -[1-(2-pyridyl)ethylidene]morpholine-4-carbothiohydrazide
Pepeb	3-{[4-(4-pyridylethenyl)phenyl]ethenyl}benzoate
Phe	phenylalanine
PstsH2	5-phenylsulfonamide-1,3,4-thiadiazole-2-sulfonamide
Py	pyridine
Pya	4-pyridylacrylate
Pyb	4-pyridylbenzoate
Pym	pyrimidine
PymoH	2-hydroxypyrimidine
Pyta	4-pyridylthioacetate
Pyz	pyrazolate
Pz	pyrazine
Pzdc	pyrazine-2,3-dicarboxylate
QtmCp	1-(8-Quinolyl)-2,3,4,5-tetramethylcyclopentadiene
S-t-C ₄ H ₉	tert.-butanethiolate
Sal	salicylaldehyde
Sphe	4-sulfo-l-phenylalaninate
Tbdc	2,3,5,6-tetramethyl-1,4-benzenedicarboxylate
(+)-tfc	3-((trifluoromethyl)hydroxymethylene)-(+) -camphorate
Tpm	tris(4-pyridyl)methanol
Tpt	2,4,6-tris(4-pyridyl)-1,3,5-triazine
TtaH6	4,4',4''-tris(<i>N,N</i> -bis(4-carboxyphenyl)(amino) triphenylamine
Tu	thiourea
TPPB-	tris[3-(2-pyridyl)-pyrazol-1-yl]borate

1

Introduction to Coordination Polymers

1.1 Coordination Space

Material and life sciences have contributed to human well-being and prosperity and atoms and molecules play a central role in this respect. The syntheses of molecules have been a major theme in the previous century. Molecules are architectures composed of atoms, while the supramolecular chemistry developed in the last century deals with architectures built from molecules, paving the way for nanoscience [1]. In addition to the framework entity, space surrounded and partitioned by atoms and molecules could be another world of science. If we build nanosized spaces, what kind of materials can be created and what discoveries for molecules in the space can be made? In a nanosized world, walls, which are composed of atoms and molecules and apportioned space, have a considerable effect on orientation, correlation, and assembled structure of guest molecules. We can, therefore, control such states

of the guest molecules by changing the shapes and materials of walls. When molecules are confined in a space and undergo stress caused by a deviation from thermodynamically and kinetically stable structures of the ambient surroundings, such stress brings about effective energy conversion and new chemical reactions. Space apportioned by atoms and molecules creates new functions based on its shape and dynamics characteristic of the nanoworld. At the end of the last century, chemists focused on supramolecular frameworks composed of molecules, while in the 21st century a new area of nanospace chemistry by creating and opening up various types of spaces. We have to develop new synthetic routes to build the desired nanosized space effectively and on a large scale, and this is a basic methodology required for nanotechnologies. The most practical methods to build nanosized space are chemical self-assembly and self-organization and coordination bonds are the key to the development of the required new synthetic technologies. Coordination bonds are not as strong as covalent bonds and not as weak as hydrogen bonds. Constituent organic molecules and metal ions are assembled into a variety of spatial structures under mild conditions.

In this area, the molecules were designed to build space that gives an opportunity to find new phenomena based on molecular coagulation, molecular stress, and activation of molecules. For this purpose, a new chemistry that allows us to control structures and functionality of spaces was needed. Space motifs built by molecular blocks are: (1) reactions of metal ions (connector) with organic ligands (linker) to give coordination crystals with infinite structures. We can build spaces with different sizes composed of several or tens of molecules; (2) surfaces of bulk material and nanoparticles can be recognized as coordination space; and (3) the coordination space of metal complexes embedded in a protein has the hidden possibility of a new functionalized space.

1.2 Coordination Polymer

Coordination polymer is a general term used to indicate an infinite array composed of metal ions which are bridged by certain

ligands among them. This is a general term that incorporates a wide range of architectures including simple one-dimensional chains with small ligands to large mesoporous frameworks [2, 3]. Generally, the formation process proceeds automatically and, therefore, is called a self-assembly process. In general, the type and topology of the product generated from the self-assembly of inorganic metal nodes and organic spacers depend on the functionality of the ligand and valences and the geometric needs of the metal ions used. Organic ligands are very important in design and construction of desirable frameworks, since changes in flexibility, length, and symmetry of organic ligands can lead to the formation of a class of materials with diverse architectures and functions [4].

Depending on the metal element that is used in the polymer, and its valence, different geometries may be created, e.g., linear, trigonal-planar, T-shaped, tetrahedral, square-planar, squarepyramidal, trigonal-bipyramidal, octahedral, trigonal-prismatic, pentagonal-bipyramidal, and their distorted forms [5]. Organization of building blocks can lead to the formation of metal-organic frameworks of various dimensions: one-, two- or three-dimensional architectures. Dimension is usually determined through the nodes (metal centers) [6]. Metal coordination polymers have been studied widely as they represent an important interface between synthetic chemistry and materials science, and they have specific structures, properties, and reactivities that are not found in mononuclear compounds. They may have potential applications in catalysis, molecular adsorption, magnetism, nonlinear optics, luminescence, and molecular sensing. In the last two decades, rapid developments in the crystal engineering of metal-organic coordination polymers have produced many novel materials with various structural features and properties.

A coordination polymer contains metal ions linked by coordinated ligands into an infinite array. This infinite net must be defined by coordination bonds and thus molecular species linked only by hydrogen bonding are elegant instances of molecular crystal engineering but are not coordination polymers. Similarly, a structure linked by coordination bonds in one direction and hydrogen bonds in two other directions is a 1D coordination

polymer (although an overall 3D net may be defined by both sets of interactions). Furthermore, for the purposes of this book, we largely focus on main group metals, in which the bonding is more covalent.

The coordination chemistry of main group's metal compounds with organic ligands in the widest sense has been, until relatively recently, largely unknown compared to transition metal coordination networks. This is true despite the fact that many s-block metal-organic compounds are already of commercial importance. Thus, pharmaceuticals, dyes, and pigments typically use alkali and/or alkaline earth metal cations in preference to transition or lanthanide metal ions because most of them have the advantage of being non-toxic, cheap and soluble in aqueous media. Indeed, s-block cations should not be ignored as simple "spectator" ions when it comes to properties which depend on the solid-state structure and the intermolecular interactions. This is especially relevant in pharmaceutical industry where one salt might be preferred over others for practical as well as commercial purposes. Therefore, understanding the changes of material properties caused by changing the s-block metal ion is based on consideration of the fundamental properties such as charge, size, and electronegativity of these cations and their influence on the nature of the resultant solid-state structure. Furthermore, the chemistry of main group metal ions is not limited to the classical ionic behavior as known from aqueous media, but may exhibit a more covalent character similar to transition metal compounds when polar organic solvents are used.

With the aid of modern X-ray diffraction techniques, a variety of molecular and polymeric structures can be elucidated. Coordination polymer networks are made mainly from neutral or anionic ligands (linkers) with at least two donor sites which coordinate to metal ions or aggregates (nodes) also with at least two acceptor sites, so that at least a one-dimensional arrangement is possible. Depending on the number of donor atoms and their orientation in the linker, and on the coordination number of the node, different one (1D)-, two (2D)- and three (3D)-dimensional constructs are accessible.

The development of coordination polymer research has been enforced by the growth of crystal engineering and supramolecular chemistry [7, 8]. A coordination polymer contains metal ions linked by coordinated ligands into an infinite array. Coordination polymers constitute one of the most important classes of organic–inorganic hybrid materials [9, 10] that have been the subject of intensive research in recent years [11]. The rational design via self assembly depends on a variety of parameters, basically including the suitable pre-designed organic ligands and metal centers with versatile coordination geometries [12]. Design and synthesis of novel discrete and polymeric metal–organic complexes are attracting more attention, not only for their interesting molecular topologies, but also for their potential applications as functional materials [13], ions exchange, catalysis, molecular recognition, nonlinear optics [14, 15], molecular magnetic materials, electrical conductivity [16, 17], separation and gas storage [18, 19]. The structure and properties of coordination polymers depend on the coordination habits and geometries of both metal ions and connecting ligands, as well as on the influence of secondary interactions such as hydrogen bonding, π – π stacking interactions and so on [20]. Several factors, including the coordination bonds and secondary interactions, the metal-to-ligand molar ratio, the coordinative function of the ligands, the type of metal ions, the presence of solvent molecules, counterions and organic guest molecules should be taken into account in the process of the design and synthesis of metal-coordination polymers [21, 22].

1.3 Development of Coordination Polymer

The development of coordination polymer research was reinforced by the growth of two other closely related areas: crystal engineering and supramolecular chemistry (particularly metallosupramolecular chemistry). Crystal engineering seeks to understand why molecules pack in the ways that they do and to use that knowledge to deliberately engineer the arrangements

of molecules in new materials [23]. This is important because the properties of materials are often governed by the way in which their constituent molecules are arranged. Control over this arrangement gives control over the properties. In ‘molecular’ (largely organic) crystal engineering, the interactions are weaker than coordination bonds and can range in strength from very strong hydrogen bonding to weak C–H..... A hydrogen bonds, halogen bonds, π interactions and, ultimately, van der Waals forces. The crystal engineer seeks to understand and harness all these interactions. However, despite the differences in the interactions, there is much that is common in these two areas. Indeed, coordination polymers, which essentially exist only in the solid state, should be considered as a subset of crystal engineering. Furthermore, the net-based approach for coordination polymers is equally valid for molecular species connected by well-defined interactions.

Many of the concepts and terminology in molecular crystal engineering also apply to coordination polymers. Interactions between molecules that direct their packing arrangements are known as supramolecular synthons [24]; in coordination polymers, the main synthons are coordination bonds (although weaker synthons can also be important). The building blocks used to create the structure. For coordination polymers, the tectons are metal ions and ligands. The aim of supramolecular chemistry is similar: to create assemblies of molecules, that is, not to create structures an atom at a time, but to design molecules such that when combined they spontaneously self-assemble in a predetermined fashion into larger architectures [25]. Thus crystal engineering can, in fact, be considered to be the supramolecular chemistry of the solid state.

The supramolecular chemist, like the crystal engineer, uses a range noncovalent intermolecular interactions, including hydrogen bonding and coordination bonds. Use of the later gives rise to metallosupramolecular chemistry, and much of the design and indeed the structures obtained has close relationships to coordination polymers.

1.4 Synthetic Methods

One of the challenges of this research is to obtain single crystals suitable for detailed crystallographic analysis. Unlike molecular species, most coordination polymers are insoluble once synthesized (a property which is advantageous for other aspects) and so recrystallization is not an option. If the polymers can be dissolved, it is usually through the use of strongly coordinating solvents, which are then likely to become part of the recrystallized species, which therefore becomes a different material to the original phase.

Crystals are therefore usually obtained directly from the synthetic reaction mixtures. Although some species crystallize nicely from directly mixed solutions, for other systems the key to obtaining good crystals is to slow the precipitation down. This is most commonly done by allowing two separate solutions of metals and ligands to diffuse slowly into each other, and a number of different techniques have been established to this end (Figure 1.1). The simplest method is to layer carefully one solution on top of another in a small vial or tube. Often a buffer layer of pure solvent is layered between the two and the use of solvents with different densities (e.g. MeOH versus CHCl_3) greatly aids separation. This layered solution should then be left so that the crystals can grow; typically this may take in the order of 2 weeks, although crystallization can often take much longer (or shorter) times and so the reaction should be checked regularly, preferably without disturbing the crystal growth through handling. Regular inspection is important as crystals can come and go (for kinetic products) or become flawed, overgrown or otherwise deteriorate in quality over time.

Other variations on this technique include locking one solution into a gel through the addition of a gelling agent such as tetramethoxysilane. The gel slows diffusion through reduction of convection and also provides a support for the growing crystals. Specially designed glassware such as H-tubes and U-tubes (Figure 1.1) can also be used; often these can have a frit in the middle or (in the case of U-tubes) a separating gel plug can be created at the bottom first.

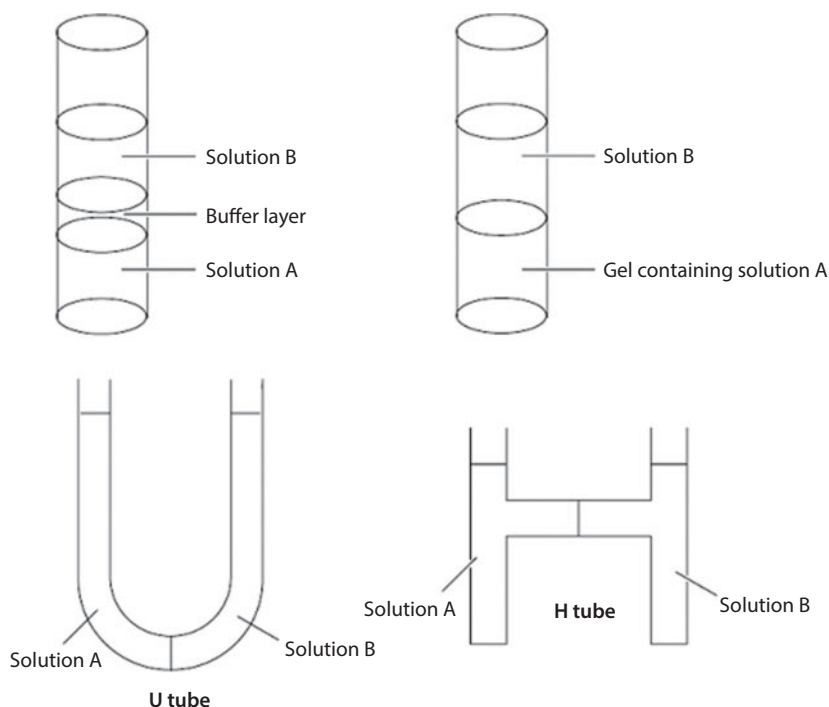


Figure 1.1 Various methods for slow growth of coordination polymer crystals.

There are a number of factors that contribute to stable crystal-line packing arrangements. For the synthetic chemist, this means that there are therefore a number of other variables that can be adjusted to produce crystals. Variation of solvent, counterion or even metal choice can be explored. More recently, the use of solvothermal techniques has become increasingly popular, both as a method of obtaining good single crystals and as a means of obtaining phases which are unavailable through bench-top techniques.

There is, overall, a large parameter space which can be explored in the quest for single crystals. However, one of the key reasons for obtaining crystal structures is to draw relationships between structures and properties and thus gain insights that can feed into the design of new materials. Therefore, it is important to recognize that the structures obtained from single crystals may be inherently

unrepresentative (because the crystallographer chooses the best crystal available, for obvious reasons) of the bulk material upon which the properties are tested. Furthermore, reactions can often give more than one product. Hence it is important to check the correlation between the single crystals and the bulk product, and this is most easily achieved through the use of techniques such as powder diffraction or (less convincingly) infrared or Raman spectroscopy.

So several different synthetic approaches have been offered for the preparation of coordination polymers. Some of them are (1) slow diffusion of the reactants into a polymeric matrix, (2) layering technique, (3) evaporation of the solvent at ambient or reduced temperatures, (4) precipitation or recrystallisation from a mixture of solvents, (5) temperature controlled cooling, (6) hydrothermal synthesis and (7) gel growth crystallization technique. We have shown another new and simple method for the construction of multi-dimensional coordination polymers, the branched tube method (Figure 1.2). The new method is straight forward, cheap and trouble-free and can be used for the preparation of other types of coordination polymers.

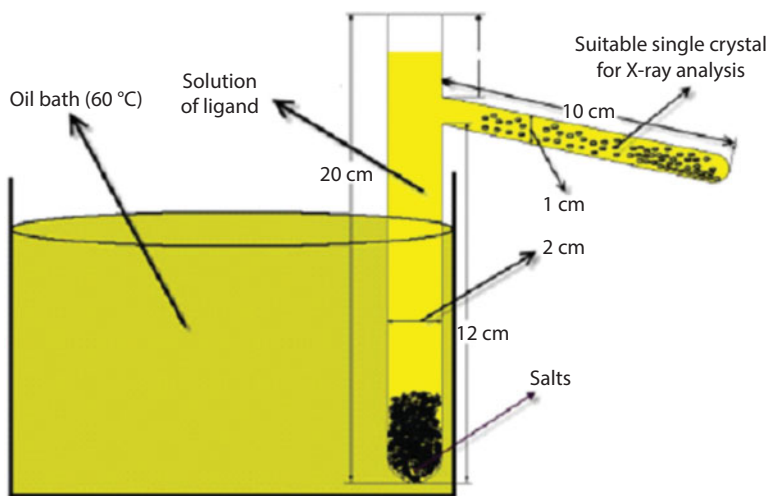


Figure 1.2 Depiction of the branched tube for syntheses and isolation of single crystals of multi-dimensional coordination polymers.

1.5 Design of Coordination Polymer

One of the most powerful techniques in crystal engineering for both the analysis and design of solids is to reduce their crystal structures to networks (or nets). Networks can aid the description and understanding of complicated structures or provide a blueprint for the targeting of particular packing arrangements and their associated properties. An early leading figure in this approach was A. F. Wells, who, in a series of seminal books [26–29], described a number of molecular and polymeric structures in terms of networks and delineated a large number of possible networks, some already seen in real structures and others that, remarkably, were still theoretical at the time. A good understanding of networks is therefore vital to the crystal engineer. But what is a net? For our purposes, a network is a polymeric collection of interlinked nodes; each link connects two nodes and each node is linked to three or more other nodes. A node cannot be connected to only two nodes; in this case it then becomes a link. Similarly, a link can only connect two nodes; if it connects more than two it is a node. And finally, since we are talking about crystal structures here, the network must also have a repeating pattern and thus a finite number of unique nodes and links.

A network is also a topological description and not a geometric one. For example, the two networks shown in Figure 1.3 are topologically identical despite the fact that they are geometrically very different. In both networks, the nodes are 3-connecting, although in one net the nodes are trigonal (leading to a hexagonal network) and in the other they are T-shaped (leading to a brick work-like network). These networks are identical because one can be converted to the other by distortions that do not break links.

By this reasoning, there is no topological difference between square-planar nodes and tetrahedral nodes – both are simply 4-connecting nodes. However, different nets are favoured by (and may even require) different node geometries. For example, (4,4) sheets are favoured by square-planar nodes, whereas the diamond net has, in its undistorted form, tetrahedral nodes. The PtS net has

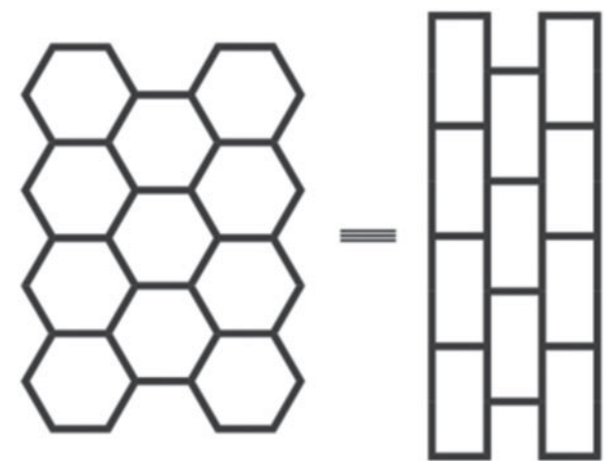


Figure 1.3 Two geometrically different but topologically identical nets.

two different sorts of 4-connecting nodes; half are tetrahedral and half are squareplanar. Hence, although geometries are not strictly a topological feature, they can still be an important factor in network selection and design, particularly for the chemist who can provide a great deal of control over different nodal geometries. In practice, there is a considerable difference between square-planar and tetrahedral nodes and therefore we will often make distinctions between different nodal geometries here.

Nonetheless, it is the connectivity of a network that defines it, not its geometry. Structures can be described as having a particular network topology even though they may be geometrically very different to the 'ideal' net. The connectivity of the node can also be very different to the local chemical geometry. This can manifest itself in a number of ways. Octahedral metals can act as 3-connecting nodes if they are bound by three chelating bridges, three monodentate bridges and three terminal (i.e. non-bridging) ligands or three pairs of monodentate bridging ligands which connect metals in pairs (Figure 1.4). It is common for square-planar nodes to be formed by octahedral metals, particularly when pyridyl donor ligands are used (it is sterically very difficult to fit six pyridyl donor groups around a first-row transition metal; more commonly four

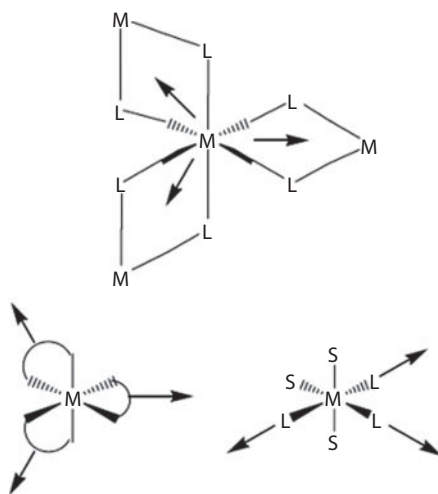


Figure 1.4 Three ways in which an octahedral metal ion can act as a 3-connecting node.

pyridyls occupy equatorial positions, while the axial positions are filled by sterically smaller terminal ligands, such as water or halide ions). Ligands with four coordination sites become simple links if they coordinate to only two metals or 3-connecting nodes if they only coordinate to three metals.

It is also important to remember that both metals and ligands can act as either nodes or links in a net (or even both if there are different types of metals or ligands in the one structure). For example, in the 3D rutile (TiO_2) net, each Ti node is connected to 10 other Ti atoms via the oxygen atoms bonded to it. This is not, however, a 10-coordinate network, because the oxygen atoms connect to three Ti atoms each and thus are themselves 3-connecting nodes. Rutile is therefore a binodal 3,6-connected network. The same applies to more complicated coordination polymers – if a metal or ligand connects to three or more metals, then it is a node and cannot be simply classed as a link.

Finally, care should be taken when choosing the interactions used to define the network. Usually this is relatively straightforward if only coordination bonds are to be used, although longer interactions can be easy to miss (e.g. Jahn–Teller distorted metals) or hard to separate

from non-bonding interactions (e.g. some Ln structures). However, it is sometimes useful also to examine weaker interactions, such as metallophilic interactions, hydrogen bonds, π stacking interactions and so forth. This can aid the understanding of the overall structure, although it should be remembered that, by definition, every crystal structure is 3D. However, if the network definition is to be extended to these interactions, then all interactions of similar strength should be used, e.g. all strong hydrogen bonds should be included rather than just selected interactions.

Care should also be taken when representing the network graphically. The distances between some nodes which are not directly linked may be shorter than or even exactly the same as the distances between nodes that truly are linked. This can often cause problems with many graphics programs and therefore the net should always be overlaid on the real structure to check that no links have been missed and that no 'false' links have been inadvertently created. Ultimately, the true test of the network approach is (a) does it increase the understanding of the structure and (b) does it correspond well to the chemical structure? If both of these criteria are not met then either the net is badly defined or this approach should not be used (some structures can be too complicated to reduce to a simple, easily understood net). A net should always simplify a structural description, not complicate it.

References

1. Lehn, J.-M., *Supramolecular Chemistry: Concepts and Perspectives*, June 1995, VCH, p. 281, 1995.
2. James, S.L., Metal-organic frameworks. *Chemical Society Reviews*, 32(5), p. 276–288, 2003.
3. Robson, R., A net-based approach to coordination polymers. *Journal of the Chemical Society, Dalton Transactions*, 2000(21), p. 3735–3744.
4. Wu, A.Q., *et al.*, Different Molecular Frameworks of Zinc(II) and Cadmium(II) Coordination Polymers Constructed by Flexible Double Betaine Ligands. *Crystal Growth & Design*, 6(2), p. 444–450, 2006.

5. Kitagawa, S. and Noro, S. 7.5 - *Coordination Polymers: Infinite Systems A2* - McCleverty, Jon A, in *Comprehensive Coordination Chemistry II*, T.J. Meyer, Editor 2003, Pergamon: Oxford. p. 231–261.
6. Robin, A.Y. and Fromm, K.M. Coordination polymer networks with O- and N-donors: What they are, why and how they are made. *Coordination Chemistry Reviews*, 250(15–16), p. 2127–2157, 2006.
7. Batten, S.R., Neville, S.M., Turner, D.R. Coordination Polymers. Design, Analysis and Application. *Angewandte Chemie International Edition*, 48(27), p. 4890–4891, 2009.
8. Abrahams, B.F., *et al.*, A Cubic (3,4)-Connected Net with Large Cavities in Solvated $[\text{Cu}_3(\text{tpt})_4](\text{ClO}_4)_3$ (tpt = 2,4,6-Tri(4-pyridyl)-1,3,5-triazine). *Angewandte Chemie International Edition* in English, 35(15), p.1690–1692, 1996.
9. Zhao, Y.-H., *et al.*, Two novel lead-carboxylate complexes based on nicotinic acid N-oxide: Synthesis, crystal structures and luminescent properties. *Inorganic Chemistry Communications*, 10(4), p. 410–414, 2007.
10. Blake, A.J., *et al.*, Inorganic crystal engineering using self-assembly of tailored building-blocks. *Coordination Chemistry Reviews*, 183(1), p. 117–138, 1999.
11. Wu, C.-D., *et al.*, Hydrothermal Synthesis, Structures, and Magnetic Properties of Three Novel 5-Aminoisophthalic Acid Ligand Bridged Transition Metal Cation Polymers. *Inorganic Chemistry*, 41(12), p. 3302–3307, 2002.
12. Du, M., Cai, H. and Zhao, X.-J. Two-dimensional CuII and first PbII coordination polymers based on a flexible 1,4-cyclohexanedicarboxylate ligand displaying different conformations and coordination modes. *Inorganica Chimica Acta*, 358(13), p. 4034–4038, 2005.
13. Xue, L., *et al.*, A noninterpenetrating 3D coordination network with rare (4,6)-connected $(4\cdot5^3\cdot6^2)2(4^2\cdot5^6\cdot6^4\cdot8^3)$ topology. *Journal of Molecular Structure*, 832(1–3), p. 132–137, 2007.
14. Youm, K.-T., *et al.*, A Noninterpenetrating Three-Dimensional 4669 Iron(ii) Coordination Polymer Built with a Trigonal-Antiprismatic Iron(iii) Metalloligand. *Angewandte Chemie International Edition*, 45(24), p. 4003–4007, 2006.
15. Chae, H.K., *et al.*, A route to high surface area, porosity and inclusion of large molecules in crystals. *Nature*, 427(6974), p. 523–527, 2004.

16. Li, G., *et al.*, Novel Pb(II), Zn(II), and Cd(II) Coordination Polymers Constructed from Ferrocenyl-Substituted Carboxylate and Bipyridine-Based Ligands. *Inorganic Chemistry*, 42(16), p. 4995–5004, 2003.
17. Hoskins, B.F. and Robson, R. Design and construction of a new class of scaffolding-like materials comprising infinite polymeric frameworks of 3D-linked molecular rods. A reappraisal of the zinc cyanide and cadmium cyanide structures and the synthesis and structure of the diamond-related frameworks $[\text{N}(\text{CH}_3)_4][\text{CuI}\text{ZnII}(\text{CN})_4]$ and $\text{CuI}[4,4',4'',4'''\text{-tetracyanotetraphenylmethane}]\text{BF}_4 \cdot x\text{C}_6\text{H}_5\text{NO}_2$. *Journal of the American Chemical Society*, 112(4), p. 1546–1554, 1990.
18. Liu, Y.-H., *et al.*, $[\text{CdII}(\text{bpdc})\cdot\text{H}_2\text{O}]_n$: A Robust, Thermally Stable Porous Framework through a Combination of a 2-D Grid and a Cadmium Dicarboxylate Cluster Chain ($\text{H}_2\text{bpdc} = 2,2'\text{-Bipyridyl-4,4'-dicarboxylic Acid}$). *Inorganic Chemistry*, 41(9), p. 2592–2597, 2002.
19. Mao, J.-G., Wang, Z. and Clearfield, A. New Lead Inorganic–Organic Hybrid Microporous and Layered Materials: Synthesis, Properties, and Crystal Structures. *Inorganic Chemistry*, 41(23), p. 6106–6111, 2002.
20. Zhang, X.-F., *et al.*, A three-dimensional lead(II) coordination polymer: $\text{poly}[\text{aqua-}\mu\text{-imidazole-4,5-dicarboxylato-lead(II)}]$. *Acta Crystallographica Section C*, 62(12), p. m617–m619, 2006.
21. Yang, J., *et al.*, Organic-Acid Effect on the Structures of a Series of Lead(II) Complexes. *Inorganic Chemistry*, 46(16), p. 6542–6555, 2007.
22. Fan, S.-R. and Zhu, L.-G. Syntheses, Structures, and Characterizations of Four New Lead(II) 5-Sulfosalicylate Complexes with Both Chelating and Bridging Neutral Ligands. *Inorganic Chemistry*, 46(16), p. 6785–6793, 2007.
23. Desiraju, G.R. Crystal Engineering. *The Design of Organic Solids*, Elsevier, Amsterdam, 1989.
24. Desiraju, G.R., Supramolecular Synthons in Crystal Engineering—A New Organic Synthesis. *Angewandte Chemie International Edition in English*, 34(21), p. 2311–2327, 1995.
25. Lehn, J.-M. Supramolecular chemistry: Concepts and perspectives. *Advanced Materials*, 1995. 8(10p. 866–868.
26. Wells, A.F. *Three-dimensional Nets and Polyhedra*, Wiley-Interscience, New York, 1977.

27. Wells, A.F. *Further Studies of Three-dimensional Nets*, ACA Monograph No. 8, American Crystallographic Association, Knoxville, TN, 1979.
28. Wells, A.F. *Structural Inorganic Chemistry*, 5th edn, Oxford University Press, Oxford, 1984.
29. Batten, S. R., Neville, S. M. and Turner, D. R. *Coordination Polymers Design, Analysis and Application*, The Royal Society of Chemistry, 2009.

2

Application of Coordination Polymers

2.1 Introduction

In this chapter we look at the application of coordination polymers. These materials have much efficiency, including magnetism (long-range ordering, spin crossover), porosity (gas storage, ion and guest exchange), non-linear optical activity, chiral networks, reactive networks, heterogeneous catalysis, luminescence, multi-functional materials and other properties, but we explain about some of these properties here.

2.2 Gas Storage

The safe storage and transport of gases in high concentrations requires compression at high pressures for the gases of interest (e.g. CH₄, H₂) at room temperature. This process consumes a great

deal of energy and does not make for safe conveyance. A solution to this is the use of solid adsorbents as carriers and is useful even at low gas pressures. Porous materials such as zeolites and activated carbons have been used thus far, but each shows limitations. Porous coordination polymers which have a large percentage of uniform microporosity (required for high efficiency) and a degree of tune ability have emerged as excellent alternative candidates for solid gas adsorbents. Gas storage potential is measured through sorption isotherm studies, but interest in developing single-crystal adsorbents has also led to structural studies of gas loaded framework materials. Such structural studies are also important for realizing preferential binding sites for the various gas molecules. These will be outlined below, but first a few important terms that reoccur throughout this section are presented. When a gas molecule is transferred from the gas phase by a solid surface (including pore surfaces) and adheres to the surface, gas adsorption is said to have occurred. This is in contrast to gas absorption, where the gas molecules are taken into the solid phase (also termed occlusion). There are two ways in which a gas can interact with a solid: first, chemisorptions, where gas molecules form chemical bonds with the solid, and second, physisorption, where gas molecules interact with the surface of the solid without forming covalent bonds. The chemisorptions process allows very high volume uptakes of gaseous molecules under ambient conditions, but requires energy input for gas release. On the other hand, as the interactions between gas and solid in the physisorption process are weak, the volumes of uptake are general low and occur only at low temperatures. Hence both processes have their drawbacks and indeed, to achieve optimum gas adsorption within solid adsorbents, porous materials are sought which show intermediate strengths of interactions (pseudo-chemisorbents). The degree of interaction between the framework and gas molecule can be quantified by determination of the heat/enthalpy of adsorption, ΔH_{ads} . This value is routinely calculated via collecting adsorption data at two temperatures (e.g. 77 and 87 K) and applying the Clausius–Clapeyron equation. Materials which have strong chemisorptions interactions, such as metal hydrides for hydrogen storage, have high ΔH_{ads} values, whereas materials which have

weaker physisorption interactions, such as activated carbons and zeolites, show low ΔH_{ads} values. Generally, when the enthalpy of adsorption is 420 kJmol^{-1} then chemical adsorption is occurring, but this is not a strict value. In the search for materials which adequately store gas molecules, intermediate ΔH_{ads} values are sought, such that they adsorb and release gas molecules at workable temperatures and pressures? Indeed, porous coordination polymers have emerged as perfect candidates for the storage and separation of a range of gases, with ΔH_{ads} values nearing the targeted range and showing respectable volumetric uptake. In comparison with other porous materials, the inner surfaces of porous coordination polymers are rich in hydrocarbons and aromatic groups, which are known to attract guest molecules. Additionally, the tuneability of pore character allows optimum properties to be readily targeted. This is particularly important as the gases of interest (i.e. H_2 , CH_4 , CO_2 , C_2H_4 , O_2) differ in size, shape and chemical nature, and as such the required pore size, shape and character of the solid adsorbent will also require variation. Examples, divided according to specific gas molecules, will now be outlined, including characteristics identified as important towards attaining greater gas storage and the target parameters for each gas.

2.3 Catalysis

The majority of interest in reactive coordination polymers lies, of course, in their application towards heterogeneous catalysis. Such materials need to be porous and contain unsaturated metal atoms or suitably active ligands to act as reactive sites. The metals can either be the nodal metals used to construct the coordination polymer or metals contained within bridging ligands. Advantages of these materials include improved catalyst recovery, enhanced stability and size or shape selectivity. Kitagawa and co-workers also described the incorporation of (achiral) Schiff bases into porous coordination polymers, but no catalytic properties were reported [1]. This same group, however, reported catalysis of Knoevenagel condensation reactions by a cadmium coordination polymer of the 3-connecting benzene-1,3,5-tricarboxylic

acid tris[N-(4-pyridyl)amide] ligand [2]. The metal ions are fully saturated (they are surrounded by six pyridyl donors) and the reaction is base catalysed by the amide groups of the ligands and is size selective. For example, the reaction of benzaldehyde with malononitrile showed 98% conversion, whereas the equivalent reaction with ethyl cyanoacetate showed only 7% conversion and no reaction was observed for cyanoacetic acid tert-butyl ester.

One of the earliest reports of heterogeneous catalysis by coordination polymers was for the (4,4) grid structure of $\text{Cd}(4,4'\text{-bipy})_2(\text{NO}_3)_2$ [3]. This material shows catalysis for the cyanosilylation of aldehydes, with shape specificity. Moderate yields (40%) were obtained for 2-tolualdehyde cyanosilylation, whereas poorer yields (18%) were obtained for 3-tolualdehyde. It was found that a- and b-naphthaldehyde reacted well whereas the larger 9-anthraldehyde did not. Later work on this material showed that it also catalysed the cyanosilylation of imines; however, absorption studies showed no detectable uptake of imines, suggesting that the catalysis is surface based (although it was noted that the reactivity is remarkably high if this is the case) [4].

2.4 Luminescence

Luminescence arises due to an electronic transition from an excited state, caused by photoexcitation, to the ground state, resulting in the emission of light [5, 6]. Depending on the nature of the excited state, luminescence is divided into two categories: fluorescence and phosphorescence. Fluorescence occurs rapidly with some energy dissipation, meaning that the emitted light is red shifted compared with that which was absorbed. Phosphorescence occurs more slowly from a triplet excited state to a singlet ground state and is the effect observed in materials that glow in the dark. Luminescent compounds usually require organic chromophoric ligands which absorb light and then pass the excitation energy to the metal ion. These 'antenna ligands' must possess an excited state that is capable of sensitising the metal ion emission. The photoexcitation in this case is referred

to as a ligand-to-metal charge-transfer process (LMCT). The reverse case is also possible, whereby the charge is transferred to the ligand (MLCT). In some cases the metal ion is not involved in the luminescence event with intraligand processes, such as $\pi-\pi^*$ transitions, responsible for fluorescence. Although organic polymers and discrete molecules can also display luminescence behaviour, coordination polymers are possibly the most versatile materials as there is the potential to couple the emission properties with guest exchange or other physical attributes. Coordination polymers can also be more thermally stable than organic species alone, making them more useful in many applications. Luminescent carboxylate-based coordination polymers have also been constructed using d-block metal ions. Cadmium-benzenetricarboxylate polymers, both 2D and 3D, have been reported that display strong fluorescence emission resulting from ligand-to-metal charge transfer (LMCT) [36]. The incorporation of DABCO co-ligands in one of the polymeric species results in a bathochromic shift of the emission band which is postulated to be caused by σ -donations from the neutral co-ligand.

2.5 Redox Activity

A number of redox-active coordination polymers have been reported [7–10]. As these are solid-state materials, designing redox activity can be a challenge. Any change in oxidation state must be compensated by either a corresponding opposite change elsewhere in the structure (either in the framework or by guests) or the absorption/desorption of the appropriate counterions.

2.6 Magnetism

There are two classes of magnetic coordination polymers that will be discussed: those displaying long-range ordering and those that display a spin crossover (SCO). Both of these phenomena involve the ordering of electrons through an external stimulus and are of great importance to the data storage and electronic industries.

2.6.1 Long-Range Magnetic Ordering

The generation of materials that order magnetically is an important goal within materials chemistry, with the main aim being to establish long-range magnetic ordering. Cooperative magnetism requires an interaction (coupling) between the spins of paramagnetic centres. A goal that has seen concerted attention is the generation of molecule-based materials with residual permanent magnetization (M) at zero field (H) with a high critical temperature (T_c). This requires a structure that allows for coupling of parallel spins, termed ferromagnetism or the antiparallel coupling of unequal spins, termed ferrimagnetism, of neighbouring paramagnetic spin carriers so that a non-zero spin of the bulk material results (Figure 2.1). When antiparallel coupling of equal spins occurs, termed antiferromagnetism, no residual spin of the bulk material is observed. An additional arrangement within these classes is termed spin canting, which occurs when the local arrangement of spins differ in magnitude such that the moment is reduced but non-zero. Other terms that are used to describe magnets are metamagnets, which show a magnetic field-dependent transformation from antiferromagnetic to ferromagnetic behaviour, and spin glass, which is a material that shows short-range magnetic ordering but no long-range ordering.

The nature of the magnetic ordering can be determined by both temperature dependent magnetic susceptibility measurements and





Ferromagnetic 	Below T_c , spins are aligned parallel in magnetic domains
Antiferromagnetic 	Below T_N , spins are aligned antiparallel in magnetic domains
Ferrimagnetic 	Below T_c , spins are aligned antiparallel but do not cancel
Paramagnetic 	Spins are randomly oriented (any of the others above T_c or T_N)

Figure 2.1 Illustration of the spin alignment.

the field dependence of the magnetization below T_c . The molar magnetic susceptibility (χ_M) of a compound in a magnetic field is the sum of its diamagnetic (repulsive) and paramagnetic (attractive) components. Ferromagnets show a temperature dependent molar magnetic susceptibility, $\chi_M T$, that increases continuously as the temperature is lowered to T_c (T_c is the Curie temperature). Ferrimagnets show a broad minimum in the $\chi_M T$ values in the paramagnetic range above T_c . The Ne'el temperature, T_N , is the critical temperature in this case. Additionally, the coercive field H_c is the reverse magnetic field required to reduce the magnetisation to zero. A hard magnet is characterised by a large H_c value (4100 Oe) and a soft magnet is characterised by a small H_c value (o10 Oe). Hard magnets are required for magnetic data storage purposes. A long-range ordered magnet is not only characterized by its critical temperature but also by field-dependent hysteresis loops. When present, hysteresis loops confer a memory effect on the system and are one of the attractive features of long range ordered materials for application in magnetic data storage. AC susceptibilities, χ_M' (in-phase), χ_M'' (out-of-phase), are also used to detect long-range ordering. It is difficult to synthesis materials which order in all three dimensions. Low dimensional materials typically show T_c values below 10 K. Intramolecular interactions (i.e. bonds) are much more efficient than intermolecular interactions (i.e. through space) at communicating magnetic information. Hence there is great interest in magnetic coordination polymers, which connect the magnetic centres through direct coordinative links. In addition, such materials have the real possibility of displaying high critical temperatures, particularly in the case of 3D ferromagnets [11].

2.6.1.1 Molecule-Based Magnets

Molecule-based magnets (MBMs) are a class of magnetic materials composed of molecular components (molecules or molecular ions) as opposed to inorganic network solids or metallic lattices, which are constructed from single atoms. Generally, MBMs are formed by transition metals, rare earth ions, free radicals or diamagnetic ligands. Molecule-based magnets include zero-dimensional isolated molecules or 1D chains, 2D layers and 3D structures where the

magnetic centres are linked directly. Such materials are commonly prepared by low-temperature, solution based methods, rather than the high-temperature methodologies often employed in inorganic network solid synthesis (e.g. metal oxides). The advantage of this design principle is that significantly more control is attained through using molecular building blocks of defined direction and connectivity where the critical temperature is potentially tunable.

2.6.1.2 *Single-Chain Magnets*

Whereas long-range ordering in magnetic materials is useful for applications in magnetic data storage, the isolation of single-chain magnets (SCM) which show magnetic ordering along the chain only may possibly be used as 1D magnetic nanowires for data storage. The general concept is to form isolated 1D chains which can be individually magnetised. While purely 1D systems are known to have no long-range ordering, the combination of large uniaxial anisotropy and large magnetic interactions between magnetic units within the chain results in long relaxation times. Thus, importantly, hysteresis or memory effects should be observed in these systems, even though 3D ordering is not present [11].

2.6.2 Spin Crossover

When a transition metal ion (d^4 – d^7) is in an octahedral environment, there is a competition between the spin pairing energy (P) and the energy gap (Δ) of the e_g and t_{2g} metal orbitals. The magnitude of the energy gap is determined by the ligand field strength of the metal coordination environment. In the case where Δ is greater than P then the d-electrons remain paired (where possible) and fill first the lowest energy, t_{2g} , orbitals, then the required e_g orbitals. The metal ground spin state for this case is defined as low spin (LS). When Δ is less than P then the d-electrons can unpair and distribute to fill both the t_{2g} and e_g orbitals. This is called the high-spin (HS) state. On the other hand, when the magnitudes of Δ and P are approximately equal, a switching between the LS and HS states can occur via an external perturbation; most

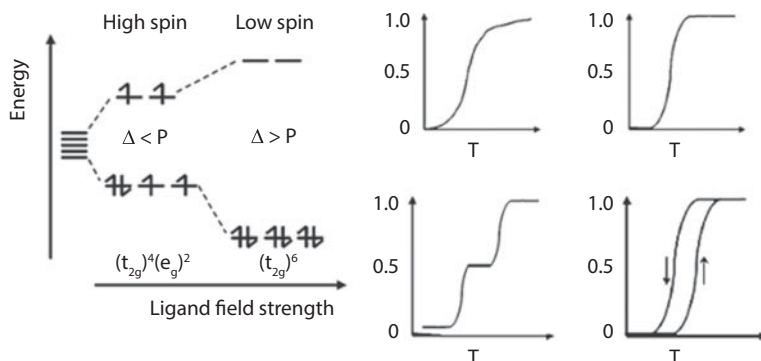


Figure 2.2 Octahedral crystal field splitting diagram showing the high-spin and low spin states for Fe^{2+} (left). The general spin transition types (HS fraction versus temperature) for gradual, abrupt, two-step and with hysteresis (right) [11].

commonly via temperature variation but also pressure or light irradiation (Figure 2.2). This phenomenon is called spin crossover (SCO), and the consequences of its incorporation into coordination polymers is the focus of the second half of this chapter. The fundamental aspects of SCO will be only briefly addressed through key examples. A final notable point is that it is possible to observe SCO in solutions of monomers where intermolecular effects are eliminated. As it is not possible to obtain 1D, 2D or 3D species in the solution phase, only solid-state SCO will be presented here. Since that SCO are about transition metal ions we don't review it further [11].

2.7 Acentric and Chiral Networks

Structures which are acentric, i.e. do not contain a centre of symmetry, are of particular interest. This symmetry is important as the following properties require acentric materials [12]:

Second-order non-linear optical (NLO) behavior: Application of a laser to a material that shows second-harmonic generation (SHG) results in the doubling of the frequency of that light (or a halving of

its wavelength). A typical example is the shining of invisible 1064 nm light from an Nd:YAG laser on a sample, resulting in its conversion to visible (green) 532 nm light. Non-linear optical materials are of significant interest for applications in photonic technology. For this reason, considerable research has been undertaken on new organic-based molecular NLO materials. Ideally, for a good SHG response a material needs to be non-centrosymmetric and have a large polarisability. Hence the organic materials best suited for this purpose have an electron donor and acceptor separated by a conjugated bridge. Coordination polymers, however, provide significant advantages for the design of new SHG active materials [13]. The structural direction provided by a network of coordination bonds can overcome unfavourable dipole–dipole interactions and coordination polymers can display high thermal and chemical robustness.

The diamond net is also a common network topology observed and is therefore fairly predictable. It is also likely to form with metals such as Zn^{II} and Cd^{II} , which have the added advantage of filled d shells, meaning that optical losses from d-d transitions are prevented. One problem with this design strategy, however, is the formation of interpenetrating nets. Although individual nets may be acentric, interpenetration may produce pairs of nets that are related by a centre of symmetry. Thus an even number of interpenetrating nets may produce an overall centrosymmetric structure and therefore it is desirable to target structures with odd numbers of interpenetrating nets. Fortunately, one of the main determining factors for the number of nets formed is the length of the bridging ligand and hence the degree of interpenetration can be controlled by varying the ligand length. Longer ligands generate higher degrees of interpenetration. The ligand L^2 with Zn^{II} or Cd^{II} gives five interpenetrating nets in the space group Cc; SHG activities are 126 and 18 times that of quartz, respectively [14]. Reaction of ligand L^3 with Zn^{II} results in five interpenetrating nets; however, in this case the nodes are $\text{Zn}_2(\mu\text{-OH})$ dimers and two of the links between the nodes are each provided by pairs of ligands related by an inversion centre [14]. As a result, the structure is centrosymmetric, despite the odd number of interpenetrating nets. By contrast, reaction of the same ligand with Cd^{II} gives seven

interpenetrating nets, the space group Ia and an SHG activity 310 times that of quartz. Use of the even longer ligand L^4 (Figure 2.3) gives eight interpenetrating diamond networks, with the Zn^{II} centres adopting both tetrahedral and octahedral geometries and the Cd^{II} centres adopting only octahedral geometry [15]. Despite the even degree of interpenetration, the structures adopt the chiral C_2 space group and display SHG activities 310 and 345 times that of quartz, respectively. Although individual results vary, it is noteworthy that the SHG efficiency, in general terms, seems to increase with increase in the number of interpenetrating networks.

Piezoelectricity: In these materials, application of a mechanical force induces electrical polarisation or, alternatively, application of an electrical field causes macroscopic strain. These materials are used in a wide range of applications to convert electrical energy into mechanical energy or vice versa.

Pyroelectricity: A pyroelectric material is one in which there is a change in the spontaneous polarisation with temperature. For this property, the structure must not just be acentric, but also possess a polar space group.

Ferroelectricity: Ferroelectric materials are pyroelectric materials in which the polarisation is reversible. These materials must not only be polar, but also contain a permanent dipole moment capable of being reversed upon application of a voltage.

Chirality: Some space groups are not just acentric, but chiral. Materials with these properties have a number of applications. Chirality is of immense interest to many chemists and the crystal engineer is no exception [16–20]. Chiral networks have possible applications as enantioselective catalysts or for the separation

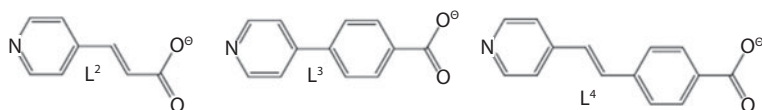


Figure 2.3 A series of asymmetric pyridylcarboxylate ligands used to construct SHG active coordination polymers.

of enantiomers from racemic solutions through enantioselective adsorption. Coordination polymers are particularly attractive for these applications as there are only two chiral zeolites known (zeolite b and titanosilicate ETS-10) and they are difficult to isolate enantiomerically pure [21, 22]. Such materials can be realised from either achiral components or, more reliably, through the use of chiral ligands. For achiral components, chirality can be induced by the geometry of the polymer, the arrangement of asymmetric ligands or by the formation of an inherently chiral network topology. However, one of the challenges for this approach (and for the use of racemic mixtures of chiral ligands) is the formation of bulk samples of crystals in which the polymers are all of the same hand, or the macroscopic resolution of crystals of the same hand (usually racemic mixtures of crystals are formed). Crystals may also be twinned, containing equal amounts of either hand within each individual crystal.

References

1. Kitaura, R., *et al.*, Immobilization of a Metallo Schiff Base into a Microporous Coordination Polymer. *Angewandte Chemie International Edition*, 43(20), p. 2684–2687, 2004.
2. Hasegawa, S., *et al.*, Three-Dimensional Porous Coordination Polymer Functionalized with Amide Groups Based on Tridentate Ligand: Selective Sorption and Catalysis. *Journal of the American Chemical Society*, 129(9), p. 2607–2614, 2007.
3. Fujita, M., *et al.*, Preparation, Clathration Ability, and Catalysis of a Two-Dimensional Square Network Material Composed of Cadmium(II) and 4,4'-Bipyridine. *Journal of the American Chemical Society*, 116(3), p. 1151–1152, 1994.
4. Ohmori, O. and Fujita, M. Heterogeneous catalysis of a coordination network: cyanosilylation of imines catalyzed by a Cd(ii)-(4,4[prime or minute]-bipyridine) square grid complex. *Chemical Communications*, 2004(14), p. 1586–1587.
5. Wang, S. and Seward, C. *Encyclopedia of Supramolecular Chemistry*, ed. J.L. Atwood and J.W. Steed, Marcel-Dekker, New York, p. 816, 2004.
6. Blasse, G. and Grabmaier, B.C. *Luminescent Materials*, Springer, Berlin, 1997.

7. Dai, J.-C., *et al.*, Synthesis, Structure, and Fluorescence of the Novel Cadmium(II)–Trimesate Coordination Polymers with Different Coordination Architectures. *Inorganic Chemistry*, 41(6), p. 1391–1396, 2002.
8. Han, J.W., Hardcastle, K.I. and Hill, C.L. Redox-Active Coordination Polymers from Esterified Hexavanadate Units and Divalent Metal Cations. *European Journal of Inorganic Chemistry*, 2006(13), p. 2598–2603, 2006.
9. Matsushita, M.M., *et al.*, Metal Coordination Complexes Composed of Photo-Electrochemically Active Ligands. *Molecular Crystals and Liquid Crystals Science and Technology. Section A. Molecular Crystals and Liquid Crystals*, 343(1), p. 87–96, 2000.
10. Noro, S.-i., *et al.*, Syntheses and crystal structures of iron co-ordination polymers with 4,4[prime or minute]-bipyridine (4,4[prime or minute]-bpy) and 4,4[prime or minute]-azopyridine (azpy). Two-dimensional networks supported by hydrogen bonding, {[Fe(azpy)(NCS)₂(MeOH)₂][middle dot]azpy} and {[Fe(4,4[prime or minute]-bpy)(NCS)₂(H₂O)₂][middle dot]4,4[prime or minute]-bpy}]. *Journal of the Chemical Society, Dalton Transactions*, 1999(10), p. 1569–1574.
11. Batten, S. R., Neville, S. M. and Turner, D. R. *Coordination Polymers; Design, Analysis and Application*, The Royal Society of Chemistry, 2009.
12. Ok, K.M., Chi, E.O. and Halasyamani, P.S. Bulk characterization methods for non-centrosymmetric materials: second-harmonic generation, piezoelectricity, pyroelectricity, and ferroelectricity. *Chemical Society Reviews*, 35(8), p. 710–717, 2006.
13. Evans, O.R. and Lin, W. Crystal Engineering of NLO Materials Based on Metal–Organic Coordination Networks. *Accounts of Chemical Research*, 35(7), p. 511–522, 2002.
14. Evans, O.R. and Lin, W. Crystal Engineering of Nonlinear Optical Materials Based on Interpenetrated Diamondoid Coordination Networks. *Chemistry of Materials*, 13(8), p. 2705–2712, 2001.
15. Lin, W., Ma, L. and Evans, O.R. NLO-active zinc(ii) and cadmium(ii) coordination networks with 8-fold diamondoid structures. *Chemical Communications*, 2000(22), p. 2263–2264.
16. Gruselle, M., *et al.*, Enantioselective self-assembly of chiral bimetallic oxalate-based networks. *Coordination Chemistry Reviews*, 250(19–20), p. 2491–2500, 2006.
17. Kesanli, B. and Lin, W. Chiral porous coordination networks: rational design and applications in enantioselective processes. *Coordination Chemistry Reviews*, 246(1–2), p. 305–326, 2003.

18. Lin, W., Homochiral porous metal-organic frameworks: Why and how? *Journal of Solid State Chemistry*, 178(8), p. 2486–2490, 2005.
19. Bradshaw, D., *et al.*, Design, Chirality, and Flexibility in Nanoporous Molecule-Based Materials. *Accounts of Chemical Research*, 38(4), p. 273–282, 2005.
20. He, C., *et al.*, Chirality Transfer through Helical Motifs in Coordination Compounds. *European Journal of Inorganic Chemistry*, 2007(22), p. 3451–3463, 2007.
21. Newsam, J.M., *et al.*, *Structural Characterization of Zeolite Beta*. Proceedings of the Royal Society of London. A. Mathematical and Physical Sciences, 420(1859), p. 375–405, 1988.
22. Anderson, M.W., *et al.*, Structure of the microporous titanosilicate ETS-10. *Nature*, 367(6461), p. 347–351, 1994.

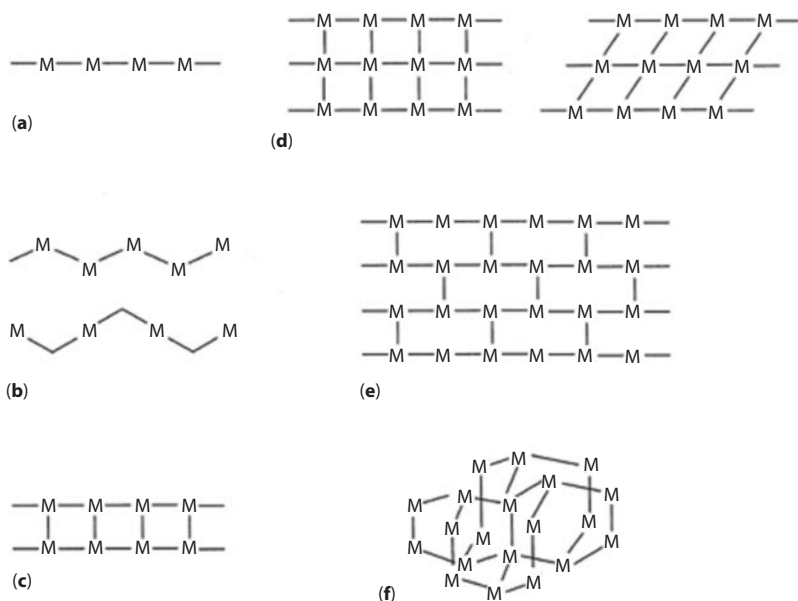
3

Zinc(II) Coordination Polymers

3.1 Introduction to Zinc(II) Coordination Polymers

During the last two decades, coordination polymers have received much attention and the number of synthesized compounds is still growing, which is mainly due to their potential application in such fields as microelectronics, nonlinear optics, molecular selection, ion exchange and catalysis. The group 12 elements are rather a special case when considering the chemistry of the main group elements [1]. The construction of coordination polymers and networks by the self-assembly of polydentate ligands and transition metal ions is a rapidly growing area of research. The considerable interest is driven by the impact on basic structural chemistry as well as by possible applications in a number of fields. As for polymeric Zn complexes, some of the compounds reviewed in the following

sections show photoluminescent and nonlinear optical (NLO) properties or have robust and thermally stable open-framework structures giving rise to permanent porosity which is a prerequisite for sorption or selective inclusion of guest molecules. As a d^{10} metal ion Zn^{2+} is particularly suited for the construction of coordination polymers and networks. The spherical d^{10} configuration is associated with a flexible coordination environment so that geometries of Zn complexes can vary from tetrahedral through trigonal bipyramidal and square pyramidal to octahedral and severe distortion of the ideal polyhedron easily occurs. Furthermore, due to the general lability of Zn complexes the formation of coordination bonds is reversible which enables metal ions and ligands to rearrange during the process of polymerization to give highly ordered network structures. Consequently, Zn can readily accommodate all kind of architectures and a selection of topological types of 1D, 2D and 3D Zn polymers is given in Scheme 3.1 [2]. In many cases rather similar ligands



Scheme 3.1 Some topological types of coordination polymers: (a) linear chain; (b) zigzag chains; (c) ladder structure; (d) square and rhombic grid, (e) brick wall; (f) diamond-related net.

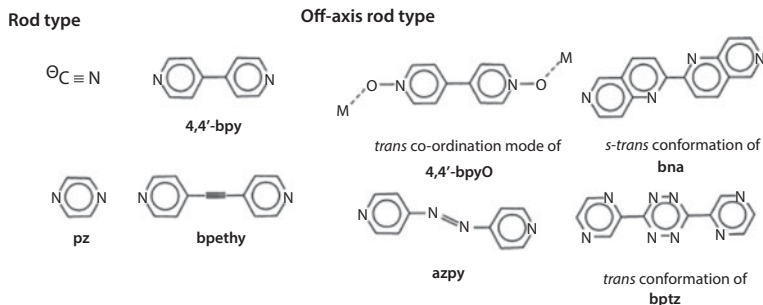
lead to completely different coordination arrays and the understanding of the structure-determining factors is of fundamental importance in coordination polymer chemistry.

3.1.1 Coordination Polymers Constructed from Rigid Two-Connecting Ligands

3.1.1.1 Rod-Type Ligands

Rod like ligands that have been employed as rigid, linear bridging units for the construction of Zn coordination polymers are summarized in Scheme 3.2. The simplest ligand recognized as a useful diatomic building block in polydimensional extended structures is the cyanide ion.

In $\{\text{Zn}(\text{CN})_2\}_n$ tetrahedral metal centers are linked by bridging CN^- groups into a robust, diamondoid network structure having relatively large adamantane-like cavities despite the small size of the bridging units [3]. Because nature tends to avoid void volume, two identical, independent copies of the framework interpenetrate each other so that each diamondoid net fills the cavities of the other. Interpenetration of $\text{Zn}(\text{CN})_2$ nets does not occur when counterions are present to occupy the cavities. Since Cu(I) forms tetrahedral complexes, self-assembly of Cu(I), Zn(II) and CN^- in the presence of $\text{N}(\text{CH}_3)_4^+$ cations affords a coordination



Scheme 3.2 Rod-type ligands in Zn coordination polymers.

polymer of composition $\{N(CH_3)_4[Cu(I)Zn(II)(CN)_4]\}_n$ with the cyanide ions linking Cu and Zn into a network of the zinc blend type [3]. Two different kinds of adamantane cavities are present in the network, namely cavities built up by four Cu^{2+} ions and six Zn^{2+} ions (4Cu/6Zn) and 4Zn/6Cu cavities. The $N(CH_3)_4^+$ cations occupy the 4Zn/6Cu cavities, thus preventing interpenetration of the network by a second one.

Pyrazine is the shortest linear linker next to cyanide. In $[Zn(pz)Cl_2]_n$ linear, parallel Zn–pz–Zn chains with octahedral metal centers are connected through double μ -Cl bridges into a 2D layer structure. Contrasting with this, $[Zn(pz)Br_2]_n$ is a 1D zigzag chain polymer with Zn adopting a tetrahedral coordination geometry [4]. $[Zn(pz)Br_2]_n$ can be converted into a 2D square-grid (4,4) network (Scheme 3.1d) by solid-state reaction with pyrazine. In $[Zn(pz)_2Br_2]_n$ the octahedral Zn ions are coordinated by four nitrogens of four distinct pyrazine ligands and two axial bromide ligands and thus act as the nodes of a (4,4) net.

4,4'-Bipyridine has been employed as a rod-type two connector in numerous studies to construct transition metal networks having, e.g. diamondlike, honeycomb, square-grid, ladder or brick-wall structures [5, 6]. In $\{[Zn(4,4'\text{-bpy})_2(H_2O)_2]SiF_6 \cdot 2H_2O\}_n$ the octahedral Zn ions are surrounded by four bridging 4,4'-bpy ligands in a square planar geometry so that infinite sheets with an ca. square grid structure are built up. In the crystal packing parallel sheets are off-set stacked so that the Zn centers are vertically above the midpoints of the Zn_4 squares of the adjacent layers. An equivalent set of stacks is arranged in planes perpendicular to the first set giving rise to an interpenetration mode that is described as diagonal/diagonal inclined interpenetration [7]. In $\{[Zn_2(4,4'\text{-bpy})_3(NO_3)_4] \cdot 2H_2O\}_n$ the Zn centers are coordinated by two chelating nitrates and three bpy nitrogens in a pentagonal bipyramidal geometry and represent T-shaped nodes [8]. Two 1D chains running perpendicularly to each other are joined by 4,4'-bpy bridges. This way, bilayers are formed that pack by partial interdigitation. There are 1D microchannels present that allow for the reversible adsorption (1,1)-bridging mode.

The rod type two-connector bpethy contains an acetylene spacer between the two pyridyl rings. Cocrystallization of $\text{Zn}(\text{NO}_3)_2$ with the bispyridyl ligand yields polycatenated molecular ladders [9]. Pentagonal bipyramidal Zn ions having two chelating nitrate ligands represent T-shaped nodes for the formation of these ladders. Two distinct sets of ladders are present with the ladders of one set being catenated by those of the other set. As schematically displayed in Figure 3.1, every mesh of a ladder is catenated by two other ladders in $[\text{Zn}_2(\text{bpethy})_3(\text{NO}_3)_4]_n$.

Analogously to 4,4'-bpy, the corresponding *N,N'*-dioxide 4,4'-bpyO can be employed as a universal, two-connecting building block for the construction of Zn grid structures. When adopting the *trans* coordination mode, 4,4'-bpyO represents a ligand with "off-axis rod" geometry.

Self-assembly of Zn^{2+} and the off-axis rod-type ligands bna {bna: 2,2'-bi-1,6-naphthyridine} and azpy yields planar 2D (4,4) frameworks. In $[\text{Zn}(\text{NCS})_2(\text{bna})_2]_n$ Zn is coordinated in a square planar fashion by four bna ligands that adopt the *s-trans* conformation, while two NCS^- ligands complete the octahedral Zn coordination geometry [10]. The ligand provides a bridging distance of about 16 Å, which allows for an inclined interpenetration mode such that each grid window has parts of two other sheets passing through it. In this regard, the 3D interlocked structure of $[\text{Zn}(\text{NCS})_2(\text{bna})_2]_n$ differs from the 1×1 interpenetration found in the (4,4) square grid structure of $\{[\text{Zn}(4,4'\text{-bpy})_2(\text{H}_2\text{O})_2][\text{SiF}_6 \cdot 2\text{H}_2\text{O}]\}_n$. Azpy produces a 2D rhombic grid

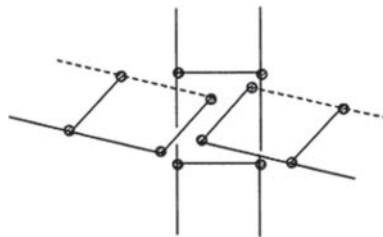
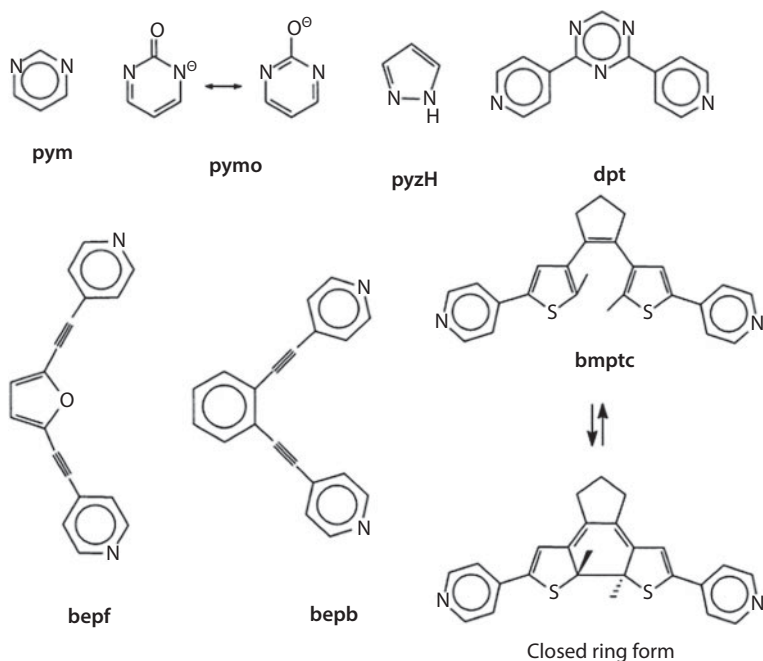


Figure 3.1 Schematic representation of the polycatenated ladders in $[\text{Zn}_2(\text{bpethy})_3(\text{NO}_3)_4]_n$.

structure of composition $\{[\text{Zn}(\text{azpy})_2(\text{H}_2\text{O})_2]\text{SiF}_6 \cdot \text{H}_2\text{O}\}_n$ with two sets of parallel layers giving rise to perpendicular interpenetration [11]. When sulfate is used as the counterion, 1D chains of alternating $\{\text{Zn}(\text{SO}_4)\}_2$ and $\{\text{Zn}(\text{SO}_4)\}_4$ rings are formed [12]. Hydrogen-bonding interactions involving Zn bound water leads to 2D sheets that are joined by azpy pillars.

3.1.1.2 Angular, Rigid Two-Connectors

Two-connecting, angular building blocks that have been assembled with Zn^{2+} are listed in Scheme 3.3. Except for pymo that links Zn^{2+} ions into a 3D diamond-related structure, these angular-type connecting units afford 1D chain structures with zigzag, wedge-shaped and helical geometries or doubly bridge Zn^{2+} ions into linear chains. Pyrimidine provides a 120° angle and connects the Zn^{2+} ions in $[\text{Zn}(\text{pym})\text{Cl}_2]_n$ into infinite zigzag chains. Linkage of these by double $\mu\text{-Cl}$ bridges results in an undulate, 2D sheet



Scheme 3.3 Ligands providing angular connectivities.

structure. Analogously to pyrimidine, the anion of pymoH represents a 120° building block, when coordination occurs via the two ring nitrogens. Unlike in $[\text{Zn}(\text{pym})\text{Cl}_2]_n$, however, the Zn ions in $[\text{Zn}(\text{pymo})_2]_n$ bind to four nitrogens of different pyrimidinolate ligands in a tetrahedral coordination geometry to give a non-interpenetrated diamond-like framework [13].

In $[\text{Zn}(\text{pymo})_2(\text{N}_2\text{H}_4)_2]_n$ octahedrally coordinated Zn centers having two mutually *trans* phenolate oxygens are doubly bridged by two N_2H_4 molecules at a distance of about 4.0 Å.

Dpt binds to Zn through the pyridyl nitrogens and links the metal ions into 21 helical chains. Two polymorphs of $[\text{Zn}(\text{NO}_3)_2(\text{dpt})]_n$, **A** and **B**, exist that differ in their nitrate binding modes [14]. In **A**, Zn is coordinated in a *cis* arrangement by two pyridyl nitrogens, one chelating and one monodentate nitrate. In **B** two chelating nitrate anions push the pyridyl donors together so that the helix pitch decreases from 22.6 Å in **A** to 19.0 Å in **B** while the helix diameter increases from 6.3 to 8.9 Å. In another Zn coordination polymer obtained with dpt, $\{[\text{Zn}(\text{dpt})_2(\text{H}_2\text{O})_2][\text{Zn}(\text{dpt})_2(\text{CH}_3\text{CN})_2](\text{ClO}_4)_4 \cdot 2\text{CH}_3\text{CN}\}_n$, two nets that have different chemical composition and different handedness interpenetrate each other [15]. Every individual net is composed of helices with two Zn ions and two dpt ligands per helical turn that are interlinked by further dpt ligands so that a second type of helix is present. In this second type of helix one helical pitch includes six metal ions and six ligands. Interpenetration of net I containing right-handed helices of composition $[\text{Zn}(\text{dpt})_2(\text{H}_2\text{O})_2]^{2+}$ and net II containing left-handed helices of composition $[\text{Zn}(\text{dpt})_2(\text{CH}_3\text{CN})_2]^{2+}$ results in a chiral network.

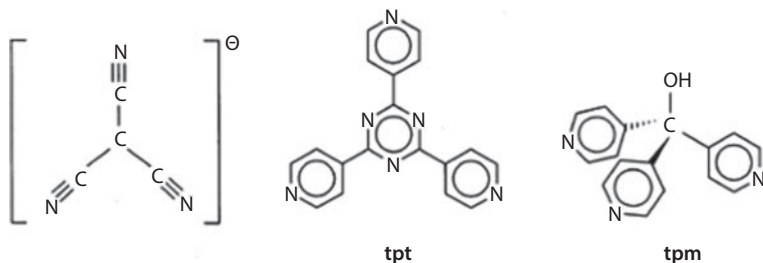
Bmptc was shown to produce infinite zigzag chains by binding to the axial positions of $\text{Zn}(\text{facac})_2$ {facac: 1,1,1,5,5,5-hexafluoroacetylacetonate} units through the pyridyl nitrogens [16]. Upon irradiation of the crystalline coordination polymer with 578 nm light the ligand is converted into the closed-ring form isomer (Scheme 3.3). Thus, $[\text{Zn}(\text{facac})_2(\text{bmptc})]_n$ exhibits photochromic reactivity in the single-crystalline state.

3.1.2 Coordination Polymers Constructed from Rigid, Trigonal Three-Connectors

Rigid, trigonal building blocks that have been used for the construction of Zn networks are summarized in Scheme 3.4. Another group of triangular building blocks comprises the inorganic anions CO_3^{2-} , BO_3^{-3} and NO_3^- that form various open-framework structures with zinc.

One possible structure resulting from self-assembly of trigonal ligands with half as many octahedral metal centers is the rutile-type framework and 2-fold interpenetrated rutile nets are realized in $[\text{Zn}\{\text{C}(\text{CN})_3\}_2]_n$ [17].

Two coordination polymers constructed from tpt have been described that possess remarkable topologies, $[\text{Zn}(\text{tpt})_{2/3}(\text{SiF}_6)(\text{H}_2\text{O})_2(\text{CH}_3\text{OH})]_n$ [18] and $\{[\text{Zn}(\text{CN})(\text{NO}_3)(\text{tpt})_{2/3}]\cdot 18\text{Solv}\}_n$ [19]. $[\text{Zn}(\text{tpt})_{2/3}(\text{SiF}_6)(\text{H}_2\text{O})_2(\text{CH}_3\text{OH})]_n$ is a rare example of a (10,3)-a net. Each Zn is coordinated by two water molecules, a methanol molecule and a SiF_6^{2-} ion in a square-planar fashion which leaves two *trans* positions for binding of tpt. The three pyridyl nitrogens of tpt link the Zn centers into a (10,3)-a net that features helical arrays. Interpenetrated (10,3)-a nets are particularly interesting. As realized by Wells 25 years ago, for intrinsically enantiomorphous (10,3)-a nets interpenetration can occur with an identical net of the same handedness as well as with a net of the opposite handedness [20].



Scheme 3.4 Ligands used as rigid, trigonal building blocks.

In $[\text{Zn}(\text{tpt})_{2/3}(\text{SiF}_6)(\text{H}_2\text{O})_2(\text{CH}_3\text{OH})]_n$ eight independent nets interpenetrate each other, four of one handedness (41-helices) and four of the other (43-helices) giving rise to a 3D racemate. Helices of independent nets with the same handedness pair to give double helices. The most remarkable and unique feature of the second Zn coordination polymer derived from tpt, $\{[\text{Zn}(\text{CN})(\text{NO}_3)(\text{tpt})_{2/3}]\cdot 18\text{Solv}\}_n$, is the presence of large, isolated and sealed-off chambers that accommodate 18 solvent molecules. Each metal ion is surrounded by one chelating nitrate, two cyanides in *cis* positions and two *trans* pyridyl nitrogens. Four Zn ions and four bridging cyanides constitute squares. Six $\{\text{Zn}_4(\text{CN})_4(\text{NO}_3)_4\}$ squares are connected by eight μ_3 -tpt ligands to build a cage structure with the centers of the trigonal building blocks sitting at the corners of a cube as outlined in Figure 3.2.

The overall infinite 3D structure consists of cages sharing the Zn_4 -faces. Two identical copies of this framework interpenetrate each other. There is a second and considerably larger type of cage. The larger cages of one framework encapsulate the smaller ones from the other. This affords isolated and sealed-off chambers that are surrounded by double shells. These cavities are large enough to host nine $\text{C}_2\text{H}_2\text{Cl}_4$ and nine methanol molecules which are highly disordered and essentially liquid.

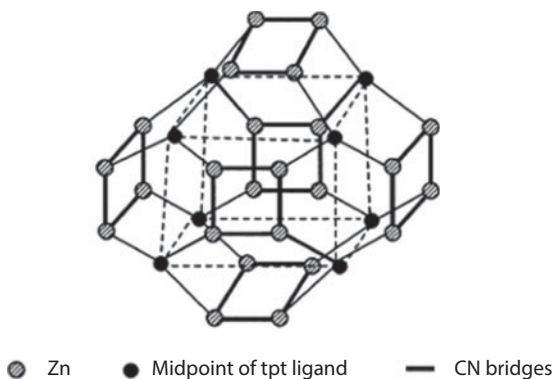
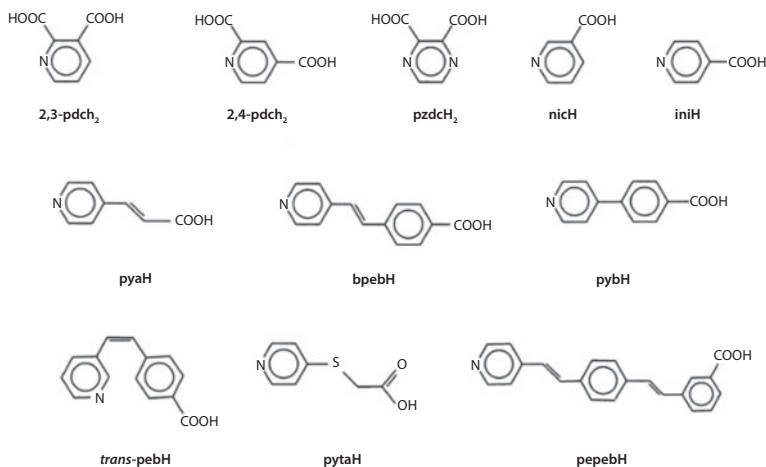


Figure 3.2 Schematic representation of the cage structure formed by six square $\{\text{Zn}_4(\text{CN})_4(\text{NO}_3)_4\}$ entities and eight μ_3 -tpt ligands in $\{[\text{Zn}(\text{CN})(\text{NO}_3)(\text{tpt})_{2/3}]\cdot 18\text{Solv}\}_n$.

3.1.3 Coordination Polymers Constructed from Carboxylates, Pyridine Carboxylates and Pyrazine Carboxylates

Several aliphatic and aromatic dicarboxylates have been employed for the synthesis of Zn coordination polymers. Two *trans* oxygens of squarate coordinate to two Zn ions and generate the 1D coordination polymer $[\text{Zn}(\text{C}_4\text{O}_4)(\text{H}_2\text{O})_4]_n$ [21] and the 3D framework structure $\{[\text{Zn}(\text{C}_4\text{O}_4)(\text{H}_2\text{O})_2] \cdot 1/3\text{CH}_3\text{COOH} \cdot 1/3\text{H}_2\text{O}\}_n$ containing cavities to accommodate CH_3COOH and water molecules [22]. The oxalate dianion has been shown to connect $\{\text{Zn}(\text{py})_2\}$ fragments into an infinite zigzag chain, while with no other ligands being bound to Zn a 2D honeycomb net results from self-assembly of six Zn and six oxalate ligands into hexagons in $\{(\text{mpyH})_2[\text{Zn}_2(\text{ox})_3]\}_n$ [23]. 1,2-Bdc forms infinite zigzag chains with $\text{Zn}(\text{im})_2$ fragments in $[\text{Zn}(\text{im})_2(1,2\text{-bdc})]_n$, while in $[\text{Zn}(\text{mim})(1,2\text{-bdc})]_n$ two Zn ions and two carboxylate ligands constitute 14-membered rings that are parts of infinite chains, since one carboxylate group of each 1,2-bdc acts as a 1,3-bridging ligand [24]. The mixed ligand complexes $[\text{Zn}(1,2\text{-bdc})\text{py}_2]_n$, $[\text{Zn}(1,2\text{-bdc})(3\text{-mpy})_2]_n$, $[\text{Zn}(1,2\text{-bdc})(4\text{-mpy})_2]_n$ and $[\text{Zn}(1,2\text{-bdc})(4\text{-mpy})]_n$ all represent chain-type coordination polymers, although the dicarboxylate ligand displays distinct coordination patterns in the individual compounds (1,6- and 1,3-bridging, monatomic bridges, monodentate, bidentate and chelating coordination) [25].

The pyridine and pyrazine carboxylate ligands displayed in Scheme 3.5 have been shown to act as connecting units in Zn coordination networks with diamondoid, 2D grid, herringbone, pillar-type and helical topologies. Pyridine-2,3-dicarboxylate (2,3-pdc) chelates one Zn through the pyridine nitrogen and one *ortho* carboxylate oxygen and binds to the next Zn ion through one oxygen of the carboxylate group in *meta* position. 2,3-pdc creates a diamondoid Zn network two copies of which interpenetrate each other in $\{\text{K}_2[\text{Zn}(2,3\text{-pdc})_2]\}_n$ [26]. In $\{[\text{ZnCu}(2,4\text{-pdc})_2(\text{H}_2\text{O})_3(\text{dmf})]\cdot\text{dmf}\}_n$ 2,4-pdc serves as a two-connecting unit to generate an interesting microporous, heteronuclear coordination polymer [27].



Scheme 3.5 Pyridine and pyrazine carboxylates in Zn coordination polymers.

Nicotinate has been applied by Lin *et al.* as a bifunctional, bridging ligand for the construction of an infinite chiral square grid [28]. The Zn centers in $[\text{Zn}(\text{nic})_2]_n$ are hexacoordinated by two chelating carboxylate groups and two pyridyl nitrogens of four different ligands. The bent configuration of nicotinate allows for a planar arrangement of the Zn ions in the 2D network. Since the Zn coordination polyhedra lack a center of symmetry and have all the same handedness, $[\text{Zn}(\text{nic})_2]_n$ represents a chiral 2D network. $[\text{Zn}(\text{nic})_2]_n$ is thermally stable up to 420 °C and shows second-order non-linear (NLO) properties. Requirements for NLO effects are the absence of a center of symmetry and the presence of asymmetric ligands that can introduce electronic asymmetry (push–pull effect).

3.1.4 Coordination Polymers Constructed from Secondary Building Blocks (SBUs)

Aromatic and other rigid di- and tricarboxylates have been recognized as powerful ligands for the construction of robust frameworks that show permanent porosity and adsorptive behavior [29]. Aromatic polycarboxylates impart a high degree of rigidity to the

structure so that in many cases guest molecules can be removed or exchanged without destruction of the porous framework or even without loss of crystallinity. In such compounds the carboxylate groups act as bridging bidentate ligands and form clusters that are referred to as secondary building units (SBU). Depending on the geometry of the cluster and the polycarboxylate ligand SBUs can represent, e.g. square, tetrahedral, octahedral, trigonal prismatic or pentagonal antiprismatic nodes for the formation of extended structures. Since the pioneering work of Yaghi [30] various open-framework structures containing Zn carboxylate clusters have been reported many of which have interesting structural features and properties. By using 1,4-bdc open-framework structures based on di-, tri- and tetranuclear secondary building blocks have been generated. $\{[\text{Zn}(1,4\text{-bdc})(\text{H}_2\text{O})].\text{dmf}\}_n$ is built up by dinuclear paddle-wheel SBUs that represent square building block. These cluster units are connected into a 2D microporous square-grid structure [31]. Adjacent layers are stacked in parallel and linked through hydrogen-bonding interactions involving water ligands and carboxylate oxygens. This way, channels are generated that have diameters of $\sim 5 \text{ \AA}$ and host the dmf molecules. Permanent porosity of $\{[\text{Zn}(1,4\text{-bdc})(\text{H}_2\text{O})].\text{dmf}\}_n$ was manifested by the observation of rapid and reversible sorption of N_2 and CO_2 by the evacuated $[\text{Zn}(1,4\text{-bdc})]_n$ framework.

While 1,4-abdc leads to the same square-grid framework as found in $\{[\text{Zn}(1,4\text{-bdc})(\text{H}_2\text{O})].\text{dmf}\}_n$, tbdc gives a double layer structure built up by tetrahedral $\{\text{Zn}_2(\text{tbdc})_6\}^{8-}$ building blocks [32]. In the case of 1,4-ndc hexameric entities containing four tetrahedral Zn, four octahedral Zn, two $\mu_3\text{-OH}$ groups, two bound dmf molecules and ten dicarboxylate ligands are obtained [33]. These SBUs have a pentagonal antiprismatic geometry and form a six-connected, channeled network hosting dmf molecules.

The tricarboxylate btc and $\text{Zn}(\text{NO}_3)_2$ yield a rigid and highly stable porous 3D framework that reversibly includes alcohols [34]. The basic structural motif of $\{[\text{Zn}_2(\text{btc})(\text{NO}_3)(\text{EtOH})_3].\text{H}_2\text{O}.2\text{EtOH}\}_n$ is composed of two Zn centers that are bridged by three carboxylate groups of three different btc ligands. One chelating nitrate and three ethanol molecules give rise to five- and hexa

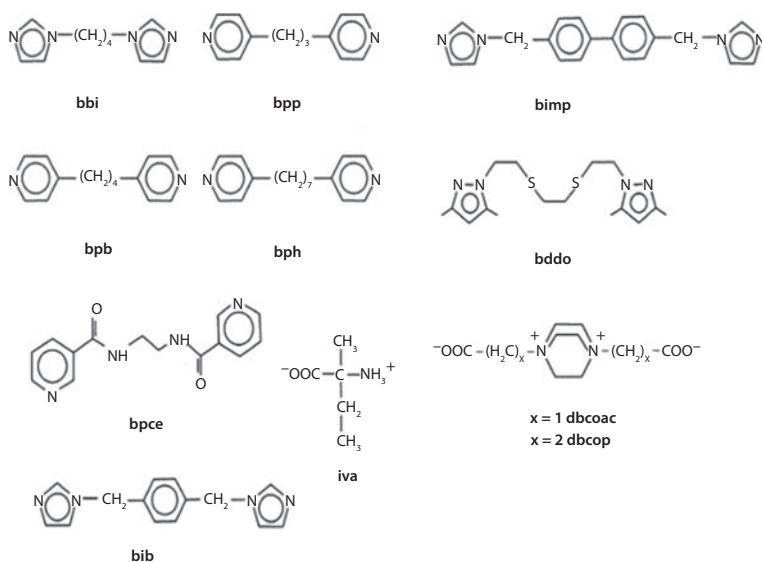
coordinated metal ions. The porous structure of the network results from large fused rings composed of five dinuclear Zn_2 building blocks. The nitrate anions and the bound ethanol molecules point towards the centers of the rings. The 3D overall structure features channels with a diameter of about 14 Å that host water and (uncoordinated) ethanol molecules. Most of the bound and unbound ethanol can be removed without loss of the structural integrity of the framework.

Ctc is structurally similar to btc. However, the extended structure of its Zn complex of composition $[\text{Zn}_3(\text{ctc})_2(\text{py})_2(\text{dmf})_2]_n$ is two-dimensional and is based on trinuclear building blocks [35]. Three collinear Zn ions are bridged by six carboxylate groups four of which form three-atom bridges. The other two carboxylate groups form single-atom bridges. Two of the three Zn ions have additional pyridine and dmf ligands. The building blocks are linked through the remaining carboxylate functionalities into a 2D layer three Zn centers thick.

3.1.5 Coordination Polymers Constructed from Conformational Flexible Ligands

While the rigid ligands with fixed bridging angles discussed in the previous sections are suitable candidates for a more rational design of network structures, bidentate ligands with conformational flexible spacers that preclude prediction and control of the resultant structures are well suited to accommodate a wide variety of architectures and offer a high degree of adaptability to, e.g. the inclusion of counterions or other guest molecules. Conformational flexible ligands that have been used to synthesize Zn coordination polymers are presented in Scheme 3.6.

In bib two imidazole residues are separated by an aromatic spacer. This ligand is known to form catenane and rotaxane structures with transition metal ions [36] and a 2D polyrotaxane structure has been reported for the Zn complex $\{[\text{Zn}(\text{bib})_2(\text{NO}_3)_2] \cdot 4.5\text{H}_2\text{O}\}_n$ [37]. The cyclic units of the polyrotaxane are built up by two Zn centers and two bridging bib ligands. As outlined in



Scheme 3.6 Conformational flexible ligands used to synthesize Zn coordination polymers.

Figure 3.3a these $\{Zn_2(bib)_2\}$ macrocycles are connected by bib bridges into an infinite 2D array. Each Zn is surrounded by four imidazole nitrogens in a distorted tetrahedral geometry. Interpenetration of two independent nets results in the polyrotaxane structure shown in Figure 3.3b. When the imidazole residues of the ligand are separated by two phenyl groups instead of one, a double-stranded Zn helix can be obtained.

In $\{[Zn(bimp)(CH_3CO_2)_2] \cdot 6H_2O\}_n$ bridging bimp ligands generate infinite 21 helical chains, while the acetate ligands bind in a monodentate fashion to the metal centers [38]. Two independent strands are interwoven with each other and the resulting double helix is held together by H bonds and weak face-to-face π - π interactions. In contrast to the chelating binding mode observed in other transition metal complexes, bddo acts as a bidentate, bridging ligand towards Zn and connects the Zn ions of $[Zn(bddo)(NCS)_2]_n$ into an infinite chain [39].

The two carboxylate groups of zwitterionic dbcop link Zn ions into a 2-fold interpenetrated polymer of composition $\{[Zn(dbcop)_2]$

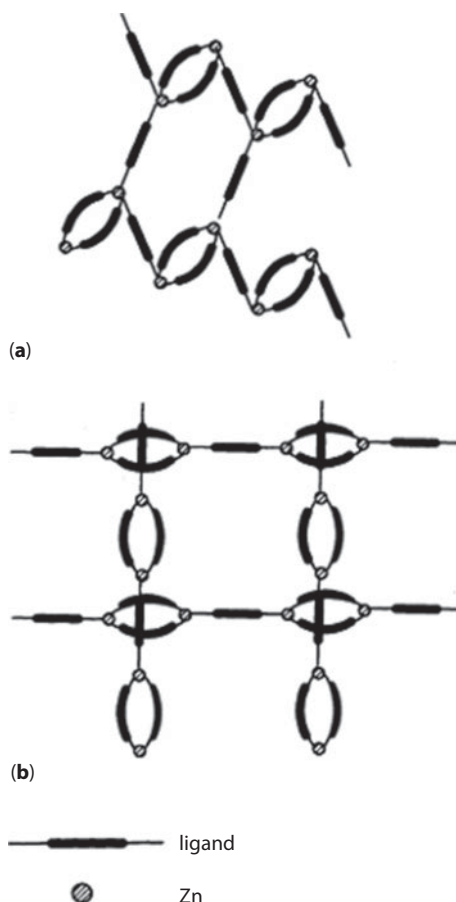


Figure 3.3 Schematic representation of the 2D structure of $\{[\text{Zn}(\text{bib})_2(\text{NO}_3)_2] \cdot 4.5\text{H}_2\text{O}\}_n$ (a) and the polyrotaxane structure generated by interpenetration (b).

$(\text{ClO}_4)_2\}_n$ [40]. With the structurally related ligand dbcoac 1D and 2D coordination polymers have been obtained, namely $\{[\text{Zn}(\text{dbcoac})\text{Br}_2] \cdot \text{H}_2\text{O}\}_n$ (infinite zigzag chains) and $\{[\text{Zn}(\text{dbcoac})(\text{H}_2\text{O})_2](\text{ClO}_4)_2 \cdot 4\text{H}_2\text{O}\}_n$ (wavy layer network) [41].

In $[\text{Zn}_3\text{Cl}_2(\text{iva})_4]_n$ Zn ions are linked by the α -amino acid isovaline into a 2D grid structure [42]. The compound contains two types of Zn ions. One type is chelated by two iva ligands, thus having $\text{N}_2\text{O}_2\text{Cl}$ environments. The carboxylate groups of these

$\{\text{ZnCl(iva)}_2\}$ moieties form monatomic bridges to the second type of Zn ions having a distorted tetrahedral O_4 environment so that the $\{\text{ZnCl(iva)}_2\}$ units are connected into 2D layers.

3.1.6 Coordination Polymers Constructed from Phosphate and Phosphonate Ligands

A wide variety of interesting chain, layer, open-framework and channel structures have been derived from phosphate and phosphonates. Transition metal phosphonates are of interest due to their potential applicability in ion exchange and sorption. Phosphate and phosphonate based coordination polymers have been reviewed by Cao and Mallouk [43] and by Clearfield [44] and some recent examples are listed under [45]. In $[\text{Zn}_2(\text{en})(\text{HPO}_3)_2]_n$ and $[\text{Zn}_2(4,4'\text{-bpy})(\text{PO}_3\text{F})_2]_n$ ethylenediamine and 4,4'-bpy serve as bidentate linking units between inorganic $\text{Zn}-\text{O}_3\text{P}$ layers [46, 47]. In $[\text{Zn}_2(\text{en})(\text{HPO}_3)_2]_n$ alternating ZnO_3N and HPO_3^{-2} tetrahedra form neutral sheets with 4.8^2 topology. Neighboring sheets are connected through $\text{Zn}-\text{NH}_2-(\text{CH}_2)_2-\text{NH}_2-\text{Zn}$ linkages. In the crystal lattice two independent networks interpenetrate each other with the $\text{Zn}-\text{en}-\text{Zn}$ chains of one network threading the eight-membered circuits of the other. Like en, 4,4'-bpy connects adjacent layers built up by ZnO_3N and PO_3F^- tetrahedra, thus serving as a pillaring group. The larger 4,4'-bpy ligand, however, generates a non-interpenetrated channel structure in $[\text{Zn}_2(4,4'\text{-bpy})(\text{PO}_3\text{F})_2]_n$. $[\text{Zn}_2(\text{en})(\text{HPO}_3)_2]_n$ and $[\text{Zn}_2(4,4'\text{-bpy})(\text{PO}_3\text{F})_2]_n$ can be structurally compared with pillared Zn compounds derived from biphosphonates like $[\text{Zn}_2(\text{pbp})(\text{H}_2\text{O})_2]_n$ [48], $[\text{Zn}_2(\text{bpbp})(\text{H}_2\text{O})_2]_n$ [49], $[\text{Zn}_2(\text{ebp})(\text{H}_2\text{O})_2]_n$ [50] and $[\text{Zn}_2(\text{pbp})]_n$ [50] where neighboring inorganic $\text{Zn}-\text{O}_3\text{PC}$ layers are cross-linked by the diaryl or alkyl groups of the phosphonates.

3.2 Nano Zinc(II) Coordination Polymers

The Zn(II) ions as metal centers have been used extensively for the synthesis of various organic-inorganic networks [51–54].

To date, the synthesis of nano coordination polymers have been generated interest and they are synthesized with different methods and conditions such as microwave, sonochemistry [55–57], the coordination modulation, hydrothermal/solvothermal and so on [58, 59]. By decreasing the size of coordination polymers (CPs) from bulk powder crystalline to nano-size, the properties and applications of them would be improved.

A quite elegant approach used in the synthesis of nanomaterials is sonochemistry [60]. In this method molecules are promoted to form nano-sized straw-like by the application ultrasound radiation. Reaction between mixture of 4,4'-bipy and 3-bpdb with a mixture of zinc(II) acetate and sodium perchlorate led to the formation of the new zinc(II) 2D coordination polymer $\{[\text{Zn}(\mu\text{-}4,4'\text{-bipy})(\mu\text{-}3\text{-bpdb})(\text{H}_2\text{O})_2](\text{ClO}_4)_2 \cdot 4,4'\text{-bipy} \cdot 3\text{-bpdb} \cdot \text{H}_2\text{O}\}_n$ {4,4'-bipy = 4,4'-bipyridine and 3-bpdb = 1,4-bis(3-pyridyl)-2,3-diaza-1,3-butadiene}. Nano-straws of complex were obtained by ultrasonic irradiation in a water solution and single crystalline material was obtained using a slow evaporation. The complex in the solid state (Figure 3.4) consists of two-dimensional polymeric units, i.e. the structure can be considered a coordination polymer of zinc(II) consisting of linear chains formed by bridging 4,4'-bipy and 3-bpdb

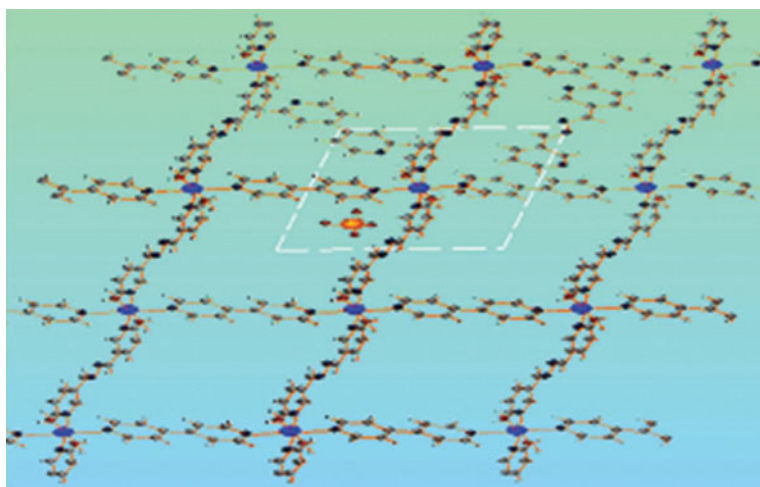


Figure 3.4 A fragment of the two-dimensional polymer in up compound.

ligands. The coordination number in this complex is six and the geometry can be regarded as distorted octahedral.

The morphology of compound prepared by the sonochemical method is very interesting and it is composed of belts of similar straw (Figure 3.5) [61].

The yellowish crystalline material of the general formula $\{[\text{Zn}(\mu\text{-}4,4'\text{-bipy})(\mu\text{-}3\text{-bpdh})(\text{H}_2\text{O})_2](\text{ClO}_4)_2 \cdot (4,4'\text{-bipy})_{0.5}\}_n$ was provided from slow evaporation of a saturated solution; a mixture of two organic compounds as bridging ligand (4,4'-bipy and 3- bpdh) and two inorganic salts as center atom and counter ion (zinc(II) acetate dehydrate, sodium perchlorate). Determination of the structure of compound $\{[\text{Zn}(\mu\text{-}4,4'\text{-bipy})(\mu\text{-}3\text{-bpdh})(\text{H}_2\text{O})_2](\text{ClO}_4)_2 \cdot (4,4'\text{-bipy})_{0.5}\}_n$ by X-ray crystallography), showed this structure is a novel two-dimensional coordination polymer (Figure 3.6). The zinc(II) atoms can be considered to be six-coordinate as octahedral with ZnN_4O_2 coordination

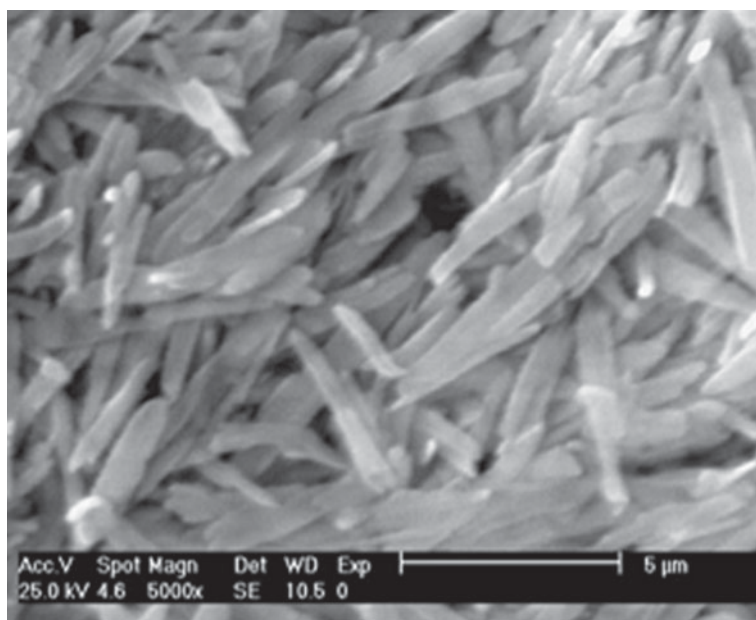


Figure 3.5 SEM photograph of $\{[\text{Zn}(\mu\text{-}4,4'\text{-bipy})(\mu\text{-}3\text{-bpdh})(\text{H}_2\text{O})_2](\text{ClO}_4)_2 \cdot 4,4'\text{-bipy} \cdot 3\text{-bpdh} \cdot \text{H}_2\text{O}\}_n$ nano-straw.

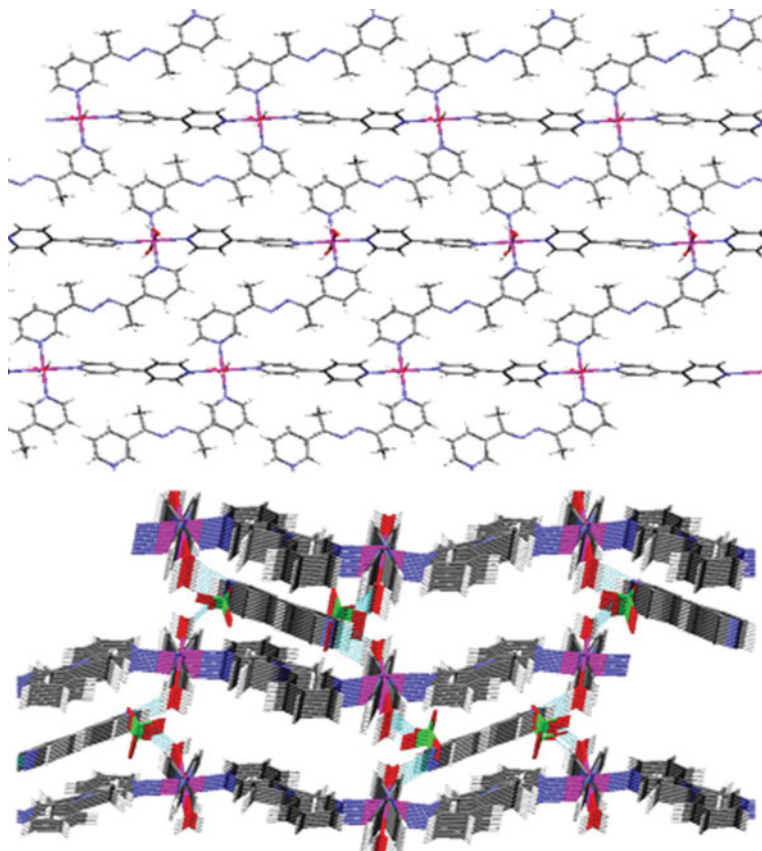


Figure 3.6 A fragment of the two-dimensional chain in compound along crystallographic b axis (top) and showing of three-dimensional supramolecular of compound formed by hydrogen bonding of perchlorate anions and uncoordinated 4,4'-bipyridine molecules (bottom).

sphere, the coordinated nitrogen atom is from 3-pyridine and 4-pyridine groups of 3-bpdh and 4,4'-bipy ligands.

Two water molecules have been coordinated to the zinc atoms by oxygen atoms. The perchlorate anions as counter ion and some molecules of 4,4'-bipy as guest molecule are fixed in the structure by hydrogen bonding. Hydrogen bonding is the main reason for growing the structure in three dimensions.

The compound $\{[\text{Zn}(\mu\text{-}4,4'\text{-bipy})(\mu\text{-}3\text{-bpdh})(\text{H}_2\text{O})_2](\text{ClO}_4)_2 \cdot (4,4'\text{-bipy})_{0.5}\}_n$ has been synthesized in nano-size by ultrasonic

method. The morphology, structure and size of the nanostructure of compound 1 were investigated by Scanning Electron Microscopy (Figure 3.7). Figure 3.7 indicates the original morphology is the nanorods that have been prepared by sonochemical process [62].

The shiny crystalline material of the general formula $\{[\text{Zn}(\mu\text{-3-bpdb})(3\text{-bpdb})_2(\text{H}_2\text{O})_2](\text{ClO}_4)_2 \cdot 3\text{-bpdb}\}_n$ was provided from slow evaporation of a saturated solution of 3-bpdb, zinc(II) acetate dehydrate and sodium perchlorate. Also, the nano-rods of compound $\{[\text{Zn}(\mu\text{-3-bpdb})(3\text{-bpdb})_2(\text{H}_2\text{O})_2](\text{ClO}_4)_2 \cdot 3\text{-bpdb}\}_n$ with good morphologies were synthesized by sonochemical method.

Determination of the structure of compound $\{[\text{Zn}(\mu\text{-3-bpdb})(3\text{-bpdb})_2(\text{H}_2\text{O})_2](\text{ClO}_4)_2 \cdot 3\text{-bpdb}\}_n$ by X-ray crystallography showed this structure is a new one-dimensional coordination polymer. The zinc(II) atoms have been coordinated by six atoms and have octahedral coordination sphere as ZnN_4O_2 . Four 3-bpdb molecules coordinate to each zinc(II) atom by nitrogen atoms of pyridyl groups. One molecule of ligand 3-bpdb connects to zinc(II) atom as bi-donor and two other ones coordinate just by one nitrogen atom. Also, two water molecules coordinate to zinc(II) atom. The perchlorate anions act as counter ion; these ions and un-coordinated 3-bpdb ligand were filled the space between of one-dimensional chains. The hydrogen bonds and π - π stacking are the main causes for growing this polymer in two and three-dimension networks (Figure 3.8).

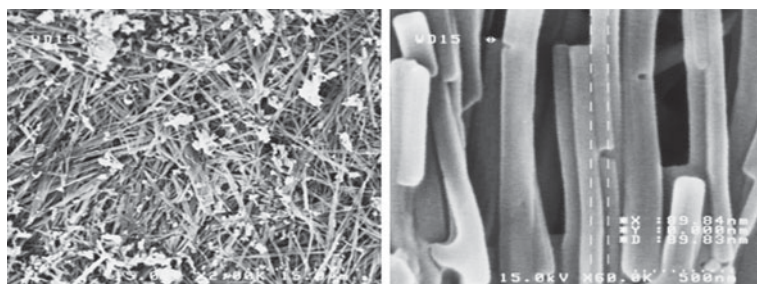


Figure 3.7 The SEM images of compound $\{[\text{Zn}(\mu\text{-4,4'-bipy})(\mu\text{-3-bpdb})(\text{H}_2\text{O})_2](\text{ClO}_4)_2 \cdot (4,4'\text{-bipy})_{0.5}\}_n$ nanorods prepared by sonochemical method.

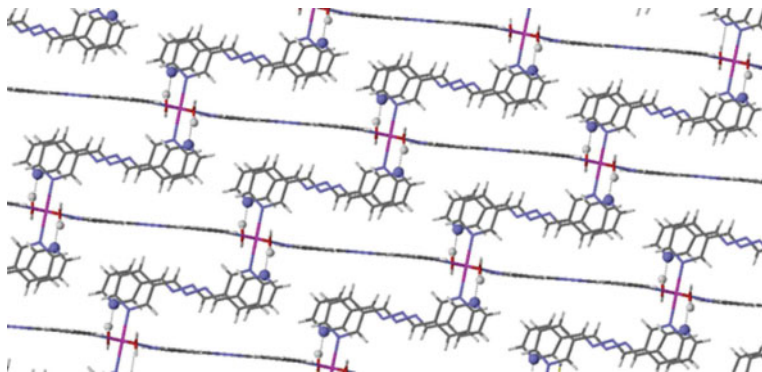


Figure 3.8 A view of π - π stacking and hydrogen bonding interactions between two chains the perchlorate ions were omitted for clarity (Zn = violet, O = red, C = gray, N = blue, Chloride = green).

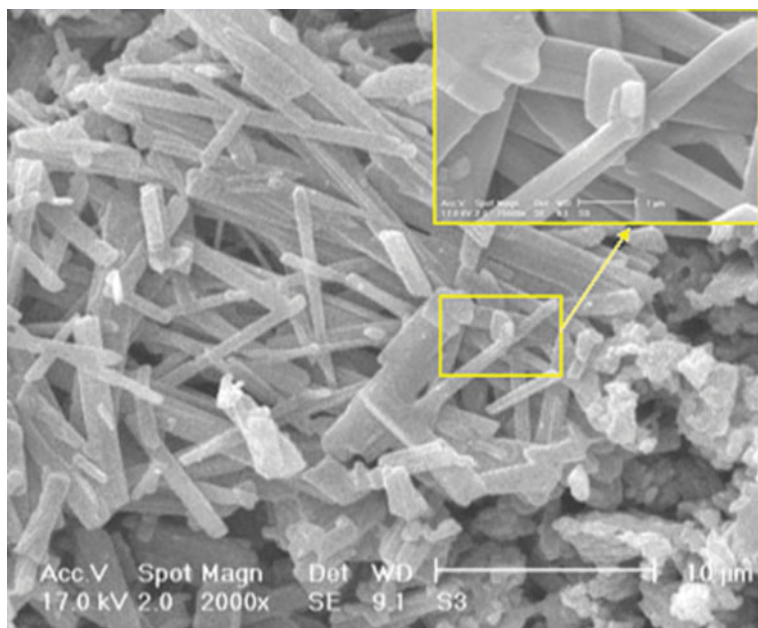


Figure 3.9 The SEM images of nano-rods compound $\{[\text{Zn}(\mu\text{-3-bpdb})(\text{3-bpdb})_2(\text{H}_2\text{O})_2](\text{ClO}_4)_2 \cdot \text{3-bpdb}\}_n$.

The morphology, structure and size of compound $\{[\text{Zn}(\mu\text{-3-bpdb})(\text{3-bpdb})_2(\text{H}_2\text{O})_2](\text{ClO}_4)_2 \cdot \text{3-bpdb}\}_n$ in nano size were investigated by scanning electron microscopy (Figure 3.9) [63].

3.3 Conclusion

As manifested by the structures reviewed in this part, the versatile coordination properties of the Zn^{2+} ion allow for a large variety of architectures resulting from the self-assembly of Zn^{2+} with organic ligands. A number of open-framework structures derived from conformationally rigid polydentate ligands are available to date that are promising candidates for applications due to properties like permanent porosity and (selective) adsorptive behavior.

References

1. Pitt, M.A. and Johnson, D.W. Main group supramolecular chemistry. *Chemical Society Reviews*, 36(9), p. 1441–1453, 2007.
2. Mahmoudi, G. and Morsali, A. Counter-ion influence on the coordination mode of the 2,5-bis(4-pyridyl)-1,3,4-oxadiazole (bpo) ligand in mercury(ii) coordination polymers, $[\text{Hg}(\text{bpo})_n\text{X}_2]$: $\text{X} = \text{I}^-$, Br^- , SCN^- , N_3^- and NO_2^- ; spectroscopic, thermal, fluorescence and structural studies. *CrystEngComm*, 9(11), p. 1062–1072, 2007.
3. Hoskins, B.F. and Robson, R. Design and construction of a new class of scaffolding-like materials comprising infinite polymeric frameworks of 3D-linked molecular rods. A reappraisal of the zinc cyanide and cadmium cyanide structures and the synthesis and structure of the diamond-related frameworks $[\text{N}(\text{CH}_3)_4][\text{CuI}\text{ZnII}(\text{CN})_4]$ and $\text{CuI}[4,4',4'',4'''\text{-tetracyanotetraphenylmethane}]\text{BF}_4 \cdot x\text{C}_6\text{H}_5\text{NO}_2$. *Journal of the American Chemical Society*, 112(4), p. 1546–1554, 1990.
4. Bourne, S.A., Kilkenny, M. and Nassimbeni, L.R. One- and two-dimensional coordination polymers of zinc(II) with pyrazine. Solid state reactions and decomposition kinetics of the interconversion reactions. *Journal of the Chemical Society, Dalton Transactions*, 2001(8), p. 1176–1179.
5. Blake, A.J., *et al.*, Inorganic crystal engineering using self-assembly of tailored building-blocks. *Coordination Chemistry Reviews*, 183(1), p. 117–138, 1999.
6. Yaghi, O.M., *et al.*, Synthetic Strategies, Structure Patterns, and Emerging Properties in the Chemistry of Modular Porous Solids. *Accounts of Chemical Research*, 31(8), p. 474–484, 1998.

7. Gable, R.W. Hoskins, B.F. and Robson, R. A new type of interpenetration involving enmeshed independent square grid sheets. The structure of diaquabis-(4,4[prime or minute]-bipyridine) zinc hexafluorosilicate. *Journal of the Chemical Society, Chemical Communications*, 1990(23), p. 1677–1678.
8. Kondo, M., *et al.*, Three-Dimensional Framework with Channeling Cavities for Small Molecules: $\{[M_2(4,4'\text{-bpy})_3(\text{NO}_3)_4]\cdot x\text{H}_2\text{O}\}_n$ (M = Co, Ni, Zn). *Angewandte Chemie International Edition in English*, 36(16), p. 1725–1727, 1997.
9. Carlucci, L. Ciani, G. and Proserpio, D. M. Self-assembly of novel co-ordination polymers containing polycatenated molecular ladders and intertwined two-dimensional tilings. *Journal of the Chemical Society, Dalton Transactions*, 1999(11), p. 1799–1804.
10. Wu, H.-P., *et al.*, 2,2[prime or minute]-Bi-1,6-naphthyridine metal complexes: a new ligand and a novel 2 [times] 2 inclined interpenetration of (4,4) nets or formation of helicoidal chains[dagger]. *Chemical Communications*, 1998(23), p. 2637–2638.
11. Carlucci, L. Ciani, G. Proserpio, D.M. *New J. Chem.* 1998(40), p. 1319.
12. Kondo, M., *et al.*, Syntheses and Structures of Zn Coordination Polymers with 4,4'-Bipyridine and 4,4'-Azopyridine. Effect of Counter Anions on the Network System. *Chemistry Letters*, 28(4), p. 285–286, 1999.
13. Masciocchi, N., *et al.*, *Thermally Robust Metal Coordination Polymers: The Cobalt, Nickel, and Zinc Pyrimidin-2-olate Derivatives*. *European Journal of Inorganic Chemistry*, 2000(12), p. 2507–2515.
14. Barnett, S.A., *et al.*, Synthesis and structural characterisation of cadmium(II) and zinc(II) coordination polymers with an angular dipyridyl bridging ligand: parallel interpenetration of two-dimensional sheets with 4.8² topology. *Journal of the Chemical Society, Dalton Transactions*, 2001(5), p. 567–573.
15. Sasa, M., *et al.*, Spontaneously Resolved Chiral Interpenetrating 3-D Nets with Two Different Zinc Coordination Polymers. *Journal of the American Chemical Society*, 123(43), p. 10750–10751, 2001.
16. Matsuda, K., Takayama, K. and Irie, M. Single-crystalline photochromism of a linear coordination polymer composed of 1,2-bis[2-methyl-5-(4-pyridyl)-3-thienyl]perfluorocyclopentene and bis(hexafluoroacetylacetonato)zinc. *Chemical Communications*, 2001(4), p. 363–364.

17. Batten, S.R., Hoskins, B.F. and Robson, R. 3D Knitting patterns. Two independent, interpenetrating rutile-related infinite frameworks in the structure of $\text{Zn}[\text{C}(\text{CN})_3]_2$. *Journal of the Chemical Society, Chemical Communications*, 1991(6), p. 445–447.
18. Abrahams, B.F., *et al.*, A wellsian ‘three-dimensional’ racemate: eight interpenetrating, enantiomorphic (10,3)-a nets, four right- and four left-handed. *Chemical Communications*, 1996(11), p. 1313–1314.
19. Batten, S.R., Hoskins, B.F. and Robson, R. Two Interpenetrating 3D Networks Which Generate Spacious Sealed-Off Compartments Enclosing of the Order of 20 Solvent Molecules in the Structures of $\text{Zn}(\text{CN})(\text{NO}_3)(\text{tpt})2/3.\text{cntdot.solv}$ ($\text{tpt} = 2,4,6\text{-tri}(4\text{-pyridyl})\text{-}1,3,5\text{-triazine}$, $\text{solv} = .\text{apprx.}3/4\text{C}_2\text{H}_2\text{Cl}_4.\text{cntdot.}3/4\text{CH}_3\text{OH}$ or $.\text{apprx.}3/2\text{CHCl}_3.\text{cntdot.}1/3\text{CH}_3\text{OH}$). *Journal of the American Chemical Society*, 117(19), p. 5385–5386, 1995.
20. Wells, A.F. *Three-Dimensional Nets and Polyhedra*, Wiley-Interscience, New York, 1977.
21. Robl, C. and Kuhs, W.F. Hydrogen bonding in the chain-like coordination polymer $\text{ZnC}_4\text{O}_4 \cdot 4\text{H}_2\text{O}$: A neutron diffraction study. *Journal of Solid State Chemistry*, 75(1), p. 15–20, 1988.
22. Weiss, A., Riegler, E. Robl, C. Transition Metal Squarates, II, Z. *Naturforsch.* 1986(41b), p.1329
23. Evans, O.R. and Lin, W. Synthesis of Zinc Oxalate Coordination Polymers via Unprecedented Oxidative Coupling of Methanol to Oxalic Acid. *Crystal Growth & Design*, 1(1), p. 9–11, 2001.
24. Baca, S.G., *et al.*, Zinc(II) carboxylates with imidazole and 2-methylimidazole: unprecedented cyclic dimer and polynuclear coordination polymers based on bridging phthalate ions. *Inorganica Chimica Acta*, 344, p. 109–116, 2003.
25. Baca, S.G., *et al.*, Synthesis and X-ray diffraction study of Zn(II) complexes with *o*-phthalic acid and aromatic amines. *Polyhedron*, 20(9–10), p. 831–837, 2001.
26. Gutschke, S.O.H., Slawin, A.M.Z. and Wood, P.T. Coordination complexes with infinite lattice structures: solvothermal synthesis and X-ray crystal structures of $\text{K}_2\text{M}[\text{NC}_5\text{H}_3(\text{CO}_2)_2]_2$ ($\text{M} = \text{Mn}$, Zn). *Journal of the Chemical Society, Chemical Communications*, 1995(21), p. 2197–2198.
27. Noro, S.-i., *et al.*, New microporous coordination polymer affording guest-coordination sites at channel walls. *Chemical Communications*, 2002(3), p. 222–223.

28. Lin, W., *et al.*, Supramolecular Engineering of Chiral and Acentric 2D Networks. Synthesis, Structures, and Second-Order Nonlinear Optical Properties of Bis(nicotinato)zinc and Bis{3-[2-(4-pyridyl)ethenyl]benzoato}cadmium. *Journal of the American Chemical Society*, 120(50), p. 13272–13273, 1998.
29. Eddaoudi, M., Li, H. and Yaghi, O.M. Highly Porous and Stable Metal–Organic Frameworks: Structure Design and Sorption Properties. *Journal of the American Chemical Society*, 122(7), p. 1391–1397, 2000.
30. Eddaoudi, M., *et al.*, Modular Chemistry: Secondary Building Units as a Basis for the Design of Highly Porous and Robust Metal–Organic Carboxylate Frameworks. *Accounts of Chemical Research*, 34(4), p. 319–330, 2001.
31. Li, H., *et al.*, Establishing Microporosity in Open Metal–Organic Frameworks: Gas Sorption Isotherms for Zn(BDC) (BDC = 1,4-Benzenedicarboxylate). *Journal of the American Chemical Society*, 120(33), p. 8571–8572, 1998.
32. Braun, M.E. Steffek, C.D. Kim, J. Rasmussen, P.G. Yaghi, O.M. 1,4-Benzenedicarboxylate Derivatives as Links in the Design of Paddle-Wheel Units and Metal–Organic Frameworks. *Chem. Commun.*, 120, p. 2532–2533, 2001.
33. Vodak, D.T. Braun, M.E. Kim, J. Eddaoudi, M. Yaghi, O.M. Metal–Organic Frameworks Constructed from Pentagonal Antiprismatic and Cuboctahedral Secondary Building Units. *Chem. Commun.* 120, p. 2534–2535, 2001.
34. Yaghi, O.M., *et al.*, Selective Guest Binding by Tailored Channels in a 3-D Porous Zinc(II)–Benzenetricarboxylate Network. *Journal of the American Chemical Society*, 119(12), p. 2861–2868, 1997.
35. M. Yaghi, O., *et al.*, Construction of a new open-framework solid from 1,3,5-cyclohexanetricarboxylate and zinc(II) building blocks. *Journal of the Chemical Society, Dalton Transactions*, 1997(14), p. 2383–2384.
36. Hoskins, B.F., Robson, R. and Slizys, D.A. An Infinite 2D Polyrotaxane Network in $\text{Ag}_2(\text{bix})_3(\text{NO}_3)_2$ (bix = 1,4-Bis(imidazol-1-ylmethyl)benzene). *Journal of the American Chemical Society*, 119(12), p. 2952–2953, 1997.
37. Hoskins, B.F., Robson, R. and Slizys, D.A. The Structure of $[\text{Zn}(\text{bix})_2(\text{NO}_3)_2] \cdot 4.5 \text{ H}_2\text{O}$ (bix = 1,4-Bis(imidazol-1-ylmethyl)benzene): A New Type of Two-Dimensional Polyrotaxane. *Angewandte Chemie International Edition in English*, 36(21), p. 2336–2338, 1997.

38. Zhu, H.-F., *et al.*, Self-assembly of a snake-like blue photoluminescent coordination polymer from 4,4[prime or minute]-bis(imidazol-1-ylmethyl)biphenyl and zinc acetate. *New Journal of Chemistry*, 26(10), p. 1277–1279, 2002.
39. aanstra, W.G., *et al.*, Unusual chelating properties of the ligand 1,8-bis(3,5-dimethyl-1-pyrazolyl)-3,6-dithiaoctane (bddo). Crystal structures of $\text{Ni}(\text{bddo})(\text{NCS})_2$, $\text{Zn}(\text{bddo})(\text{NCS})_2$ and $\text{Cd}_2(\text{bddo})(\text{NCS})_4$. *Journal of the Chemical Society, Dalton Transactions*, 1989(11), p. 2309–2314.
40. Wei, P.-R., *et al.*, Interpenetrating network structure of a polymeric complex of zinc(II) perchlorate with 1,4-Diazoniobicyclo[2.2.2] Octane-1,4-Dipropionate. *Polyhedron*, 15(22), p. 4041–4046, 1996.
41. Wei, P.-R., *et al.*, Crystal structures of polymeric complexes of zinc(II) bromide and perchlorate with 1,4-diazoniabicyclo [2.2.2] octane-1,4-diacetate. *Journal of Chemical Crystallography*, 27(10), p. 609–615, 1997.
42. Strasdeit, H., *et al.*, Syntheses and Properties of Zinc and Calcium Complexes of Valinate and Isovalinate: Metal α -Amino Acidates as Possible Constituents of the Early Earth's Chemical Inventory. *Chemistry – A European Journal*, 7(5), p. 1133–1142, 2001.
43. Cao, G., Hong, H.G. and Mallouk, T.E. Layered metal phosphates and phosphonates: from crystals to monolayers. *Accounts of Chemical Research*, 25(9), p. 420–427, 1992.
44. Clearfield, A., Metal-phosphonate chemistry. *Progress in inorganic chemistry*, 47, p. 371–510, 1998.
45. Song, H.-H., *et al.*, Zinc Diphosphonates Templated by Organic Amines: Syntheses and Characterizations of $[\text{NH}_3(\text{CH}_2)_2\text{NH}_3]\text{Zn}(\text{hedpH}_2)_2 \cdot 2\text{H}_2\text{O}$ and $[\text{NH}_3(\text{CH}_2)_n\text{NH}_3]\text{Zn}_2(\text{hedpH})_2 \cdot 2\text{H}_2\text{O}$ ($n = 4, 5, 6$) (hedp = 1-Hydroxyethylidenediphosphonate). *Inorganic Chemistry*, 40(19), p. 5024–5029, 2001.
46. Rodgers, J.A. and Harrison, W.T.A. Ethylenediamine zinc hydrogen phosphite, $[\text{H}_2\text{N}(\text{CH}_2)_2\text{NH}_2]0.5 [\text{middle dot}]\text{ZnHPO}_3$, containing two independent, interpenetrating, mixed inorganic/organic networks. *Chemical Communications*, 2000(23), p. 2385–2386.
47. Shiv Halasyamani, P., Drewitt, M. J. and O'Hare, D. Hydro(solvo) thermal synthesis and structure of a three-dimensional zinc fluorophosphate: $\text{Zn}_2(4,4[\text{prime or minute}]\text{-bipy})(\text{PO}_3\text{F})_2$. *Chemical Communications*, 1997(9), p. 867–868.
48. Poojary, D.M., *et al.*, Synthesis and X-ray Powder Structures of Covalently Pillared Lamellar Zinc Bis(phosphonates). *Inorganic Chemistry*, 35(18), p. 5254–5263, 1996.

49. Zhang, B., Poojary, D.M. and Clearfield, A. Synthesis and Characterization of Layered Zinc Biphenylenebis(phosphonate) and Three Mixed-Component Arylenebis(phosphonate)/Phosphates. *Inorganic Chemistry*, 37(8), p. 1844–1852, 1998.
50. Poojary, D.M., Zhang, B. and Clearfield, A. Pillared Layered Metal Phosphonates. Syntheses and X-ray Powder Structures of Copper and Zinc Alkylenebis(phosphonates). *Journal of the American Chemical Society*, 119(51), p. 12550–12559, 1997.
51. Erxleben, A., Structures and properties of Zn(II) coordination polymers. *Coordination Chemistry Reviews*, 246(1–2), p. 203–228, 2003.
52. Katsenis, A.D., *et al.*, Initial use of 1-hydroxybenzotriazole in the chemistry of group 12 metals: An 1D zinc(II) coordination polymer and a mononuclear cadmium(II) complex containing the deprotonated ligand in a novel monodentate ligation mode. *Inorganic Chemistry Communications*, 12(2), p. 92–96, 2009.
53. Gkioni, C., Psycharis, V. and Raptopoulou, C.P. Investigation of the zinc(II) acetylacetonate/benzotriazole reaction system in the presence of bridging N,N'-ligands: Pentanuclear, enneanuclear and polymeric complexes. *Polyhedron*, 28(16), p. 3425–3430, 2009.
54. Morsali, A. and Kempe, R. A Novel One-Dimensional Coordination Polymer Involving Weak Hg-Hg Interactions. *Helvetica Chimica Acta*, 88(8), p. 2267–2271, 2005.
55. Morsali, A. and Mahjoub, A.R. Structural influence of counterions in lead(II) complexes: $[\text{Pb}(\text{phen})_n(\text{NO}_2)_X]$, $X = \text{CH}_3\text{COO}^-$, NCS^- and, phen = 1,10-phenanthroline. *Solid State Sciences*, 7(11), p. 1429–1437, 2005.
56. Sadeghzadeh, H., *et al.*, Sonochemical syntheses of strawberry-like nano-structure mixed-ligand lead(II) coordination polymer: Thermal, structural and X-ray powder diffraction studies. *Inorganica Chimica Acta*, 363(5), p. 841–845, 2010.
57. Aboutorabi, L. and Morsali, A. Sonochemical synthesis of a new nano-plate lead(II) coordination polymer constructed of maleic acid. *Acta Inorganica Chimica*, 363(11), p. 2506–2511, 2010.
58. Diring, S., *et al.*, Controlled Multiscale Synthesis of Porous Coordination Polymer in Nano/Micro Regimes. *Chemistry of Materials*, 22(16), p. 4531–4538, 2010.
59. Ranjbar, Z.R. and Morsali, A. Sonochemical syntheses of a new nano-sized porous lead (II) coordination polymer as precursor for preparation of lead (II) oxide nanoparticles. *Journal of Molecular Structure*, 936(1), p. 206–212, 2009.

60. Sadeghzadeh, H. and Morsali, A. Hedge balls nano-structure of a mixed-ligand lead(II) coordination polymer; thermal, structural and X-ray powder diffraction studies. *CrystEngComm.*, 12(2), p. 370–372, 2010.
61. Khanpour, M., Morsali, A. and Retailleau, P. Sonochemical syntheses of a straw-like nano-structure two-dimensional mixed-ligand zinc(II) coordination polymer as precursor for preparation of nano-sized ZnO. *Polyhedron*, 29(5), p. 1520–1524, 2010.
62. Ranjbar, Z.R. and Morsali, A. Sonochemical synthesis of a novel nano-rod two-dimensional zinc (II) coordination polymer; preparation of zinc (II) oxide nanoparticles by direct thermolyses. *Ultrasonics sonochemistry*, 18(2), p. 644–651, 2011.
63. Ranjbar, Z.R., Morsali, A. and Retailleau, P. Thermolysis preparation of zinc(II) oxide nanoparticles from a new micro-rods one-dimensional zinc(II) coordination polymer synthesized by ultrasonic method. *Inorganica Chimica Acta*, 376(1), p. 486–491, 2011.

4

Cadmium(II) Coordination Polymers

4.1 Introduction to Cadmium(II) Coordination Polymers

Cd^{2+} , as a d^{10} metal ion, is particularly suited for the construction of supramolecular compounds and networks. The spherical d^{10} configuration is associated with a flexible coordination environment, so that geometries of these complexes can vary from tetrahedral ($\text{CN} = 4$) to dodecahedral ($\text{CN} = 8$) and severe distortions in the ideal polyhedron easily occur. Furthermore, due to the general lability of Cd(II) complexes, the formation of coordination bonds is reversible, which enables metal ions and ligands to rearrange during the process of polymerization to give highly ordered network structures. Consequently, Cd can readily accommodate all kind of architectures and a selection of topological types of 1D, 2D and 3D polymers is given [1–10]. Thus, their preparation is challenging owing to their ability to tailor their physical and chemical properties [11].

4.1.1 One-Dimensional Coordination Polymers

However, there is an unfavorable investigation on the MOFs containing flexible bridging carboxylate ligands [12–16]. Compared with the rigid ligands, the skew and versatile coordination orientation of the flexible bridging ligands is favorable for constructing novel structures [17–20]. Disulfide bridging phenyl carboxylate ligands possess flexibility owing to the presence of –S–S– spacers between the phenyl rings and can adopt various conformations according to geometric requirements when they react with different metal salts, the flexible and multifunctional coordination sites provide a high likelihood for build novel coordination frameworks with high dimensions. Whereas, there have been few reports of studies on flexible disulfide derivatives of carboxylates [21–25]. Considering the points mentioned above, to further explore the coordination characteristics of flexible disulfide bridging aromatic dicarboxylate ligand, here chose 2,2-dithiobisbenzoic acid (H_2dtbb) as primary ligand to construct Cd(II) photoluminescent coordination polymers by taking advantage of its multicarboxylate bridging coordination ability together with the flexibility of its C–S–S–C bonds, incorporating the auxiliary ligands. Herein, report the syntheses, crystal structures and photoluminescent properties of four Cd(II) complexes with these ligands: $[Cd(Hdtbb)(dtbb)_{0.5}(DMF)]_n$ (1), $\{[Cd(dtbb)(2,2'-bpy)(H_2O)].2DMA\}_n$ (2) [$dtbb$: 2,2'-dithiobis(benzoato)]. The crystallographic analysis reveals that 1 is a one dimensional chain coordination polymer. Complex 1 crystallizes in the monoclinic system, C2/c space group. The asymmetric unit of 1 contains one crystallographically nonequivalent Cd (II) ion (Cd1), one $Hdtbb^-$ ligand, half $dtbb^{2-}$ ligand and one DMF molecule. Cd1 is six-coordinated by three oxygen atoms from two carboxylic groups of two $dtbb^{2-}$ ligands, two oxygen atoms from two carboxylic groups of two $Hdtbb^-$ ligands and one oxygen atom from DMF molecule, exhibiting the distorted octahedral geometry. X-ray crystallographic analysis reveals that 2 crystallizes in a monoclinic space group P21/c and there are one Cd(II) ion (Cd1), one $dtbb^{2-}$ ligand, one 2,2'-bpy ligand, one H_2O molecule and two free DMA molecules

in the asymmetric unit. The Cd(II) ion is seven-coordinated by four oxygen atoms from two carboxylic groups of two different dtbb²⁻ ligands, two nitrogen atoms from one 2,2'-bpy molecule and one O atom from water molecule in a pentagonal bipyramidal geometry. The solid-state emission spectra of the free H₂dtba ligand and complexes 1, 2 were measured at room temperature. The main emission peak of H₂dtbb is at 465 nm ($\lambda_{\text{exc}} = 389$ nm), which may be attributed to $\pi \rightarrow \pi^*$ transition. The compounds 1, 2 show emissions at about 455 nm ($\lambda_{\text{exc}} = 396$ nm) and 468 nm ($\lambda_{\text{exc}} = 395$ nm), respectively. It should be pointed out that the emissions of compounds 1, 2 are neither metal-to-ligand charge transfer (MLCT) nor ligand-to metal charge transfer (LMCT) in nature since the Cd²⁺ ions are difficult to oxidize or to reduce due to their d¹⁰ configuration, which are mainly based on the luminescence of ligands. They can probably be assigned to the intraligand $\pi \rightarrow \pi^*$ transitions of dtbb²⁻ ligand. Different intensity emission bands of 1, 2 are probably due to the variation of the metal ions and the coordination environment around them because the photoluminescence behavior is closely associated with the metal ions and the ligands coordinated around them [26–28].

Anion influence in the structural diversity of 1D cadmium coordination polymers constructed from a pyridine based Schiff base ligand has been reported by Khandar *et al.* [29]. Among the effective factors to design CPs counterions have been paid particular attention in the past few years, since they not only show a co-ligand effect, but also can direct and/ or template the formation of assemblies, thus leading to structural diversity [30, 31]. Furthermore, some counterions such as carboxylate, nitrate, azide and thiocyanate have various coordination modes and can act as a monodentate, chelate, or bridging ligands within the framework, which may further enrich the structural diversity. Moreover the geometries of organic ligands can have a great impact on the structural architecture of coordination polymers [32]; therefore much effort has been devoted to the design and modification of the organic ligands to control the products. Herein has been described self-assembly of the potentially tetradentate chelating bridging ligand (2-pyridinecarbaldehyde

isonicotinoyl hydrazone) with divalent cadmium(II) salts as the nodes. The ligand which have prepared to design and construction of CPs has potential to form different types of complexes due to the multiple coordination sites and the tautomeric effect of enol and keto form. A series of seven coordination polymers based on Cd and potentially tetradentate pyridine based Schiff base ligand with different anions (CH_3COO^- , NO_2^- , Cl^- , I^-) [$\text{Cd}(\text{L})(\text{CH}_3\text{COO})(\text{OH}_2)]_n$ (**1**), $\{[\text{Cd}_2(\text{L})_2(\text{NO}_2)_2(\text{CH}_3\text{OH})_2] \cdot \text{CH}_3\text{OH}\}_n$ (**2**), $\{[\text{Cd}_2(\text{L})_2\text{Cl}_2(\text{CH}_3\text{OH})_2] \cdot \text{CH}_3\text{OH}\}_n$ (**3**) and $[\text{Cd}(\text{HL})\text{I}_2]_n$ (**4**) {HL = 2-pyridinecarbaldehyde isonicotinoyl hydrazone (HPCIH)} in order to rationalize the effect of the anion, have been synthesized and characterized by elemental analyses, FT-IR spectroscopy, single crystal X-ray data diffraction, etc. The results show the influence of the counter ions on the coordination mode of the cadmium ion that is capable of forming compounds with five-, six- and seven- coordination numbers. The ligand acts as a negatively charged tetradentate N_3O -donor ligand and coordinates to the cadmium center in the enolic form ($=\text{N}-\text{N}=\text{C}=\text{O}$) in **1-3** while in compound **4** coordinates as N_3 - donor neutral ligand in keto form ($=\text{N}-\text{NH}-\text{C}=\text{O}$). There are some major similarities between structures of **1-4**. For instance all of them crystallize in monoclinic system and consist of $\text{P2}(1)/c$ space group [$\text{P2}(1)/n$, for **1**] except **4** that crystallized in Pc . In all of the compounds the ligand HL acts as N_3O -donor except in **4** as N_3 -donor chelating-bridging agent, leading to formation of coordination polymers. In all compounds one of the coordination positions of Cd(II) centers is occupied by the *Para*-N of pyridyl group of the adjacent molecule and three other positions are occupied by the *Ortho*-N of pyridyl group, imine nitrogen and oxygen of Schiff base ligand. In the case of **4** the oxygen atom of the ligand doesn't participate in coordination. The individual 1D polymeric chains in **1-4** are almost parallel to each other and linked by weak hydrogen bonding. There are also aromatic π - π stacking interactions between parallel pyridyl rings of the adjacent chains in these compounds except in **4**. In compounds **1-4** the hydrogen bonding and π - π stacking interactions between adjacent chains grow 1D chains into the 3D networks. The 1D to 3D interpenetration of **1** is illustrated in Figure 4.1 as an example.

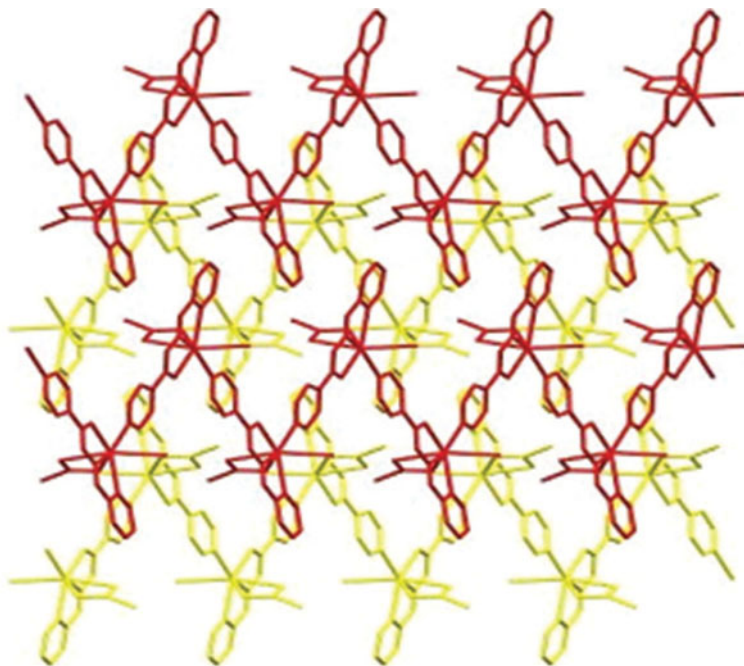


Figure 4.1 The 1D to 3D Chains interpenetration and a view of 3D network in **1**.

4.1.2 Two-Dimensional Coordination Polymers

Recent years, a series of multi-dentate N-containing ligands, especially the bridging ligands with bis-imidazole [33–37], bis-triazole [38–42] and bis-tetrazol [43–48] groups have been widely employed to construct coordination polymers with fascinating architectures and interesting properties. However, the semi-rigid N-donor ligands with different N-containing groups have rarely been investigated [49, 50], and they may be excellent candidates to construct novel structures such as helical, interpenetrating frameworks. 5-(4-((1H-1,2,4-triazol-1-yl)methyl)phenyl)-1H-tetrazole (HL), as a semi-rigid multi-dentated ligand, has the following characteristics: The ligand HL possesses multiple potential coordinate sites involving four tetrazole N atoms and two triazole N atoms. It is therefore likely that some of the N atoms

will remain uncoordinated to the metal centers in the prospective coordination solids. Such unbounded N donors provide two potentially interesting avenues for exploring functional coordination networks. (i) they could H-bond with the available H-bond donors and create composite networks built on both H-bond and coordination bonds. (ii) these unbounded N donors could remain free-standing, and, when installed in a porous framework, could provide for effective binding to metal guests (e.g., to take up metal ions into the channels).” In addition, Cd(II)-containing coordination polymers have attracted extensive interests due to the amiability to bond with different donors simultaneously, the large radius, various coordination modes and potential applications in catalysis, fluorescent materials, NLO materials and so on. Inspired by the above consideration, synthesize CPs with novel structures and special properties through combining respective merits of HL ligand and Cd(II) ion have been done. As expected, successfully obtained three new 2D and 3D coordination polymers, formulated as $[\text{Cd}(\text{L})_2(\text{H}_2\text{O})_2]_n$ (1), $[\text{Cd}_3(\text{L})_2(\mu_3\text{-OH})_2(\mu_2\text{-Cl})_2(\text{H}_2\text{O})_2]_n$ (2), $\{[\text{Cd}_2(\text{L})_2(\text{nic})_2(\text{H}_2\text{O})_2] \cdot \text{H}_2\text{O}\}_n$ (3) (Hnic= nicotinic acid). Furthermore, the luminescence properties of 1–3 were studied in the solid state at room temperature.

A single-crystal X-ray diffraction study reveals that complex 1 crystallizes in the monoclinic space group P21/n and features a two-dimensional (2D) layer-like structure with helices. The asymmetric unit of 1 contains one six-coordinated Cd(II) atom, one L ligand and one coordination water molecule. Each Cd(II) atom is coordinated in a distorted octahedral geometry. Complex 2 crystallizes in the triclinic space group $P\bar{1}$ and displays a 2D framework with the asymmetric unit of $[\text{Cd}_2(\text{L})(\mu_3\text{-OH})(\mu_2\text{-Cl})(\text{H}_2\text{O})]$. The two crystallographically independent Cd(II) atoms exhibit similar coordination environments. The Cd1 adopts a lightly distorted octahedral coordinated geometry and is surrounded by two N atoms (N6, N6A) of two separated L[−] ligands, two $\mu_3\text{-O}$ atoms (O1, O1A) and two $\mu_2\text{-Cl}$ atoms (Cl1, Cl1A). When the auxiliary ligand nicotinic acid (Hnic) was introduced into the assembled system, a distinct 3D network was produced. Complex 3 crystallizes in the monoclinic space group P21/n and

the asymmetric unit consists of one crystallographically independent Cd(II) atom, one L^- ligand, one nic^- anion, one coordination water molecule and one lattice water molecule. Each Cd(II) atom is six-coordinated, displaying as lightly distorted octahedral coordinated geometry formed by four N atoms from three different L^- ligands and one nic^- ligand, and two O atoms from one nic^- ligand and one terminal water molecule [51].

Recently, focused on the construction of CPs based on the mixed multicarboxylates and flexible N-containing ligands [52]. Flexible N-containing ligands are often used as bridging ligands to produce diverse CPs due to their different conformations [53]. On the other hand, the multicarboxylates can be employed as ancillary ligands because of their versatile coordination modes, high structural stability and the ability to balance the positive charges [54]. The combination of these O-donor and N-donor ligands with metal ions has greatly contributed to the structural and topological diversity of CPs. And it is found that the structure of a coordination polymer can be greatly affected by the choice of carboxylate. So, in order to extend this part and explore the influence of the skeletons of dicarboxylate ligands on the structures, has been chosen flexible 1,4-bis(2-methylimidazol-1-ylmethyl)-2,3,5,6-tetramethylbenzene (bmimx) as bridging ligand, five dicarboxylate ligands, namely, 1,2-benzenedicarboxylic acid (1,2- H_2BDC), homophthalic acid (H_2HMPH), 1,3-benzenedicarboxylic acid (1,3- H_2BDC), 1,3-adamantanediactic acid (1,3- H_2ADA) and adipic acid (H_2ADI) are employed as ancillary ligands and five new complexes, $[Cd(bmimx)_{0.5}(1,2-BDC)]_n$ (1), $\{[Cd(bmimx)(HMPH)].H_2O\}_n$ (2), $\{[Cd(bmimx)(1,3-BDC)].1.5H_2O\}_n$ (3), $\{[Cd(bmimx)_{0.5}(ADA)].H_2O\}_n$ (4) and $\{[Cd(bmimx)(ADI)].2H_2O\}_n$ (5) are obtained under hydro(solvo)thermal conditions.

Although complexes 1–5 display 2D layer structures, the topologies of their networks show notable structural disparities because of the different dicarboxylate ligands used. Generally, the role of dicarboxylate ligands can be explained in terms of their differences in the positions of the carboxylate groups, the flexible abilities and the spacer groups of the carboxylate anions. Complexes 1 and 2 imply

the influence of the flexibility of the carboxylate ligands on the resulting frameworks. Although the two carboxylate groups of 1,2- H_2BDC and H_2HMPH are located in the 1,2-positions of benzene ring, 1,2- H_2BDC is a rigid ligand, while one carboxylate group of H_2HMPH possesses flexibility owing to the presence of the $-\text{CH}_2-$ spacer, which allows the carboxylate group to bridge the metal ions from different directions. As a result, complex 1 exhibits a binodal (3,4)-connected layer with $3,4\text{L}8^3$ topology, while complex 2 shows a 44-sql layer with left- and right-handed helical chains. Complexes 1 and 3 show the effects of carboxylate positions on the structures of their complexes. Although both 1,2- H_2BDC and 1,3- H_2BDC act as dicarboxylate anions with the rigid benzene ring spacers, the two carboxylate groups of 1,2- H_2BDC are located in the 1,2-positions of benzene ring, whereas those of 1,3- H_2BDC are in the 1,3-positions. Consequently, complex 1 presents a binodal (3,4)-connected layer with $3,4\text{L}8^3$ topology, whereas 3 shows a pleated net with the 44-sql topology. Obviously, the position discrimination of the carboxylate ligand leads to the structural difference of 1 and 3. Comparing 2 and 3, it has been found that both 2 and 3 are 2D 44-sql networks. But left- and right-handed helical chains are present in the structure of 2. This is because of the flexibility of H_2HMPH . Complexes 4 and 5 show the effects of the carboxylate spacers. 1,3- H_2ADA and H_2ADI are both flexible ligands, however, the former is based on bulky adamantane spacer, and the latter is based on the $-\text{CH}_2-$ spacer. Thus, the employment of 1,3- H_2ADA gives a binodal (3,4)-connected layer with $3,4\text{L}8^3$ topology, while the use of H_2ADI provides a 3-connected hcb topology.

Luminescent properties of compounds containing d^{10} metal centers are of intense interest due to their potential applications, such as in chemical sensors, photochemistry and electroluminescent display, and so on [14]. Hence, the solid-state luminescent properties of the free ligands bmimx, 1,2- H_2BDC , H_2HMPH , 1,3- H_2BDC together with complexes 1–5 (Figure 4.2) have been determined at room temperature. The main emission peaks of the bmimx, 1,2- H_2BDC , H_2HMPH and 1,3- H_2BDC were observed at 305 nm ($k_{\text{ex}} = 272$ nm), 342 nm ($k_{\text{ex}} = 307$ nm), 440 nm ($k_{\text{ex}} = 374$ nm), 356 nm ($k_{\text{ex}} = 310$ nm), which can be assigned to the $n \rightarrow \pi^*$ or $\pi \rightarrow \pi^*$

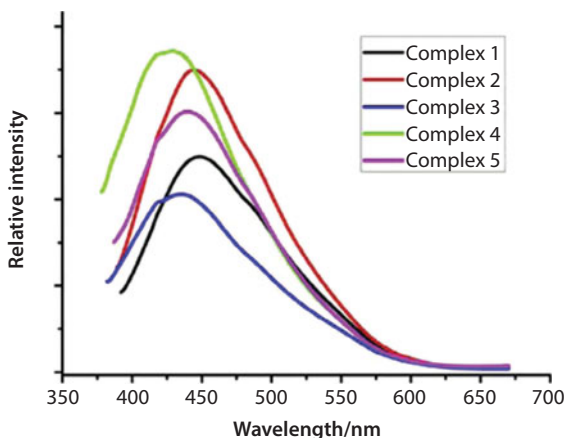


Figure 4.2 Solid-state emission spectra of complexes 1–5 at room temperature [58].

transitions. Complexes 1 and 3 show emission bands with the maximum peak at 449 nm ($k_{\text{ex}} = 374$ nm) and 435 nm ($k_{\text{ex}} = 366$ nm), respectively. Notably, the large redshifts occur in complexes 1 and 3 in contrast with free 1,2- H_2BDC and 1,3- H_2BDC , suggesting that the ligand-to-metal charge transfer makes a major contribution to the photoluminescences of 1 and 3 [55]. Complex 2 exhibits an emission at 445 nm ($k_{\text{ex}} = 374$ nm), which is similar to that of the free H_2HMPH ligand. Therefore, the emission band of the complex 2 can be mainly attributed to the intraligand (H_2HMPH) emission. Complexes 4 and 5 exhibit emission peaks at 429 nm ($k_{\text{ex}} = 363$ nm) and 440 nm ($k_{\text{ex}} = 368$ nm), respectively. Because the solid 1,3- H_2ADA [56] and H_2ADI [57] ligands do not possess any luminescence at room temperature, such significant red-shifts in 4 and 5 as compared with the ligand *bmimx* may be tentatively assigned to ligand-to-metal charge transfer [58].

4.1.3 Three-Dimensional Coordination Polymers

A new 3D metal–organic coordination polymer $[\text{Cd}(\text{H}_3\text{BPTC})_2(\text{bpy})]_n$ (1) (H_4BPTC = 1,1'-biphenyl- 2,2',6,6'-tetracarboxylic acid, *bpy* = 4,4'-bipyridine) has been synthesized

and characterized by single X-ray diffraction and IR spectroscopy. The one-dimensional metal-organic chains of the title complex, namely $[\text{Cd}(\text{H}_3\text{BPTC})_2]_n$, are held together through hydrogen bonding and bridging “second” ligand 4,4'-bpy to give a three-dimensional metal-organic network. In each unit, there are one Cd(II) center ion, two H_3BPTC^- anions, and one bridging bpy molecule. Cd1 displays an axisymmetrical N_2O_4 octahedral geometry, and the related bond distances and bond angles are all symmetrically equivalent. Two N(1) atoms from two different bpy ligands and two carboxylate O(8) atoms of two H_3BPTC^- anions comprise the equatorial plane [59]. It is worth noting that each Cd(II) ion is coordinated by four different H_3BPTC^- ligands, and each H_3BPTC^- anion acts as bis-monodentate ligand to ligate two Cd(II) ions along the *c* axis into an infinite polymeric chain $[\text{Cd}(\text{H}_3\text{BPTC})_2]_n$, in which the strong O–H \cdots O interactions between the carboxylate O atoms of H_3BPTC^- anions make the chain more stable. At the same time, neighboring parallel chains are connected via the third hydrogen bond interaction along the *a* axis. However, the peculiar structural feature of complex **1** is that each $[\text{Cd}(\text{H}_3\text{BPTC})_2]_n$ chain is connected to four adjacent parallel chains through the second bridging 4,4'-bpy (bpy) ligands along four different directions to form a 3D metal-organic network (Figure 4.3).

However, flexible bis(pyridine) ligands based upon the open-chain polyether $-\text{O}-\text{CH}_2-\text{CH}_2-\text{O}-$ group received relatively less attentions [60]. On the other hand, the construction of porous MOFs based on flexible open-chain polyether-bridged ligands is challenging, owing to an unavoidably large amount of framework interpenetration. The introduction of rigid organic ligand might be a useful approach to effectively reduce the MOFs interpenetration. Taking the above into consideration, here reported a $-\text{O}-\text{CH}_2-\text{CH}_2-\text{O}-$ bridging ligand 1,2-bis[4-(pyridin-3-yl)phenoxy]ethane (L) to construct coordination frameworks in the presence of a rigid 1,4-benzenedicarboxylic acid (H_2BDC) co-ligand. Two new Cd(II)-coordination polymers, namely $\{[\text{Cd}(\text{L})(\text{BDC})].(\text{EtOH}).(\text{DMF})\}_n$ (**1**) and $\{[\text{Cd}_{1.5}(\text{L})_2(\text{BDC})_{1.5}].0.5(\text{MeOH}).0.5(\text{H}_2\text{O})\}_n$ (**2**) (H_2BDC = 1,4 benzenedicarboxylic acid, DMF = N,N-dimethylformamide)

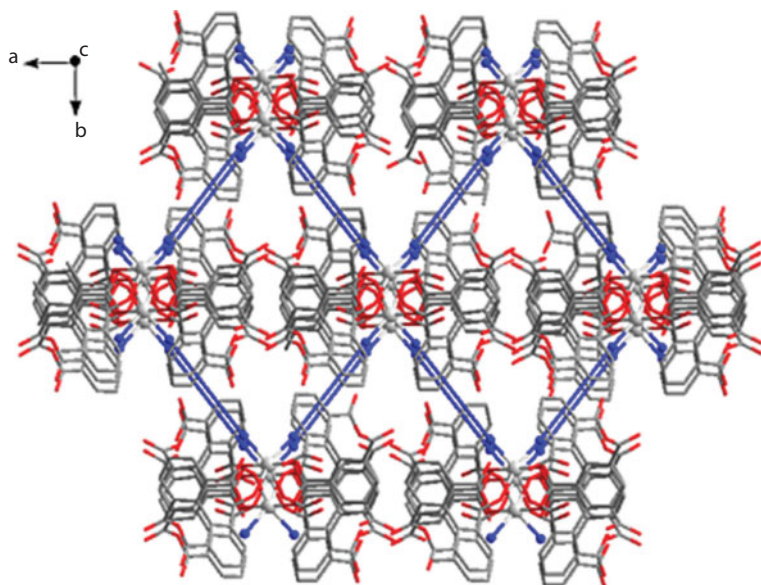


Figure 4.3 The 3D supramolecular structure of **1**: the bridging “second” ligand 4,4'-bpy is highlighted as blue line [59].

have been synthesized, and were characterized by single-crystal X-ray analyses, IR spectra and element analyses.

Single crystal X-ray analysis reveals that complex **1** crystallizes in the triclinic system with $\overline{P}1$ space group, and exhibits a three dimensional network. There are one Cd(II), two half-molecule of the L and BDC ligands, one DMF and one ethanol in the asymmetric unit. Each Cd(II) atom displays a distorted octahedral coordination geometry, which is completed by four O atoms from three BDC ligands and two N atoms from two L ligands. To further understand the structure of **1**, the topological analysis was carried out. In **1**, each $\text{Cd}_2(\text{CO}_2)_2$ cluster is linked by four BDC ligands and two pairs of L ligands, so it could be considered as 6-connected node. Meanwhile, each BDC and L ligands could be regarded as 2-connected linkers. When the reaction was conducted under hydrothermal condition, a new 3D coordination polymer $\{[\text{Cd}_{1.5}(\text{L})_2(\text{BDC})_{1.5}]\cdot 0.5(\text{CH}_3\text{OH})\cdot 0.5(\text{H}_2\text{O})\}_n$ was obtained. Single-crystal X-ray analysis indicates that complex **2** crystallizes in the triclinic space group $\overline{P}1$. There are one and half a Cd(II) atoms, two

L ligands, one and half a BDC ligands, half lattice H_2O molecule and half methanol in the asymmetric unit. The crystallographically independent Cd1 and Cd2 atoms display different coordination conditions. The Cd1 atom displays distorted octahedral coordination geometry, coordinated by four O atoms from three carboxylate groups and two N atoms from two L ligands [61].

4.2 Nano Cadmium(II) Coordination Polymers

The crystalline material $\{[\text{Cd}(\text{bpa})(4,4'\text{-bipy})_2(\text{H}_2\text{O})_2](\text{ClO}_4)_2\}_n$ was obtained from the reaction between cadmium(II) acetate and sodium perchlorate with a mixture of bpa and 4,4'-bipy. Determination of the structure of compound 1 by X-ray crystallography has shown that the polymer in the solid state consists of one-dimensional chains. The cadmium atoms are linked by two nitrogen atoms of the bpa ligands, two nitrogen atoms of 4,4'-bipy ligands and two oxygen atoms of water molecules (Figure 4.4). Compound $\{[\text{Cd}(\text{bpa})(4,4'\text{-bipy})_2(\text{H}_2\text{O})_2](\text{ClO}_4)_2\}_n$ could be considered as a six-coordinated moiety with a N_4O_2 donor atom array. The coordination around Cd is octahedral and the two coordinated bpa ligands, as well as 4,4'-bipy and waters molecules, are located in trans positions. So, the cadmium ion lies on an inversion center. The aromatic rings of the coordinated bpa are coplanar. There are face-to-face π - π stacking interactions between every set of aromatic rings of the 4,4'-bipy ligands with the pyridine rings of 4,4'-bipy ligands in neighboring chains.

Compound $\{[\text{Cd}(\text{bpa})(4,4'\text{-bipy})_2(\text{H}_2\text{O})_2](\text{ClO}_4)_2\}_n$ has been synthesized in the nanocrystalline form by the addition of reagents in ultrasonic baths with different powers (138W and 305 W). The morphology, structure and size of the nanostructure of compound $\{[\text{Cd}(\text{bpa})(4,4'\text{-bipy})_2(\text{H}_2\text{O})_2](\text{ClO}_4)_2\}_n$ under different powers (138 W and 305 W) of ultrasound irradiation were investigated by Scanning Electron Microscopy (Figure 4. 5a and b). These images show that a smaller size of compound is obtained with the higher ultrasound power [62].

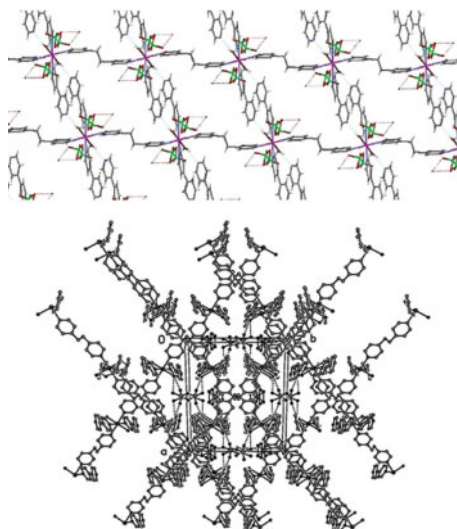


Figure 4.4 (up) The two-dimensional sheet and (down) the three-dimensional network of compound $\{[\text{Cd}(\text{bpa})(4,4'\text{-bipy})_2(\text{H}_2\text{O})_2](\text{ClO}_4)_2\}_n$.

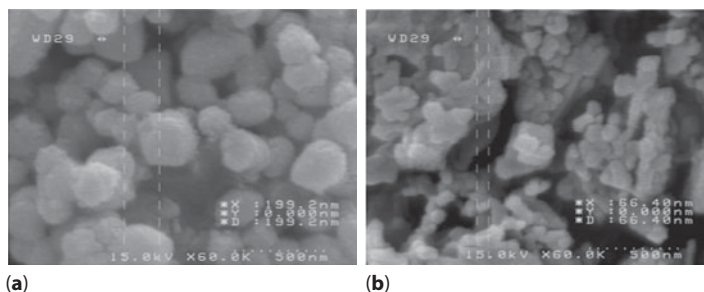


Figure 4.5 SEM images of compound $\{[\text{Cd}(\text{bpa})(4,4'\text{-bipy})_2(\text{H}_2\text{O})_2](\text{ClO}_4)_2\}_n$ nano-structure with two different powers of ultrasound irradiation, (a) 0.138 kW and (b) 305 W.

In other work has been reported on synthesis of two nano Cd(II) complexes with (4,4-di-tert-bu-bipy) and (4,4'-dmbpy) ligands $[\text{Cd}(4,4\text{-di-tert-bubipy})\text{Cl}_2(\text{DMSO})]$ (1) and $[\text{CdI}_2(4,4'\text{-dmbpy})(\text{DMSO})]$ (2). In addition the nano-structures of supramolecular complexes have been synthesized nano-sized compounds 1 and 2, were obtained by ultrasonic irradiation in a MeOH solution.

Reaction of ligands (4,4'-di-tert-butyl-2,2'-bipyridine) with CdCl_2 and (4,4'-di-methyl-2,2'-bipyridine) with CdI_2 led to the formation of two Cd(II) complexes $[\text{Cd}(4,4\text{-di-tert-bu-bipy})\text{Cl}_2(\text{DMSO})]$ (1) and $[\text{CdI}_2(4,4'\text{-dmbpy})(\text{DMSO})]$ (2). The unit cell of compound 1 and 2 has been shown in Figure 4.6.

SEM photograph shows a broad distribution of the particle size, the average size of the particles in compounds 1 and 2, are 35 nm, as shown in Figure 4.7 [63].

Reaction of 1H-1,2,4-triazole-3-carboxylate (L^-) with cadmium(II) chloride leads to formation of a 3D supramolecular $[\text{Cd}(\text{L})_2(\text{H}_2\text{O})_2]$. Nanoparticles of compound were obtained in

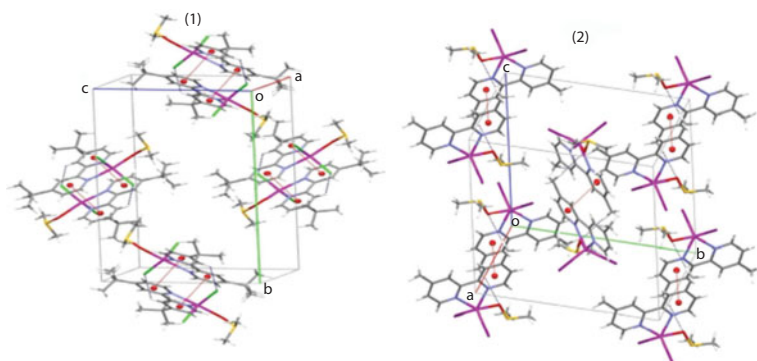


Figure 4.6 The unit cell of $[\text{Cd}(4,4\text{-di-tert-bu-bipy})\text{Cl}_2(\text{DMSO})]$ (1) and $[\text{CdI}_2(4,4'\text{-dmbpy})(\text{DMSO})]$ (2).

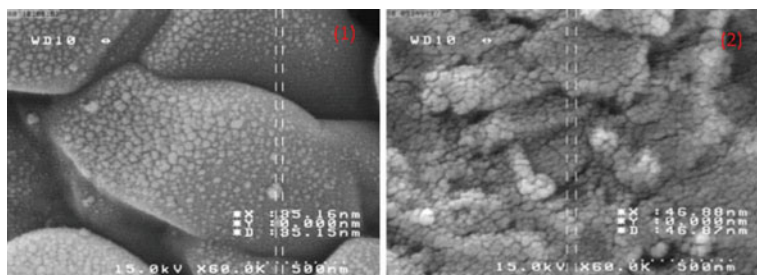


Figure 4.7 SEM photograph of compounds 1 and 2 nano-particles produced by sonochemical method.

aqueous solution by ultrasonic irradiation, while single crystals of compound $[\text{Cd}(\text{L})_2(\text{H}_2\text{O})_2]$ were obtained using a heat gradient applied to an aqueous solution of the reagents (the “branched tube method”). Figure 4.8 gives an overview of the methods used for the synthesis of $[\text{Cd}(\text{L})_2(\text{H}_2\text{O})_2]$ using the two different routes.

The structure of compound $[\text{Cd}(\text{L})_2(\text{H}_2\text{O})_2]$ has been reported by J. Zhu *et al.* [64]. The complex in the solid state is a 3D supramolecular framework that consists of one Cd(II) ion, two de-protonated L^- and two terminal coordinated water molecule. A view of the coordination environment around the cadmium(II) ion and packing of compound $[\text{Cd}(\text{L})_2(\text{H}_2\text{O})_2]$ is shown in Figure 4.9.

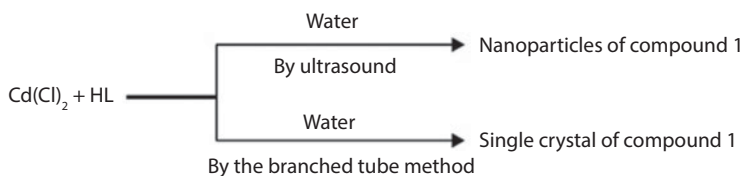


Figure 4.8 Materials produced and synthetic methods.

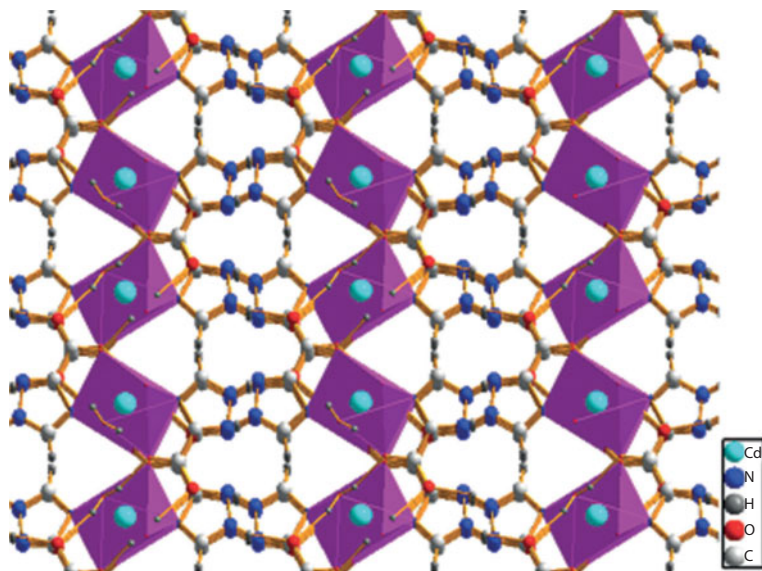


Figure 4.9 A fragment of the 3D framework in compound $[\text{Cd}(\text{L})_2(\text{H}_2\text{O})_2]$, viewed along c direction.

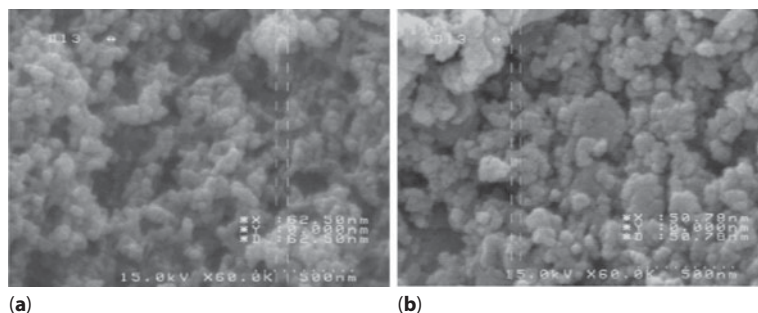


Figure 4.10 SEM photograph of compound $[\text{Cd}(\text{L})_2(\text{H}_2\text{O})_2]$ nanoparticles prepared in concentration of initial reagents (a) $[\text{Cd}^{2+}] = [\text{L}^-] = 0.01 \text{ M}$ and (b) $[\text{Cd}^{2+}] = [\text{L}^-] = 0.05 \text{ M}$.

The morphology and size of compound $[\text{Cd}(\text{L})_2(\text{H}_2\text{O})_2]$ prepared by the sonochemical method was characterized by scanning electron microscopy (SEM) and shows that it is composed of particles with sizes of about 62 nm. Figure 2.30 shows the scanning electron microscopy (SEM). Appropriate nano-sized particles of compound $[\text{Cd}(\text{L})_2(\text{H}_2\text{O})_2]$ were obtained at both concentrations of 0.01 and 0.05 M (Figures 4.10 a and b). Particle sizes of the nanoparticles depend on the concentration of initial reagents. In order to investigate the role of concentration of initial reagents on the nature of products, reactions were performed with two different concentrations. Comparison between the samples with different concentrations shows that high concentration of initial reagents increases particles size. Thus, particles sizes produced using lower concentrations of initial reagents (0.01 M, Figure 4.10a) are smaller than particles size produced using higher concentration (0.05 M, Figure 4.10b) [65].

4.3 Conclusion

The structural diversity indicates that the different conformations of ligand and various coordination modes of second ligand significantly affect the topological structures of the reported coordination polymers. Moreover, the luminescent behaviors were closely associated with the diverse structures. Consequently, Cd

can readily accommodate all kind of architectures and a selection of topological types of 1D, 2D and 3D polymers is given. Thus, their preparation is challenging owing to their ability to tailor their physical and chemical properties.

References

1. Suen, M.-C. and Wang, J.-C. Synthesis and structural characterization of three new cadmium(II) coordination polymers containing thiocyanato and pyridyl ligands. *Journal of Coordination Chemistry*, 60(3), p. 257–268, 2007.
2. Payehghadr, M. and Moasali, A. Thermolysis preparation of cadmium(II) oxide nanoparticles from a new three-dimensional cadmium(II) supramolecular compound. *Journal of Structural Chemistry*, 54(4), p. 787–791, 2013.
3. Notash, B. Safari, N. Abedi, A. Amani, V. Khavasi, H. Reza, Cadmium(II) complexes containing 2,2'-dimethyl-4,4' -bithiazole ligand: synthesis, characterization, and crystal structure. *Journal of Coordination Chemistry*, 62, p. 1638–1649, 2009.
4. Banerjee, S., Drew, M.G.B. and Ghosh, A. Construction of coordination polymers of cadmium(II) with mixed hexamethylenetetramine and terephthalate or thiocyanate ligands. *Polyhedron*, 22(21), p. 2933–2941, 2003.
5. Blake, K.M., *et al.*, Effect of pendant arm length and nitrogen donor disposition on the topology of luminescent cadmium phenylenedicarboxylate coordination polymers with bis(pyridylmethyl)piperazine co-ligands. *Inorganica Chimica Acta*, 363(1), p. 88–96, 2010.
6. Shyu, E., *et al.*, Control of topology and dimensionality by aromatic dicarboxylate pendant arm position and length in cadmium coordination polymers incorporating a hydrogen-bonding capable kinked dipyridine ligand. *Inorganica Chimica Acta*, 362(7), p. 2283–2292, 2009.
7. Xia, S.-Q., *et al.*, Syntheses and structures of 1D, 2D, 3D cadmium(II) coordination polymers with oxalate and aromatic co-ligands. *Polyhedron*, 23(6), p. 1003–1009, 2004.
8. Chen, L.-F., *et al.*, Syntheses, crystal structures and photoluminescence of two new pyrazinecarboxylate-based cadmium(II) coordination polymers. *Journal of Molecular Structure*, 892(1–3), p. 278–282, 2008.

9. Ding, J., *et al.*, Anion-dependent structural diversity in cadmium coordination polymers of flexible bis (1, 2, 4-triazol-1-yl) butane. *Inorganic Chemistry Communications*, 11(9), p. 1079–1081, 2008.
10. Braverman, M.A., Supkowski, R.M. and LaDuca, R.L. Luminescent zinc and cadmium complexes incorporating 1,3,5-benzenetricarboxylate and a protonated kinked organodiimine: From a hydrogen-bonded layer motif to thermally robust two-dimensional coordination polymers. *Journal of Solid State Chemistry*, 180(6), p. 1852–1862, 2007.
11. Ciurtin, D.M., *et al.*, Two Versatile N,N'-Bipyridine-Type Ligands for Preparing Organic-Inorganic Coordination Polymers: New Cobalt- and Nickel-Containing Framework Materials. *Inorganic Chemistry*, 40(12), p. 2825–2834, 2001.
12. Xiao, D.-R., *et al.*, A Bridge between Pillared-Layer and Helical Structures: A Series of Three-Dimensional Pillared Coordination Polymers with Multiform Helical Chains. *Chemistry – A European Journal*, 12(25), p. 6528–6541, 2006.
13. Zang, S., *et al.*, One Dense and Two Open Chiral Metal–Organic Frameworks: Crystal Structures and Physical Properties. *Inorganic Chemistry*, 45(7), p. 2972–2978, 2006.
14. Xiao, D.-R., *et al.*, Syntheses and Structures of Three Unprecedented Metal–Ciprofloxacin Complexes with Helical Character. *Crystal Growth & Design*, 7(3), p. 506–512, 2007.
15. Hawxwell, S.M., *et al.*, Ligand flexibility and framework rearrangement in a new family of porous metal-organic frameworks. *Chemical Communications*, 2007(15), p. 1532–1534.
16. Li, S.-L., *et al.*, Structures and Luminescent Properties of Seven Coordination Polymers of Zinc(II) and Cadmium(II) with 3,3',4,4'-Benzophenone Tetracarboxylate Anion and Bis(imidazole). *Crystal Growth & Design*, 8(2), p. 675–684, 2008.
17. Han, L. and Hong, M. Recent advances in the design and construction of helical coordination polymers. *Inorganic Chemistry Communications*, 8(4), p. 406–419, 2005.
18. Hou, H., *et al.*, First Octameric Ellipsoid Lanthanide(III) Complexes: Crystal Structure and Nonlinear Optical Absorptive and Refractive Properties. *Inorganic Chemistry*, 43(4), p. 1323–1327, 2004.
19. Su, C.-Y., Smith, M.D. and zur Loye, H.-C. Columnar Supramolecular Architecture Self-Assembled from S4-Symmetric Coordination Nanotubes Encapsulating Neutral Guest Molecules. *Angewandte Chemie International Edition*, 42(34), p. 4085–4089, 2003.

20. Davis, A.V. and Raymond, K.N. The Big Squeeze: Guest Exchange in an M4L6 Supramolecular Host. *Journal of the American Chemical Society*, 127(21), p. 7912–7919, 2005.
21. Du, J.-L., *et al.*, Metal Coordination Architectures of 2,3-Bis(triazol-1-ylmethyl)quinoxaline: Effect of Metal Ion and Counterion on Complex Structures. *European Journal of Inorganic Chemistry*, 2008(7), p. 1059–1066, 2008.
22. Cai, S. and Jin, G.-X. Trinuclear Rh₂M Complexes (M = Ni, Pd) Bridged by Butyl Selenolato and Carborane Diselenolato Ligands. *Organometallics*, 26(22), p. 5442–5445, 2007.
23. Fromm, K.M., Doimeadios, J.L.S. and Robin, A.Y. *Concomitant crystallization of two polymorphs—a ring and a helix: concentration effect on supramolecular isomerism*. *Chemical Communications*, 2005(36): p. 4548–4550.
24. Tzeng, B.-C., *et al.*, Anion-directed assembly of supramolecular zinc(ii) halides with N,N[prime or minute]-bis-4-methyl-pyridyl oxalamide. *New Journal of Chemistry*, 29(10), p. 1254–1257, 2005.
25. Hou, L. and Li, D. A new ligand 4'-phenyl-4,2':6',4''-terpyridine and its 1D helical zinc(II) coordination polymer: syntheses, structures and photoluminescent properties. *Inorganic Chemistry Communications*, 8(2), p. 190–193, 2005.
26. Fu, Z.-Y., *et al.*, The Structure and Fluorescence Properties of Two Novel Mixed-Ligand Supramolecular Frameworks with Different Structural Motifs. *European Journal of Inorganic Chemistry*, (10), p. 2730–2735, 2002.
27. Wang, X., *et al.*, Syntheses, Structures, and Photoluminescence of a Novel Class of d10 Metal Complexes Constructed from Pyridine-3,4-dicarboxylic Acid with Different Coordination Architectures. *Inorganic Chemistry*, 43(6), p. 1850–1856, 2004.
28. Yu, J., *et al.*, Cd(II) coordination polymers constructed from flexible disulfide ligand: Solvothermal syntheses, structures and luminescent properties. *Inorganica Chimica Acta*, 376(1), p. 222–229, 2011.
29. Khandar, A.A., *et al.*, Anion influence in the structural diversity of cadmium coordination polymers constructed from a pyridine based Schiff base ligand. *Inorganica Chimica Acta*, 427, p. 87–96, 2015.
30. Huang, Y.-Q., *et al.*, Metal-organic frameworks with oxazoline-containing tripodal ligand: structure changes via reaction medium and metal-to-ligand ratio. *CrystEngComm*, 12(12), p. 4328–4338, 2010.

31. Halper, S.R., *et al.*, Topological Control in Heterometallic Metal–Organic Frameworks by Anion Templating and Metalloligand Design. *Journal of the American Chemical Society*, 128(47), p. 15255–15268, 2006.
32. Fujita, M., Metal-directed self-assembly of two- and three-dimensional synthetic receptors. *Chemical Society Reviews*, 27(6), p. 417–425, 1998.
33. Fan, J., *et al.*, Syntheses, Structures, and Magnetic Properties of Inorganic–Organic Hybrid Cobalt(II) Phosphites Containing Bifunctional Ligands. *Inorganic Chemistry*, 45(2), p. 599–608, 2006.
34. Xu, J., *et al.*, Metal–organic frameworks with six- and four-fold interpenetration and their photoluminescence and adsorption property. *CrystEngComm*, 11(12), p. 2728–2733, 2009.
35. Li, Z.-X., *et al.*, Adjusting the Porosity and Interpenetration of Cadmium(II) Coordination Polymers by Ligand Modification: Syntheses, Structures, and Adsorption Properties. *Crystal Growth & Design*, 10(3), p. 1138–1144, 2010.
36. Carlucci, L., Ciani, G. and Proserpio, D.M. A new type of entanglement involving one-dimensional ribbons of rings catenated to a three-dimensional network in the nanoporous structure of $[\text{Co}(\text{bix})_2(\text{H}_2\text{O})_2](\text{SO}_4) \cdot 7\text{H}_2\text{O}$ [bix = 1,4-bis(imidazol-1-ylmethyl)benzene]. *Chemical Communications*, 2004(4): p. 380–381.
37. Carlucci, L., Ciani, G. and Proserpio, D.M. Parallel and inclined (1D \rightarrow 2D) interlacing modes in new polyrotaxane frameworks $[\text{M}_2(\text{bix})_3(\text{SO}_4)_2][\text{M} = \text{Zn(II), Cd(II)}; \text{bix} = 1, 4\text{-bis(imidazol-1-ylmethyl)benzene}]$. *Crystal Growth & Design*, 5(1), p. 37–39, 2005.
38. Meng, X., *et al.*, Hydrothermal Syntheses, Crystal Structures, and Characteristics of a Series of Cd–btx Coordination Polymers (btx = 1,4-Bis(triazol-1-ylmethyl)benzene). *Inorganic Chemistry*, 43(11), p. 3528–3536, 2004.
39. Li, B., *et al.*, Supramolecular isomers in the same crystal: a new type of entanglement involving ribbons of rings and 2D (4,4) networks polycatenated in a 3D architecture. *Chemical Communications*, 2005(18): p. 2333–2335.
40. Du, J.-L., *et al.*, Tuning silver(I) coordination architectures by ligands design: from dinuclear, trinuclear, to 1D and 3D frameworks. *CrystEngComm*, 10(12), p. 1866–1874, 2008.
41. Ding, B., *et al.*, Structural Variations Influenced by Ligand Conformation and Counteranions in Copper(II) Complexes with

- Flexible Bis-Triazole Ligand. Crystal Growth & Design*, 9(1), p. 593–601, 2009.
42. Wang, D.-Z., *et al.*, Metal-organic coordination architectures of bis(1,2,4-triazole) ligands bearing different spacers: syntheses, structures and luminescent properties. *CrystEngComm*, 12(11), p. 3587–3592, 2010.
43. Tao, J., *et al.*, Synthesis and Characterization of a Tetrazolate-Bridged Coordination Framework Encapsulating D_{2h}-Symmetric Cyclic (H₂O)₄ Cluster Arrays. *Inorganic Chemistry*, 43(20), p. 6133–6135, 2004.
44. Dinca, M., A.F. Yu, and J.R. Long, Microporous metal-organic frameworks incorporating 1, 4-benzeneditetrazolate: syntheses, structures, and hydrogen storage properties. *Journal of the American Chemical Society*, 128(27), p. 8904–8913, 2006.
45. Li, J.-R., *et al.*, A pcu-type metal-organic framework with spindle [Zn₇(OH)₈]₆⁺ cluster as secondary building units. *Chemical Communications*, 2007(15), p. 1527–1529.
46. Tong, X.-L., *et al.*, Zinc and cadmium coordination polymers with bis (tetrazole) ligands bearing flexible spacers: synthesis, crystal structures, and properties. *Crystal Growth and Design*, 9(5), p. 2280–2286, 2009.
47. Ouellette, W., *et al.*, A Thermally and Hydrolytically Stable Microporous Framework Exhibiting Single-Chain Magnetism: Structure and Properties of [Co₂(H_{0.67}bdt)₃].20H₂O. *Angewandte Chemie International Edition*, 48(12), p. 2140–2143, 2009.
48. Liu, W.-T., *et al.*, Spontaneous resolution of four-coordinate Zn(II) complexes in the formation of three-dimensional metal-organic frameworks. *CrystEngComm*, 12(11), p. 3487–3489, 2010.
49. Su, Z., *et al.*, Synthesis, structure and fluorescence of novel cadmium(II) and silver(I) complexes with in situ ligand formation of 1-(5-tetrazolyl)-4-(imidazol-1-ylmethyl)benzene. *Journal of Solid State Chemistry*, 182(6), p. 1417–1423, 2009.
50. Chen, L.-Z., *et al.*, A 2-D tetrazole-based Zn(II) coordination polymer: crystal structure, dielectric constant, and luminescence. *Journal of Coordination Chemistry*, 64(4), p. 715–724, 2011.
51. Yuan, G., *et al.*, Synthesis, crystal structures, and luminescent properties of Cd(II) coordination polymers assembled from semi-rigid multi-dentate N-containing ligand. *Journal of Solid State Chemistry*, 196, p. 87–92, 2012.
52. Mu, Y., *et al.*, Effect of Organic Polycarboxylate Ligands on the Structures of a Series of Zinc(II) Coordination Polymers Based on

- a Conformational Bis-triazole Ligand. *Crystal Growth & Design*, 12(3), p. 1193–1200, 2012.
53. Song, X.-Z., *et al.*, Syntheses, structures, and photoluminescent properties of coordination polymers based on 1, 4-bis (imidazol-1-yl-methyl) benzene and various aromatic dicarboxylic acids. *Crystal Growth & Design*, 12(1), p. 253–263, 2011.
 54. Ren, C., *et al.*, Structural diversity of coordination polymers assembled from adamantane dicarboxylates and conformational bis-triazole ligand. *CrystEngComm*, 13(16), p. 5179–5189, 2011.
 55. Tao, J., *et al.*, Hydrothermal Syntheses, Crystal Structures and Photoluminescent Properties of Three Metal-Cluster Based Coordination Polymers Containing Mixed Organic Ligands. *European Journal of Inorganic Chemistry*, 2004(1), p. 125–133, 2004.
 56. Jin, J.-C., *et al.*, An Unusual Independent 1D Metal– Organic Nanotube with Mesohelical Structure and 1D→ 2D Interdigitation. *Crystal Growth & Design*, 10(5), p. 2029–2032, 2010.
 57. Uebler, J.W., *et al.*, Control of Self-Penetration and Dimensionality in Luminescent Cadmium Succinate Coordination Polymers via Isomeric Dipyrindylamide Ligands. *Crystal Growth & Design*, 13(5), p. 2220–2232, 2013.
 58. Ran, Y., *et al.*, A series of 2D Cd(II) coordination polymers constructed from dicarboxylate acids and a flexible imidazole-based ligand. *Inorganica Chimica Acta*, 425, p. 17–27, 2015.
 59. Mei, C.-Z., Shan, W.-W. and Liu, B.-T. Synthesis, crystal structure and luminescent properties of one 3D Cd(II) coordination polymer $[\text{Cd}(\text{H}_3\text{BPTC})_2(\text{bpy})]_n$ (H_4BPTC = 1,1'-biphenyl-2,2',6,6'-tetracarboxylic acid, bpy = 4,4'-bipyridine). *Spectrochimica acta. Part A, Molecular and biomolecular spectroscopy*, 81(1), p. 764–768, 2011.
 60. Wu, D., *et al.*, The structures of three $\text{Hg}_2\text{X}_4\text{L}_2$ macrocycles $\{X = \text{Cl}, \text{Br} \text{ and } \text{I}, \text{ and } L = 1,2\text{-bis}[4\text{-(pyridin-3-yl)phenoxy}] \text{ethane}\}$ assembled from ether-bridged dipyrindyl ligands. *Acta Crystallogr., Sect. C: Cryst. Struct. Commun.* 68, p. 156–160, 2012.
 61. Wang, L., *et al.*, M(II)-coordination polymers (M = Zn and Cd) constructed from 1,2-bis[4-(pyridin-3-yl)phenoxy]ethane and 1,4-benzenedicarboxylic acid. *Journal of Molecular Structure*, 1084, p. 1–8, 2015.
 62. Ranjbar, Z.R. and Morsali, A. Ultrasound assisted syntheses of a nano-structured two-dimensional mixed-ligand cadmium(II) coordination polymer and *direct thermolyses for the preparation*

- of cadmium(II) oxide nanoparticles. Polyhedron*, 30(6), p. 929–934, 2011.
63. Hashemi, L., *et al.*, Sonochemical synthesis of two new nanostructured cadmium(II) supramolecular complexes. *Journal of Inorganic and Organometallic Polymers and Materials*, 23(3), p. 519–524, 2013.
64. Zhu, J., *et al.*, *Diaquabis(1H-1,2,4-triazole-3-carboxylato) cadmium(II)*, *Acta Crystallogr. Sect. E: Struct. Rep. Online*, 2008. (64) m119.
65. Safarifard, V. and Morsali, A. Sonochemical syntheses of a nanoparticles cadmium(II) supramolecule as a precursor for the synthesis of cadmium(II) oxide nanoparticles. *Ultrasonics sonochemistry*, 19(6), p. 1227–1233, 2012.

5

Mercury(II) Coordination Polymers

5.1 Introduction Mercury(II) Coordination Polymers

Coordination polymers of transition metals ions, the formation of polymers with main group metal ions such as mercury(II) is disproportionately sparse when compared with those of other metals. Because of the effects of mercury on environment and its polymers' applications, it is necessary to understand mercury's ability to bind donors and form complexes or coordination polymers. This part provides an overview of some reported coordination polymers of mercury(II) after 1990 and a summary of their properties. One-dimensional polymers, constituted the majority of the mercury(II) coordination polymers and the most frequent coordination number for mercury(II) is four.

In spite of attractive properties of mercury(II) compounds in terms of their potential applications in paper industry, paints, cosmetics, preservatives, thermometers, manometers, energy efficient fluorescent light bulbs and mercury batteries (although somehow limited due to mercury's toxicity), formation of polymers with Hg^{2+} ion are disproportionately sparse when compared with that of Zn^{2+} and Cd^{2+} metals. Grednic [1] defines the nearest neighbours of mercury in a crystal structure as those which are in "contact" with it. In a free molecule (e.g. in the vapor state) these contacts are chemical bonds and their number is defined by valency or coordination number. With a crystal structure the position is less clear, and it is necessary to restrict the consideration of nearest neighbours (the atoms in the coordination sphere) of mercury to those within a defined distance. All atoms surrounding mercury at a distance of less than the sum of van der Waals radii are considered to belong to the mercury coordination sphere [1]. Mercury(II) has atomic, ionic, covalent (tetragonal) and van der Waals radii of $1.50 < r(\text{Hg}) < 1.73$, 1.04, 1.48 and 1.50 Å, respectively [1]. In addition van der Waals radii 1.55 [2], 1.75(7) [3] and 1.71–1.76 Å [4] have been cited. Distances smaller than the sum of van der Waals radii, are taken as effective coordination number.

5.1.1 One-Dimensional Coordination Polymers

One-dimensional (1D) complexes which are the simplest topological type of coordination arrays represent a good starting point for modeling and investigating infinite polymeric compounds to develop strategies for engineering supramolecular polymers [5]. In one-dimensional motifs the metal ion is coordinated with two ligand molecules, metal ions and organic ligands alternate "infinitely", leading to a chain. The most important motifs among one dimensional coordination polymers are linear chains, zigzag chains, double chains, ladder-like chains, fish-bone, railroad and helix. For example in compounds $[\text{Hg}(4\text{-pye})_2]_n$ [6] and $[\text{Hg}(4\text{-tfp})_2]_n$ [7],

Hg(II) centers are coordinated by two C atoms and one N atom in a T-shaped geometry to give infinite zigzag polymeric chains (Figure 5.1). In the complex $[\text{Hg}(2\text{-cpa})_2]_n$ [8] mercury is bonded linearly to two carboxylate oxygen atoms to form a polymer link to a third oxygen giving triangular coordination about the mercury.

Combination of neutral tetrakis-monodentate tecton **I** (Figure 5.2) and HgCl_2 leads to the formation of a 1D coordination polymer [9]. The empty spaces in the network are occupied by $\text{C}_2\text{H}_2\text{Cl}_4$ and H_2O solvent molecules without any specific interactions with the networks. Connection between the organic bis-monodentate tectons **II** and **III** (Figure 5.2) and HgCl_2 [10, 11] and tecton **IV** (Figure 5.2) with HgX_2 ($\text{X} = \text{Cl}, \text{Br}, \text{I}$) leads to the formation of zigzag polymeric chains. When tecton **IV** is combined with HgX_2 ($\text{X} = \text{Cl}, \text{Br}, \text{I}$), two 1D chains have opposite directions and packed orthogonally leading to the formation of a 2D network with basket wave type. The formation of the overall structure results from the parallel packing of braided sheet [11]. Again, connection between the organic tecton **V** (Figure 5.2) and HgCl_2 leads to an

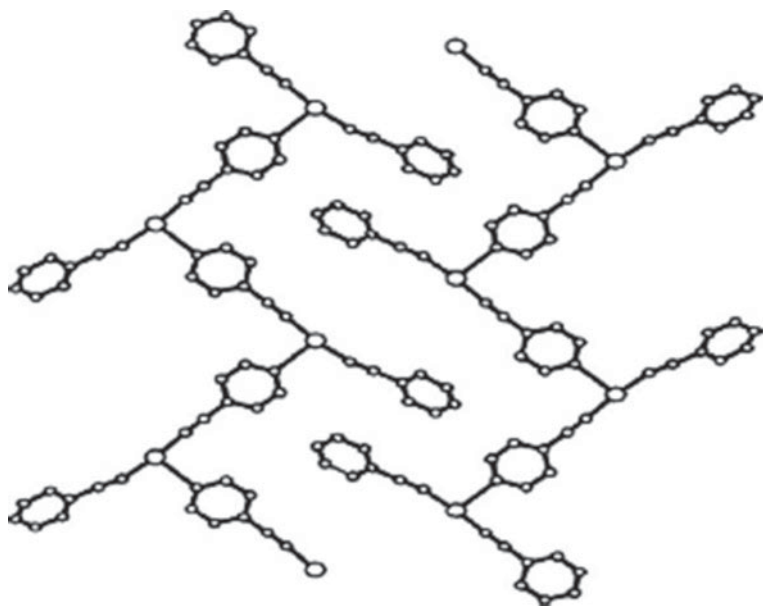


Figure 5.1 Zigzag chain structure of $[\text{Hg}(4\text{-pye})_2]_n$ [6].

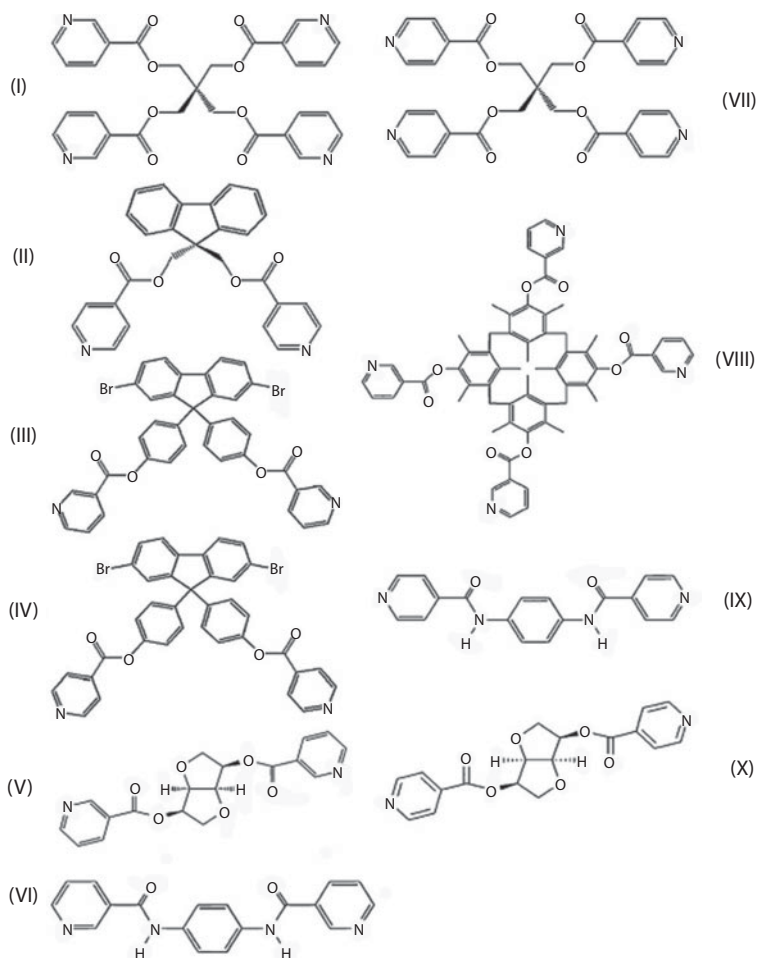


Figure 5.2 Tectons used in mercury(II) coordination polymers.

enantiomerically pure neutral single stranded infinite helix with P helicity [12]. In all the compounds above the coordination sphere around Hg(II) is composed of two halide anions and two N atoms belonging to two consecutive tectons in a distorted tetrahedral coordination geometry.

Compound $[(\text{HgI}_2)_2\text{TPyP}]\cdot 2\text{TCE}$ [13] has a nanoporous 1D polymeric architecture with each HgI_2 tetrahedrally coordinated by a pyridyl moiety of two TPyP molecules. A supramolecular cavity is formed between the linked porphyrins with an effective cavity

size of $2.5 \text{ \AA} \times 7.7 \text{ \AA}$. The 1D coordination polymers are arranged in layers inducing another supramolecular cavity (effective cavity size, $2.4 \text{ \AA} \times 3.0 \text{ \AA}$). The 2D layers are offset stacked at 5.5 \AA and form a partially open porous network. The TCE molecules are sandwiched between the layers and cap the supramolecular cavities. In complex $[(\text{HgBr}_2)_2\text{TPyP}] \cdot 6\text{TCE}$ [13], there are three TCE molecules per TPyP between the layers, and the 1D polymers stack (porphyrin cavity directly over supramolecular cavity) at an 8.1 \AA separation. Complex $[(\text{HgI}_2)_2\text{TPyP}] \cdot 4\text{TCE}$ [13], is a 1D polymer and has a bilayer structure, which exhibits solvation and stacking features of both $[(\text{HgI}_2)_2\text{TPyP}] \cdot 2\text{TCE}$ and $[(\text{HgBr}_2)_2\text{TPyP}] \cdot 6\text{TCE}$; but is solvated with four TCE molecules per formula. Alternating layers have either one (between offset stacked layers as in $[(\text{HgI}_2)_2\text{TPyP}] \cdot 2\text{TCE}$ or three (between stacked layers as in $[(\text{HgBr}_2)_2\text{TPyP}] \cdot 6\text{TCE}$) TCE molecules per TPyP with interlayer separations of 5.4 and 8.3 \AA , respectively (Figure 5.3). Indeed, these two stacking distances correspond to the interlayer stacking distances of $[(\text{HgI}_2)_2\text{TPyP}] \cdot 2\text{TCE}$ (5.5 \AA) and $[(\text{HgBr}_2)_2\text{TPyP}] \cdot 6\text{TCE}$ (8.1 \AA). The crystal structures of $[(\text{HgI}_2)_2\text{TPyP}] \cdot 2\text{TCE}$, $[(\text{HgBr}_2)_2\text{TPyP}] \cdot 6\text{TCE}$ and $[(\text{HgI}_2)_2\text{TPyP}] \cdot 4\text{TCE}$ demonstrate an interesting ability to include variable numbers of identical neutral guest molecules by subtle rearrangement of the stacking of layers (Figure 5.3).

The complexes $[\text{Hg}(3,5\text{-Cl}_2\text{py})_2(\text{Cl})_2]_n$, $[\text{Hg}(3,5\text{-Br}_2\text{py})_2(\text{Cl})_2]_n$ and $[\text{Hg}(3,5\text{-Me}_2\text{py})_2(\text{Cl})_2]_n$ [14] have isomorphous infinite polymeric chains with six-coordinated mercury centers. Polymeric

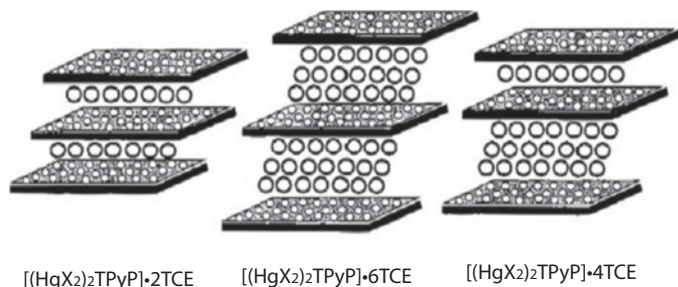


Figure 5.3 Identical neutral guest molecules in crystal structures of $[(\text{HgI}_2)_2\text{TPyP}] \cdot 2\text{TCE}$, $[(\text{HgBr}_2)_2\text{TPyP}] \cdot 6\text{TCE}$ and $[(\text{HgI}_2)_2\text{TPyP}] \cdot 4\text{TCE}$ [13].

complex $[\text{Hg}(3,5\text{-Br}_2\text{py})_2(\text{Br})_2]_n$ has two symmetrically independent mercury(II) cations, both located in crystallographic inversion centers and each metal is coordinated in a pseudo-octahedral fashion [14]. Complexes $[\text{Hg}(\text{C}_5\text{H}_4\text{NCOOMe})(\text{Cl})_2]_n$, $[\text{Hg}(\text{C}_5\text{H}_4\text{NCOOEt})(\text{Cl})_2]_n$ [15] and $[\text{Hg}(\text{MeC}_5\text{H}_3\text{NCOOEt})(\text{Cl})_2]_n$ [16] exist as polymeric chains with highly distorted octahedral mercury(II) centers that are doubly bridged by two Cl atoms. Picolinate ligands behave as chelates, whereas in complex $[\text{Hg}(\text{C}_5\text{H}_4\text{NCOO})_2]_n$ [16], 2-pyridinecarboxylate ligands behave as chelates and simultaneously bridge two consecutive mercury atoms to form one-dimensional chain.

In complex $[\text{Hg}(4,4'\text{-bipy})(\mu\text{-OAc})(\text{OAc})]_n \cdot n/2\text{H}_2\text{O}$ [17] each Hg(II) atom has a coordination number of seven and the environment is a distorted pentagonal bipyramid with an O_5N_2 coordination sphere. The carboxylate group of one acetate ligand acts only as a bidentate chelating group. In the second mode two OAc^- anions act as both a chelating and a bridging group (totally tridentate). These metallacycle nodes are connected through four 4,4'-bipy bridges to two other nodes, resulting in one-dimensional double-chains. Solvate water molecules are found in the lattice of this compound and are involved in a hydrogen bonding network. The coordinated water molecules are acting as hydrogen bond donors towards the O atoms of the coordinated acetate ligands. Consequently, the 1D structure is grown by the hydrogen bonds into a hybrid 2D network. The maximum emission of this compound in the solid state is in the blue region (446.4 nm) and the emission bands cover much of the blue region, giving the observed blue luminescence. Also in complex $[\text{Hg}(\text{nbs})_2(\text{H}_2\text{O})_3]_n$ [18] the mercury(II) ion has a distorted pentagonal bipyramidal coordination environment. The HgN_2O_3 units, in which mercury(II) ion is coordinated by two nbs (*p*-nitrobenzoxasulfamate) nitrogen atoms and three water oxygen atoms, are bridged by the nitro oxygen atoms of the adjacent units, forming polymeric chains. The water oxygen atoms form intermolecular hydrogen bonds with the sulfonyl and nitro oxygen atoms of the nbs ligands in the neighbouring units and the polymeric chains of HgN_2O_3 units are held together by these hydrogen bonds forming a 3D network.

5.1.2 Two-Dimensional Coordination Polymers

Two-dimensional compounds are obtained with three or four ligand molecules coordinating around the metal ion and the elementary motif expands now in two directions; the most important motifs among two-dimensional coordination polymers are square grids, rhombic and rectangular grids based on square grids, 2D motifs with T-shape nodes like brick wall or other parquet floor, honeycomb and pseudo-honeycomb grid, herringbone and bilayer.

In the compound $[\text{Hg}_2(\mu\text{-}2,5\text{-dmpyr})(\mu\text{-SCN})_2(\text{SCN})_2]_n$ [19] the geometry of the Hg(II) is trigonal bipyramidal with the two S and the N atom of the SCN^- anions forming a trigonal planar HgS_2N_1 unit that is augmented on one side by the N atom of the bridging 2,5-dmpyr ligand (2,5-dimethylpyrazine) and on the other side by a vacant space at the mercury ion. Of the SCN^- anions one acts as a monodentate ligand, whereas the other forms a bridge to a mercury atom of an adjacent moiety. $[\text{MeHg}(3\text{-SC}_6\text{H}_4\text{NH}_2)_2]_n$ [20] has two crystallographically independent molecules in an asymmetric unit. Each Hg(II) atom is bonded linearly to C and S atoms and form a centrosymmetric dimer through Hg...S bonds. Further bonding, between amino groups and mercury, links the dimers into sheet networks. The geometry around Hg(II) is pseudo-octahedral with two *cis*-positions vacant.

In compound $[\text{Hg}_2(2\text{-bpdb})\text{I}_4]_n$ [21], ligand 2-bpdb [1,4-bis(2-pyridyl)-2,3-diaza-1,3-butadiene] chelating with each one nitrogen atom of the pyridyl and diaza groups on one side of the molecule coordinating to a mercury(II) ion. Of the I^- anions one acts as a monodentate ligand, whereas the other forms a full halogen bridge to a mercury atom of an adjacent $\text{I}_2\text{Hg}(2\text{-bpdb})$ moiety. The geometry around Hg(II) is distorted tetragonal pyramid. The compound $[\text{Hg}_3(3\text{-bpdh})_{1.5}(\text{SCN})_6]_n$ [22] has a polymeric structure and contain two parts, 2D (part A) and 1D (part B) coordination polymers. Part A consists of mercury(II) ions bridged by both 3-bpdh [2,5-bis(3-pyridyl)-3,4-diaza-2,4-hexadiene] and

thiocyanate ligands and the environment of each Hg(II) is a distorted square pyramidal. Part B consists of linear double chains formed by bridging 3-bpdh ligands. The two individual adjacent 1D (part B) and 2D (part A) in this compound are almost parallel to each other and further linked by weak Hg...S and this interaction extends the structure into a three-dimensional coordination polymer. The 2D net (part A) is polycatenated by the 1D double chain (part B) (Figure 5.4) which is a very rare case of 2D+ 1D= 2D polycatenation [23].

If the weak S...Hg interaction is taken into account the “ladders” connect every other two layers with the result of a twofold interpenetrated nets with complex topology (Figure 5.5).

The structure of complex $[\text{Hg}(\text{pom})\text{Br}_2]_n$ [24] is polymeric through six bridging atoms. The very distorted octahedral mercury(II) is bonded to two O atoms from two pom ligands (3-methyl-4-nitropyridine-1-oxide) and four Br atoms. In polymeric complex $[\text{Hg}(\text{picOH})\text{Cl}]_n$ [25] both carboxylate oxygen atoms of the deprotonated picolinic acid are involved in coordination with two neighbouring mercury atoms to bridge them and form infinite zigzag chains. Mercury(II) also binds to N and Cl atoms and forms infinite two-dimensional layers with two more long Hg...O contacts.

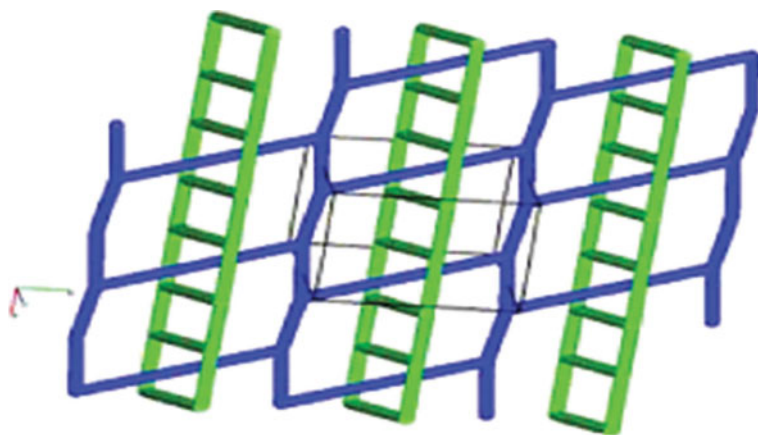


Figure 5.4 Representation of 2D+ 1D= 2D polycatenation in compound $[\text{Hg}_3(3\text{-bpdh})_{1.5}(\text{SCN})_6]_n$.

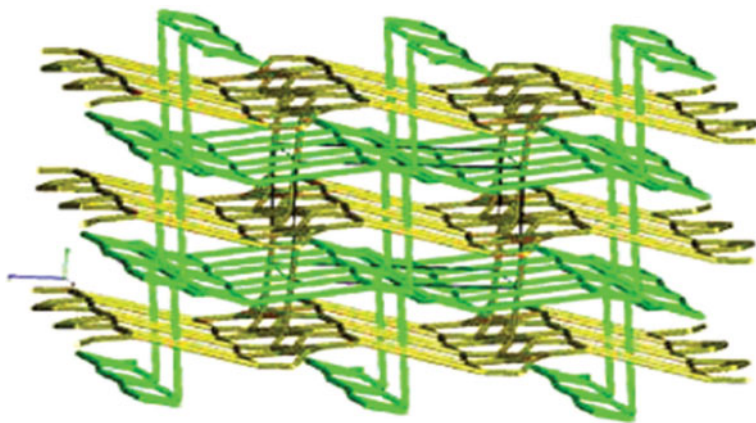


Figure 5.5 Representation of a twofold interpenetrated nets generated by weak S...Hg in $[\text{Hg}_3(3\text{-bpdh})_{1.5}(\text{SCN})_6]_n$.

In compounds $\{[\text{Hg}(\mu\text{-Pym})_2](\text{NO}_3)_2\}_n$ [pym: pyrimidine (1,3-diazine)] and $\{[\text{Hg}(\mu\text{-pyr})_2](\text{ClO}_4)_2\}_n$ [pyr: pyrazine (1,4-diazine)] [26] four N-donor ligands are bridged between Hg(II) centers forming two-dimensional coordination polymers in which the nitrate and perchlorate ions attach bidentately to mercury(II) centers.

5.1.3 Three-Dimensional Coordination Polymers

Three-dimensional structures can be built with metal ions of higher coordination number (tetrahedral or octahedral nodes); the most important motifs among three-dimensional coordination polymers are Diamondoid net, Octahedral net, NbO-, ThSi_2 -, PtS_2 -, SrSi_2 - and CdSO_4 -like motifs.

In complex $[\text{Hg}_8(\mu\text{-}n\text{-C}_3\text{H}_7\text{Te})_{12}(\mu_2\text{-Br})\text{Br}_3]$ [27] closely packed subunits of $[\text{Hg}_8(\mu\text{-}n\text{-C}_3\text{H}_7\text{Te})_{12}(\mu_2\text{-Br})]^{3+}$ are linked with a centered Br^- to form a three-dimensional network through six bromo-bridges (Figure 5.6). This finally enables a three-dimensional linking of the cluster units and a close packing in the solid state.

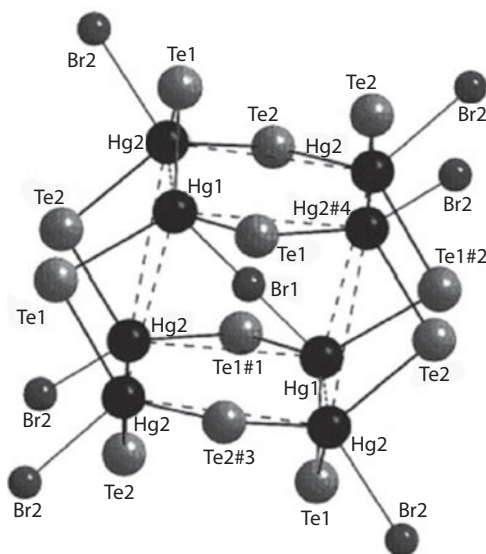


Figure 5.6 Representation of the cluster units of $[\text{Hg}_8(\mu\text{-}n\text{-C}_3\text{H}_7\text{Te})_{12}(\mu_2\text{-Br})\text{Br}_3]$.

The eight mercury atoms of the cluster units are in a distorted cubic arrangement with the $\mu_2\text{-Br}$ atom in its center. The coordination environment of Hg(2) is a distorted trigonal pyramid, whereas that of Hg(1) is intermediate between a trigonal pyramid and a tetrahedron [27].

Complex $[\text{Hg}(\mu\text{-}2,6\text{-dmpyr})(\mu\text{-SCN})_2]_n$ (dmpyr: dimethylpyrazine) consists of one-dimensional linear chains, with $[\text{Hg}(\mu\text{-}2,6\text{-dmpyr})]$ building blocks. The individual parallel polymeric chains are further bridged by the bidentate thiocyanate anions, resulting in a three dimensional framework. The coordination geometry around the mercury(II) ion is irregular and is distorted octahedral. As already pointed out in $(\text{HgCl}_2)_2(\text{hmt})$ hmt ligands (hmt: hexamethylenetetramine) connect to four HgCl_2 , generating 2D (4,4) sheets (Figure 5.7).

But these sheets stack so that the HgCl_2 molecules of adjoining sheets associate to form chains through long $\text{Hg} \cdots \text{Cl}$ interactions (3.105 Å) (Figure 5.8).

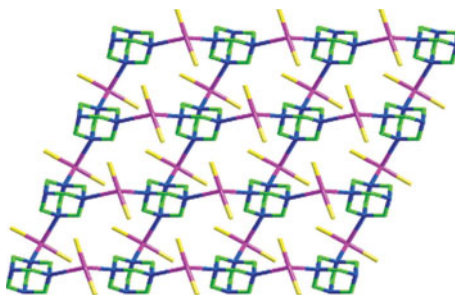


Figure 5.7 2D (4,4) sheet in the structure of $(\text{HgCl}_2)_2(\text{hmt})$

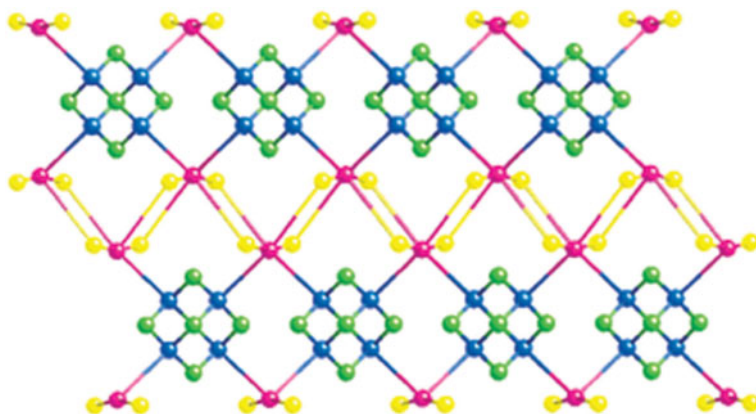


Figure 5.8 Adjacent sheets in the structure of $(\text{HgCl}_2)_2(\text{hmt})$, viewed side-on, linked by 1D chains of weak Hg-Cl interactions running across the page.

When taking into account the lateral interconnections, a three dimensional coordination polymer of compound $(\text{HgCl}_2)_2(\text{hmt})$ is achieved and these interactions complete the pseudo-octahedral geometry of the mercury(II) [28].

5.2 Nano Mercury(II) Coordination Polymers

Among various metal coordination polymers, Hg(II) complexes are of interest because they possess the properties of both transition and non-transition elements and biological activity. They form

various dimensional supramolecular coordination assemblies due to their wide variety of coordination configurations and coordination numbers. In addition, organic ligands are very important in the design and construction of desirable frameworks.

The reaction of 5,5'-di-*tert*-but-bpy, with HgBr_2 and HgI_2 led to the formation of two Hg(II) complexes, $[\text{Hg}(5,5'\text{-di-}t\text{-but-bpy})(\mu\text{-Br})\text{Br}]_2[\text{Hg}(5,5'\text{-di-}t\text{-but-bpy})\text{Br}_2]$ (1) and $[\text{Hg}(5,5'\text{-di-}t\text{-but-bpy})\text{I}_2]$ (2). Nano-sized compounds of 1 and 2 were obtained by ultrasonic irradiation in methanol solution. The structure of 1 by X-ray crystallography (Figure 5.9a) shows that the complex has two types of Hg(II) -ions and two primary structural units. Hg^{I} has coordination number of 5 with trigonal bipyramid geometry and an $\text{Hg}^{\text{I}}\text{Br}_3\text{N}_2$ coordination sphere. Two N-atoms from 5,5'-dtbu-2,2'-bpy chelate the Hg^{I} -ion. Two Br^- ions bridge two Hg^{I} -atoms and another Br^- ion is a terminal group. The Hg^{II} -ion is coordinated by two Br^- anions and one neutral ligand molecule, resulting in a four-coordinate Hg^{II} complex with a HgBr_2N_2 chromophore. The structure of 2 by X-ray crystallography (Figure 5.9b) shows that the Hg(II) -ion is coordinated by two I^- ions and 5,5'-dtbu-2,2'-bipy ligands resulting in a four coordinate complex with a HgI_2N_2 chromophore.

The SEM photograph of 1 and 2 shows a broad distribution of particle size with an average size of 35 nm (Figure 5.10). This

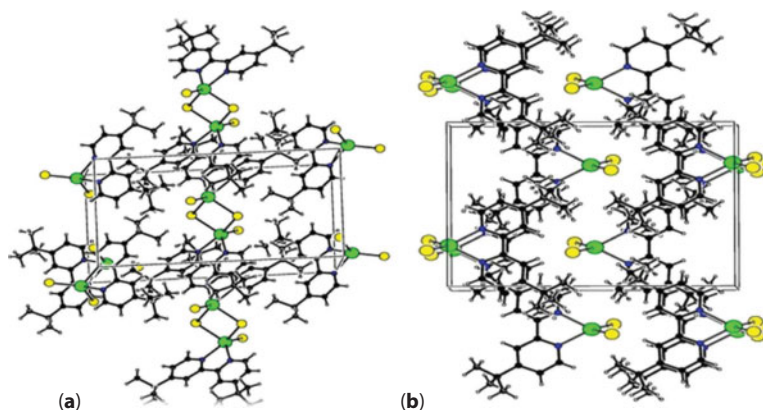


Figure 5.9 Unit cell of (a) compound 1 and (b) compound 2.

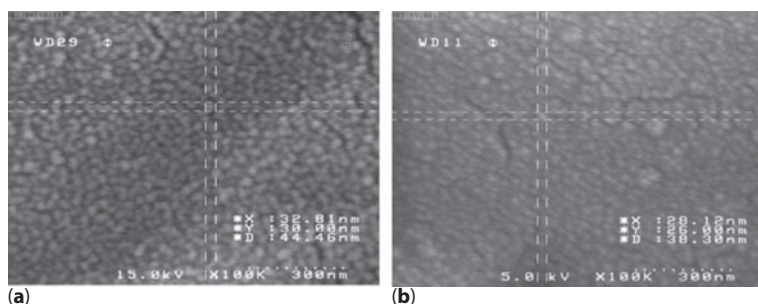


Figure 5.10 SEM photograph of (a) 1 and (b) 2 nanoparticles produced sonochemically.

result indicates that ultrasound can be used as an alternative synthetic procedure to form coordination polymers on a nano-meter scale [29].

Two mercury(II) complexes $[\text{Hg}(4\text{-mtrt})\text{Cl}_2]$ and $[\text{Hg}(4\text{-mtrt})\text{Br}_2]$, have been synthesized from reaction of ligand 4-methyl-4H-1,2,4-triazole-3-thiol (4-mtrt) with HgCl_2 and HgBr_2 . Structures of compound $[\text{Hg}(4\text{-mtrt})\text{Cl}_2]$ and $[\text{Hg}(4\text{-mtrt})\text{Br}_2]$ have been characterized by elemental analysis, IR spectroscopy and single crystal X-ray diffraction. The nanoparticles of compound $[\text{Hg}(4\text{-mtrt})\text{Cl}_2]$ and $[\text{Hg}(4\text{-mtrt})\text{Br}_2]$ have been prepared by sonochemical method. The new nano-structures were characterized by scanning electron microscopy, elemental analysis, IR spectroscopy and X-ray diffraction (XRD). The size of the samples prepared by sonochemical method are about 50 and 60 nm in compounds $[\text{Hg}(4\text{-mtrt})\text{Cl}_2]$ and $[\text{Hg}(4\text{-mtrt})\text{Br}_2]$, respectively [30].

Determination of the structure of compound $[\text{Hg}(4\text{-mtrt})\text{Cl}_2]$ by X-ray crystallography showed that Hg(II) has coordination number of four with HgS_2Cl_2 coordination sphere. Two S atom from 4-methyl-4H-1,2,4-triazole-3-thiol and two of the Cl^- anions coordinated to Hg(II) atoms. Determination of the structure of compound $[\text{Hg}(4\text{-mtrt})\text{Br}_2]$ by X-ray crystallography showed that the Hg(II) ion is coordinated by two Br^- and 4-methyl-4H-1,2,4-triazole-3-thiol ligand, resulting in a four-coordinate complex with a HgS_2Br_2 chromophore (Figure 5.11).

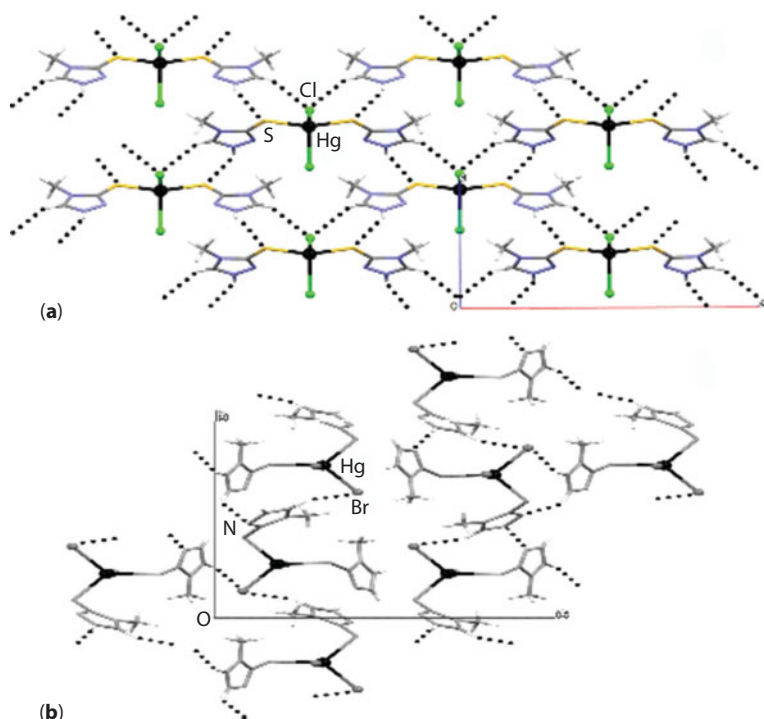


Figure 5.11 The unit cell and packing diagram of (a) $[\text{Hg}(4\text{-mtrt})\text{Cl}_2]$ in *b* direction and (b) $[\text{Hg}(4\text{-mtrt})\text{Br}_2]$ in *a*-direction.

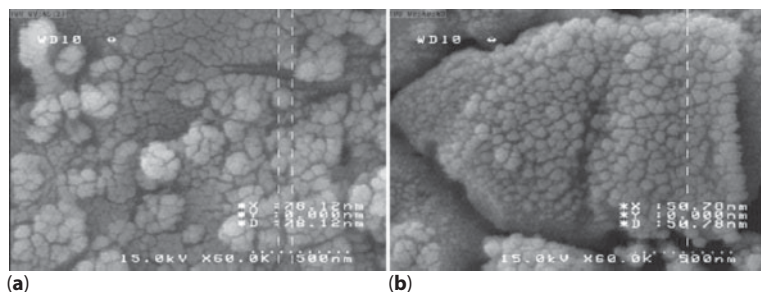


Figure 5.12 SEM photograph of compound $[\text{Hg}(4\text{-mtrt})\text{Cl}_2]$ (a) and $[\text{Hg}(4\text{-mtrt})\text{Br}_2]$ (b) nano-particles produced by sonochemical method.

The significant broadening of the peaks in typical samples of compounds $[\text{Hg}(4\text{-mtrt})\text{Cl}_2]$ and $[\text{Hg}(4\text{-mtrt})\text{Br}_2]$ prepared by the sonochemical process indicates that the particles are of nanometer dimensions. SEM photograph shows a broad distribution of the particle size (Figure 5.12), the average size of the

particles in compounds $[\text{Hg}(4\text{-mtrt})\text{Cl}_2]$ and $[\text{Hg}(4\text{-mtrt})\text{Br}_2]$ are 55 and 45 nm respectively [30].

5.3 Conclusion

Considering the structures discussed in this part, one dimensional polymers constitute a great portion of coordination polymers of mercury(II), among which zigzag structure with counter ion iodide is drastically dominant. This dominance of zigzag structures may be due to the steric effect of the counter ion, in particular iodide group, the rigidity of the ligands, and the preference of Hg(II) for tetrahedral coordination geometry [31–33]. Mercury(II) exhibits greater tendency to forming one-dimensional coordination polymers and three-dimensional polymers are less common. This may be related to mercury's greater radii, mercury's tendency for having a smaller coordination number and taking a tetrahedral coordination geometry by mercury(II). Moreover, the effects related to structure, size and rigidity of ligands as well as number and size of anions, are important in explaining the greater number of one-dimensional coordination polymers [34].

References

1. Grdenic, D., The structural chemistry of mercury. *Quarterly Reviews*, Chemical Society, 19(3), p. 303–328, 1965.
2. Bondi, A., van der Waals Volumes and Radii. *The Journal of Physical Chemistry*, 68(3), p. 441–451, 1964.
3. Pyykkö, P. and Straka, M. *Ab initio* studies of the dimers $(\text{HgH}_2)_2$ and $(\text{HgMe}_2)_2$. Metallophilic attraction and the van der Waals radii of mercury. *Physical Chemistry Chemical Physics*, 2(11), p. 2489–2493, 2000.
4. Canty, A.J. and Deacon, G.B. The van der Waals radius of mercury. *Inorganica Chimica Acta*, 45, p. L225–L227, 1980.
5. Khlobystov, A.N., *et al.*, Supramolecular design of one-dimensional coordination polymers based on silver(I) complexes of aromatic nitrogen-donor ligands. *Coordination Chemistry Reviews*, 222(1), p. 155–192, 2001.

6. Hoskins, B.F., Robson, R. and Sutherland, E.E. Bis(4-pyridylethynyl) mercury. *Journal of Organometallic Chemistry*, 515(1), p. 259–260, 1996.
7. Tyrra, W., Aboulkacem, S. and Pantenburg, I. Silver compounds in synthetic chemistry. Part 3. 4-Tetrafluoropyridyl silver(I), AgC₅F₄N – A reagent for redox transmetalations with group 12–14 elements. *Journal of Organometallic Chemistry*, 691(3), p. 514–522, 2006.
8. Mak, T., *et al.*, Heavy-Metal Complexes With (2-Chlorophenoxy) acetic Acid: The Crystal Structures of Polymeric Mercury(II) (2-Chlorophenoxy)acetate and the Thallium(I) (2-Chlorophenoxy) acetate(2-Chlorophenoxy)acetic Acid Adduct. *Australian Journal of Chemistry*, 43(8), p. 1431–1437, 1990.
9. Grosshans, P., *et al.*, Gradual increase in the dimensionality of cobalt and mercury coordination networks based on conformation of tetradentate tectons. *New Journal of Chemistry*, 27(5), p. 793–797, 2003.
10. Grosshans, P., *et al.*, Molecular tectonics: design of coordinating tectons based on fluorene bearing pyridines and structural analysis of their coordination networks generated in the presence of mercury and cobalt salts. *New Journal of Chemistry*, 27(12), p. 1806–1810, 2003.
11. Jouaiti, A., *et al.*, Molecular tectonics: generation and packing of 1-D coordination networks formed between dibromofluorene based tectons bearing two pyridines and metal halides. *CrystEngComm*, 8(12), p. 883–889, 2006.
12. Grosshans, P., *et al.*, Molecular tectonics: design and structural analysis of enantiomerically pure tectons and helical coordination networks. *Comptes Rendus Chimie*, 7(2), p. 189–196, 2004.
13. Sharma, C.V.K., *et al.*, Design Strategies for Solid-State Supramolecular Arrays Containing Both Mixed-Metalated and Freebase Porphyrins. *Journal of the American Chemical Society*, 121(6), p. 1137–1144, 1999.
14. Hu, C., Kalf, I. and Englert, U. Pyridine complexes of mercury (II) halides: Implications of a soft metal center for crystal engineering. *CrystEngComm*, 9(7), p. 603–610, 2007.
15. Álvarez-Larena, A., *et al.*, Mercury(II) halide adducts of esters of 2-pyridinecarboxylic acid. Crystal structures and structural variations within the series [HgCl₂(C₅H₄NCOOR)], R=Me, Et, Prn, Pri. *Inorganica Chimica Acta*, 266(1), p. 81–90, 1997.
16. González-Duarte, P., *et al.*, Reactions of mercury(II) with 2-pyridinecarboxylic and 6-methyl-2-pyridinecarboxylic acids and

- corresponding esters. Crystal structures of $[\text{Hg}(\text{C}_5\text{H}_4\text{NCOO})_2]$, $[\text{HgX}_2(\text{C}_5\text{H}_4\text{NCOOPri})]$, $\text{X} = \text{Br}$ or I and $[\text{HgCl}_2(\text{MeC}_5\text{H}_3\text{NCOOEt})]$. *Polyhedron*, 17(9), p. 1591–1600, 1998.
17. Mahmoudi, G., *et al.*, $[\text{Hg}(\mu\text{-}4,4'\text{-bipy})(\mu\text{-AcO})(\text{AcO})]_n \cdot n/2\text{H}_2\text{O}$, one-dimensional double-chain coordination polymer, syntheses, characterization, thermal, fluorescence, porous and structural studies. *Inorganica Chimica Acta*, 360(10), p. 3196–3202, 2007.
 18. Yilmaz, V.T., *et al.*, Bis(p-nitrobenzoxasulfamato) Complexes of Cadmium(II) and Mercury(II) - Synthesis, Spectra, and X-Ray Crystal Structures. *Zeitschrift für anorganische und allgemeine Chemie*, 628(8), p. 1908–1912, 2002.
 19. Mahmoudi, G. and Morsali, A. Counter-ion influence on the coordination mode of the 2, 5-bis (4-pyridyl)-1, 3, 4-oxadiazole (bpo) ligand in mercury (ii) coordination polymers, $[\text{Hg}(\text{bpo})_n \text{X}_2]$: $\text{X} = \text{I}^-$, Br^- , SCN^- , N_3^- and NO_2^- ; spectroscopic, thermal, fluorescence and structural studies. *CrystEngComm*, 9(11), p. 1062–1072, 2007.
 20. Almagro, X., *et al.*, Schiff bases derived from mercury (II)–aminothiolate complexes as metalloligands for transition metals. *Journal of Organometallic Chemistry*, 623(1), p. 137–148, 2001.
 21. Mahmoudi, G. and Morsali, A. Crystal-to-crystal transformation from a weak hydrogen-bonded two-dimensional network structure to a two-dimensional coordination polymer on heating. *Crystal Growth and Design*, 8(2), p. 391–394, 2007.
 22. Mahmoudi, G. and Morsali, A. Novel rare case of $2\text{D} + 1\text{D} = 2\text{D}$ polycatenation $\text{Hg}(\text{II})$ coordination polymer. *CrystEngComm*, 11(1), p. 50–51, 2009.
 23. Carlucci, L., Ciani, G. and Proserpio, D.M. Polycatenation, polythreading and polyknotting in coordination network chemistry. *Coordination Chemistry Reviews*, 246(1), p. 247–289, 2003.
 24. Hu, S.-Z., *et al.*, Structure of a 1:1 addition compound of mercuric bromide with 3-methyl-4-nitropyridine 1-oxide. *Acta Crystallography C*, 48, p. 1597–1599, 1992.
 25. Popović, Z., *et al.*, Coordination modes of 3-hydroxypicolinic acid: Synthesis and structural characterization of polymeric mercury(II) complexes. *Polyhedron*, 26(5), p. 1045–1052, 2007.
 26. Meyer, G. and Nockemann, P. Affinity of Divalent Mercury Towards Nitrogen Donor Ligands. *Zeitschrift für anorganische und allgemeine Chemie*, 629(9), p. 1447–1461, 2003.
 27. Schulz Lang, E., *et al.*, $[\text{Hg}_8(\mu\text{-}n\text{-C}_3\text{H}_7\text{Te})_{12}(\mu\text{-Br})\text{Br}_3]$ — Synthesis and Structure. *Zeitschrift für anorganische und allgemeine Chemie*, 628(13), p. 2815–2817, 2002.

28. Batten, S.R., *et al.*, Crystal Engineering with Mercuric Chloride. *Crystal Growth & Design*, 2(2), p. 87–89, 2002.
29. Abedini, J., *et al.*, Thermal and Fluorescence Properties of New Nanostructured Hg(II) -2,2'-Bipyridine Derivative Complexes. *Journal of Inorganic and Organometallic Polymers and Materials*, 22(5), p. 1221–1227, 2012.
30. Paqhaleh, D.M.S., *et al.*, Synthesis of two new nano-structured mercury(II) complexes with 4-methyl-4H-1,2,4-triazole-3-thiol ligand by sonochemical method. *Inorganica Chimica Acta*, 407, p. 1–6, 2013.
31. Niu, Y., *et al.*, The syntheses, crystal structures and optical limiting effects of HgI₂ adduct polymers bridged by bipyridyl-based ligands. *Inorganica Chimica Acta*, 355, p. 151–156, 2003.
32. Niu, Y., *et al.*, The synthesis and crystal structure of a new coordination polymeric adduct containing mercury iodide. *Journal of Chemical Crystallography*, 36(10), p. 679–684, 2006.
33. Niu, Y., Hou, H. and Zhu, Y. Self-assembly of d10 metal adduct polymers bridged by bipyridyl-based ligands. *Journal of Cluster Science*, 14(4), p. 483–493, 2003.
34. Morsali, A. and Masoomi, M.Y. Structures and properties of mercury(II) coordination polymers. *Coordination Chemistry Reviews*, 253(13–14), p. 1882–1905, 2009.

6

Lead(II) Coordination Polymers

6.1 Introduction

Divalent lead, with its electronic configuration $[\text{Xe}] 4f^{14} 5d^{10} 6s^2$, is a heavy toxic metal [1], easy to extract, dense, highly malleable and stable to corrosion [2]. Problem of environmental contamination is widespread owing to several industrial activities, mainly battery making and recycling, oil refining, paint manufacturing [3], metal alloys, glasses, ceramic and radiation shielding materials [4]. Lead(II) contains the $6s^2$ lone pair, which can cause distortion in coordination sphere [5–10] and frequently discussed in considering the “stereo-chemical activity” of valence shell electron lone pairs [11–17]. In 1998, Shimoni-Livny discussed the possible stereo-chemical activity of the lone pair of lead(II) compounds based on a thorough review of crystal data available in the CSD. They classify lead coordination as holodirected which refers to complexes in which the bonds to ligand atoms are directed

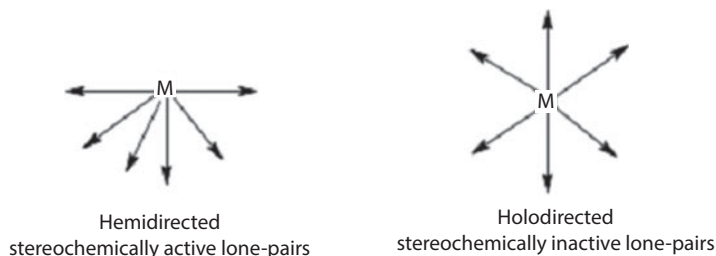
throughout the surface of encompassing sphere, while hemidirected refers to those cases where the bonds to ligand atoms are directed only to a part of the coordination sphere, leaving a gap in the distribution of bonds to the ligand (Scheme 6.1) [18–23].

Lone pair activity may depend on the following factors: (1) low versus high coordination number, (2) hard versus soft ligands, (3) attractive versus repulsive interactions among ligands, (4) whether the lone pair has p character, (5) fewer or more electron donation from ligands to metal [24]. Lead(II) complexes are interesting and frequently discussed in considering the coordination and forms stable complexes with both soft and hard donor atom ligands [25–31]. The effects of ligands on the construction of the coordination polymers are studied and play a role in determining the network structure of a coordination polymer.

6.2 Mono-donor Coordination Mode

6.2.1 Discrete Complexes

$[\text{Pb}(\text{H}_3\text{Dtpa})]\cdot 2\text{H}_2\text{O}$ (1) [32] forms discrete coordination polymer only with carboxylate group of the related ligand. $[\text{Pb}(\text{phen})_2(\text{L})_2]\cdot 2.5\text{H}_2\text{O}$ (2) [33], $(\text{pipz})[\text{Pb}(2\text{-}6\text{-pydc})_2]\cdot 2\text{H}_2\text{O}$ (3) [34], $[\text{Pb}(\text{OAc})_2\text{BPh}_4]_2$ (4), $[\text{Pb}(\text{L}_3)_2(\text{bpy})]$ (5) [35], $[\text{Pb}(\text{H}_2\text{Edta})(\text{tu})]$ (6), $\text{Pb}(\text{H}_2\text{Edta})\cdot 2\text{tu}\cdot \text{H}_2\text{O}$ (7) [36], $(\text{tataH}_2)_2[\text{Pb}(\text{pydc})_2]\cdot 2\text{tata}\cdot 4\text{H}_2\text{O}$ (8) [37], $[\text{Pb}(\text{L}_4)_2(\text{phen})]\cdot \text{H}_2\text{O}$ (9) [38], $[\text{Pb}(\text{L}_5)_2(\text{phen})_2]\cdot 2.5\text{H}_2\text{O}$ (10) [39] and $[\text{Pb}(\text{qina})_2(\text{DMSO})]\cdot \text{H}_2\text{O}$ (11) [40], form novel



Scheme 6.1 Lone pair stereo-chemical properties.

mixed-ligand lead(II) complexes that one of them has possessed carboxylate groups.

HL, 2-chlorobenzoic acid; L₂, 1,4,7-triazacyclononane; L₃, o-fluorobenzoic acid; L₄, 5-nitroisophthalate; L₅, 2-bromobenzoato.

Compounds 6 and 11 contain two-dimensional supramolecular compound formed through hydrogen bonding and π - π stacking interactions. Compound 6 is linked in twin polymeric chains (ribbons) through strong hydrogen bonding. In complex 11 the coordination number of Pb(II) ion is four and two qina- ligands coordinate to the Pb(II) ions with two nitrogen atoms and two mono-donor carboxylate oxygen atoms (Figure 6.1).

In compound 9, the coordination geometry of the Pb(II) atom is best described as highly distorted tetrahedral, made up of two nitrogen atoms of a phenanthroline ligand and two oxygen atoms from two mono-donor carboxylate groups from two 5- nitroisophthalate anions (Figure 6.2). In compound 5 each Pb(II) atom is coordinated by two nitrogen and two oxygen atoms, to complete a significantly distorted PbN₂O₂ polyhedron. The molecules form

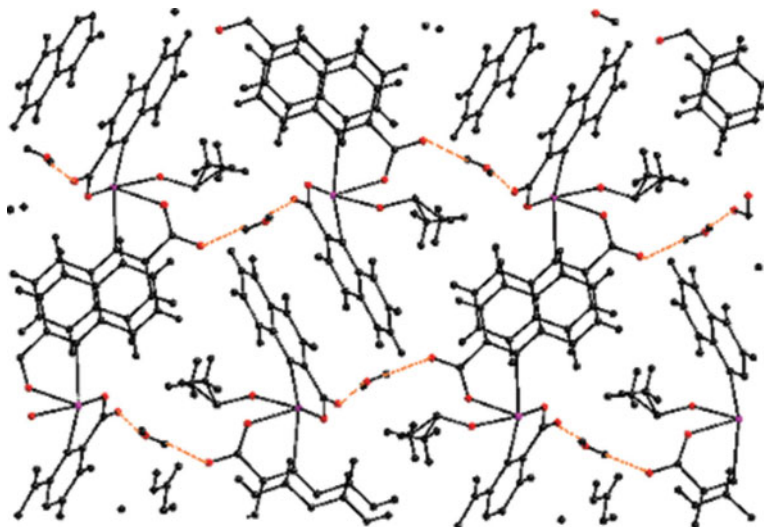


Figure 6.1 Two-dimensional net structure in compound 11.

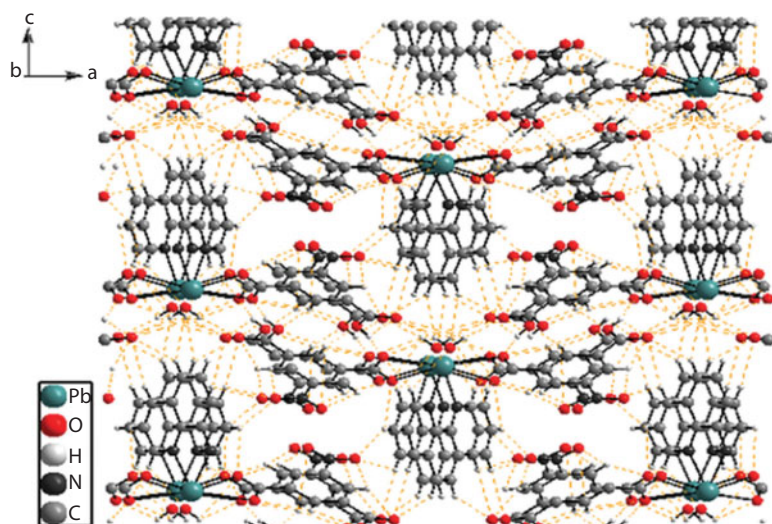


Figure 6.2 Three-dimensional network formed by hydrogen bonding and π - π stacking interactions in compound 9.

1D chains along the *a*-axis via weak $\text{Pb}\cdots\text{O}$ and $\text{Pb}\cdots\text{Pb}$ interactions. The chains are connected to each other via weak intermolecular hydrogen bonding. These interactions form the 3D network.

6.2.2 One-Dimensional Coordination Polymers

Compounds $[\text{Pb}(\text{H}_2\text{Edta})]\cdot 1.5\text{H}_2\text{O}$ [41], $[\text{Pb}(\text{Htpaa})]_2$ [42], $[\text{Pb}(\text{INO})_2]\cdot 3\text{H}_2\text{O}$ [43] and $[\text{Pb}(\text{pro})(\text{H}_2\text{O})]_n$ [44] form 1D coordination polymers only with carboxylate group of the related ligand. Compounds $[\text{Pb}(\text{H}_2\text{tpaa})\text{Cl}]$ and $[\text{Pb}(\text{Hdpaea})\text{Cl}]$ [42] form mixed-ligand lead(II) complexes. In compound $[\text{Pb}(\text{INO})_2]\cdot 3\text{H}_2\text{O}$ each Pb(II) center has a tetrahedral environment coordinated by four oxygen atoms. The oxygen atoms are located on one side of the Pb(II) ion which adopts a hemidirected structural geometry and shows the presence of a stereo-chemically active lone electron pair. All INO ligands adopting a bidentate-bridged coordination mode, through mono-donor carboxylate moieties and pyridyl N-oxide groups link to a pair of lead(II) centers to form $[\text{Pb}_2(\text{INO})_2]$ units. These units are expanded into a 1D infinite chain through corner

sharing lead(II) polyhedrons. The 1D chains are further extended into a 3D supramolecular framework through Pb...O interactions [45] and multipoint hydrogen bonding between water molecules and carboxylate oxygen atoms. Compound $[\text{Pb}(\text{pro})(\text{H}_2\text{O})]_n$ is a 1D chain polymer as a result of water bridging. Coordination number of Pb(II) is six with a 'stereo-chemically active' lone electron pair, and the coordination sphere is hemidirected.

6.2.3 Two-Dimensional Coordination Polymers

In $[\text{Pb}(\text{3-PYD})_2]_n$ [46], ligand 3-PYD bridges Pb(II) atoms through its pyridyl nitrogen atom and mono-donor carboxylate group, generating a head-to-tail aggregated $\{\text{Pb}(\text{3-PYD})\}_4$ ring. The $\{\text{Pb}(\text{3-PYD})\}_4$ rings are further extended into a 2D wave-like layer by sharing Pb(II) joints and ligand 3-PYD edges.

Compound $[\text{Pb}(\text{rctt-tpcb})(\text{O}_2\text{CCF}_3)_2]$ [47] has formed from upright squares zigzag structure. The bottom edges of the squares are bonded to the adjacent rows alternately to form this 2D coordination polymeric sheet with the layer thickness of 8.7 Å. This connectivity generates larger ring linked by the edges of four squares and empty spaces are occupied by the free non-bonded pyridyl rings of the rctt-tpcb ligands.

6.2.4 Three-Dimensional Coordination Polymers

Compound $[\text{Pb}(\text{INO})_2]_2 \cdot 7\text{H}_2\text{O}$ [48] contains two alternate 1D nano-channels (A and B) with different sizes and shapes. Such biporous materials with two (or more) distinct channels may be used as the simultaneous isolation or transportation of two different guests possible. Channel A is approximately a square, whereas channel B is roughly a rectangle. In complex $[\text{Pb}(\text{INO})_2]_2 \cdot 7\text{H}_2\text{O}$, notably, (1) two distinct 1D channels were observed in a 3D coordination network; (2) the lattice water molecules fill in two distinct channels in different manners, and (3) leading to an array of

1D water tube with a double-stranded chain and an ordered 1D water chain involving a cyclic $(\text{H}_2\text{O})_4$ unit.

6.3 Bi-donor Coordination Polymers

6.3.1 Bridging ($\mu^2-\mu^1:\mu^1$) Mode

6.3.1.1 Discrete Complexes

Two equivalent $[\text{Pb}(\text{H}_2\text{L}_6)]^+$ units in $[\text{Pb}_2(\text{H}_2\text{L}_6)_2(\mu^2-\text{OAc})]^+$ [49] are connected by a bridging acetate group to form a dimer lead(II) complex, $[\text{Pb}_2(\text{H}_2\text{L}_6)_2(\mu^2-\text{OAc})]^+$. The uncoordinated acetate counter-ion is involved in intermolecular hydrogen bonding with the oxygen atom of consecutive cations (Figure 6.3). In compound $[\text{Pb}_2(\text{H}_2\text{L}_6)_2(\mu^2-\text{OAc})]^+$ both lead(II) centers have an irregular geometry, bound by five atoms with the sixth coordination site comprising the remaining $6s^2$ lone pair.

6.3.1.2 One-Dimensional Coordination Polymers

Compounds $[\text{Pb}(\text{sdac})\cdot\text{H}_2\text{O}]$ [50] and $[\text{Pb}(\text{DABT})]_n$ [51] are 1D coordination polymers in which hydrogen bonding help to stabilize the structure and form two-dimensional supramolecule. $\{[\text{Pb}(\text{phen})_2(\text{ox})]\cdot 5\text{H}_2\text{O}\}_n$ [52], $[\text{Pb}(\text{phen})(\text{OAc})_2]$ [53], form 1D mixed-ligand lead(II) complexes. In compound $\{[\text{Pb}(\text{phen})_2(\text{ox})]\cdot 5\text{H}_2\text{O}\}_n$ each Pb(II) atom is eight-coordinated and generates a N_4O_4 environment with a square-antiprismatic geometry (D_{4d} symmetry). Each ox group acts as a bischelate coordination mode, further bridges to Pb(II) atom, generating a one-dimensional chain. Phen ligands are alternately attached to both

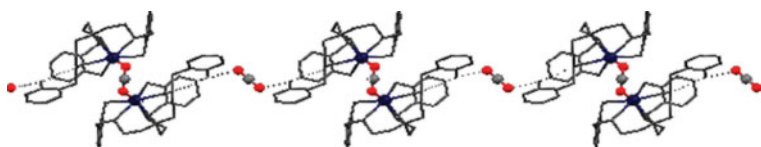


Figure 6.3 The arrangement of 1D chain containing $[\text{Pb}(\text{H}_2\text{L}_6)]^+$ units in compound $[\text{Pb}_2(\text{H}_2\text{L}_6)_2(\mu^2-\text{OAc})]^+$.

sides of the chain and adjacent polymeric chains are packed through inter-calation of the lateral phen ligands in a zipper-like fashion into a two dimensional layer exhibiting very strong inter-chain π - π stacking interactions with the face-to-face distance of 3.25 Å. There are two crystallographic positions for the five water molecules in the $[\text{Pb}(\text{phen})_2(\text{ox})]\cdot 5\text{H}_2\text{O}$ unit, to generate one-dimensional ribbons running along the b-axis. The water molecule intercalates into the two adjacent layers and further connects via hydrogen bonding with the ox oxygen atoms within the π - π stacked layers, hence forming a three-dimensional network in the lattice.

6.3.1.3 Two-Dimensional Coordination Polymers

In compound $[\text{Pb}(\text{INO})(\text{N}_3)(\text{H}_2\text{O})]_n$ [54] each azide ligand bridges three Pb(II) ions to form a two-dimensional three-connected 6^3 topology network. The carboxylate group of the isonicotinate unit and the aqua ligand act as coligands to bridge Pb(II) ions. Adjacent two-dimensional layers are connected by hydrogen-bonding interactions between the isonicotinate nitrogen atom and the water molecule, resulting in an extended three-dimensional network. In the structure of $[\text{Pb}(\text{fum})(\text{dpdp})]\cdot \text{H}_2\text{O}$, each fum ligand bridges four Pb(II) centers in a tetradentate mode, generating a novel layer structure. Additionally, the interplanar distance between two neighboring dpdp ligands of adjacent layers are ca. 3.54 and 3.50 Å, indicating the presence of face-to-face $\Pi - \Pi$ interactions that extend the layers to a unique 3D supramolecular structure. The carboxylate moiety of the 4-pyc⁻ ligand in compounds $[\text{Pb}(\mu\text{-4-pyc})(\mu\text{-NCS})-(\mu\text{-H}_2\text{O})]_n$ and $[\text{Pb}(\mu\text{-4-pyc})(\mu\text{-N}_3)(\mu\text{-H}_2\text{O})]_n$ [55] act as a bridging group in a bridging ($\mu^2\text{-}\mu^1\text{:}\mu^1$) coordination mode. The X-Pb-Y angles suggest that there is a vacant site in the coordination sphere of the lead(II) ion due to lone pair-bond pair repulsion (Figures 6.4a and 6.5a). Nano-sized particles of compounds $[\text{Pb}(\mu\text{-4-pyc})(\mu\text{-NCS})-(\mu\text{-H}_2\text{O})]_n$ and $[\text{Pb}(\mu\text{-4-pyc})(\mu\text{-N}_3)(\mu\text{-H}_2\text{O})]_n$ have been prepared by sonochemical method in aqueous solution. The average size of the particles is around 88 and 96 nm for compounds 33 and 34, respectively (Figures 6.4b and 6.5b).

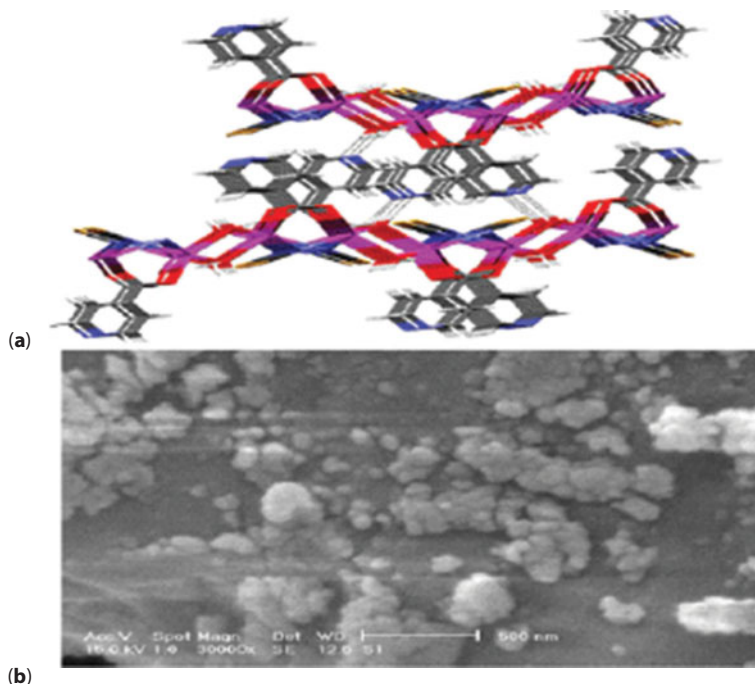


Figure 6.4 (a) A fragment of the 2D polymer and showing hydrogen bonding in compound $[\text{Pb}(\mu\text{-4-ptyc})(\mu\text{-NCS})-(\mu\text{-H}_2\text{O})]_n$ and (b) SEM photograph of compound $[\text{Pb}(\mu\text{-4-ptyc})(\mu\text{-NCS})-(\mu\text{-H}_2\text{O})]_n$ nano-particles prepared by sonochemical method.

6.3.1.4 Three-Dimensional Coordination Polymers

Compounds $[\text{Pb}_4(\text{H}_2\text{L}_8)(\text{SIP})_2(\text{H}_2\text{O})_4 \cdot 2\text{H}_2\text{O}]$ [56], $[\text{Pb}_4(\text{OH})_4(\text{INO})_4] \cdot n\text{H}_2\text{O}$ [57] and $\{[\text{Pb}(4\text{-sb})(4,4'\text{-bipy})_{1/2}] \cdot (4,4'\text{-bipy})_{1/2}\}_n$ [58] form mixed-ligand three-dimensional coordination polymers. In complex $[\text{Pb}_4(\text{OH})_4(\text{INO})_4] \cdot n\text{H}_2\text{O}$ each hepta-coordinated Pb(II) center is bound to three hydroxyl oxygen atoms through $\mu_3\text{-OH}$ atoms, and each $\mu_3\text{-OH}$ bridges to three Pb(II); thus, it forms a usual M_4O_4 core. The Pb_4O_4 core is bonded to four carboxylate groups from four different INO ligands to expand to four different orientations. The INO ligand acts as a tetra-donor ligand and bridges four lead(II) ions through two carboxylate O atoms and one N-oxide oxygen atom. The resulting 3D network contains 1D square nano channels. Compound $\{[\text{Pb}(4\text{-sb})(4,4'\text{-bipy})_{1/2}] \cdot (4,4'\text{-bipy})_{1/2}\}_n$ displays a 3D network, in

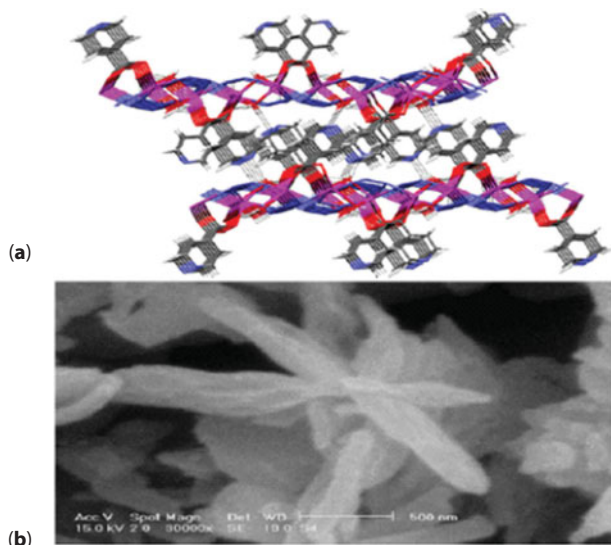


Figure 6.5 (a) A fragment of the 2D polymer and showing hydrogen bonding in compound $[\text{Pb}(\mu\text{-4-ptyc})(\mu\text{-N}_3)(\mu\text{-H}_2\text{O})]_n$ and (b) SEM photograph of compound $[\text{Pb}(\mu\text{-4-ptyc})(\mu\text{-N}_3)(\mu\text{-H}_2\text{O})]_n$ nano-rods prepared by sonochemical method.

which each Pb(II) center is eight-coordinated in a dicapped trigonal prism with a PbNO_7 chromophore. The carboxylate group in this complex acts as bridging ($\mu^2\text{-}\mu^1\text{:}\mu^1$) mode. There are $\pi\text{-}\pi$ interactions not only between coordinated 4,4'-bipyridine and free 4,4'-bipyridine ligands but also between coordinated 4,4'-bipyridine and 4-sb, as well as between free 4,4'-bipyridine ligand and 4-sb ligand.

6.4 Tri-donor Coordination Polymers

6.4.1 Bridging ($\mu^3\text{-}\mu^1\text{:}\mu^2$) Mode

6.4.1.1 Two-Dimensional Coordination Polymer

In compound $\{[\text{Pb}(3\text{-sb})(\text{H}_2\text{O})_2]\cdot 4,4'\text{bpy}\}_n$, the Pb(II) atoms are linked by 3- sulfonatobenzoate anions as μ_4 -bridging coordination mode to give double layers. The carboxylate groups are

coordinated to two Pb(II) atoms through a tri-donor bridging mode, and form a two-dimensional coordination polymer. Ligand 4,4'-bipyridine is uncoordinated and is linked to coordinated water molecules via O–H...N hydrogen bonding. As a result of hydrogen bondings between uncoordinated 4,4'-bipyridine and coordinated water molecules the double layer structure is extended to give a 3D supramolecular network [59]. In compound $[\text{Pb}(2\text{-pyc})(\text{NCS})]_n$ the lead(II) ions are coordinated by both NCS^- and pyc^- anions, resulting in a two-dimensional framework [60]. The carboxylate moiety of the pyc^- ligand acts as tri-donor bridging ($\mu^3\text{-}\mu^1\text{:}\mu^2$) coordination mode. Nano-particles of compound $[\text{Pb}(2\text{-pyc})(\text{NCS})]_n$ have been prepared by sonochemical method and the average size of the particles is around 55 nm.

6.4.1.2 Three-Dimensional Coordination Polymers

In compound $[\text{PbCl}(\text{N,N'}\text{-diacetate imidazolium})]_n$ [61] each of the zwitterionic N,N'-diacetate imidazolium anions acts as bridging ligand and links four lead(II) atoms. The Pb(II) atoms are eight-coordinated with a significantly distorted monocapped pentagonal bipyramidal geometry by two $\mu_2\text{-Cl}$ and six oxygen atoms from four carboxylate groups. Along c-axis, the monocapped pentagonal bipyramidally coordinated Pb(II) atoms are connected by the N,N'-diacetate imidazolium anions into one-dimensional right-handed helical chains (Figure 6.6a). Each helical unit includes five Pb(II) atoms and four zwitterionic ligands, and the right-handed helix is generated from the crystallographic 4_1 axis. The infinitely right-handed helical chains are held together to form a 3D homochiral porous metal–organic framework. A space-filling model shows the open rectangular channels in the individual framework (Figure 6.6b).

Compounds $[\text{Pb}_2(4\text{-pyc})_2\text{I}_2(\text{H}_2\text{O})]_n$ and $[\text{Pb}(3\text{-pyc})\text{I}]_n$ [62] are three-dimensional neutral metallopolymer bridged by 4-pyc $^-$ and 3-pyc $^-$, water and iodide ligands, thus forming infinite frameworks. The carboxylate moiety of the pyc $^-$ ligands in these compounds acts as both a bi-donor and a bridging group (totally tri-donor) in $\mu^3\text{-}\mu^1\text{:}\mu^2$ coordination mode, where two

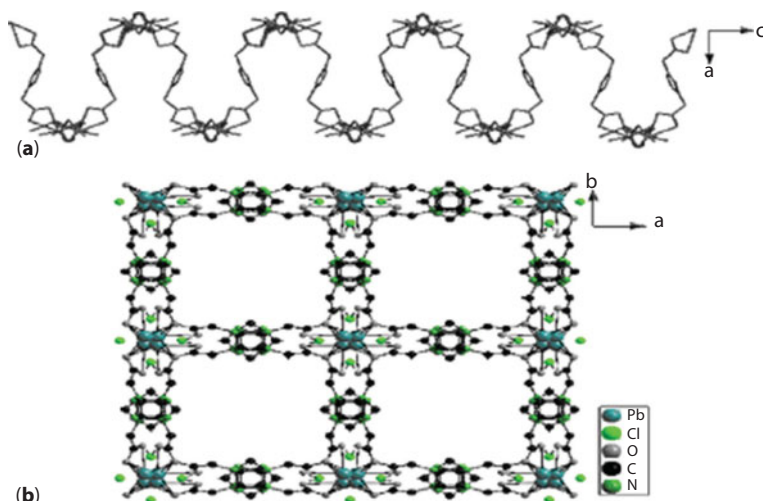


Figure 6.6 (a) View of the right-handed helical chain in $[\text{PbCl}(\text{N},\text{N}'\text{-diacetate imidazolium})]_n$ and (b) a space-filling model showing the open rectangular nano-channels in the individual framework of compound $[\text{PbCl}(\text{N},\text{N}'\text{-diacetate imidazolium})]_n$

oxygen atoms of the carboxylate group bidentately coordinate to a lead(II) ion, creating a four-membered chelate ring. Nano-particles of compounds $[\text{Pb}_2(4\text{-pyc})_2\text{I}_2(\text{H}_2\text{O})]_n$ and $[\text{Pb}(3\text{-pyc})\text{I}]_n$ were prepared by sonochemical method. The SEM photograph shows that the compounds $[\text{Pb}_2(4\text{-pyc})_2\text{I}_2(\text{H}_2\text{O})]_n$ and $[\text{Pb}(3\text{-pyc})\text{I}]_n$ are nano-fiber and nano-particles, respectively.

6.5 Tetra-donor Coordination

6.5.1 Chelating, Bridging ($\mu^3\text{-}\mu^1$: μ^2 : μ^1) Mode

6.5.1.1 One-Dimensional Coordination Polymers

The acetate anions in the compounds $[\text{Pb}(\text{phen})(\text{OAc})(\text{O}_2\text{NO})]$ [63] and $[\text{Pb}(\text{phen})(\text{OAc})(\text{O}_2\text{ClO}_2)]$ [64] act as a tetradonor ligands with both chelating and bridging ($\mu^3\text{-}\mu^1$: μ^2 : μ^1) mode. In compound $[\text{Pb}(\text{phen})(\text{OAc})(\text{O}_2\text{NO})]$ the Pb(II) atom has an asymmetrical eight coordination and the arrangement of ligands suggests a hemidirected geometry.

6.5.1.2 Two-Dimensional Coordination Polymers

The structure of $\{[\text{Pb}(\mu\text{-OAc})(\mu\text{-ebp})](\text{ClO}_4)\}_n$ [65] consists of $[\text{Pb}(\mu\text{-OAc})(\mu\text{-ebp})]^+$ cations and ClO_4^- anions. The cationic complex is a two-dimensional framework, in which Pb(II) atoms are bridged by both OAc^- and ebp ligands as illustrated in Figure 6.7.

The carboxylate moiety of the OAc^- ligand acts as both bidentate and bridging group (totally tetra-donor) where the two oxygen atoms of the carboxylate group bidentately coordinate to Pb(II) atoms, creating a four-membered chelate ring, and one of them also bridges two adjacent Pb(II) atoms, yielding an one-dimensional chain. These one-dimensional chains are further linked by the ebp ligands and thus creating a two-dimensional coordination polymer (Figure 6.7). Although ClO_4^- anions act as a counter-ion, it also makes weak interactions with the Pb(II) center. The arrangement of the ligands exhibits hemidirected geometry, and the coordination gap around the Pb(II) ion is possibly occupied by an active lone pair of electrons.

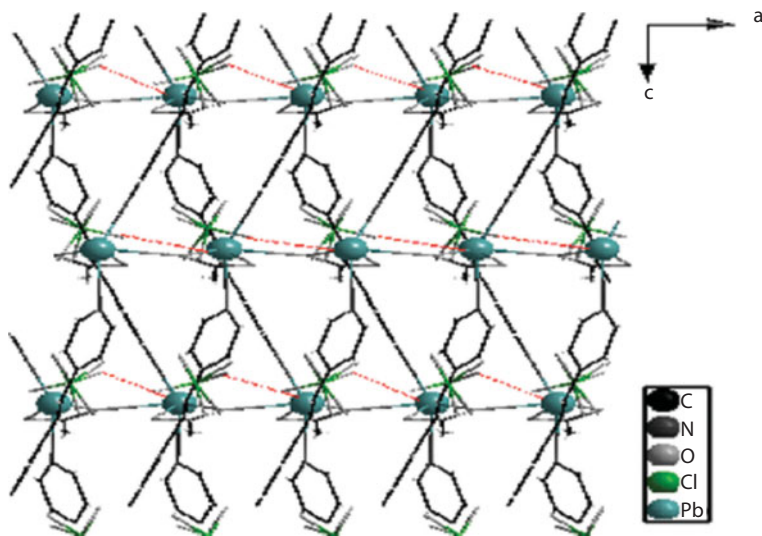


Figure 6.7 Fragment of the two-dimensional layer in $\{[\text{Pb}(\mu\text{-OAc})(\mu\text{-ebp})](\text{ClO}_4)\}_n$ viewed along the b-axis.

6.5.1.3 Three-Dimensional Coordination Polymers

Compounds $[\text{Pb}_9(\text{L-2H})_3(\text{ClO}_4)_6(\text{OH})_6] \{ \text{L: calix[4]diquinone bis(acid); sac, saccharinate; trz, 1,2,4-triazole} \}$ [66], $[\text{Pb}(\text{H}_2\text{O})(\mu\text{-OAc})(\mu\text{-sac})]_n$ [67] and $[\text{Pb}_2(\text{trz})_2(\text{OAc})(\text{NO}_2)]_n$ form three-dimensional coordination polymers. In compound $[\text{Pb}_9(\text{L-2H})_3(\text{ClO}_4)_6(\text{OH})_6]$ there are three independent lead(II) atoms in its structure. The lead(II) atom is ten or eleven coordinate and the $[\text{Pb}_9(\text{L-2H})_3(\text{ClO}_4)_6(\text{OH})_6]$ trimer contains a small channel around the 3-fold axis filled with disordered solvent molecules. In addition there is a much larger channel that is relatively free from significant electron density though the presence of highly mobile and thus disordered solvent molecules cannot be ruled out.

6.6 Nano Lead(II) Coordination Polymers

The sonochemical method has been used for preparation of nano-scale lead(II) coordination polymers. Sonochemistry is the research area in which molecules undergo a reaction due to the application of powerful ultrasound radiation (20 kHz–10 MHz) [68]. Ultrasound induces chemical or physical changes during cavitation, a phenomenon involving the formation, growth, and instantaneously implosive collapse of bubbles in a liquid, which can generate local hot spots having temperatures of roughly 5000 °C, pressures of about 500 atm, and a lifetime of a few microseconds [69]. These extreme conditions can drive chemical reactions, but they can also promote the formation of nano-sized particles, mostly by the instantaneous formation of a plethora of crystallization nuclei [69, 70]. This has been widely used to fabricate nano-sized particles of a variety of compounds, and in recent years many kinds of nano-sized materials have been prepared by this method [71–76].

Nano-structures of two new Pb(II) three-dimensional coordination polymers, $[\text{Pb}_2(4\text{-pyc})_2\text{I}_2(\text{H}_2\text{O})]_n$ (1), {4-Hpyc = 4-pyridinecarboxylic acid} and $[\text{Pb}(3\text{-pyc})\text{I}]_n$ (2), {3-Hpyc = 3-pyridinecarboxylic acid} were synthesized by sonochemical method.

The new nano-structures were characterized by scanning electron microscopy, X-ray powder diffraction, IR spectroscopy and elemental analyses. The thermal stability of compounds 1 and 2 both their bulk and nano-size were studied by thermal gravimetric and differential thermal analyses and compared. PbO block-structures were obtained by calcination of the nano-structures of compounds 1 and 2 at 400 °C. The compounds 1 and 2 were obtained by reaction of 4-pyridinecarboxylate (4-pyc⁻) or 3-pyridinecarboxylate (3-pyc⁻) and sodium iodide with lead(II) acetate trihydrate in water. Single crystalline material was obtained using a heat gradient applied to an aqueous solution of the reagents (the “branched tube method”) and nano-structured particles were prepared by ultrasonication of the aqueous solution.

The carboxylate moiety of the “pyc” ligand in compounds 1 and 2 acts as both a bidentate and a bridging group (totally tridentate) in a μ -1,3 mode, where two oxygen atoms of the carboxylate group bidentately coordinate to a lead(II) ion, creating a four-membered chelate ring. One of them also bridges two adjacent lead(II) ions, yielding a three-dimensional coordination polymer. The coordination number in 1 is seven and each lead atom is coordinated by three oxygen atoms of 4-pyc⁻ ligands, one oxygen atom of water molecule, one nitrogen atoms of 4-pyc⁻ anion and two iodide atoms (Figure 6.8a). In compound 2 also the Pb(II) atoms are bridged by the 3-pyc⁻ and I⁻ anions. The coordination number in 2 is also seven and each lead atom is coordinated by three oxygen atoms of 3-pyc⁻ ligands, one nitrogen atoms of 3-pyc⁻ anions and three iodide atoms (Figure 6.8b).

The SEM photographs show that the compounds 1 and 2 have nano-fiber (Figure 6.9) and nano-particles (Figure 6.10) morphologies, respectively. For further investigation have been used other solvents such as methanol, acetonitrile, dichloromethane, benzene and chloroform by the sonochemical process, but the particle sizes of compounds were not completely good [77].

In compound $\{[\text{Pb}(\text{bpacb})(\text{OAc})].\text{DMF}\}_n$, {Hbpacb: 3,5-bis[(4-pyridylamino)carbonyl]benzoic acid} the Pb(II) atoms are in the hemidirected geometry. One of oxygen atoms from bpacb⁻ ligand

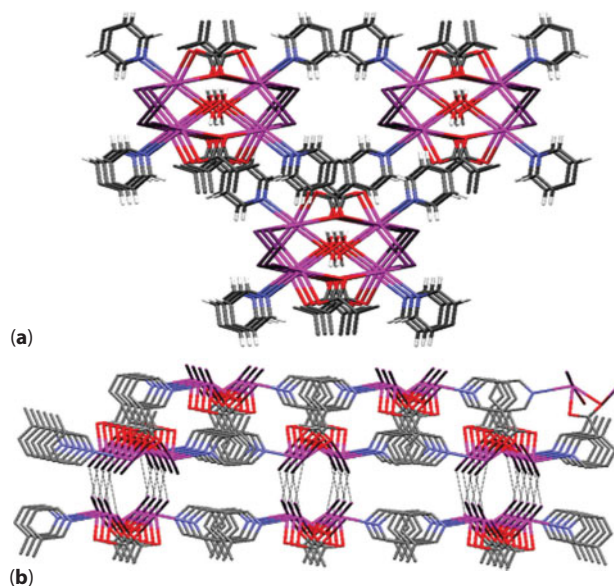


Figure 6.8 A fragment of the three-dimensional polymer and showing Pb---I interactions (a) in compound (1) and (b) in compound (2).

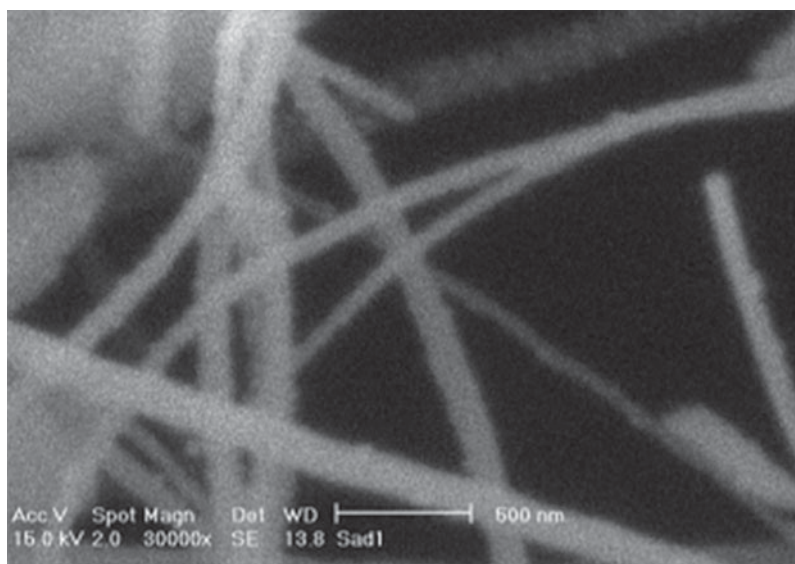


Figure 6.9 SEM photographs of $[\text{Pb}_2(4\text{-pyc})_2\text{I}_2(\text{H}_2\text{O})]_n$ (1) nano-fibers.

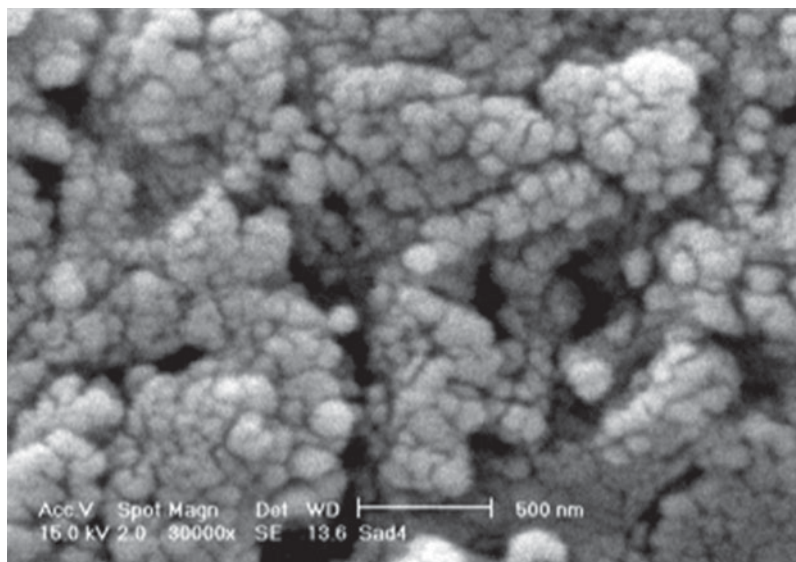


Figure 6.10 SEM photographs of $[\text{Pb}(3\text{-pyc})\text{I}]_n$ (2) nano-particles [77].

is a bridging (μ^2) and connects lead(II) atoms to each other. The polymeric structure has large pores that consist of DMF as guest molecules and the hydrogen bonding is the important interaction for DMF stability in pores. Oxygen atoms of DMF molecule and acetate anion connect to amidic nitrogen of terminal pyridine rings of ligand bpacb^- by hydrogen bonding ($\text{O}\cdots\text{N}-\text{H}$) (Figure 6.11a). The nano-sized compound $\{[\text{Pb}(\text{bpacb})(\text{OAc})]\cdot\text{DMF}\}_n$ is prepared by ultrasonic irradiation and characterized by powder XRD and SEM. The average size of the particles is 60 nm (Figure 6.11b) [78].

Also nanobelts of a lead(II) coordination polymer in $[\text{Pb}(3\text{-pyc})_2]_n$, are synthesized by a sonochemical method with average size of about 90 nm (Figure 6.12b). The carboxylate moiety of the 3-pyc $^-$ ligand acts in chelating (μ^2) mode, where two oxygen atoms of the carboxylate group bidentately coordinate to a lead(II) ion, creating a four-membered chelate rings (Figure 6.12a) [79].

In $[\text{Pb}(2\text{-pyc})(\text{N}_3)(\text{H}_2\text{O})]_n$ [80] the lead(II) ion is coordinated by 2-pyc $^-$, water and N_3^- ligand and coordination number in this complex is six. The building blocks of $[\text{Pb}_2(\mu\text{-H}_2\text{O})_2]$ are bridged by the N_3^- and 2-pyc $^-$ anions and each lead(II) atom is coordinated

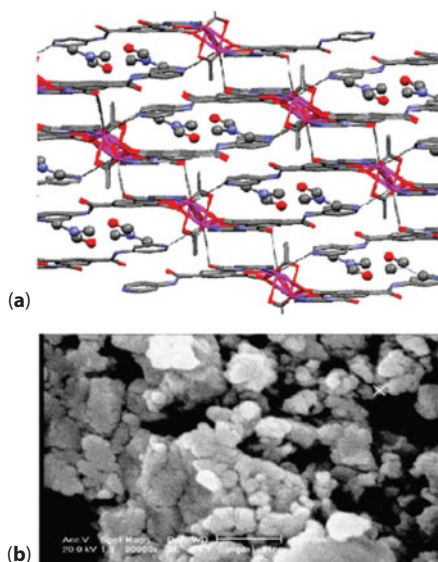


Figure 6.11 (a) A perspective view of the packing down the b-axis in compound $\{[\text{Pb}(\text{bpac})(\text{OAc})]\cdot\text{DMF}\}_n$, showing the free DMF molecules lying in the pores and (b) SEM image of nano-sized compound $\{[\text{Pb}(\text{bpac})(\text{OAc})]\cdot\text{DMF}\}_n$ [78].

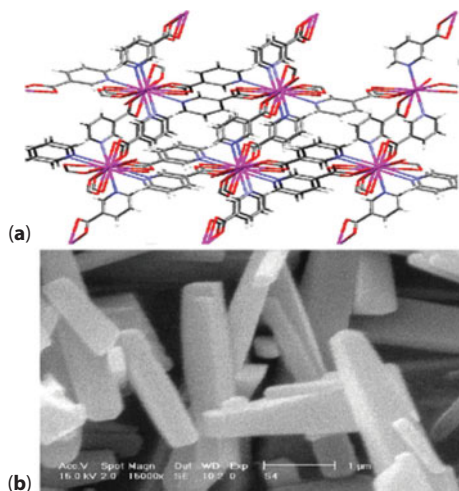


Figure 6.12 (a) Depiction of three-dimensional network in compound $[\text{Pb}(\text{3-pyc})_2]_n$ and (b) SEM photograph of compound $[\text{Pb}(\text{3-pyc})_2]_n$ nanobelts [79].

by three oxygen atoms of 2- pyc^- ligands, two water molecules and three nitrogen atoms of azide anions. The carboxylate moiety of the 2- pyc^- ligand acts as a bridging group where two oxygen atoms of the carboxylate group bidentately coordinate to a lead(II) ion, creating a four-membered chelate ring (Figure 6.13a). One of them also bridges two adjacent lead(II) ions. There is not any vacant site on lead(II) environment and the X–Pb–X angle shows that the coordination sphere of the lead(II) is holodirected. Nanostructure of compound $[\text{Pb}(\text{2-pyc})(\text{N}_3)(\text{H}_2\text{O})]_n$ is prepared by sonochemical method and the SEM shows that it is composed of rods with size of about 80 nm, with all rods arranged so that they form a strawberry network (Figure 6.13b).

Two isostructure lead(II) complexes, $[\text{Pb}_2(\text{2-pyc})_2(\text{I})_2]_n$ and $[\text{Pb}_2(\text{2-pyc})_2(\text{Br})_2]_n$ [81], are synthesized by a sonochemical method and produce the nano-sized coordination polymers. The average size of the particles is around 98 and 95 nm for compounds $[\text{Pb}_2(\text{2-pyc})_2(\text{I})_2]_n$ and $[\text{Pb}_2(\text{2-pyc})_2(\text{Br})_2]_n$, respectively. The carboxylate moiety of the pyc^- ligand in these compounds acts as both a bi-donor and a bridging group (totally tri-donor) in a $\mu_2-\mu^2:\mu^1$ mode (Figures 6.14 and 6.15).

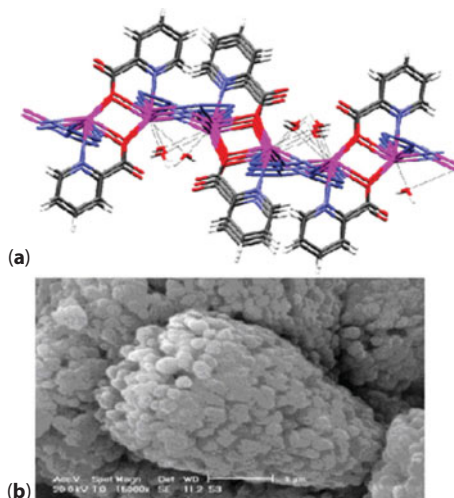


Figure 6.13 (a) Fragment of the two-dimensional polymer in $[\text{Pb}(\text{2 pyc})(\text{N}_3)(\text{H}_2\text{O})]_n$ and (b) SEM photograph of compound $[\text{Pb}(\text{2-pyc})(\text{N}_3)(\text{H}_2\text{O})]_n$ nano-strawberry [80].

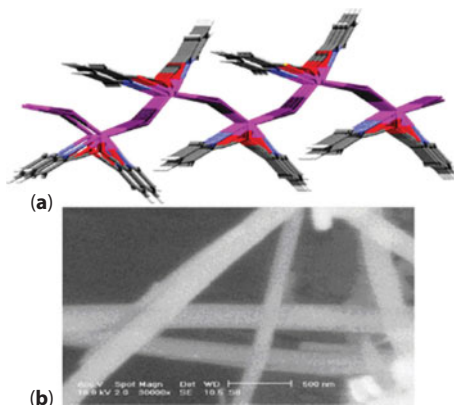


Figure 6.14 (a) A two-dimensional packing of compound $[\text{Pb}_2(2\text{-pyc})_2(\text{I})_2]_n$ and (b) SEM photograph of compound $[\text{Pb}_2(2\text{-pyc})_2(\text{I})_2]_n$ nano-wires [81].

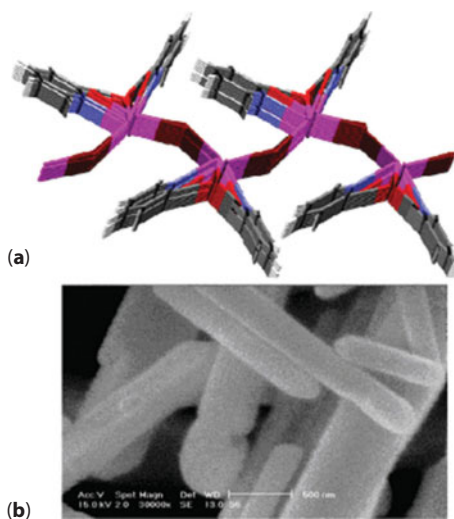


Figure 6.15 (a) A two-dimensional packing of compound $[\text{Pb}_2(2\text{-pyc})_2(\text{Br})_2]_n$ and (b) SEM photograph of compound $[\text{Pb}_2(2\text{-pyc})_2(\text{Br})_2]_n$ nano-rods [81].

Reaction of 1,6-bis(2-pyridyl)-2,5-diaza-1,5-hexadiene (2-bpdbe) and lead(II) nitrate lead to the formation of a new lead(II) complex $[\text{Pb}_2(\mu\text{-2-bpdbe})_2(\text{NO}_3)_4]_n$. single crystalline material was obtained using a thermal gradient. Determination of the structure of 1 by X-ray crystallography showed the Pb(II) ion to be coordinated by

nitrate and 1,6-bis(2-pyridyl)-2,5-diaza-1,5-hexadiene ligands. The structure consists of Pb(II) units coordinated by NO_3^- and 2-bpdbe ligands that form infinite layers as illustrated (Figure 6.16). This is an eight-coordinate complex with a PbO_4N_4 chromophore. The structure is considered a coordination polymer of Pb(II) of linear chains that run parallel to the c-axis, with a building block of $[\text{Pb}_2(\text{NO}_3)_2]_n$. The X–Pb–Y angles suggest a hole in the coordination sphere of the Pb(II) ion due to a stereo-chemically active lone pair. The Pb(II) ion, thus, has a hemidirected geometry as is observed for Pb(II) with high coordination numbers (9–10) [82]. The activity of the lone pair in the coordination sphere of Pb atoms in $[\text{Pb}_2(\mu\text{-2-bpdbe})_2(\text{NO}_3)_4]_n$ is probably due to the presence of eight hard donor O and N atoms.

Nano-sized $[\text{Pb}_2(\mu\text{-2-bpdbe})_2(\text{NO}_3)_4]_n$ was obtained by ultrasonic irradiation in a MeOH solution. An SEM micrograph shows a broad distribution of the particle size, the average size of the particles is 40 nm, which is in agreement with that observed by scanning electron microscopy, as shown in Figure 6.17 [83].

In other report, 3-bpdh and $\text{Pb}(\text{NO}_3)_2$ lead to the formation of a new lead(II) 2D coordination polymer, $[\text{Pb}_2(3\text{-bpdh})(\mu\text{-NO}_3)_3(\text{NO}_3)]_n$. Single crystalline material was obtained using a slow evaporation.

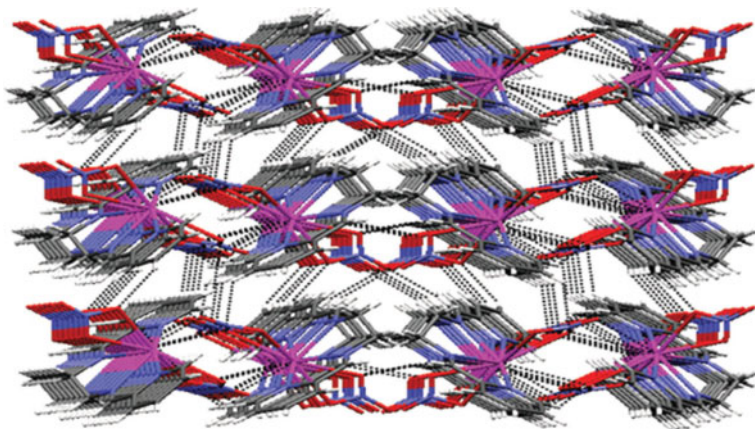


Figure 6.16 3-D supramolecular compound $[\text{Pb}_2(\mu\text{-2-bpdbe})_2(\text{NO}_3)_4]_n$ formed by π - π stacking and weak hydrogen-bonding.

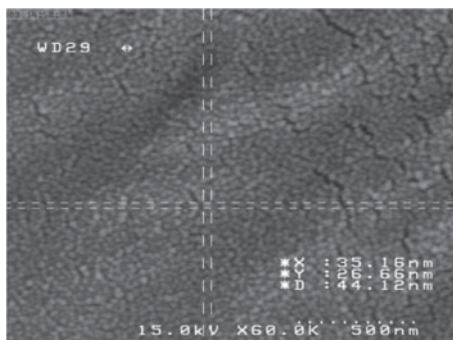


Figure 6.17 SEM photograph of compound $[\text{Pb}_2(\mu\text{-2-bpdbe})_2(\text{NO}_3)_4]_n$ nanopowder produced by the sonochemical method.

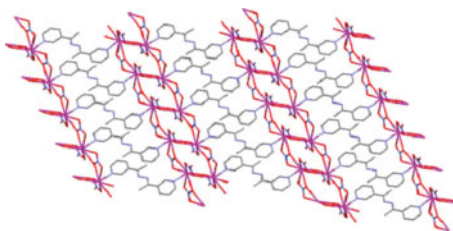


Figure 6.18 Showing the 2D structure of $[\text{Pb}_2(\mu\text{-3-bpdh})(\mu\text{-NO}_3)_3(\text{NO}_3)]_n$.

Single crystal X-ray diffraction analysis reveals that the lead(II) ion is coordinated by four nitrate anions and one neutral 3-bpdh molecule, and results in a nine-coordinate complex with a PbO_8N chromophore. Although the coordination geometry around lead is irregular, presumably associated with steric constraints arising from the shape of the ligands, it is best described as a distorted mono-capped pentagonal prism. On the other hand, the structure may be considered a coordination polymer of lead(II) consisting of one-dimensional linear chains running parallel to the *c* axis, with a building block of $[\text{Pb}_2(\mu\text{-NO}_3)_3(\text{NO}_3)]_n$ (Figure 6.18).

Nano-sized $[\text{Pb}_2(3\text{-bpdh})(\mu\text{-NO}_3)_3(\text{NO}_3)]_n$ was obtained by ultrasonic irradiation in a water solution. The SEM image (Figure 6.19) shows a broad distribution of the particle size with an average particle size of 95 nm [84].

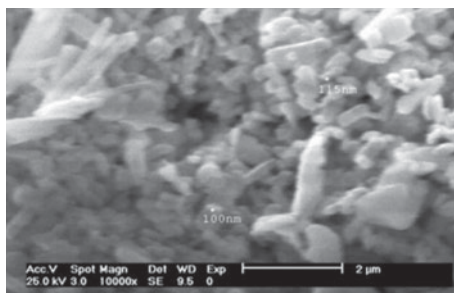


Figure 6.19 SEM photographs of $[\text{Pb}_2(3\text{-bpdh})(\mu\text{-NO}_3)_3(\text{NO}_3)]_n$ nanoparticles produced sonochemically.

6.7 Conclusion

Lead(II), with its large radius, flexible coordination environment and various stereo-chemical activities, provides unique opportunities for formation of unusual network topologies with interesting properties. Lead(II) compounds are a potential class of functional materials and ideal systems for investigation of structure–property relationships. The largest class of coordination polymers is those containing carboxylate ligands and until now a variety of hybrid materials with different dimensions has been designed with the use of carboxylate groups. The carboxylate group due to its rich coordination modes usually binds either a mono-donor, a bi-donor, a tri-donor or a tetra-donor to a metal ion and lead(II) forms discrete, one-, two- and three-dimensional coordination polymers. Also lead(II) can form one-, two- and three-dimensional coordination polymer via secondary interactions such as, hydrogen-bonding, π – π stacking interactions and non-covalent bonding. The different coordination modes of carboxylate groups increase the strength and stability of the resulting architectures. Carboxylate groups in the lead(II) coordination polymers have been coordinated in binding modes ranging from μ^1 , bridging (μ^2 – μ^1 : μ^1), chelating (μ^2), bridging (μ_2 – μ_2), bridging (μ_3 – μ^1 : μ^2), chelating, bridging (μ_2 – μ^2 : μ^1) to chelating, bridging (μ_3 – μ^1 : μ^2 : μ^1) and chelating, bridging (μ_4 – μ^2 : μ^2). So, the researchers found that carboxylate groups in many of lead(II) coordination polymers form more than one type of coordination

mode and among all of these modes maximum number belonged to chelating (μ^2) mode.

References

1. Soudi, A.A., Morsali, A. and Moazzenchi, S. A first 1,2,4-triazole PbII Complex: Thermal, spectroscopic and structural studies, $[\text{Pb}_2(\text{trz})_2(\text{CH}_3\text{COO})(\text{NO}_2)]_n$. *Inorganic Chemistry Communications*, 9(12), p. 1259–1262, 2006.
2. Casas, J.S., *et al.*, New insights on the Lewis acidity of diorganolead (IV) compounds: Diphenyllead (IV) complexes with N, O, S-chelating ligands. *Polyhedron*, 27(1), p. 1–11, 2008.
3. Di Vaira, M., Mani, F. and Stoppioni, P. Lead(II) and Bismuth(III) Complexes with Macrocyclic Ligands. *European Journal of Inorganic Chemistry*, 1999(5), p. 833–837, 1999.
4. Davidovich, R.L., *et al.*, Stereochemistry of lead(II) complexes with oxygen donor ligands. *Coordination Chemistry Reviews*, 253(9–10), p. 1316–1352, 2009.
5. Zhang, K.-L., *et al.*, Syntheses, characterization and luminescent properties of two lead(II) fumarate metal-organic frameworks. *Polyhedron*, 28(4), p. 647–652, 2009.
6. Mahjoub, A.R. and Morsali, A. Syntheses and characterization of lead(II) salts with 4, 4'-bithiazole ligand: X-ray crystal structures of $[(\text{BTZ})_2\text{Pb}(\text{NO}_3)_2]$ and $[(\text{BTZ})\text{Pb}(\text{SCN})_2]_n$ (a new polymeric compound). *Polyhedron*, 21(2), p. 197–203, 2002.
7. Ahmadzadi, H., Marandi, F. and Morsali, A. Structural and X-ray powder diffraction studies of nano-structured lead(II) coordination polymer with $\eta^2 \text{Pb} \cdots \text{C}$ interactions. *Journal of Organometallic Chemistry*, 694(22), p. 3565–3569, 2009.
8. Marandi, F., Morsali, A. and Soudi, A.A. Labile Interactions in Aza-aromatic Base Adducts of Lead(II) Thenoyltrifluoroacetate. *Zeitschrift für anorganische und allgemeine Chemie*, 633(4), p. 661–665, 2007.
9. Morsali, A. and Ramazani, A. One-Dimensional Holodirected Lead(II) Coordination Polymer, $[\text{Pb}(\mu_2\text{-TPPZ})(\text{NO}_3)(\text{ClO}_4)]_n$ (TPPZ = 2, 3, 5, 6-tetra(2-pyridyl)pyrazine). *Zeitschrift für anorganische und allgemeine Chemie*, 631(10), p. 1759–1760, 2005.
10. Soudi, A.A., *et al.*, $[\text{Pb}_2(2,2'\text{-bipy})_2(\mu\text{-}4,4'\text{-bipy})(\text{NO}_3)_4]$: A novel hemidirected dimeric mixed-ligands lead(II) complex extended in

- holodirected two-dimensional polymer by weak Pb–Onitrate interactions. *Inorganic Chemistry Communications*, 8(9), p. 773–776, 2005.
11. Hu, M.L., *et al.*, Synthesis and crystal structure of two novel PbII compounds of $[\text{Pb}(\text{endc})_2(\text{phen})]_n$ and $[\text{Pb}(\text{endc})(\text{phen}) \cdot 3\text{H}_2\text{O}]_2$. *Inorganic Chemistry Communications*, 9(9), p. 962–965, 2006.
 12. Morsali, A. and Mahjoub, A. The first hemidirected nine coordinate lead(II) complex, crystal and molecular structure of $[\text{Pb}(\text{BzImH})_2\text{py}(\text{H}_2\text{O})_2(\text{NO}_3)_2] \cdot (\text{BzImH})_2\text{py} \cdot \text{H}_2\text{O}$, ($\text{BzImH})_2\text{py}$ =2,6-Bis(2-benzimidazolyl)pyridine. *Inorganic Chemistry Communications*, 7(7), p. 915–918, 2004.
 13. Abedini, J., Morsali, A. and Zeller, M. Three-dimensional Hemidirected Mixed-ligand Lead(II) Coordination Polymer, $[\text{Pb}_2(\text{bpa})_2(\text{SCN})_3(\text{NO}_3)]_n$ (bpa = 1,2-di(4-pyridyl)ethane). *Zeitschrift für anorganische und allgemeine Chemie*, 634(14), p. 2659–2662, 2008.
 14. Marandi, F., *et al.*, A Novel 1D Coordination Polymer $[\text{Pb}(\text{phen})(\mu\text{-N}_3)(\mu\text{-NO}_3)]_n$ with the First $\text{Pb}_2(\mu\text{-N}_3)_2$ Unit (phen = 1,10-phenanthroline). *Zeitschrift für anorganische und allgemeine Chemie*, 632(15), p. 2380–2382, 2006.
 15. Aslani, A., *et al.*, 2D Holodirected lead(II) bromide coordination polymers constructed of rigid and flexible ligands. *Inorganica Chimica Acta*, 362(5), p. 1506–1510, 2009.
 16. Morsali, A. and Mahjoub, A. Coordination polymers of lead(II) with 4,4'-bipyridine: syntheses and structures. *Polyhedron*, 23(15), p. 2427–2436, 2004.
 17. Askarinejad, A., Morsali, A. and Zhu, L.-G. Secondary interactions in thallium(I) coordination, $[\text{Tl}_2(\text{DBM})_2]_n$, DBM= 1, 3-diphenylpropane-1, 3-dionate (dibenzoylmethanide). *Solid State Sciences*, 8(5), p. 537–540, 2006.
 18. Shimoni-Livny, L., Glusker, J.P. and Bock, C.W. Lone Pair Functionality in Divalent Lead Compounds. *Inorganic Chemistry*, 37(8), p. 1853–1867, 1998.
 19. Aslani, A. and Morsali, A. Sonochemical synthesis of nano-sized metal-organic lead(II) polymer: A precursor for the preparation of nano-structured lead(II) iodide and lead(II) oxide. *Inorganica Chimica Acta*, 362(14), p. 5012–5016, 2009.
 20. Aslani, A., *et al.*, Hydrothermal and sonochemical synthesis of a nano-sized 2D lead(II) coordination polymer: A precursor for nano-structured PbO and PbBr 2. *Journal of Molecular Structure*, 929(1), p. 187–192, 2009.

21. Noshiranzadeh, N., *et al.*, Novel coordination mode of chloride ion in holo- and hemidirected one-dimensional PbII coordination polymer. *Inorganic Chemistry Communications*, 10(7), p. 738–742, 2007.
22. Aslani, A., Morsali, A. and Zeller, M. Novel homochiral holodirected three-dimensional lead(II) coordination polymer, $[\text{Pb}_2(\mu\text{-bpa})_3(\mu\text{-NO}_3)_2(\text{NO}_3)_2]_n$: Spectroscopic, thermal, fluorescence and structural studies. *Solid State Sciences*, 10(7), p. 854–858, 2008.
23. Morsali, A., 2,9-Dimethyl-1,10-phenanthroline as Ligand in the Holo- and Hemidirected 1:1 and 1:2 Lead(II) Complexes. *Z. Naturforsch.* 60b, p. 149–154, 2005.
24. Marandi, F., *et al.*, New mixed-anion 2-aminomethylpyridine (AMP) lead(II) complexes, $\text{Pb}(\text{AMP})_n(\text{ClO}_4)_X$, ($X=\text{CH}_3\text{COO}$ and $n=1$ or $X=$ and $n=2$); crystal and molecular structure of $[\text{Pb}(\text{AMP})_2](\text{ClO}_4)(\text{NO}_3)$. *Journal of Coordination Chemistry*, 58(14), p. 1233–1239, 2005.
25. Davidovich, R.L., Stavila, V. and Whitmire, K.H. Stereochemistry of lead(II) complexes containing sulfur and selenium donor atom ligands. *Coordination Chemistry Reviews*, 254(17–18), p. 2193–2226, 2010.
26. Morsali, A., Mahjoub, A.R. and Hosseini, A. Syntheses and characterization of lead(II) complexes, $\text{Pb}(\text{dmphen})X$ 2 and $\text{dmphen}=2,9\text{-dimethyl-1,10-phenanthroline}$, and crystal structure of $[\text{Pb}(\text{dmphen})(\text{NO}_3)_2]_n$, a new polymeric compound with holodirected geometry. *Journal of Coordination Chemistry*, 57(8), p. 685–692, 2004.
27. Morsali, A., Two new lead(II) nitrite complexes, crystal structure of $[\text{Pb}(\text{phen})_2(\text{NO}_2)_2]$ an eight-coordinate lead(II) complex. *Journal of Coordination Chemistry*, 58(17), p. 1531–1539, 2005.
28. Abedini, J., *et al.*, Lead(II) complexes of 2,2'-diamino-4,4'-bithiazole (DABTZ) including crystal structure of a novel 1D chain polymer, $[\text{Pb}(\text{DABTZ})(\mu\text{-SCN})(\mu\text{-NO}_3)]_n$. *Journal of Coordination Chemistry*, 58(18), p. 1719–1726, 2005.
29. Soudi, A.A., *et al.*, 1D & 2D Supramolecular assemblies dominated by crystal structure of Pb(II) oxoanion (and) complexes with 3-(2-pyridyl)-5,6-diphenyl-1,2,4-triazine (PDPT). *Journal of Coordination Chemistry*, 59(10), p. 1139–1148, 2006.
30. Morsali, A., Mercury(II) and Lead(II) complexes with 2,2'-Bis(4,5-dimethylimidazole) – syntheses, characterization and crystal structures of $[\text{M}(\text{DmImH})(\text{SCN})_2]$, ($\text{M}=\text{Hg}$ and Pb). *Journal of Coordination Chemistry*, 59(9), p. 1015–1024, 2006.

31. Souidi, A.A., *et al.*, Lead(II): misleading or merely hermaphroditic? *C. R. Chim*, 8 p. 157–168, 2005.
32. Ilyukhin, A.B., *et al.*, Crystal structures of lead(II) complexes with anions of iminodiacetic, hydroxyethyliminodiacetic, nitrilotriacetic, hexamethylene-1,6-diaminetetraacetic, and diethylenetriaminepentaacetic acids, *Kristallografiya* 43, p. 812–828, 1998.
33. Guo, H.M. Zhang, B.-S. Wang, Y.H. Crystal structure of bis(1,10-phenanthroline-N,N')bis(2-chlorobenzoato)-lead(II) hydrate (1:2.5), $[\text{Pb}(\text{C}_7\text{H}_4\text{O}_2\text{Cl})_2(\text{C}_{12}\text{H}_8\text{N}_2)_2] \cdot 2.5\text{H}_2\text{O}$ *Z. Kristallogr, New Cryst. Struct*, 221 p. 352–354, 2006.
34. Aghabozorg, H. Ghasemikhah, P. Ghadermazi, M. Sheshmani, S. Piperazinedium bis(pyridine-2,6-dicarboxylato)plumbate(II) dihydrate, *Acta Crystallogr. Sect. E: Struct. Rep. Online* 62, p. m2835–m2837, 2006.
35. Zhang, B.S. Crystal structure of (2,2'-bipyridine-N,N')bis(2-fluorobenzoato)lead(II), $\text{Pb}(\text{C}_7\text{H}_4\text{O}_2\text{F})_2(\text{C}_{10}\text{H}_8\text{N}_2)_2$, *Z. Kristallogr, New Cryst. Struct.* 221 p. 355, 2006.
36. Davidovich, R.L. Popov, D.Y. Gerasimenko, A.V. Logvinova, V.B. Neorg. Zh. *Khim.* 49 p. 574, 2004.
37. Sharif, M.A., *et al.*, Novel Proton Transfer Compounds Containing 2,6-Pyridinedicarboxylic Acid and Melamine and Their PbII Complex: Synthesis, Characterization, Crystal Structure and Solution Studies, *Polish Journal of Chemistry*. 80 p. 847–863, 2006.
38. Xiao, H.P. Yuan, J.X. Bis(hydrogen 5-nitroisophthalato)(1,10-phenanthroline)lead(II) monohydrate, *Acta Crystallogr. Sect. E: Struct. Rep. Online* 60, p. m1501–m1503, 2004.
39. Zhang, B.S. Crystal structure of bis(1,10-phenanthroline-N,N')-bis(2-bromobenzoato)lead(II) hydrate (1:2.5), $[\text{Pb}(\text{C}_7\text{H}_4\text{O}_2\text{Br})_2(\text{C}_{12}\text{H}_8\text{N}_2)_2] \cdot 2.5\text{H}_2\text{O}$. *Z. Kristallogr, Z. Kristallogr, New Cryst. Struct.* 221 p. 511, 2006.
40. Zhang, W., *et al.*, Synthesis and Crystal Structure of Complex $[\text{Pb}(\text{qina}) \sim 2(\text{DMSO})] \cdot \text{H} \sim 2\text{O}$. *Chinese Journal of Structural Chemistry*, 26(3), p. 357, 2007.
41. A.L. Poznyak, G.N. Kupriyanova, I.F. Burshtein, A.B. Ilyukhin, *Koord. Khim.* 24 (1998) 825.
42. Pellissier, A., *et al.*, Relating Structural and Thermodynamic Effects of the Pb(II) Lone Pair: A New Picolinate Ligand Designed to Accommodate the Pb(II) Lone Pair Leads to High Stability and Selectivity. *Inorganic Chemistry*, 46(9), p. 3714–3725, 2007.

43. Zhao, Y.-H., *et al.*, A Series of Lead(II)-Organic Frameworks Based on Pyridyl Carboxylate Acid N-Oxide Derivatives: Syntheses, Structures, and Luminescent Properties. *Crystal Growth & Design*, 8(10), p. 3566–3576, 2008.
44. Marandi, F. and N. Shahbakhsh, Lead(II) complexes of proline. *Journal of Coordination Chemistry*, 60(23), p. 2589–2595, 2007.
45. Tiekink, E.R., Molecular architecture and supramolecular association in the zinc-triad 1, 1-dithiolates. Steric control as a design element in crystal engineering? *CrystEngComm*, 5(21), p. 101–113, 2003.
46. Li, X., *et al.*, Syntheses and Characterizations of Multidimensional Metal-Organic Frameworks Based on Rings and 1D Chains. *European Journal of Inorganic Chemistry*, 2005(2), p. 321–329.
47. Peedikakkal, A.M.P., Koh, L.L. and Vittal, J.J. Photodimerization of a 1D hydrogen-bonded zwitter-ionic lead(ii) complex and its isomerization in solution. *Chemical Communications*, 2008(4), p. 441–443.
48. Zhao, Y.-H., *et al.*, Syntheses, Characterization, and Luminescent Properties of Three 3D Lead–Organic Frameworks with 1D Channels. *Crystal Growth & Design*, 7(3), p. 513–520, 2007.
49. Bhattacharyya, P., Parr, J. and Slawin, A.M.Z. Novel bimetallic lead(II) complexes of polydentate amine-phenol ligands. *Inorganic Chemistry Communications*, 2(3), p. 113–115, 1999.
50. Kiosse, G.A. Bologa, O.A. Filippova, I.G. Gerbeleu, N.V. Lozan, V.I. *Kristallografiya*. 42, p. 1041, 1997.
51. Liu, B.X. Nie, J.J. Xu, D.J. *Catena-Poly[(2,2'-diamino-4,4'-bi-1,3-thiazole- κ 2N,N')lead(II)]-di- μ -isonicotinato- κ 4O:O']*, *Acta Crystallogr. Sect. E: Struct. Rep.* Online 62, p. m2122–m2124, 2006.
52. Zhu, L.-H., *et al.*, Hydrothermal Synthesis and Crystal Structure of a New Oxalato-bridged Lead(II) Polymer: {[Pb(phen)₂(ox)]·5H₂O}_n (phen = 1, 10-phenanthroline, ox = oxalate). *Zeitschrift für anorganische und allgemeine Chemie*, 630(6), p. 952–955, 2004.
53. M.Q. Cheng, L.F. Ma, L.Y. Wang, Crystal structure of catena-[(1,10-phenanthroline-N,N')- bis(μ -acetato-O,O')lead(II)], Pb(C₁₂H₈N₂)(CH₃COO)₂. *Z. Kristallogr, New Cryst. Struct.* 221 p. 299–300, 2006.
54. Huang, G. *et al.*, *Poly[(μ_2 -aqua- κ^2 O:O)(μ_3 -azido- κ^3 N1:N1:N³)(μ_2 -isonicotinato- κ^2 O:O')lead(II)]*, *Acta Crystallogr. Sect. C: Cryst. Struct. Commun.* 64, m369–m371, 2008.
55. Fard-Jahromi, M.J.S. and Morsali, A. *Sonochemical synthesis of nanoscale mixed-ligands lead(II) coordination polymers as*

- precursors for preparation of $Pb_2(SO_4)O$ and PbO nanoparticles; thermal, structural and X-ray powder diffraction studies. *Ultrasonics sonochemistry*, 17(2), p. 435–440, 2010.
56. Du, Z.-Y., Ying, S.-M. and Mao, J.-G. Two new lead(II) diphosphonates with second ligands as an intercalated species or a multidentate metal linker. *Journal of Molecular Structure*, 788(1–3), p. 218–223, 2006.
 57. Swamy, K.C.K., Day, R.O. and Holmes, R.R. A new structural form of tin in a cubic cluster. *Journal of the American Chemical Society*, 109(18), p. 5546–5548, 1987.
 58. Zhang, L.-P. and Zhu, L.-G. Influence of neutral amine ligands on the network assembly of lead(II) 4-sulfobenzoate complexes. *Journal of Molecular Structure*, 873(1–3), p. 61–68, 2008.
 59. Wagner, C. Merzweiler, K., *Poly[[diaqua(μ_4 -3-sulfonatobenzoato) lead(II)] 4,4'-bipyridine]*, *Acta Crystallogr. Sect. E: Struct. Rep.* 63 p. m111–m113, 2007.
 60. Aslani, A., Morsali, A. and Zeller, M. Nano-structures of two new lead(II) coordination polymers: New precursors for preparation of PbS nano-structures. *Solid State Sciences*, 10(11), p. 1591–1597, 2008.
 61. Wang, X.-W., *et al.*, A Novel Chiral Doubly Folded Interpenetrating 3D Metal–Organic Framework Based on the Flexible Zwitterionic Ligand. *Crystal Growth & Design*, 7(6), p. 1027–1030, 2007.
 62. Sadeghzadeh, H., Morsali, A. and Retailleau, P. Ultrasonic-assisted synthesis of two new nano-structured 3D lead(II) coordination polymers: Precursors for preparation of PbO nano-structures. *Polyhedron*, 29(2), p. 925–933, 2010.
 63. Morsali, A., Payeghader, M. and Monfared, S.S. A New Polymer of Mixed-Anions Complex $[Pb(phen)(O_2CCH_3)(O_2NO)]_n$ (phen=1,10-phenanthroline). *Zeitschrift für anorganische und allgemeine Chemie*, 628(1), p. 12–14, 2002.
 64. Hall, A.K., *et al.*, Bonds and lone pairs in the flexible coordination sphere of lead (II). *CrystEngComm*, 2(13), p. 82–85, 2000.
 65. Morsali, A., *et al.*, Two-Dimensional Holo- and Hemidirected Lead(II) Coordination Polymers: Synthetic, Spectroscopic, Thermal, and Structural Studies of $[Pb(\mu-SCN)_2(\mu-ebp)]_{1.5}_n$ and $\{[Pb(\mu-OAc)(\mu-ebp)(ClO_4)]_n$ (ebp=4,4'-[(1E)-Ethane-1,2-diyl] bis[pyridine]; OAc=Acetato). *Helvetica Chimica Acta*, 88(9), p. 2513–2522, 2005.
 66. Beer, P.D., *et al.*, Studies of lead(II) complexes of substituted calix[4] diquinones: the remarkable self-assembly of a novel redox-active 3D channel network. *CrystEngComm*, 2(30), p. 164–168, 2000.

67. Yilmaz, V.T., *et al.*, A Three—Dimensional Lead(II) Polymer with Bridging Saccharinate and Unusually Coordinated Acetate Ligands — Synthesis, IR Spectra, and Crystal Structure of $[\text{Pb}(\text{H}_2\text{O})(\mu\text{-OAc})(\mu\text{-sac})]_n$. *Zeitschrift für anorganische und allgemeine Chemie*, 629(1), p. 172–176, 2003.
68. Suslick, K.S., *et al.*, Sonochemical synthesis of amorphous iron. *Nature*, 353(6343), p. 414–416, 1991.
69. Martos, M., *et al.*, Electrochemical properties of lead oxide films obtained by spray pyrolysis as negative electrodes for lithium secondary batteries. *Electrochimica Acta*, 46(19), p. 2939–2948, 2001.
70. Sugimoto, M. J. *Magn. Chem. Mater.* 133 p. 460, 1994.
71. Landau, M.V., *et al.*, Ultrasonically Controlled Deposition–Precipitation: Co–Mo HDS Catalysts Deposited on Wide-Pore MCM Material. *Journal of Catalysis*, 2001 (1), p. 22–36.
72. Wang, H., *et al.*, Sonochemical Fabrication and Characterization of Stibnite Nanorods. *Inorganic Chemistry*, 42(20), p. 6404–6411, 2003.
73. Zhang, J.H., *et al.*, Sonochemical method for the synthesis of antimony sulfide microcrystallites with controllable morphology. *Journal of Materials Research*, 18(08), p. 1804–1808, 2003.
74. Ding, T., Zhu, J.-J. and Hong, J.-M. Sonochemical preparation of HgSe nanoparticles by using different reductants. *Materials Letters*, 57(28), p. 4445–4449, 2003.
75. Alavi, M.A. and Morsali, A. Syntheses of BaCO_3 nanostructures by ultrasonic method. *Ultrasonics sonochemistry*, 15(5), p. 833–838, 2008.
76. Askarinejad, A. and Morsali, A. Direct ultrasonic-assisted synthesis of sphere-like nanocrystals of spinel Co_3O_4 and Mn_3O_4 . *Ultrasonics sonochemistry*, 16(1), p. 124–131, 2009.
77. Sadeghzadeh, H., *et al.*, Synthesis of PbO nano-particles from a new one-dimensional lead(II) coordination polymer precursor. *Materials Letters*, 64(7), p. 810–813, 2010.
78. Ranjbar, Z.R. and Morsali, A. Sonochemical syntheses of a new nano-sized porous lead(II) coordination polymer as precursor for preparation of lead(II) oxide nanoparticles. *Journal of Molecular Structure*, 936(1), p. 206–212, 2009.
79. Sadeghzadeh, H. and Morsali, A. Sonochemical synthesis and characterization of nano-belt lead(II) coordination polymer: New precursor to produce pure phase nano-sized lead(II) oxide. *Ultrasonics sonochemistry*, 18(1), p. 80–84, 2011.

80. Sadeghzadeh, H., *et al.*, Sonochemical syntheses of strawberry-like nano-structure mixed-ligand lead(II) coordination polymer: Thermal, structural and X-ray powder diffraction studies. *Inorganica Chimica Acta*, 363(5), p. 841–845, 2010.
81. Sadeghzadeh, H., *et al.*, Sonochemical synthesis of nano-scale mixed-ligands lead(II) coordination polymers as precursors for preparation of PbO and PbBr(OH) nano-structures; thermal, structural and X-ray powder diffraction studies. *Ultrasonics sonochemistry*, 17(3), p. 592–597, 2010.
82. Shimon-Livny, L., Glusker, J.P. and Bock, C.W. Lone Pair Functionality in Divalent Lead Compounds. *Inorganic Chemistry*, 37(8), p. 1853–1867, 1998.
83. Hashemi, L. and Morsali, A. Sonochemical synthesis of nano-structured lead(II) complex: precursor for the preparation of PbO nano-structures. *Journal of Coordination Chemistry*, 64(23), p. 4088–4097, 2011.
84. Hashemi, L. and Morsali, A. Synthesis and characterization of a new nano lead(II) two-dimensional coordination polymer by sonochemical method: a precursor to produce pure phase nano-sized lead(II) oxide. *Journal of Inorganic and Organometallic Polymers and Materials*, 20(4), p. 856–861, 2010.

7

Thallium(I) Coordination Polymers

7.1 Introduction to Thallium(I) Coordination Polymers

Thallium, when compared with the remainder of the group 13 elements, shows a preference for the oxidation state +1. This has been attributed to the effect of the inert pair of electrons which is generally used in introductory textbooks to explain the tendency of the heavier main group elements to adopt oxidation numbers that are two less than the respective group number. This phenomenon which could also be observed in Pb^{2+} and Bi^{3+} [1–6], Originates from a combination of shell structure effects and relativity. Owing to the relativistic downshift in energy of the 6s orbital, Tl does indeed favor the oxidation state +1 over +3. Moreover [7], Tl might be regarded as a relativistic alkali metal because Tl chemistry parallels that of the alkali metals in many ways [8] and the well-known toxicity of thallium compounds may also be associated with the high affinity for sulfur functions and the non-reversibility of the complexation reactions as compared

to the action of alkali cations [9]. Specially thallium(I) compounds are similar in structure and chemical properties to potassium and silver salts [10]. In modern coordination chemistry the role of most metals as clustering centers for ligands appears to be predictable and the coordination number and coordination geometry can be extrapolated for most of the common metal/ligand combinations with quite high certainty.

Although this is generally true, the situation is surprisingly difficult for main group metals in their low oxidation states in which they are assigned lone pairs of electrons [11]. Although such a pair of *s* electrons beyond a completed shell is always stereo active with an obvious gap in Tl^I coordination sphere in the thallium(I) complexes with lower coordination number (three to five), this activity cannot be predicted in complexes with higher coordination number (six to twelve) [12]. Thallium(I) has atomic, ionic, covalent and van der waals radii of $1.70 < r(\text{Tl}) < 1.90, 1.47, 1.55$ and 1.96 \AA , respectively [13, 14]. Owing to the relativistically contracted valence shell and the low electrical charge, the Tl⁺ cation is intermediate between standard hard and soft character and has affinity for both hard and soft donor atoms, like oxygen and sulfur, or chloride and iodide, and so forth [11].

The design and construction of supramolecular arrays utilizing non-covalent bonding of tectons would be called supramolecular synthesis. Thus, the supramolecular synthesis successfully exploits hydrogen bonding and other types of non-covalent interactions, in building supramolecular systems such as intermolecular coordination bonds, which leads to formation of coordination polymers, polyhapto, metallophilic or agostic interactions.

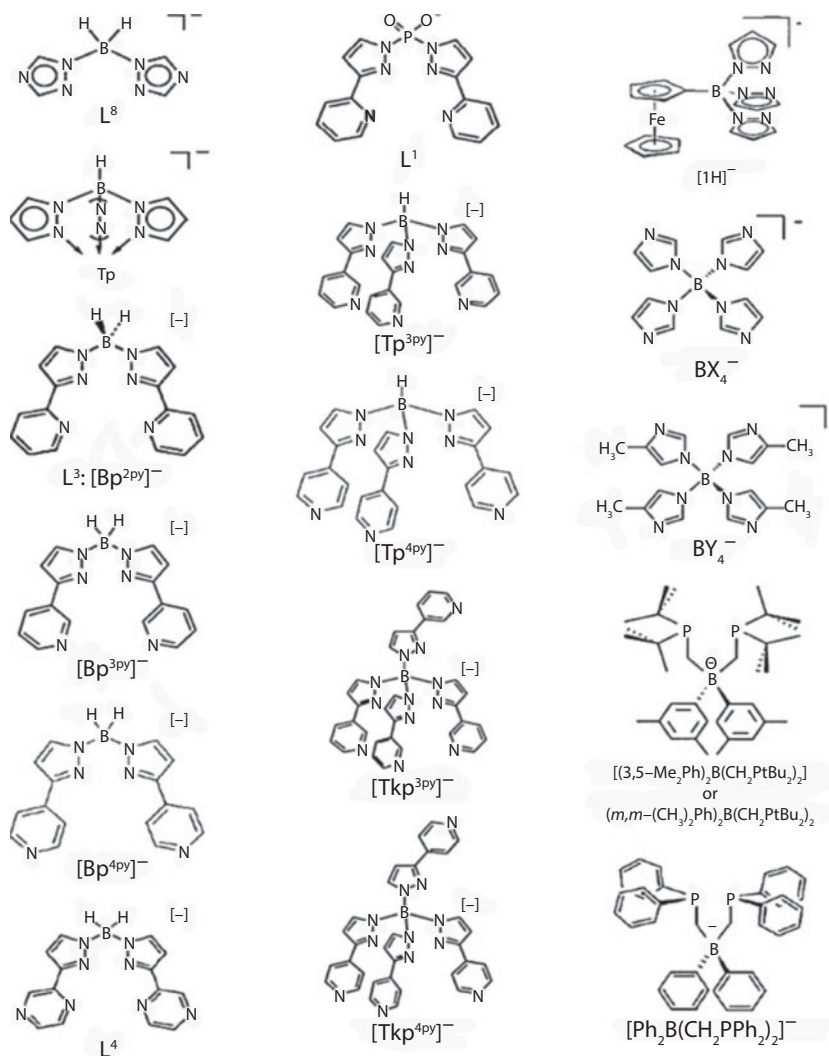
In contrast to transition-metal arene complexes, arene π - complexes of monovalent p-block metals are rather scarce [15]. Tl^I also forms π -complexes with aromatic hydrocarbons [16] as first demonstrated for the anionic cyclopentadienyl ligands in 1957, and in 1985 for neutral arenes [11], but structural reports on thallium(I) arene complexes have only appeared in the literature in the last 20 years. It was not until 1985 that Schmidbaur isolated the first structurally characterized Tl(I) arene complex, with Tl... π (centroid) distances

between 2.94 and 3.03 Å [17]. The reported Tl...C separations range is 3.20–4.00 Å in recent reported species [11, 18] and the sum of the van der Waals radii of carbon and Tl atoms is 3.66 Å [14]. The M–M bonded clusters, in which the metal ion has a +1 oxidation state and weakly interacting ns^2 lone pairs, are of particular interest due to the nature of the bonding and the unusual optical properties that can be produced by M–M interactions, in particular those in thallium(I) centers [19]. The strength of this interaction is generally considered to be of a magnitude similar to that of a typical hydrogen bond [20]. Recent *ab initio* calculations on thallocene dimers suggest energy minima with Tl...Tl distances slightly under 4 Å and interaction strengths of the order 10 kJ/mol [21]. Though positioning in a structural analysis of a H so close to the heavy Tl atom may not be given too much credibility, however M...H interactions have recently reported [20, 22–24]. This interaction is observed when the H atoms situated above the proposed site on the lone pair of Tl are oriented such that they might be thought to be forming a Tl–L_p...H–C– (L_p = lone pair) as a weak hydrogen bond [22] or Tl...H–C– as agostic interactions with distances smaller than 3.30 Å [25].

In this part we summarize three types of thallium(I) supramolecular compounds: thallium(I) coordination polymers, thallium(I) compounds aggregate from secondary interactions and finally thallium(I) polymeric compounds obtained from Tl–M (M = Pt, Au or Ni) bonds. Also we take distances that fall within the sum of the covalent or ionic radii, as primary bond and distances falling within the sum of the van der Waals radii or near it, as secondary interactions, in addition we consider much attention in Tl...C, Tl...Tl and Tl...H secondary interactions due to role of these interactions in aggregate Tl^I supramolecular compounds. Scheme 7.1 shows the figures of some complex ligands which are used to fabricate thallium(I) supramolecular compounds.

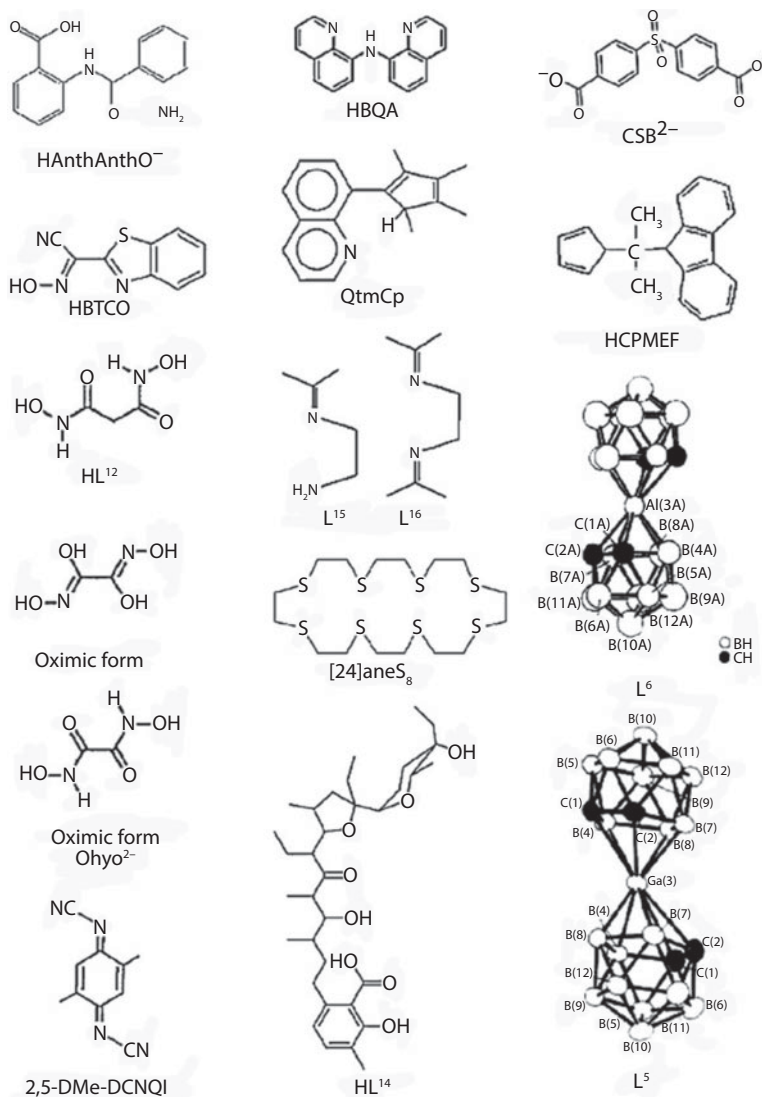
7.2 Thallium(I) Coordination Polymers

Coordination polymers are a very important topic of modern solid-state chemistry. Especially porous compounds like MOF-5



Scheme 7.1 Shows the figures of some complex ligands which used in fabricate thallium(I) supramolecular compounds. In L^5 and L^6 hydrogen atoms omitted for clarity. (*Continued*)

[26], MIL-53 [27] or HKUST-1 [28] have attracted a lot of attention due to their potential as heterogeneous catalysts or adsorbents for gases like hydrogen. Besides porosity there are also attractive aspects of non-porous coordination polymers, e.g. magnetic, luminescent, vaporochromism or conducting properties to name



Scheme 7.1 Continued.

a few [29–31]. Coordination polymers offer significant advantages over conventional molecular compounds due to very low solubility in conventional organic solvents and water, and much higher thermal stability. They have also several applications in sensors, organic light emitting diodes (OLED) and full-colored LCD displays [32]. In this section we classified coordination polymers on

the basis of their dimensions and secondary interactions in the Tl^I coordination sphere. Tl(I)–ligand bonding is generally divided into two types, primary and secondary. Primary bonding is said to exist if the Tl–X (X = hetero atom) bond distance falls within the sum of the covalent or ionic radii. Secondary bonding occurs if the Tl–X (X = hetero atom) bond distance falls within the sum of the van der Waals radii [32].

7.2.1 One-Dimensional Coordination Polymers with Secondary Interactions in Tl^I Coordination Sphere

In thallium(I) 2-amino-3-methyl-benzoate (Tl[C₈H₈NO₂]) [11] the anion is chelating the metal atom to form a wedge-like four-membered ring. These fundamental units aggregate to give dimers, the geometry also suggests intramolecular hydrogen bonding. Complexation of the metal atom through four oxygen atoms in a small quadrant of the coordination sphere is supplemented by a weak polyhapto contact with Tl. . π (centroid) distance of 3.230(11) Å. In the dinuclear units of [HAnthAnthOTl(H₂O)_{0.5}] [9], the thallium ions accommodate one nitrogen and four oxygen atoms of the anions in their coordination sphere and in addition entertain weak Tl–arene contacts forming 3D supramolecular networks. Relatively short contacts of three carbon atoms with Tl^I ion have 3.47, 3.59 and 3.47 Å distances. The water molecules are not involved in metal complexation, but contribute to a network of hydrogen bonding. In compounds catena-[bis(μ_3 - salicylato)dithallium(I)] [33] and catena-[bis(μ_3 -4-aminosalicylato)dithallium(I)] [33], adjacent units are held together by secondary Tl–O₃ interactions, resulting in stair-like, infinite one-dimensional polymers. The Tl⁺ ion is in a distorted square pyramidal geometry, with the four oxygen atoms in the basal plane and the stereoactive lone pair occupying the apex position of the pyramid, in a hydrophobic environment provided by two neighboring phenyl groups with O₄Tl · · 2 μ^6 -C₆ coordination environment. In catena-[bis(μ_3 salicylato)dithallium(I)] the distance between the planes of the

phenyl rings and the Tl^+ cation is 3.29 Å and in catena-[bis(μ_3 -4-aminosalicylato)dithallium(I)] the distance between the planes of the phenyl rings and the Tl^+ cation are 3.31 and 3.68 Å. In addition to the strong intramolecular hydrogen bond, weak hydrogen bonds are also formed between the amino protons and O_2 atoms of adjacent units, resulting in a 3D supramolecular compound. Compound catena-[bis(μ_3 salicylato)dithallium(I)] was obtained from H_2O with empirical formula of $(\text{C}_7\text{H}_5\text{O}_3\text{Tl})_2$ crystallizing in the monoclinic system with $\text{P2}_1/\text{n}$ space group.

One-dimensional polymeric chains in $[\text{Tl}(\text{Tbz})]_\infty$ [34], comprise a zigzag array of Tl and S atoms (Figure 7.1a). The full coordination sphere of the Tl ion is shown in Figure 7.1b. The vacant coordination sites on Tl interact (albeit weakly) with the π -systems of benzothiazole units in neighboring ligands with $\text{S4Tl} \cdots 2\mu^6\text{-C}_6$

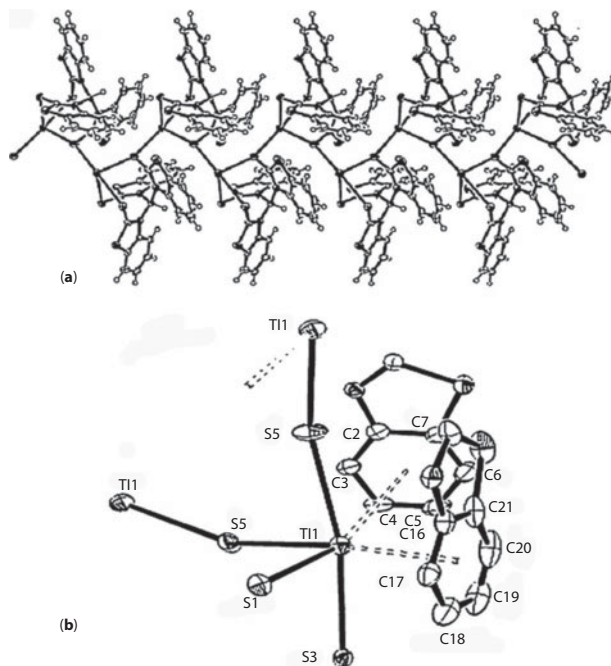


Figure 7.1 (a) A view of a section of the infinite polymeric chain in $[\text{Tl}(\text{Tbz})]_\infty$ emphasising the zigzag $-\text{Tl}-\text{S}-\text{Tl}-$ arrangement. (b) The thallium coordination sphere in TlTbz .

coordination sphere. In one case the interaction is approximately symmetrical, whereas in the other the metal is placed significantly 'off-center' with respect to the ring. In the solid-state $\text{Tl}[\text{PhTt}^{\text{t-Bu}}]$ [35] forms a one-dimensional coordination polymer. Each thallium ion is coordinated to three sulfur donors and a phenyl ring in an μ^6 -mode that may be described roughly as a three-legged piano stool coordination environment. The $\text{Tl} \cdots \text{C}$ distances range is from 3.272(8) to 3.446(8) Å.

7.2.2 One-Dimensional Coordination Polymers without Secondary Interactions in Tl^{I} Coordination Sphere

$\text{Tl}[\text{trans-Ru}(\text{DMeOPrPE})_2\text{Cl}_2]\text{PF}_6$ [32] is a 1D coordination polymer in which the $\text{Tl}(\text{I})$ centers have an unusual slightly distorted octahedral TlO_4Cl_2 coordination geometry with a stereochemically active $6s^2$ lone pair. The formation of product is solvent and temperature dependent. Complex $\text{Tl}(\text{18-crown-6})[\text{H}\{\text{ONC}(\text{CN})\text{C}(\text{O})\text{C}_6\text{H}_5\}_2]$ [36] exists as a hybrid coordination/H-bonded one-dimensional polymer with eight-coordinate thallium. The polymeric chain can be formally described to consist of macrocyclic cations $\text{Tl}(\text{18-crown-6})$, oximate anions $(\text{bco})^-$ and oxime molecules $\text{H}(\text{bco})$. Complex hydrogen oximate anions $\text{H}(\text{bco})_2^-$ that possess a centrosymmetric structure with two (bco) fragments being symmetry equivalents.

7.2.3 Two-Dimensional Coordination Polymers with Secondary Interactions in Tl^{I} Coordination Sphere

In 2D coordination polymer of $\text{Tl}(\text{m-Nbs})$ [37], both $\text{Tl}(\text{I})$ cation and the sulfonate group display high coordinating ability: one thallium(I) cation is surrounded by nine oxygen atoms and one

sulfonate anion is coordinated to six different thallium(I) cations. The Tl/O distances are at long end of the range for Tl(I)–O distances, suggesting a predominantly ionic character for metal–ligand bonding in this complex. This might be interpreted as an indication that the $6s^2$ lone pair of thallium ion is not stereochemically active. The crystal structure can be viewed as consisting of inorganic and organic layers (Figure 7.2). The organic layers are formed by *m*-Nbs[–] anions arranged in columnar stacks along the *z*-axis. The sulfonate groups are situated outside these layers and directed towards the inorganic layers within which they interact with the Tl⁺ cations. Besides the ionic and stacking interactions, the packing is stabilized by the C–H/O hydrogen bonds. A relatively short contact between Tl(I) cation and aromatic proton H(2) equal to 3.05 Å and thalophilic interactions at a distance of 3.857(1) Å also deserves attention, resulting in O₉Tl⁺ ··· TlH coordination sphere.

In Tl(Ohyo), the coordination polyhedron around the Tl^I can be described as a distorted dodecahedron; the eight Tl–O bonds are divided into sets of six short and two long, the latter lying at one side of the Tl^I ion which show the lone pair electrons are stereoactive. The oxalohydroxamate groups comprise a hydrogen-bonded, two-dimensional ligand layer; layers of this type are, in turn, interlinked by the aforementioned strong hydrogen bonds to form a three-dimensional supramolecular network.

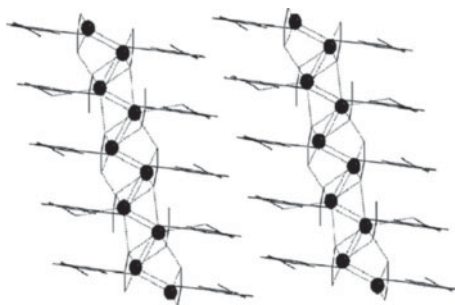


Figure 7.2 Packing diagram of Tl(*m*-Nbs) [37], as viewed along the *y*-axis, of the stacked *m*-nitrobenzenesulfonate anions arranged in columns along the *z*-axis.

The main structural unit of the polynuclear thallium complex with dialkyldithiocarbamates is the centrosymmetric binuclear molecule $\text{Tl}_2\{\text{S}_2\text{CN}(\text{CH}_2)_6\}_n$ [38] ($\text{Tl} \cdots \text{Tl}$ 3.6776 Å) involving two bridging ligands. Both thallium atom simultaneously coordinate all four S atoms of two dithio ligands. The geometry of the dimer can be represented by a tetragonal bipyramid with four equatorial S atoms and the thallium atoms as its vertices. The geometry of the seven-membered heterocyclic fragments $-\text{N}(\text{CH}_2)_6-$ can be approximately represented as a “twist chair”. The complexing metal in structure $\text{Tl}_2\{\text{S}_2\text{CN}(\text{CH}_2)_6\}_n$ becomes coordinatively saturated via additional coordination of the S atoms of adjacent dimeric molecules. Thus, each binuclear fragment is united with two neighbors through pairs of additional $\text{Tl}-\text{S}$ bonds and the resulting zigzag polymer chain is aligned with the crystallographic z-axis. In turn, polymer chains are united into a layer through additional coordination by each Tl atom and an S atom in an adjacent chain. The distance between the closest Tl atoms in adjacent chains is 3.7264 Å. The thallium atom has two agostic interactions with two hydrogen atoms too, thus attaining the total coordination sphere of $\text{S}_6\text{Tl} \cdots \text{H}_2\text{Tl}_2$.

7.2.4 Two-Dimensional Coordination Polymers without Secondary Interactions in Tl^{I} Coordination Sphere

$[\text{Tl}(\mu\text{-DNB})]_n$ [39] is a novel two dimensional polymer with eight-coordinate Tl atoms. Each DNB^- anion is octadentate connecting eight Tl^{I} ions. The carboxylate group of the DNB^- ligand is both bidentate chelating, and bridging. One of the nitro groups of this ligand has chelating and the other nitro group has only bridging coordination behavior. Structural determination of $\{\text{Tl}[(\text{H})\text{phthalate}]\}_n$ [40] shows the formation of two-dimensional coordination polymer. The coordination number of the Tl_1 ion is six with the coordination environment of TlO_6 . The arrangement of the O atoms suggests a gap in the

coordination geometry around the thallium atom in compound $\{\text{Tl}[(\text{H})\text{phthalate}]\}_n$, due to a stereochemically ‘active’ electron lone pair of Tl^{I} .

The layer structure of $\text{Tl}_2[\text{Ag}\{\text{N}(\text{SO}_2\text{Me})_2\}_3]$ [41], displays two unprecedented characteristics; one $(\text{MeSO}_2)_2\text{N}^-$ ion that strongly deviates from the C_2 -symmetric standard conformation of this species and approximates to mirror symmetry and a tris(dimesylamido)argentate anion featuring a trigonal planar AgN_3 core. The independent thallium ions are coordinated by the complex anions to form monolayer substructures, in which $\text{Tl}(\text{I})$ attains an O_6 and $\text{Tl}(2)$ an O_5 environment; the monolayers are associated into bilayers via one independent set of $\text{Tl}(2)\text{--O}$ bonds that concomitantly raise the coordination number for $\text{Tl}(2)$ to six. The two-dimensional Ag--N/Tl--O bonding system is reinforced by a three-dimensional network of weak $\text{C--H} \cdots \text{O}$ hydrogen bonds.

7.2.5 Three-Dimensional Coordination Polymers with Secondary Interactions in Tl^{I} Coordination Sphere

$\text{Tl}(\text{4-np})$ [42] and $[\text{Tl}(\text{2,4-dnp})]$ [43] have approximately similar ligands, they show different structural motifs. The structure of $\text{Tl}(\text{4-np})$ is based on a tetranuclear cubane motif with TlO_3 coordination sphere. $\text{Tl} \cdots \text{Tl}$ interactions within the cube are $3.858(2)$ Å and $[\text{Tl}(\text{O-phenoxide})]_4$ units linked into a three-dimensional network by further $\text{Tl} \cdots \text{O--nitro}$ interactions from adjacent units. The crystal structure of $[\text{Tl}(\text{2,4-dnp})]$ shows a three dimensional polymer as a result of bridging 2,4-dnp ligands. In $[\text{Tl}(\text{2,4-dnp})]$, the Tl atoms have TlO_2 coordination sphere with weak thalophilic interactions (3.740 Å), $\pi\text{--}\pi$ -stacking interactions between the parallel aromatic rings also exist. $[\text{Tl}_4(\mu_8\text{-SB})_2]_n$ [44], another compound with phenolic group, is a novel three-dimensional coordination polymer involving the tetranuclear cubic cage nodes as a result of bridging “ SB_2^- ” ligands with basic repeating $[\text{Tl}_4(\mu_8\text{-SB})_2]$ units. There are four thallium atoms with

different coordination spheres ($\text{Tl}1\text{O}_4$, $\text{O}_4\text{Tl}2 \cdot \cdot \text{Tl}_2$, $\text{O}_4\text{Tl}3 \cdot \cdot \text{Tl}$ and $\text{O}_3\text{Tl}4 \cdot \cdot \text{Tl}$) in the cubic cage. These thallium atoms contain an irregular coordination sphere with stereochemically active lone pair and thallium–thallium interactions.

$[\text{K}_2\text{Tl}(\mu\text{-succinate})(\mu\text{-NO}_3)]_n$ [45] with mixed succinate and nitrate ligands, shows two types of K^+ -ions with coordination numbers of seven and eight and one Tl^+ -ion with a coordination number of five. Two hydrogen atoms of succinate situated 3.26 Å above the proposed site on the lone pair of Tl^I is oriented in such a way that it might be forming a weak $\text{Tl-Lp} \cdot \cdot \text{H-C}$ hydrogen bond or agostic interaction, thus attaining a coordination environment of $\text{O}_5\text{Tl} \cdot \cdot \text{H}_2$.

7.2.6 Three-Dimensional Coordination Polymers without Secondary Interactions in Tl^I Coordination Sphere

CSB^{2-} ligand in compound $[\text{Tl}_2(\mu_{10}\text{-CSB})]_n$ [46] is similar to SB^{2-} but with carboxylate donor groups instead of phenolate group. In $[\text{Tl}_2(\mu_{10}\text{-CSB})]_n$ the thallium atoms have an irregular coordination sphere containing a stereochemically active lone pair with TlO_5 coordination environment. There are two known forms of $[\text{Tl}(\text{picrate})]$ [47], showing approximately similar coordination environments for the thallium atoms but the ‘high temperature’, yellow form has a bond to the phenoxide oxygen atom which is 0.2 Å shorter than the equivalent bond in the ‘low temperature’, red form. The yellow polymorph of $[\text{Tl}(\text{picrate})]$ has TlO_9 and the red polymorph of $[\text{Tl}(\text{picrate})]$ has $\text{O}_{11}\text{Tl} \cdot \cdot \text{C}$ coordination sphere with $\text{Tl} \cdot \cdot \text{C}$ distance of 3.463 Å, finally resulting in a 3D coordination polymer with inactive lone pair in both polymorphs. Transition from the red to the yellow polymorph occurs in the solid state only at 400 K and above, but the yellow polymorph does not transform to red, neither on heating nor on cooling. Addition of a small amount of solvent to

the system accelerates the transformations in both directions. In $\text{Tl}\{\text{ONC}(\text{CN})_2\}$ [48], the thallium(I) center has four shorter bonds than the sum of the ionic radii bonds (three with N and one with O atoms) and three longer electrostatic (ionic) contacts with the anion. The $6s^2$ lone pair is stereoactive, and the coordination polyhedron is best described as a distorted square pyramid. The $\text{ONC}(\text{CN})_2^-$ anion in this complex is planar and in the nitroso form.

Compound $\text{Tl}\{\text{ONC}(\text{CN})_2\}$ at 293 K exhibited structured metal-based red photoluminescence in the range of 690–800 nm that depends on the excitation wavelengths. An assignment of a metal-to-ligand charge transfer (MLCT) state from $\text{Tl}(\text{I})$ to π^* of the $\text{ONC}(\text{CN})_2^-$ anion is very likely since thallium is known to form a stable $\text{Tl}(\text{III})$ oxidation state.

$[\text{Tl}(\text{SC}_6\text{H}_5)]$ [49], is built up by the two novel structure units; $[\text{Tl}_7(\text{SC}_6\text{H}_5)_6]^+$ and $[\text{Tl}_5(\text{SC}_6\text{H}_5)_6]^-$ with six different Tl^{I} ions as Tl1 , Tl2 , Tl5 with TlS_1 coordination sphere, Tl3 and Tl4 with TlS_3 coordination sphere and finally Tl6 with TlS_4 coordination sphere, resulting in a 3D coordination polymer with stereoactive electron lone pair.

7.3 Nano Thallium(I) Coordination Polymers

A new thallium(I) two-dimensional supramolecular polymer, $[\text{Tl}_6(\text{biphO})_4(\text{biphOH})_4(\text{NO}_3)_2]_n$, biphOH = 4-hydroxy biphenyl, has been synthesized and characterized by elemental analyzes and IR spectroscopy. Compound $[\text{Tl}_6(\text{biphO})_4(\text{biphOH})_4(\text{NO}_3)_2]_n$ was structurally characterized by single-crystal X-ray diffraction and in addition to three types of Tl^{I} ions has secondary $\text{Tl}\dots\pi$ interactions. Two different Tl_2O_3 nano-structures have been prepared by direct calcination of $[\text{Tl}_6(\text{biphO})_4(\text{biphOH})_4(\text{NO}_3)_2]_n$ at two different temperatures. These Tl_2O_3 nano-structures were characterized by scanning electron microscopy, X-ray powder diffraction (XRD) and IR spectroscopy.

Determination of the structure of this compound by X-ray crystallography showed that the compound has three types of Tl⁺ ions. In addition to NO₃⁻ anion, Tl atoms in [Tl₆(biphO)₄(biphOH)₄(NO₃)₂]_n are coordinated with protonated and deprotonated phenolic oxygen atoms. Thus we could consider Tl1O₃, Tl2O₁ and Tl3O₃ coordination sphere for them. In addition to short Tl...O bonds, Tl1 and Tl3 atoms in [Tl₆(biphO)₄(biphOH)₄(NO₃)₂]_n have two weak interactions with oxygen atoms of phenolic ligands. Existence of these strong and weak Tl...O interactions in [Tl₆(biphO)₄(biphOH)₄(NO₃)₂]_n, result in formation of two-dimensional supramolecular network in crystallographic bc plane. Another secondary interaction in [Tl₆(biphO)₄(biphOH)₄(NO₃)₂]_n is the intra-plane hydrogen bonding network which does not increase dimension of this polymer from 2D to 3D network (Figure 7.3).

Nano-structures of Tl₂O₃ have been generated by direct calcinations at 430 and 570 °C. The final product upon thermal decomposition of compound [Tl₆(biphO)₄(biphOH)₄(NO₃)₂]_n, based on their IR spectrum and XRD pattern is Tl₂O₃. Sharp diffraction peaks in PXRD indicate good crystallinity of Tl₂O₃ nanostructures prepared and the broadening of the peaks indicated that the particles were of nanometer scale in agreement with that observed from SEM images (Figure 7.4) [50].

Two thallium(I) coordination polymers, [Tl(3-np)]_n and [Tl(2,4-dnp)]_n, 3-np⁻=3 nitrophenoxide and 2,4-dnp⁻=2,4-dinitrophenoxide, have been synthesized and characterized by

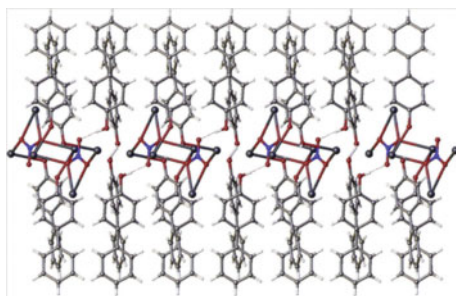


Figure 7.3 Side view of formation H-bonding network along the 2D supramolecular polymer of [Tl₆(biphO)₄(biphOH)₄(NO₃)₂]_n.

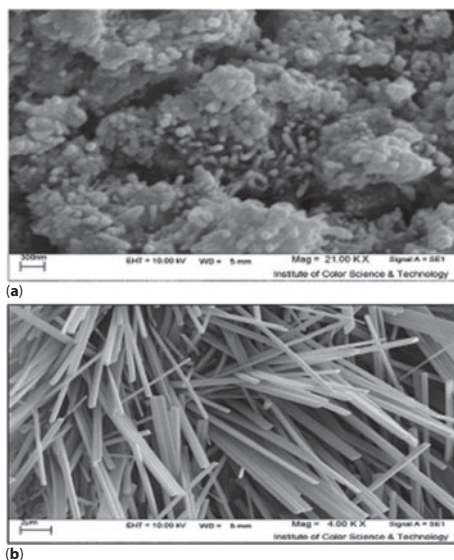


Figure 7.4 SEM micrograph of Tl_2O_3 nano-structures produced by direct calcination of compound $[\text{Tl}_6(\text{biphO})_4(\text{biphOH})_4(\text{NO}_3)_2]_n$ at a) 430 °C and b) 570 °C, respectively.

elemental analyses and IR spectroscopy. Flower-like nano structure and nano-powders thallium(III) oxide, Tl_2O_3 , have been prepared by direct thermal decomposition of two different Tl(I) coordination polymers, $[\text{Tl}(\text{3-np})]_n$ and $[\text{Tl}(\text{2,4-dnp})]_n$. The nano-materials were characterized by scanning electron microscopy, X-ray powder diffraction (XRD) and IR spectroscopy. The thermal stability of nano-structure Tl_2O_3 was studied by thermal gravimetric and differential thermal analyses and showed that there is no reportable loss of weight in the TGA curves that proves the existence of thallium(III) oxide. This study demonstrates that coordination polymers may be suitable precursors for the preparation of nanoscale materials with different and interesting morphologies.

Reaction either of 3-nitrophenoxide (3-np^-) or 2,4-dinitrophenoxide (2,4-dnp^-) ligands with thallium(I) nitrate provided powdered materials analyzing as $[\text{Tl}(\text{3-np})]_n$ and $[\text{Tl}(\text{2,4-dnp})]_n$, respectively. The structure of compounds $[\text{Tl}(\text{3-np})]_n$ and $[\text{Tl}(\text{2,4-dnp})]_n$ were reported in [43] and in the solid state are three-dimensional polymers and crystallize in the triclinic with space group P21/c and

$[\text{Tl}(3\text{-np})]_n$ and $[\text{Tl}(2,4\text{-dnp})]_n$, respectively. The morphology and size of the particles are different in the two samples obtained by two different polymers. This point shows the influence of crystal packing of coordination polymers upon morphology and size of nano-materials produced from their calcinations [51].

7.4 Conclusion

Tl^{I} favors to form neutral species with anionic ligands. One-dimensional polymers constitute a great portion of thallium(I) supramolecular compounds and two and three-dimensional polymers are less common. This may be related to existence of a vacant site on thallium(I) environment and hemidirected coordination sphere of Tl^{I} ion due to the stereochemical activity of its lone pair (however the stereochemical activity of the lone pair was also observed in 2D and 3D supramolecular compounds) and effects which relate to structure, size and rigidity of ligands. In addition thallium(I) usually favors the formation of $\text{Tl}^{\cdot} \cdots \text{Tl}$, $\text{Tl}^{\cdot} \cdots \text{C}$, $\text{Tl}^{\cdot} \cdots \text{H}$ secondary interactions especially through the stereochemically active lone pair indicating that thallium(I) ions act as both a Lewis acid and a Lewis base.

References

1. Sadeghzadeh, H. and Morsali, A. New Reversible Crystal-to-Crystal Conversion of a Mixed-Ligand Lead(II) Coordination Polymer by De- and Rehydration. *Inorganic Chemistry*, 48(23), p. 10871–10873, 2009.
2. Sadeghzadeh, H. and Morsali, A. Hedge balls nano-structure of a mixed-ligand lead(II) coordination polymer; thermal, structural and X-ray powder diffraction studies. *CrystEngComm*, 12(2), p. 370–372, 2010.
3. Aslani, A., Morsali, A. and Zeller, M. Dynamic crystal-to-crystal conversion of a 3D-3D coordination polymer by de- and re-hydration. *Dalton Transactions*, 2008(38), p. 5173–5177.
4. Aslani, A. and Morsali, A. Crystal-to-crystal transformation from a chain polymer to a two-dimensional network by thermal desolvation. *Chemical Communications*, 2008(29), p. 3402–3404.

5. Soltanzadeh, N. and Morsali, A. Metal–organic supramolecular assemblies generated from bismuth(III) bromide and polyimine ligands. *Polyhedron*, 28(4), p. 703–710, 2009.
6. Soltanzadeh, N. and Morsali, A. Syntheses and characterization nano-structured bismuth(III) oxide from a new nano-sized bismuth(III) supramolecular compound. *Polyhedron*, 28(7), p. 1343–1347, 2009.
7. Mudring, A.-V. and Rieger, F. Lone Pair Effect in Thallium(I) Macrocyclic Compounds. *Inorganic Chemistry*, 44(18), p. 6240–6243, 2005.
8. Askarinejad, A. Torabi, A.A. Morsali, A. Thallium(I) Salicylate and Phthalate: Syntheses and Structural Characterization, *Z. Naturforsch.* 61b p. 565–569, 2006.
9. Wiesbrock, F. and Schmidbaur, H. Interactions of a β -dipeptide with monovalent metal cations: crystal structures of (anthranoyl) anthranilic acid and its lithium, sodium and thallium salts. *Journal of Inorganic Biochemistry*, 98(3), p. 473–484, 2004.
10. Hünig, S., *et al.*, A conducting thallium salt of 2,5-dimethyl-N, N'-dicyanoquinone-diimine, [2,5-DMe-DCNQI]₂Tl: Comparison with other related radical anion salts. *Advanced Materials*, 2(8), p. 361–363, 1990.
11. Wiesbrock, F. and Schmidbaur, H. Complexity of Coordinative Bonding in Thallium(I) Anthranilates and Salicylates. *Journal of the American Chemical Society*, 125(12), p. 3622–3630, 2003.
12. Huang, S.-H., Wang, R.-J. and Mak, T.C.W. Preparation and crystal structure of the complexes thallium(I) oxalohydroxamate(1-) and malono-hydroxamate(1-). *Journal of the Chemical Society, Dalton Transactions*, 1991(5), p. 1379–1381.
13. Emsley, J. *The Elements*, Clarendon Press, Oxford, UK, 1995, p. 192.
14. Bondi, A. *van der Waals Volumes and Radii*, *Journal of Physical Chemistry*. 68 p. 441–451, 1964.
15. Schmidbaur, H., Arene Complexes of Univalent Gallium, Indium, and Thallium. *Angewandte Chemie International Edition in English*, 24(11), p. 893–904, 1985.
16. Bochmann, M., Highly electrophilic main group compounds: Ether and arene thallium and zinc complexes. *Coordination Chemistry Reviews*, 253(15), p. 2000–2014, 2009.
17. Schmidbaur, H., *et al.*, [{1, 3, 5-(CH₃)₃H₃C₆}_6Tl₄][GaBr₄]₄ Synthesis and Structure of a Mixed Mono-and Bis (arene) thallium Complex. *Angewandte Chemie International Edition in English*, 24(5), p. 414–415, 1985.

18. Waezsada, S.D., *et al.*, [2, 6- $i\text{Pr}_2\text{C}_6\text{H}_3$ (Me_3Si) NTL] $_4$ —A Covalent Thallium(I)-Nitrogen Compound with Weak Arene–Thallium Interactions. *Angewandte Chemie International Edition* in English, 33(13), p. 1351–1352, 1994.
19. Wright, R.J., *et al.*, Synthesis and Reactivity of Dimeric $\text{Ar}'\text{TlTlAr}'$ and Trimeric $(\text{Ar}''\text{Tl})_3$ (Ar' , Ar'' = Bulky Terphenyl Group) Thallium (I) Derivatives: Tl (I)–Tl (I) Bonding in Species Ligated by Monodentate Ligands. *Journal of the American Chemical Society*, 127(13), p. 4794–4799, 2005.
20. Ghosh, P., Rheingold, A.L. and Parkin, G. Synthesis and Molecular Structure of Bis(pyrazolyl)hydroborato Thallium $\{[\text{Bp}]\text{Tl}\}_2$: A $[\text{BpRR}']\text{Tl}$ Complex with an Unbridged Close $\text{Tl}^I \cdots \text{Tl}^I$ Contact. *Inorganic Chemistry*, 38(23), p. 5464–5467, 1999.
21. Pyykkö, P., Strong Closed-Shell Interactions in *Inorganic Chemistry*. *Chemical Reviews*, 97(3), p. 597–636, 1997.
22. Hancock, R.D., Reibenspies, J.H. and Maumela, H. Structural Effects of the Lone Pair on Lead(II), and Parallels with the Coordination Geometry of Mercury(II). Does the Lone Pair on Lead(II) Form H-Bonds? Structures of the Lead(II) and Mercury(II) Complexes of the Pendant-Donor Macrocyclic DOTAM (1,4,7,10-Tetrakis(carbamoylmethyl)-1,4,7,10-tetraazacyclododecane). *Inorganic Chemistry*, 43(9), p. 2981–2987, 2004.
23. Fillebeen, T., Hascall, T. and Parkin, G. Bis- and Tris (pyrazolyl) hydroborato Ligands with Bulky Triptycyl Substituents: The Synthesis and Structural Characterization of Tl $[\text{BpTrip}]$ and Tl $[\text{TpTrip}]$. *Inorganic Chemistry*, 36(17), p. 3787–3790, 1997.
24. Dowling, C., Ghosh, P. and Parkin, G. Structural characterization of bis(pyrazolyl)hydroborato thallium complexes: monomeric “two-coordinate” thallium derivatives supplemented by $[\text{Tl} \cdots \text{H}-\text{B}]$ interactions. *Polyhedron*, 16(19), p. 3469–3473, 1997.
25. Brookhart, M., M.L. Green, and L.L. Wong, Carbon-Hydrogen-Transition Metal Bonds. *Progress in Inorganic Chemistry*, Volume 36, 1988; p. 1–124.
26. Li, H., *et al.*, Design and synthesis of an exceptionally stable and highly porous metal-organic framework. *Nature*, 402(6759), p. 276–279, 1999.
27. Loiseau, T., *et al.*, A rationale for the large breathing of the porous aluminum terephthalate (MIL-53) upon hydration. *Chem. Eur. J.*, 10 p. 1373–1382, 2004.
28. Chui, S.S.Y., *et al.*, A chemically functionalizable nanoporous material $[\text{Cu}_3(\text{TMA})_2(\text{H}_2\text{O})_3]$. *Science*, 283, p. 1148–1150, 1999.

29. Cheetham, A.K. and Rao, C.N.R. There's Room in the Middle. *Science*, 318(5847), p. 58–59, 2007.
30. Morsali, A. and Masoomi, M.Y. Structures and properties of mercury(II) coordination polymers. *Coordination Chemistry Reviews*, 253(13–14), p. 1882–1905, 2009.
31. Akhbari, K. and Morsali, A. One-Dimensional Corrugated Tape AgI Coordination Polymers Constructed of Ag–C Bonds. *Crystal Growth & Design*, 7(10), p. 2024–2030, 2007.
32. Szymczak, N.K., Han, F. and Tyler, D.R. Arrested chloride abstraction from trans-RuCl₂(DMeOPrPE)₂ with TlPF₆; formation of a 1-D coordination polymer having unusual octahedral coordination around thallium(I). *Dalton Transactions*, 2004(23), p. 3941–3942.
33. Kristiansson, O., Structures of Complexes of Thallium(I) and Functionalized Benzoate Ligands with Pronounced Stereoactivity of the Lone Pair of Electrons and Metal–Phenyl π -Bonding. *European Journal of Inorganic Chemistry*, 2002(9), p. 2355–2361, 2002.
34. Ojo, J.F., *et al.*, The synthesis of soft tripodal ligands: restrictions on the preparation of hydrotris(thiazolyl)borate anions from borohydride melts. *Inorganica Chimica Acta*, 313(1–2), p. 15–20, 2001.
35. Schebler, P.J., *et al.*, Phenyltris((tert-butylthio)methyl)borate: A Second Generation S₃-Ligand That Enforces Tetrahedral Coordination. *Inorganic Chemistry*, 37(19), p. 4754–4755, 1998.
36. Ponomarova, V.V. and K.V. Domasevitch, Structure of M (18-crown-6)⁺(M= Tl, NH₄) oximate complexes: effective control of the molecular geometry employing a crystal engineering approach. *Crystal engineering*, 5(2), p. 137–145, 2002.
37. harma, R.P., *et al.*, Coordination network: synthesis, characterization, crystal structure and packing of thallium m-nitrobenzenesulfonate, Tl(m-NO₂C₆H₄SO₃). *Journal of Molecular Structure*, 738(1–3), p. 247–252, 2005.
38. Ivanov, A.V., *et al.*, Structures of polynuclear thallium(I) and copper(II)-thallium(I) complexes with dialkyldithiocarbamates: ¹³C and ¹⁵N CP/MAS NMR, EPR, and X-ray diffraction studies. *Russian Journal of Coordination Chemistry*, 32(5), p. 339–349, 2006.
39. Askarinejad, A., *et al.*, Syntheses and structural characterization of New Tl⁺ and K⁺ complexes of 3,5-dinitrobenzoic acid (HDNB), [Tl(μ -DNB)]_n and [K(μ -DNB)(μ -HDNB)]_n. *J of Coordination Chemistry*, 60 p. 753–761, 2007.
40. Askarinejad, A. and Morsali, A. Synthesis and structural characterization of a new two-dimensional polymeric thallium (I)

- compound, {Tl [(H) phthalate)]} n . *Journal of Coordination Chemistry*, 59(9), p. 997–1005, 2006.
41. Latorre, V., *et al.*, Polysulfonylamine. CLXIV Kristallstrukturen von Metall-di(methansulfonyl)amiden. Dithallium-tris(dimesylamido-N) argentat: Ein zweidimensionales Koordinationspolymer. *Zeitschrift für anorganische und allgemeine Chemie*, 629(9), p. 1515–1521, 2003.
42. Harrowfield, J.M., *et al.*, Structural Systematics of 2/4-Nitrophenoxide Complexes of Closed-Shell Metal Ions. III 2/4-Nitrophenoxides of Univalent Heavy Metals. *Australian Journal of Chemistry*, 51(8), p. 735–746, 1998.
43. Mahjoub, A.R., Morsali, A. and Bagherzadeh, H. Syntheses and characterization of thallium(I) complexes with 3-nitrophenoxide [Tl(3-np)], 4-nitrobenzoate [Tl(4-nb)] and 2,4-dinitrophenoxide [Tl(2,4-dnp)]: X-ray crystal structures of [Tl(3-np)] $_n$ and Tl(2,4-dnp) (two new polymeric compounds). *Polyhedron*, 21(25–26), p. 2555–2560, 2002.
44. Askarinejad, A. and Morsali, A. TII three-dimensional coordination polymer involving tetranuclear cubic cage nodes, [Tl $_4(\mu_8$ -SB) $_2$] n {H $_2$ SB = 4-[(4-hydroxyphenyl)sulfonyl]-1-benzenol}. *Inorganic Chemistry Communications*, 9(2), p. 143–146, 2006.
45. Askarinejad, A. and Morsali, A. Potassium(I)thallium(I) heterometallic 3D polymeric mixed-anions compound, succinate–nitrate [K $_2$ Tl(μ -C $_4$ H $_4$ O $_4$)(μ -NO $_3$)] $_n$. *Inorganica Chimica Acta*, 359(10), p. 3379–3383, 2006.
46. Askarinejad, A. and Morsali, A. Thermal and structural studies of two new Tl three-dimensional coordination polymers, [Tl $_2(\mu$ -CSB)] $_n$ and [Tl $_2(\mu$ -ADC)] $_n$, CSB=4-[(4-carboxyphenyl)sulfonyl]-1-benzenecarboxylate and ADC=acetylendicarboxylate. *Journal of Coordination Chemistry*, 60(17), p. 1903–1912, 2007.
47. Botoshansky, M. Herstein, F.H. Kapon, M. *Crystallography of metal picrates. II. Crystal structure of yellow thallium(I) picrate; relations among various M(I) picrate phases*, *Acta Crystallogr*, B50 p. 589–596, 1994.
48. Glover, G., *et al.*, Monovalent K, Cs, Tl, and Ag Nitrosodicyanomethanides: Completely Different 3D Networks with Useful Properties of Luminescent Materials and Nonelectric Sensors for Gases. *Inorganic Chemistry*, 48(6), p. 2371–2382, 2009.
49. Krebs, B. and Brömmelhaus, A. Thallium (I)-Thiolate: Darstellung, Struktur und Eigenschaften von TlSC $_6$ H $_5$, TlS-t-C $_4$ H $_9$ und TlSC $_7$ H $_7$. *Zeitschrift für anorganische und allgemeine Chemie*, 595(1), p. 167–182, 1991.

50. Mohammadi, M., *et al.*, Synthesis of one-dimensional Tl_2O_3 nano-structures from thermolyses of a new two-dimensional thallium(I) supramolecular polymer with secondary polyhapto $\text{Tl}\cdots\text{C}$ interactions. *Journal of Organometallic Chemistry*, 733, p. 15–20, 2013.
51. Mohammadi, M. and A. Morsali, Different thallium(III) oxide nano-structures from direct thermal decomposition of two thallium(I) coordination polymers. *Materials Letters*, 63(27), p. 2349–2351, 2009.

8

Bismuth(III) Coordination Polymers

8.1 Introduction to Bismuth Coordination Polymers

Bismuth has two major oxidation states (Bi(III) with ionic radii of 1.03 and 1.17 Å for CN 6 and 8, respectively and Bi(V) with an ionic radius of 0.76 Å for CN 6), with the trivalent being the most common and stable form. Pentavalent bismuth is a powerful oxidant in aqueous solutions with a Bi(V)/Bi(III) potential of $E^\circ = 2.03$ V. Bi(III) readily hydrolyzes in aqueous solutions ($pK_a = 1.51$) and has a high affinity to both oxygen and nitrogen ligands [1, 2]. However, it prefers to coordinate to thiolate groups (–SR) when thiol containing ligands such as cysteine and glutathione are available [3–5]. Corresponding to its various coordination numbers from 3 to 10 [6, 7], the structures of Bi(III) compounds are irregular, from pyramidal (CN: 3), octahedral (CN: 6, $[\text{Bi}_6\text{O}_4\text{OH}]_4^{6+}$) [8], bicapped trigonal prism (CN: 8, $[\text{Bi}(\text{HEDTA})] \cdot 2\text{H}_2\text{O}$) [9] and square antiprism [10, 11] to tricapped trigonal prism (CN: 9, $[\text{Bi}(\text{OH}_2)_9](\text{CF}_3\text{SO}_3)_3$) [12]. Most

of the Bi(V) complexes are five-coordinated [13], although Bi(V) in triarylbi-smuthate complexes such as $\text{Ar}_3\text{Bi}(\text{HCO}_2)_2$ (where $\text{Ar} = \text{Ph}, p\text{-Tol}$) [14], are six-coordinated. Almost all of Bi(V) complexes are very unstable in aqueous media except a recently reported seven-coordinated Bi(V) tropolonato complex, tri(aryl) tropolonatobismuth(V). The stability of this Bi(V) complex may be attributed to the steric shielding of the bismuth ion [15]. In some Bi(V) complexes such as $\text{BiR}_3(\text{O}_2\text{CR}')_2$, synthesized *via* the reaction of BiR_3Cl_2 with $\text{Ag}(\text{O}_2\text{CR}')$, the Bi(V) centre shows interesting unusual stereoselectivity towards the chiral ligand R^*CO_2^- . $\text{BiR}_3(\text{O}_2\text{CR}')_2$ can be used as building units for the assembly of extended structures *via* hydrogen-bonding. So, because of unstable complexes in aqueous media for Bi(V) we discuss only bismuth(III) coordination polymers here.

Compounds of Bi(III) have received increased interest recently due to their multiple applications in diverse areas including medicine, materials, organic synthesis, and catalysis. Even though bismuth is a p-block element, it is one of the more metallic of that part of the periodic table and forms stable complexes with aminopolycarboxylate (APC) and polyaminopolycarboxylate (PAPC) ligands. In this part, the Bi(III) complexes with APC and PAPC ligands are systematized by the number of nitrogen atoms of the ligands in mono-, di- and polyaminopolycarboxylates.

According to Pearson's hard-soft acid-base theory, Bi(III) is a borderline metal ion, but it has a high affinity for multidentate ligands containing O and N donor atoms. Hence, anions of aminopolycarboxylic and polyaminopolycarboxylic acids are highly versatile ligands towards Bi(III). The stability constants of these Bi(III) APC and PAPC complexes are usually very high: e.g. K_{BiL} of $\text{Bi}(\text{edta})^-$ was reported and is 26.7, while that of $\text{Bi}(\text{dota})^-$ reaches an even higher value of 30.3. As result, these complexes are stable and can be isolated even at low pH. Although Bi(III) has a strong tendency to hydrolyze, in the presence of these strongly chelating ligands it is stabilized up to pH 10. Increasing the number of donor atoms of the ligands and the number of chelating rings formed usually results in higher stability of the complexes. The high number of donor atoms of the ligands and of chelating

rings are not always reflected in high values of the stability constants; other factors that should be considered are the charge of the ligand, the preorganization, and the steric efficiency in which the ligand surrounds the Bi(III) ion to form a cage-like structure. A significant increase in complex stability is observed in Bi(III)–cdta compared to Bi(III)–edta complex. The cyclohexyl moiety leads to a conformation in which the donor atoms are held in optimized positions for complex formation. As a result, a four order increase in the stability constant is observed.

The increasing interest in Bi(III) APC and PAPC complexes has ensued as a result of a variety of factors:

- i. bismuth(III) complexes with aminopolycarboxylate and polyaminopolycarboxylate ligands have found many applications in analytical chemistry, including complexometric titrations.
- ii. ^{212}Bi and ^{213}Bi radioisotopes are among the most promising candidates for radioimmunotherapy. Medical chelation therapy requires chelate ligands forming radiometal complexes of high stability *in vivo* for the period of time the agent is in the body.
- iii. APC and PAPC ligands are used as chelate agents in different processes for preparation of metallic bismuth nanoparticles, and other high-tech materials, such as bismuth oxide or chalcogenide materials.
- iv. bismuth(III) heterometallic APC and PAPC complexes are attractive as single-source molecular precursors to mixed oxide systems with promising properties.

For some of these applications all that is necessary is an APC or PAPC ligand that will bind Bi(III) strongly to form highly stabilized structures; however, for biomedical applications, other factors, such as kinetic inertness and biocompatibility play an important role, too. Another important factor is the structure of the complex. For instance, involving water or other additional ligands in the coordination sphere, as well as the formation of polynuclear species could influence the utility of the specific complexes.

8.2 Bismuth(III) Complexes with Monoaminopoly Carboxylate

8.2.1 Bi(III) Complexes with Iminodiacetate Ligands

Bismuth(III) in solution and in the solid state forms stable complexes with anions of iminodiacetic acid. The complexation of Bi(III) with ida^{2-} has been studied spectrophotometrically. In the pH range 0.6–2 the formation of a 1:1 Bi–ida {H₂ida Iminodiacetic acid} complex was proposed. However in solid state only the 1:2 complex was isolated, namely Bi(Hida)(ida), which has a poor solubility in water (0.2 g in 100 g of H₂O at 90 °C). The compound can be recrystallized from its aqueous solutions, which are slightly acidic (pH 5). Bi(Hida)(ida) proved to be stable in air and does not lose weight upon heating to 200 °C. At 220 °C the complex starts to decompose, giving rise ultimately to Bi₂O₃ by 480 °C. IR spectroscopic data suggest a polymeric structure of Bi(Hida)(ida), involving Bi–O bridging bonds. The X-ray structure determination of Bi(Hida)(ida) confirmed the IR data. In the polymeric chain structure of [Bi(Hida)(ida)] each Bi atom is coordinated by one N atom and two carboxylate O atoms of the ida^{2-} –ligand, four O donor atoms of the Hida[–] bridging ligands, each of them being also coordinated to three other bismuth atoms. Additionally, Bi(III) forms a bridging bond with the O atom of ida^{2-} –ligand of the neighbor unit. Bi(III) has a distorted octa-coordinate environment.

8.2.2 Bi(III) Complexes with Nitrilotriacetate

Complexation of Bi(III) with anions of H₃nta {H₃nta: Nitrilotriacetic acid} in solution has been investigated by several different methods. Potentiometric titration of Bi(III) with H₃nta in aqueous solution showed that two types of complexes are formed, but no stability constants were determined. Reaction of bismuth(III) perchlorate and H₃nta has been monitored by means of UV spectroscopy. Ershova *et al.* studied the interaction of [BiCl₆]^{3–} with

nitrilotriacetic acid by potentiometry in a large pH range. The formation constants of the mixed ligand complex $[\text{Bi}(\text{Hnta})_2\text{Cl}_2]^{3-}$ and a deprotonated $[\text{Bi}(\text{nta})_2]^{3-}$ complex were reported to be 14.9 and 27.6. Both 1:1 and 1:2 Bi(III)–nta complexes have been isolated in solid state. $\text{Bi}(\text{nta}) \cdot 2\text{H}_2\text{O}$ was obtained by interaction of equimolar quantities of $\text{Bi}(\text{OH})_3$ and H_3nta and by reaction of $(\text{BiO})_2\text{CO}_3$ and H_3nta . Complexes of the general formula $\text{M}_3[\text{Bi}(\text{nta})_2] \cdot n\text{H}_2\text{O}$ ($\text{M}^+ = \text{Li}^+, \text{Na}^+, \text{K}^+, \text{Rb}^+, \text{Cs}^+, \text{NH}_4^+$, and guanidinium CH_6N_3^+) were isolated by dissolution of equimolar quantities of $\text{Bi}(\text{OH})_3$ and H_3nta , and addition of MOH to achieve pH 5. Complexes $\text{M}_2[\text{Bi}(\text{nta})(\text{Hnta})] \cdot \text{H}_2\text{O}$ ($\text{M}^+ = \text{K}^+, \text{NH}_4^+$), containing both nta and Hnta ligands have also been obtained. These complexes proved to be isostructural. Examples of other mixed-ligand Bi(III)–nta complexes include $\text{Bi}(\text{nta}) \cdot 3\text{tu}$ and $(\text{NH}_4)_4[\text{Bi}(\text{nta})_2(\text{NCS})] \cdot \text{H}_2\text{O}$. The reaction of $[\text{Bi}(\text{nta})(\text{H}_2\text{O})_2]$, H_3nta and KOH at pH 5 results in formation of $\text{K}_2[\text{Bi}(\text{nta})(\text{Hnta})] \cdot \text{H}_2\text{O}$. In the crystal structure of this mixed ligand complex the H atom in the Hnta^{2-} ligand is localized on the N atom. The Bi atom is coordinated by the nta^{3-} ligand in a tetradentate–chelate mode and by three betaine Hnta^{2-} ligands. In its turn, each Hnta^{2-} ligand represents a hexadentate bridge between three bismuth atoms. The CN of the Bi atom in $\text{K}_2[\text{Bi}(\text{nta})(\text{Hnta})] \cdot \text{H}_2\text{O}$ is equal to $7 + 3$. When the reaction of $\text{Bi}(\text{OH})_3 \cdot \text{H}_3\text{nta}$ (ratio 1:2) and ammonia is performed in the presence of NH_4NCS , $(\text{NH}_4)_4[\text{Bi}(\text{nta})_2(\text{NCS})] \cdot \text{H}_2\text{O}$ is obtained. The crystal structure of this mixed-ligand complex is formed by NH_4^+ cations $[\text{Bi}(\text{nta})_2(\text{NCS})]^{4-}$ complex anions and H_2O molecules. In the $[\text{Bi}(\text{nta})_2(\text{NCS})]^{4-}$ anions, the two nta^{3-} ligands exhibit a tetradentate–chelate mode ($\text{N} + 3\text{O}$), each using the N donor atom and three O atoms of the acetate groups. The NCS ligand is involved in coordination to the Bi atom through the N atom ($\text{Bi}-\text{N}$ 2.71(1) Å), which is close to the Bi–N bond lengths in $\text{Rb}[\text{Bi}(\text{NCS})_4]$.

8.2.3 Bi(III) Complexes with 2-hydroxyethyliminodiacetate

The reaction of Bi^{3+} with anions of H_3heida { H_3heida : β -Hydroxyethyliminodiacetic acid} has been investigated by

means of spectrophotometry and shows a 1:1 stoichiometry of the complex with the formation constant equal to 14.82 ± 0.03 [16]. The same value for the stability constant was reported in [17]. The reaction of $[\text{BiCl}_6]^{3-}$ with equimolar amounts of H_3heida was studied by means of potentiometry [18]. It was established that at pH 2.2–3.48 no complexation occurs, while at pH > 3.48 the precipitation of BiOCl was observed. Interaction of $[\text{BiCl}_6]^{3-}$ with excess H_3heida , however, led to the formation of both 1:1 and 1:2 complexes. The stability constants of $[\text{Bi}(\text{H}_2\text{heida})(\text{Hheida})\text{Cl}_2]^{2-}$ and $[\text{Bi}(\text{Hheida})_2]^-$ are reported to be 18.7 (pH 2.0–4.5) and 24.3 (pH 6.0–9.0).

The hydroxyethyl group of the Hheida^{2-} -ion can be deprotonated under certain conditions, leading to heida^{3-} ions. The interaction of $\text{Bi}(\text{OH})_3$ with H_3heida in aqueous solution for both 1:1 and 1:2 ratios leads to $\text{Bi}(\text{heida})_2 \cdot 2\text{H}_2\text{O}$ [19, 20]. It should be noted that this complex is highly soluble in the presence of H_3heida . Reaction of two equivalents of H_3heida with $\text{Bi}(\text{OH})_3$ in the presence of some alkali metal, ammonium or guanidinium cations leads to the formation of well-soluble $\text{MBi}(\text{Hheida})_2 \cdot n\text{H}_2\text{O}$, where $\text{M}^+ = \text{Na}^+$ [88], K^+ , Rb^+ , Cs^+ , NH_4^+ or CH_6N_3^+ [20], $n = 1$ –3, as well as $(\text{CH}_6\text{N}_3)_2\text{Bi}(\text{Hheida})(\text{heida}) \cdot 3\text{H}_2\text{O}$ [20]. $(\text{CH}_6\text{N}_3)_2\text{Bi}(\text{Hheida})_2 \cdot \text{H}_2\text{O}$ was obtained as a first fraction from the solution, which resulted from dissolution of guanidinium carbonate in a mixture of $\text{Bi}(\text{OH})_3$ – H_3heida in 1:2 ratio. The second fraction that precipitated from the solution was $(\text{CH}_6\text{N}_3)_2\text{Bi}(\text{Hheida})(\text{heida}) \cdot 3\text{H}_2\text{O}$.

$[\text{Bi}(\text{heida})(\text{H}_2\text{O})] \cdot \text{H}_2\text{O}$ has a polymeric structure [21]. The distorted bicapped trigonal prismatic environment for bismuth involves two O atoms of deprotonated acetate groups, one O atom of the deprotonated hydroxyethyl group, the nitrogen atom, one water molecule O atom, and three carboxylate O atoms of the neighboring complexes. In $[\text{Bi}(\text{heida})(\text{H}_2\text{O})] \cdot \text{H}_2\text{O}$ the heida^{3-} ligand exhibits a tetradentate–chelate ($\text{N} + 3\text{O}$) and a triply-bridging (3O) function. The Bi polyhedra are united in dimers ($\text{Bi} \cdots \text{Bi}' = 3.83 \text{ \AA}$) by means of the bridging O atom of the hydroxyethyl group. The dimers are connected in layers

(Bi \cdots Bi \cdots = 5.14 Å) by both oxygen atoms of the two acetate groups of the neighboring complexes.

8.2.4 Bi(III) Complexes with Pyridinedicarboxylate Ligands

Bismuth(III) complexes with aromatic nitrogen-donor carboxylate ligands include 2,3-, 2,5-, and 2,6-pyridinedicarboxylates. Postel and co-workers [22, 23] studied the reaction of Bi₂O₃ and 2,3-, 2,5-, and 2,6-pyridinedicarboxylic acids (H₂L) in aqueous solution and, based on elemental analysis and IR spectra, proposed the same Bi(HL)₂(OH) composition for all three complexes. When Bi₂O₃ is reacted with pyridine-2,6-dicarboxylic acid (H₂pydc) in water at reflux, with subsequent recrystallization of the product from DMSO, a dimeric complex [Bi(2,6-Hpydc)(2,6-pydc)(DMSO)]₂ is formed. The compound is not soluble in common organic solvents, but is soluble in hot DMF and DMSO. In the dimeric structure of [Bi(2,6-Hpydc)(2,6-pydc)(DMSO)]₂, two bismuth atoms are connected by bridging carboxylic groups of the dipicolinate ions [23]. Each bismuth center is surrounded by four oxygen atoms and two nitrogen atoms of the dipicolinate ions, a bridging oxygen atom from the neighboring complex and one oxygen atom of a DMSO molecule (Bi–O 2.209(8)–2.507(6) Å; Bi–N 2.418(9) and 2.481(9) Å; Bi–O_{bridging} = 2.577(4) Å, Bi–ODMSO 2.613(6) Å). Reaction of a solution of bismuth(III) subnitrate Bi₅O(OH)₉(NO₃)₄ in HCl with pyridine-2,6-dicarboxylic acid in the presence of pyridine-2,6-diamine results in formation of [{BiCl(H₂O)(pydc)}₂]_n [24]. The structure of this compound is composed of dimers, linked into an infinite system by means of bridging carboxylate groups. Bismuth has a distorted pentagonal bipyramidal environment, in which the equatorial plane contains the three donor atoms of a pydc²⁻ ligand, the oxygen donor atom of a water molecule and the Bi₂O₂ ring, while the axial sites are occupied by an oxygen atom of the neighboring pydc²⁻ ligand, and by a chlorine atom (Bi–O 2.365(3)–2.633(3) Å; Bi–N 2.384(4) Å; Bi–Cl = 2.562(1) Å).

8.3 Bismuth(III) Complexes with Diaminopolycarboxylate Ligands

Bismuth complexes with anions of ethylenediaminetetraacetic acid ($H_4\text{edta}$) are far the most widely investigated of the diaminopolycarboxylates because the acid and its disodium salt are readily available and form stable complexes with the bismuth(III) ion in aqueous solutions. As a result, there is a substantial literature dealing with the study of bismuth(III) ethylenediaminetetraacetates while the data concerning other diaminopolycarboxylatobismuthates(III) are more limited.

8.3.1 Bi(III) Complexes with Ethylenediaminetetraacetate

Due to the large volume of data, Bi(III) complexes with edta will be further subdivided according to the charge, nature and composition of the outer-sphere cation and the presence of additional ligands in the coordination sphere of Bi(III) (mixed-ligand complexes).

8.3.1.1 *Protonated Bi(III) Ethylenediaminetetraacetate Complexes*

Bismuth(III) forms stable complexes with edta^{4-} and this was demonstrated by means of several methods: spectrophotometry, potentiometry, polarography, as well as by IR and NMR spectroscopy. Bhat and Krishna Iyer [25] investigated the reaction of Bi(III) with $H_4\text{edta}$ spectrophotometrically and by means of pH-metric titrations, the stability constant of the $[\text{Bi}(\text{edta})]^-$ complex was 26.47. The complexation reaction of Bi(III) and edta^{4-} has been also studied spectrophotometrically [26]. In the pH range 0.6–1.4, the formation of the 1:1 protonated complex $[\text{Bi}(\text{Hedta})]$ has been proposed, while at pH 1.5–10 the $[\text{Bi}(\text{edta})]^-$ exists. At higher pH the hydrolysis occurs with the formation of bismuth hydroxide. The stability constants of the protonated and anionic complex were 17.73 and 25.68, respectively. The polarimetric

studies showed, however, slightly higher values, 27.93 [27], and 27.94 [28]. In solid state Bi(III) forms with edta two types of complexes: protonated neutral [Bi(Hedta)] and deprotonated anionic [Bi(edta)]⁻ species. Synthesis of an acidic complex formulated as Bi(Hedta) was reported by Brintzinger and Munkelt as early as in 1948 [29]. Bhat and Krishna Iyer reported the synthesis of the same acidic complex, but based on the results of the elemental analysis it was formulated as Bi(Hedta).H₂O. The same authors investigated the thermal stability of this complex in an atmosphere of air and nitrogen [30]. The IR spectrum of Bi(Hedta).H₂O showed that all four acetate groups are coordinated to Bi, and Hedta³⁻ may be functioning as a hexadentate ligand [31].

8.3.1.2 *Bi(III) Ethylenediaminetetraacetate Complexes with Alkali Metal and Ammonium Cations*

The carboxylate proton in [Bi(Hedta)] has a significant acidity, the aqueous solutions showing a pH~2. Reactions of aqueous solutions of [Bi(Hedta)] and alkali metal or ammonium carbonates M₂CO₃ have been investigated for different molar ratios and at different pH (from 2.5 to 9). In the range of pH 6–9, the corresponding salts, MBi(edta).nH₂O (where $n = 4$ for M⁺ = Li⁺; $n = 3$ for M⁺ = Na⁺, K⁺ and Rb⁺ and $n = 1$ for Cs⁺ and NH₄⁺), can be isolated [101]. Reacting aqueous [Bi(Hedta)] with M₂CO₃ in molar ratios from 0.25:1.0 to 0.5:1.0 at pH 3–4, complexes of the general formula MBi₂(Hedta)(edta).nH₂O ($n = 2$ for M⁺ = K⁺, Rb⁺, NH₄⁺ and $n = 3$ for M⁺ = Cs⁺) were synthesized [32]. The same complexes can be obtained by mixing aqueous MCl and [Bi(Hedta)].2H₂O in molar ratios from 1:1 to 5:1 at pH≈3 or by addition of a diluted solution of hydrochloric acid to a solution of MBi(edta).nH₂O until pH≈3 is reached. The complexes crystallize from concentrated solution and are slightly soluble in water. Addition of corresponding K⁺, Rb⁺, Cs⁺ or NH₄⁺ carbonates or hydroxides to the aqueous MBi₂(Hedta)(edta).nH₂O and adjustment of pH to 6–8 leads to MBi(edta).nH₂O. The following alkali metal and ammonium ethylenediaminetetraacetatobismuthates(III) have been structurally characterized: Li[Bi(edta)].4H₂O [33], Na[Bi(edta)].3H₂O [34], Rb[Bi(edta)].3H₂O [35],

$\text{Cs}[\text{Bi}(\text{edta})]\cdot\text{H}_2\text{O}$, and $\text{NH}_4[\text{Bi}(\text{edta})]\cdot\text{H}_2\text{O}$. The crystal structure of $\text{Li}[\text{Bi}(\text{edta})]\cdot 4\text{H}_2\text{O}$ contains hydrated $\text{Li}(\text{H}_2\text{O})_2^+$ cations, complex $[\text{Bi}(\text{edta})]^-$ anions, and water molecules of crystallization. The $\text{Li}(\text{H}_2\text{O})_2^+$ cations link the $[\text{Bi}(\text{edta})]^-$ anions in polymeric chains via two carbonyl oxygen atoms. The coordination environment of Bi(III) contains four oxygen and two nitrogen atoms of the edta^{4-} ligand and two O atoms from two neighboring $[\text{Bi}(\text{edta})]^-$ anions. In $\text{Na}[\text{Bi}(\text{edta})]\cdot 3\text{H}_2\text{O}$ the bismuth coordination environment can be presented as square antiprismatic and includes two nitrogen atoms (Bi–N 2.491(9) and 2.497(8) Å), four oxygen atoms of carboxylate groups (Bi–O chelate 2.324(8), 2.331(8), 2.362(8), and 2.525(8) Å), and two oxygen atoms of neighboring complexes (Bi–O bridging 2.637(8) and 2.843(8) Å). The latter results in the formation of layers. The Na^+ cation has an octahedral coordination environment, formed by three O atoms of water molecules and three O atoms of edta. In the crystal structure of $\text{Na}[\text{Bi}(\text{edta})]\cdot 3\text{H}_2\text{O}$ the complex anions $[\text{Bi}(\text{edta})]^-$ are joined in layers by means of oxygen atoms. The polymeric layers are connected by cyclic carboxylate dimers. The 3D structure is completed by dimers between two Na^+ cations ($\text{Na}\cdots\text{Na}$ distance is 3.92(1) Å) connected by two bridging water molecules. Crystal structures of isostructural $\text{K}[\text{Bi}(\text{edta})]\cdot 3\text{H}_2\text{O}$ and $\text{Rb}[\text{Bi}(\text{edta})]\cdot 3\text{H}_2\text{O}$ contain octa-coordinate Bi(III) with bonding to six edta^{4-} donor atoms and two bridging carboxylate oxygen atoms of the neighboring complexes. By means of this bridging $[\text{Bi}(\text{edta})]^-$ anions the complexes are joined into polymeric layers. The crystal structure of $\text{Cs}[\text{Bi}(\text{edta})]\cdot\text{H}_2\text{O}$ contains two types of Cs^+ cations with an occupancy factor of 0.5, polymeric $[\text{Bi}(\text{edta})]_n^{n-}$ anions, and lattice water molecules.

8.3.1.3 Bi(III) Ethylenediaminetetraacetate Complexes with Divalent Metal Cations

Ethylenediaminetetraacetatobismuthates(III) with divalent metal cations of the general formula $\text{M}\{\text{Bi}(\text{edta})\}_2\cdot n\text{H}_2\text{O}$ (where $\text{M(II)} = \text{Mg(II)}, \text{Ca(II)}, \text{Sr(II)}, \text{Ba(II)}, \text{Ni(II)}, \text{Co(II)}, \text{Cu(II)}, \text{Zn(II)}, \text{Cd(II)}$, $n = 2\text{--}9$) were also described. The preparative methods include reaction of $[\text{Bi}(\text{Hedta})]$ with the appropriate

carbonates or basic metal carbonates in aqueous solutions or via exchange reactions of $\text{Ba}\{\text{Bi}(\text{edta})\}_2$ with corresponding divalent metal sulphates. Polymeric motifs have been found in crystal structures of all characterized complexes of this type: $\text{Ca}[\text{Bi}(\text{edta})]_2 \cdot 9\text{H}_2\text{O}$, $\text{Ba}[\text{Bi}_2(\text{edta})_2(\text{H}_2\text{O})] \cdot \text{H}_2\text{O}$ and in isostructural complexes $\text{Co}[\text{Bi}(\text{edta})]_2 \cdot 9\text{H}_2\text{O}$, $\text{Ni}[\text{Bi}(\text{edta})]_2 \cdot 9\text{H}_2\text{O}$, and $\text{Cu}[\text{Bi}(\text{edta})]_2 \cdot 9\text{H}_2\text{O}$. The corresponding cobalt, nickel and copper complexes, $\text{M}[\text{Bi}(\text{edta})]_2 \cdot 9\text{H}_2\text{O}$, are isostructural. The edta^{4-} ligand exhibits a hexadentate-chelate ($4\text{O} + 2\text{N}$) and di-bridging function (2O). By means of two chelate oxygen atoms the square antiprismatic polyhedra of bismuth(III) form centrosymmetric dimers. The dimers are further connected by means of double bridges in polymeric chains. The $\text{Ba}[\text{Bi}_2(\text{edta})_2(\text{H}_2\text{O})] \cdot \text{H}_2\text{O}$ crystals are triclinic, in which two crystallographically independent $[\text{Bi}(\text{edta})]^-$ complexes and the coordination water molecule form tetranuclear associates. The environments of two independent bismuth atoms ($\text{CN} = 8$) are similar, and their polyhedra can be described as distorted dodecahedra. A coordinated water molecule serves as a bridge between the two Bi centers.

8.3.1.4 *Bi(III) Ethylenediaminetetraacetate Complexes with Protonated Organic Base Cations*

Synthesis and characterization of several Bi(III)–edta complexes with some protonated organic base cations (guanidinium, aminoguanidinium, ethylenediammonium, β -alaninium, and thiosemicarbazidium) have been reported. The guanidinium salt $(\text{CH}_6\text{N}_3)\text{Bi}(\text{edta}) \cdot \text{H}_2\text{O}$ was obtained by reaction of BiF_3 and H_4edta , with subsequent addition of guanidinium carbonate to achieve a neutral or slightly basic pH. The same compound can be isolated by reaction of aqueous solutions of $[\text{Bi}(\text{Hedta})]$ with guanidinium carbonate or guanidinium chloride. The corresponding Bi–edta complex with aminoguanidinium $(\text{CH}_7\text{N}_4)\text{Bi}(\text{edta})$, can be obtained similarly, but it contains no water molecules. $(\text{CH}_6\text{N}_3)[\text{Bi}(\text{edta})(\text{H}_2\text{O})]$ was the first structurally characterized Bi–edta complex. Rhombic crystals of $(\text{CH}_6\text{N}_3)[\text{Bi}(\text{edta})(\text{H}_2\text{O})]$ are built by $(\text{CH}_6\text{N}_3)^+$ cations and $[\text{Bi}(\text{edta})(\text{H}_2\text{O})]^-$ anions. The coordination polyhedron around the metal may be described as a distorted square antiprism with a hexadentate edta ligand.

8.3.1.5 *Bi(III) Ethylenediaminetetraacetates with Metal Complex Cations*

In recent years, a number of Bi(III)–edta complexes, containing as counter-ion transition metal complex cations have been obtained and characterized. The Co(III)–Bi(III) complexes $[\text{Co}(\text{NH}_3)_4(\text{CO}_3)] [\text{Bi}(\text{edta})] \cdot 3\text{H}_2\text{O}$ and $[\text{Co}(\text{NH}_3)_4(\text{C}_2\text{O}_4)] [\text{Bi}(\text{edta})] \cdot 3\text{H}_2\text{O}$ were isolated from aqueous solutions of $\text{Na}[\text{Bi}(\text{edta})] \cdot 3\text{H}_2\text{O}$ in the presence of $[\text{Co}(\text{NH}_3)_4(\text{CO}_3)]^+$ and $[\text{Co}(\text{NH}_3)_4(\text{C}_2\text{O}_4)]^+$ salts. Both complexes have a polymeric structure. The bismuth polyhedral in the two complexes was described as square antiprismatic. The Bi–O and Bi–N bond lengths are quite similar for the two complexes. *Trans*- $[\text{Co}(\text{NH}_3)_4(\text{NO}_2)_2] [\text{Bi}(\text{edta})(\text{H}_2\text{O})] \cdot 2\text{H}_2\text{O}$ was prepared by reaction of aqueous *trans*- $[\text{Co}(\text{NH}_3)_4(\text{NO}_2)_2](\text{SO}_4)$ and $\text{Ba}[\text{Bi}(\text{edta})]_2$. The same method was used to obtain $[\text{Co}(\text{NH}_3)_5(\text{NCS})] [\text{Bi}(\text{edta})]_2 \cdot 4\text{H}_2\text{O}$. *Trans*- $[\text{Co}(\text{NH}_3)_4(\text{NO}_2)_2] [\text{Bi}(\text{edta})(\text{H}_2\text{O})] \cdot 2\text{H}_2\text{O}$ contains eight-coordinated Bi, bonded to an edta^{4-} ligand (2N + 4O), and further, to complete the eight-coordination, a water molecule and a carbonyl oxygen of a carboxylate group of the neighboring unit to form dimers. Antsyshkina and co-workers obtained $[\text{Co}(\text{NH}_3)_2(\text{ala})_2] [\text{Bi}(\text{edta})(\text{H}_2\text{O})] \cdot 5\text{H}_2\text{O}$ by reaction of $[\text{Co}(\text{NH}_3)_2(\text{ala})_2]\text{Cl}$ or $[\text{Co}(\text{NH}_3)_2(\text{ala})_2]\text{ClO}_4$ and $\text{Na}[\text{Bi}(\text{edta})] \cdot 3\text{H}_2\text{O}$ in aqueous solutions. A particular feature of this complex is that practically all bond distances between Bi(III) and carboxylate oxygen atoms are equal (Bi–O 2.41–2.47 Å). The bond distances to the bridging oxygen atom and water molecule are longer, 2.68 and 2.73 Å, respectively. The structure is formed by cationic Co(III) complexes and polymeric $[\text{Bi}(\text{edta})(\text{H}_2\text{O})]^-$ anions. A heterobimetallic cation–anion Cu(II)–Bi(III) ethylenediaminetetraacetate complex $[\text{Cu}(\text{Hssa})(\text{H}_2\text{O})] [\text{Bi}(\text{edta})(\text{H}_2\text{O})] \cdot 3.88\text{H}_2\text{O}$ (Hssa = monodeprotonated anion of salicylaldehyde semicarbazone) was synthesized and structurally investigated. The structure is built by complex cations $[\text{Cu}(\text{Hssa})(\text{H}_2\text{O})]^+$, centrosymmetric dimeric complex anions $[\text{Bi}(\text{edta})(\text{H}_2\text{O})]_2^{2-}$, and lattice water molecules. By means of the coordination bonds between Cu atoms and carbonylic oxygen atoms of the edta^{4-} ligands of the dimeric anion (Cu–O(8) 2.016(1) Å), complex cations $[\text{Cu}(\text{Hssa})(\text{H}_2\text{O})]^+$, two by two, are bonded with dimeric complex anions $[\text{Bi}(\text{edta})]$

$(\text{H}_2\text{O})_2]^{2-}$, resulting in tetranuclear units, which are linked by hydrogen bonds in a 3D framework.

8.3.1.6 Mixed-Ligand Bi(III) Ethylenediaminetetraacetate Complexes

The formation of mixed-ligand complexes $[\text{Bi}(\text{edta})\text{X}]^-$ (X(monodentate ligand), Br^- , I^- , SCN^- , NO_2^- , $\text{S}_2\text{O}_3^{2-}$, SO_3^{2-} , OH^- and tu) have been investigated by means of potentiometry, IR, and NMR analyses. The reaction of $[\text{BiCl}_6]^{3-}$ with H_4edta in aqueous solutions was studied by potentiometry and the formation in the range $1.72 < \text{pH} < 3.03$ of a mixed ligand complex $[\text{Bi}(\text{Hedta})\text{Cl}_2]^{2-}$ ($\log \beta = 19.44$) was presumed. According to the same authors, at $3.03 < \text{pH} < 7.25$ the complex $[\text{Bi}(\text{Hedta})\text{Cl}]^-$ dominated ($\log \beta = 23.69$), while between pH 7.25 and 9 the hydroxo-complex is dominant ($\log \beta = 31.20$). At $\text{pH} > 9$, decomposition of the complex and sedimentation of $\text{Bi}(\text{OH})_3$ was observed. The formation of mixed-ligand $\text{Bi}(\text{edta})$ -thiourea (tu) complexes was first detected in aqueous solutions. Later, a variety of Bi(III) mixed-ligand complexes containing edta^{4-} and thiourea were isolated and structurally characterized, namely $[\text{Bi}(\text{Hedta})(\text{tu})_2]$, $\text{Li}[\text{Bi}(\text{edta})(\text{tu})_2] \cdot 5.5\text{H}_2\text{O}$ [36], $\text{M}[\text{Bi}(\text{edta})(\text{tu})_2]$ ($\text{M}=\text{NH}_4$, K, Rb) [37, 38], $\text{Cs}[\text{Bi}(\text{edta})(\text{tu})_2] \cdot 3\text{H}_2\text{O}$ [37], $(\text{CH}_7\text{N}_4)[\text{Bi}(\text{edta})(\text{tu})_2] \cdot 2.5\text{H}_2\text{O}$ [38], and $(\text{CH}_7\text{N}_4)[\text{Bi}(\text{edta})(\text{tu})(\text{H}_2\text{O})] \cdot 2\text{H}_2\text{O}$ [38]. $[\text{Bi}(\text{Hedta})(\text{tu})_2]$ has been prepared by reaction of aqueous $[\text{Bi}(\text{Hedta})] \cdot 2\text{H}_2\text{O}$ and tu in the molar ratio 1:3 and crystallization by slow evaporation of the obtained solution. $\text{M}[\text{Bi}(\text{edta})(\text{tu})_2]$ and $\text{M}[\text{Bi}(\text{edta})(\text{tu})_2] \cdot n\text{H}_2\text{O}$ complexes were obtained by reaction of aqueous $\text{M}[\text{Bi}(\text{edta})] \cdot n\text{H}_2\text{O}$ and tu in a 1:2 ratio. The complexes were isolated by slow evaporation of the resulting solutions in the dark. The reaction of $[\text{Bi}(\text{Hedta})] \cdot 2\text{H}_2\text{O}$ with aminoguanidinium hydrogenocarbonate $(\text{CH}_7\text{N}_4)\text{HCO}_3$ and thiourea in 1:1:1 ratio at pH 3 results in formation of $(\text{CH}_7\text{N}_4)[\text{Bi}(\text{edta})]$. For a ratio of the starting reagents 1:2:2 or 1:2:3 two complexes can be isolated, namely $(\text{CH}_7\text{N}_4)[\text{Bi}(\text{edta})(\text{tu})_2] \cdot 2.5\text{H}_2\text{O}$ and $(\text{CH}_7\text{N}_4)[\text{Bi}(\text{edta})(\text{tu})(\text{H}_2\text{O})] \cdot 2\text{H}_2\text{O}$. In the isostructural complexes $\text{K}[\text{Bi}(\text{edta})(\text{tu})_2]$ and $\text{Rb}[\text{Bi}(\text{edta})(\text{tu})_2]$ Bi(III) has a distorted square antiprismatic environment composed of six donor atoms of edta^{4-} and two S atoms

of two thiourea molecules. In spite of evidence of the existence of multiple mixed-ligand ethylenediaminetetraacetatobismuthates (III) with acido-ligands in solution, in solid state the structures of only three complexes have been reported: $(\text{CH}_7\text{N}_4)_2[\text{Bi}(\text{edta})\text{Cl}]$ [39], $[\text{Co}(\text{NH}_3)_5(\text{NCS})]_2[(\text{edta})\text{Bi}(\mu\text{-C}_2\text{O}_4)\text{Bi}(\text{edta})]\cdot 12\text{H}_2\text{O}$ [40], and $[\text{NdBi}(\text{edta})(\text{NO}_3)_{3/2}(\text{H}_2\text{O})_{7.22}]_n$ [41].

8.3.2 Bi(III) Complexes with other than edta^{4-} diaminopolycarboxylate Ligands

Bismuth(III) complexes with other than edta^{4-} diaminopolycarboxylate ligands have been much less studied than corresponding Bi(III)– edta complexes. The stability constant of the Bi(III) complex with anions of *N,N*-hydrazinediacetic acid (H_2hzda) was reported to be 12.50. Ethylenediamine-*N,N'*-diacetic acid (H_2edda) forms a more stable complex with bismuth(III), $\log K = 18.20 \pm 0.03$. The complexation reaction of Bi(III) with *N*-(2-hydroxyethyl)ethylenediaminetriacetic acid (H_4hedta) has been studied spectrophotometrically. The acid was proposed for use in the UV spectrophotometric determination of Bi(III) at 360 nm. The selectivity of the determination is reported to be higher than that of H_4edta or 1,2-diaminocyclohexanetetraacetic acid (H_4cdta). In the crystal structure of $[\text{Bi}(\text{Hcdta})]\cdot 5\text{H}_2\text{O}$ there are two crystallographically independent $[\text{Bi}(\text{Hcdta})]$ molecules. The Bi atom is surrounded by eight donor atoms of the ligand in a square antiprismatic environment. $(\text{Hcdta})^-$ anion acts as a hexadentate ligand towards one Bi atom, the remaining two coordination positions being occupied by two O atoms of the neighboring complexes. Two acetate groups of Hcdta^- are monodentate, while the other two act as bridging groups, generating dimers. Centrosymmetric dimers formed by Bi(1) and Bi(2) are bridged by oxygen atoms and form polymeric ribbons.

The reaction of Bi_2O_3 with pyrazine-2,3-dicarboxylic acid (H_2pzdc) produces a solid, which has a very low solubility in common organic solvents. Postel and co-workers suggested a $\{\text{Bi}(\text{pzdc})(\text{OH})\}_n$

stoichiometry for this product, mainly based on IR data. Later, Devillers and co-workers obtained the same compound by reacting nitric acid solutions of $\text{Bi}(\text{NO}_3)_3$ with the corresponding acid in 1:1.5 ratio, but found the actual stoichiometry was different, $\{\text{Bi}(\text{2,3-Hpzdc})_2\text{OH}\}$, as supported by elemental analysis. However, when a 1:3 ratio of the reagents is used, the product is $\text{Bi}(\text{2,3-Hpzdc})_3 \cdot 2\text{H}_2\text{O}$ [42]. The existence of protonated carboxylic groups is supported by the presence of a strong band at 1723 cm^{-1} in the IR spectrum, attributable to the carboxyl group stretching vibrations, correlated with the broad signal at 13.24 ppm in the ^1H NMR spectrum. The actual CN of Bi(III) may be probably higher than 6. When heated in air or nitrogen both $\text{Bi}(\text{2,3-Hpzdc})_3 \cdot 2\text{H}_2\text{O}$ and $\text{Bi}_2(\text{3,5-dcp})_2 \cdot 4\text{H}_2\text{O}$ are converted into $\alpha\text{-Bi}_2\text{O}_3$ at moderate temperatures (451 and 385°C , respectively). These complexes were proposed as precursors for bismuth-based oxides. No Bi(III) pyrazine- or pyrazole-dicarboxylates have been structurally characterized.

8.4 Bismuth Complexes with Polyaminopolycarboxylate Ligands

8.4.1 Bi(III) Complexes with Diethylenetriaminepentaacetate Ligands and its Analogues

Bi(III) forms stable complexes with the anions of diethylenetriaminepentaacetic acid (H_5dtpa); however, the reported stability constants are quite different. X-ray study of $[\text{Bi}(\text{H}_2\text{dtpa})] \cdot 2\text{H}_2\text{O}$ [43] showed the $\text{H}_2\text{dtpa}^{3-}$ ligand coordinating in a heptadentate fashion to one Bi atom by means of its three nitrogen donors, three oxygen atoms of the deprotonated carboxylic groups, and the carbonyl oxygen atom of one protonated carboxylic group. In addition, the Bi atom forms a bridging bond with a carbonyl oxygen atom of the neighboring complex. The coordination polyhedron around the Bi atom is intermediate between a square antiprism and bicapped trigonal prism. The Bi–N and Bi–O bonds

in $[\text{Bi}(\text{H}_2\text{dtpa})]\cdot 2\text{H}_2\text{O}$ are in the range 2.449(3)–2.723(4) Å and 2.290(3)–2.699(3) Å, respectively. Interestingly, the bridging bond Bi–O(2) is shorter than one of the chelate Bi–O bonds. By means of the Bi–O(2) bridging bond, the $[\text{Bi}(\text{H}_2\text{dtpa})]\cdot 2\text{H}_2\text{O}$ complexes form polymeric chains.

Interaction of $\text{Bi}(\text{H}_2\text{dtpa})\cdot 2\text{H}_2\text{O}$ and ammonium or alkali metal carbonates in equivalent quantities led to the formation of the compounds $\text{M}[\text{Bi}(\text{Hdtpa})]\cdot 5\text{H}_2\text{O}$ ($\text{M}^+ = \text{Na}^+, \text{K}^+, \text{Rb}^+, \text{and } \text{NH}_4^+$). The crystal structure of the potassium salt was reported and was found to consist of K^+ cations $[\text{Bi}(\text{Hdtpa})(\text{H}_2\text{O})]^-$ anions and water molecules [44]. Nine-coordination geometry of Bi in the complex anion is imposed by three nitrogen donors (Bi–N 2.489(7)–2.669(2) Å), four oxygen atoms of deprotonated acetate groups (Bi–O 2.362(8)–2.568(8) Å), the carbonyl oxygen atom of the protonated carboxylate group (2.734(8) Å), and the oxygen atom of a coordinated water molecule (Bi–O_w 2.749(8) Å).

8.4.2 Bi(III) Complexes with Triethylenetetraaminehexaacetate Ligands

Anions of triethylenetetraaminehexaacetic acid (H_6ttha) potentially can be decadentate ligands and can form both mononuclear and binuclear complexes with metal ions. The complexation reaction of Bi(III) with H_6ttha has been studied spectrophotometrically and the stability constant of the protonated 1:1 complex was reported to be 22.59 ± 0.01 . Yingst and Martell [45] studied the potentiometric equilibrium in the Bi(III)– ttha system and suggested the formation of only 1:1 complexes, in contrast with Ln(III) and Ga(III), that can form both 1:1 and 2:1 complexes in aqueous solutions. In the solid state, however, both 1:1 and 2:1 Bi(III)– H_6ttha complexes have been isolated: $[\text{Bi}(\text{H}_3\text{ttha})]\cdot 2.5\text{H}_2\text{O}$ and $\text{Bi}_2(\text{ttha})\cdot 3.5\text{H}_2\text{O}$, respectively [46]. Two Ln–Bi heterobimetallic H_6ttha complexes, $\text{LaBi}(\text{ttha})$ and $\text{PrBi}(\text{ttha})$ were synthesized and proved to be useful precursors for Bi–Ln mixed oxide systems. The TGA investigation of the mono and heterometallic

Bi-ttha complexes showed the occurrence of three successive steps, corresponding to dehydration, ligand pyrolysis and the final evolution of CO_2 leading to the oxide or mixedoxide system. Dehydration starts at 60–85 °C and ends between 120 and 190 °C. The ligand pyrolysis starts around 270–280 °C resulting in carbonate-type compounds. The final decomposition temperatures range between 375 and 570 °C, while the final pyrolysis products are Bi_2O_3 in the case of monometallic complexes or BiLaO_3 and $\text{BiPr}^{\text{III}}_{1-x}\text{Pr}^{\text{IV}}_x\text{O}_{3+0.5x}$ in the case of corresponding Bi-Ln heterodimetallic complexes. Crystal structures of two Bi-ttha complexes are reported: $[\text{Bi}(\text{H}_3\text{ttha})]\cdot 3\text{H}_2\text{O}$ [47] and $(\text{CH}_6\text{N}_3)_2[\text{Bi}(\text{Httha})]\cdot 4\text{H}_2\text{O}$ [48]. It seemed plausible that increasing the number of donor atoms of the ligand would increase the CN of Bi(III). Indeed, in both of the two crystallographically independent $[\text{Bi}(\text{H}_3\text{ttha})]$ complexes of $[\text{Bi}(\text{H}_3\text{ttha})]\cdot 3\text{H}_2\text{O}$, Bi(III) has a CN= 10, and its coordination polyhedron may be best described as a bicapped square antiprism. The $\text{H}_3\text{ttha}^{3-}$ ligand is decadentate, using for coordination its four nitrogen and six oxygen donors. The main difference between the complexes 1A and 1B is the length of Bi–O(1) bond, 2.694(7) versus 2.912(7) Å. In contrast, in $(\text{CH}_6\text{N}_3)_2[\text{Bi}(\text{Httha})]\cdot 4\text{H}_2\text{O}$ [48], the bismuth atom adopts a nine-coordinate environment formed by four nitrogen and five oxygen atoms of the Httha^{5-} ligand. The protonated carboxylic group does not participate in coordination, the corresponding C–O bonds are quite indicative of this (1.18 Å for C–O, and 1.32 Å for C–OH bond). The coordination polyhedron in $(\text{CH}_6\text{N}_3)_2[\text{Bi}(\text{Httha})]\cdot 4\text{H}_2\text{O}$ can be best described as a monocapped square antiprism. The Bi–O bond lengths vary from 2.327(6) to 2.560(6) Å, while Bi–N bonds are very similar, from 2.619(7) to 2.688(8) Å.

8.4.3 Bi(III) Complexes with Macrocyclic Polyaminopolycarboxylate Ligands

Complexes of bismuth with anions of macrocyclic polyaminopolycarboxylic acids were shown to be kinetically inert [49]. Bismuth complexes with anions of H_3nota , H_4dota , and H_4teta

were isolated in solid state as white powders. Their aqueous solutions show UV spectra absorption bands at 285, 305, and 323 nm, respectively.

Complexes of Bi(III) with two cyclen derivatives were reported, $\text{NaBi(dota)} \cdot \text{H}_2\text{O}$ and Bi(dota-Bu) , where $\text{H}_4\text{dota} = 1,4,7,10\text{-tetraazacyclododecane-1,4,7,10-tetraacetic acid}$ and $\text{H}_3\text{dota-Bu} = 10\text{-[2,3-dihydroxy-(1-hydroxymethyl) propyl]-1,4,7,10-tetraazacyclododecane-1,4,7-triacetic acid}$. The stability constants determined with the study of the equilibria between Bi(III) and free acids, are very high, $\log K = 30.3$ for $[\text{Bi(dota)}]^-$, and 26.8 for $[\text{Bi(dota-Bu)}]$, respectively. The X-ray structure of $\text{Na[Bi(dota)]} \cdot \text{H}_2\text{O}$ showed that the ligand coordinated in an octadentate fashion. The Bi atom is deeply located in the cage formed by the nitrogen and oxygen donors; this is in accordance with the high thermodynamic stability of the complex.

8.5 Applications

Bismuth(III) complexes with APC and PAPC ligands have attracted significant interest due to a wide range of applications, from pharmaceuticals to high-tech materials. Nowadays it is commonly accepted that of all heavy metals, bismuth has one of the greatest potential for applications, from medicine to materials. Its compounds are less toxic than those of other heavy metals, and some of them are therapeutically useful. Bismuth isotopes emitting α -particles have been investigated for potential use as radiotherapeutic agents for the treatment of cancer [50–56]. A number of polyaminopolycarboxylate ligands have been considered for bismuth radioisotope chelation.

8.6 Nano Bismuth(III) Coordination Polymers

A novel bismuth (III) nano coordination polymer, $\{[\text{Bi}(\text{pcih})(\text{NO}_3)_2] \cdot \text{MeOH}\}_n$, (“pcih” is 2-pyridinecarbaldehyde isonicotinoylhydrazoneate) were synthesized by a sonochemical method.

The new nano-structure was characterized by transmission electron microscopy (TEM), scanning electron microscopy (SEM), X-ray powder diffraction, elemental analyses and IR spectroscopy. Single crystalline material was obtained using a heat gradient applied to a solution of the reagents. Compound 1 was structurally characterized by single crystal X-ray diffraction. The determination of the structure by single crystal X-ray crystallography shows that the complex forms a zig-zag one dimensional polymer in the solid state and the coordination number of Bi^{III} ions is seven, (BiN₃O₄), with three N-donor and one O-donor atoms from two “pcih” and three O-donors from nitrate anions. It has a hemidirected coordination sphere. The supramolecular features in these complexes are guided and controlled by weak directional intermolecular interactions. The chains interact with each other through π - π stacking interactions creating a 3D framework (Figure 8.1). After thermolysis of 1 at 230 °C with oleic acid, pure phase nano-sized bismuth(III) oxide was produced. The morphology and size of the prepared Bi₂O₃ samples were further observed using SEM [57].

A new nanostructured Bi(III) supramolecular compound, $\{[\text{Bi}_2(4,4'\text{-Hbipy})_{1.678}(4,4'\text{-Hbipy})_{0.322}(\mu\text{-I})_2\text{I}_{5.678}](4,4'\text{-bipy})\}, 4,4'\text{-bipy} = 4,4'\text{-bipyridine}\}$ was synthesized by a sonochemical method. The nano-structure of $\{[\text{Bi}_2(4,4'\text{-Hbipy})_{1.678}(4,4'\text{-Hbipy})_{0.322}(\mu\text{-I})_2\text{I}_{5.678}](4,4'\text{-bipy})\}$ was investigated using scanning electron microscopy, powder X-ray powder diffraction (XRD), IR spectroscopy and elemental analysis, and the crystal structure of compound $\{[\text{Bi}_2(4,4'\text{-Hbipy})_{1.678}(4,4'\text{-Hbipy})_{0.322}(\mu\text{-I})_2\text{I}_{5.678}](4,4'\text{-bipy})\}$ was determined by single crystal X-ray diffraction.

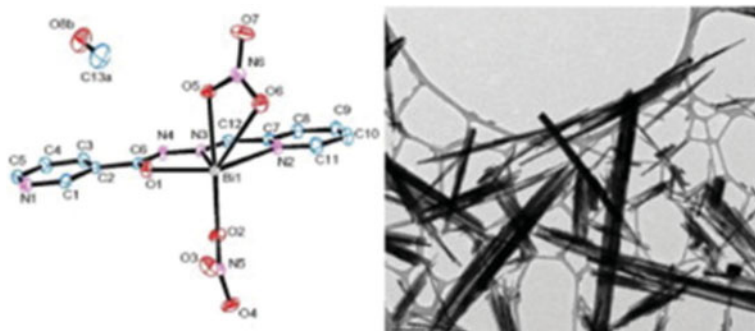


Figure 8.1 Ortep diagram of compound 1 and TEM of nano structure of 1.

$\text{I}_{5.678}](4,4'\text{-bipy})\}$ was determined by single-crystal X-ray diffraction. The thermal stability of bulk compound $\{[\text{Bi}_2(4,4'\text{-Hbipy})_{1.678}(4,4'\text{-Hbipy})_{0.322}(\mu\text{-I})_{2.5.678}](4,4'\text{-bipy})\}$ and of nano sized particles was studied by thermal gravimetric (TG) and differential thermal analyses (DTA). Bi_2O_3 and BiI_3 nano-structures were obtained by calcinations of nano-structures of compound $\{[\text{Bi}_2(4,4'\text{-Hbipy})_{1.678}(4,4'\text{-Hbipy})_{0.322}(\mu\text{-I})_{2.5.678}](4,4'\text{-bipy})\}$ at 400°C under air and nitrogen atmospheres, respectively [58].

The coordination complex was obtained by reaction between 4,4'-bipy and bismuth(III) iodide in methanol. Single crystalline material was obtained using a heat gradient applied to a solution of the reagents (the "branched tube method"), nanostructured particles were prepared by ultrasonication of the methanolic solution. The new bismuth(III) compound is an air-stable and high-melting solid that is soluble in e.g. DMSO.

The average size of the particles prepared via the sonochemical method was found to be around 115 nm, which is in agreement with the value obtained from the SEM images (Figure 8.2). Also has been investigated the use of other solvents such as water, acetonitrile, dichloromethane, benzene and chloroform) in the sonochemical procedure, but the particle sizes obtained were not in the nano scale.

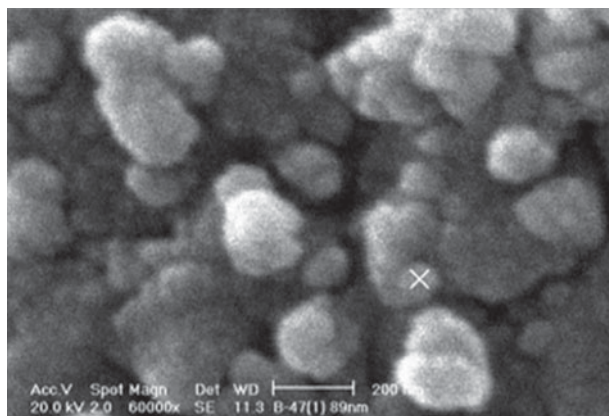


Figure 8.2 SEM photographs of nano $\{\text{Bi}_2(4,4'\text{-Hbipy})(\mu\text{-I})_2\text{I}_6\} \cdot (4,4'\text{-bipy})\}$

Thermal decomposition of the nanosized particles of $\{\text{Bi}_2(4,4'\text{-Hbipy})(\mu\text{-I})_2\text{I}_6\} \cdot (4,4'\text{-bipy})\}$ in either air or nitrogen produced Bi_2O_3 nanorods and BiI_3 nanowires, respectively. Figures 8.3a and 8.3b shows the SEM images of nanorods Bi_2O_3 and nanowires BiI_3 obtained from calcination of compound $\{\text{Bi}_2(4,4'\text{-Hbipy})(\mu\text{-I})_2\text{I}_6\} \cdot (4,4'\text{-bipy})\}$ under air and nitrogen atmosphere, respectively. The morphology and size of the structures obtained by two different methods are different [58].

In other work, has been described a simple sonochemical preparation of nano-structured particles of a new Bi(III) supramolecular compound, $\{\text{Bi}_2(\mu\text{-}4,4'\text{-bipy})\text{Cl}_{10}\} \cdot 2(4,4'\text{-Hbipy}) \cdot (4,4'\text{-H}_2\text{bipy}) \cdot 2\text{H}_2\text{O}\}$ $4,4'\text{-bipy} = 4,4'\text{-bipyridine}$ and its use for preparation of nano-particles of a- Bi_2O_3 too.

The single crystals of $\{\text{Bi}_2(\mu\text{-}4,4'\text{-bipy})\text{Cl}_{10}\} \cdot 2(4,4'\text{-Hbipy}) \cdot (4,4'\text{-H}_2\text{bipy}) \cdot 2\text{H}_2\text{O}\}$ were analyzed by X-ray diffraction (Figure 8.4). The molecular structure of the complex is built by one $[\text{Bi}_2(\mu\text{-}4,4'\text{-bipy})\text{Cl}_{10}]^{4-}$ anion, two singly protonated $4,4'\text{-Hbipy}^+$ cations and one doubly protonated $4,4'\text{-H}_2\text{bipy}^{2+}$ cation and two H_2O molecules. The $4,4'\text{-bipy}$ ligand in the dinuclear anionic complex is linking the two Bi atoms with each other which have a slightly distorted octahedral BiCl_5N coordination environment [59].

The average size of the particles prepared via the sonochemical method was found to be around 90 nm, which is in agreement with the value obtained from the SEM images (Figure 8.5). Thermal

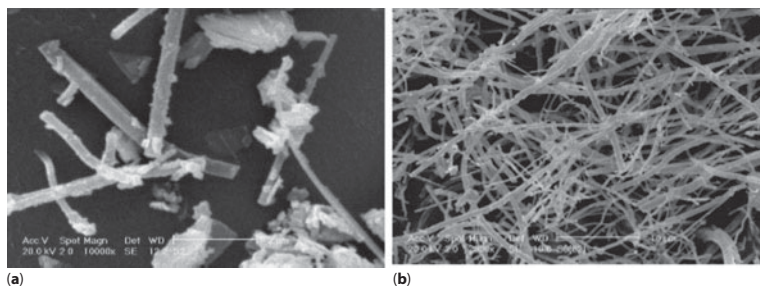


Figure 8.3 SEM photographs of (a) Bi_2O_3 nanorods and (b) BiI_3 nanowires.

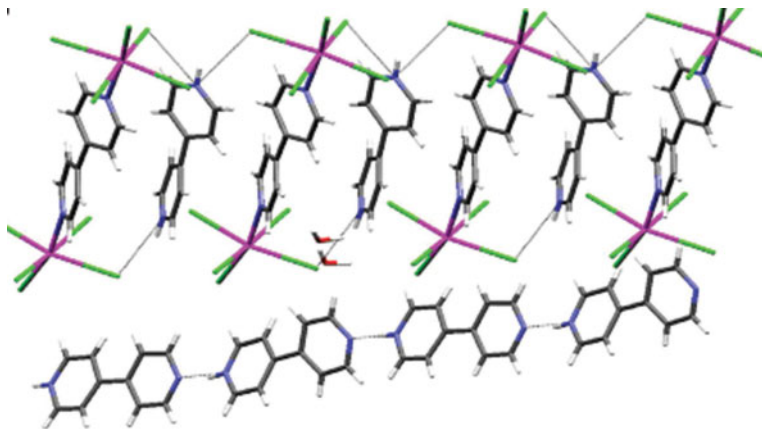


Figure 8.4 A fragment of the one-dimensional supramolecular $\{\text{Bi}_2(\mu\text{-}4,4'\text{-bipy})\text{Cl}_{10}\} \cdot 2(4,4'\text{-Hbipy}) \cdot (4,4'\text{-H}_2\text{bipy}) \cdot 2\text{H}_2\text{O}\}$

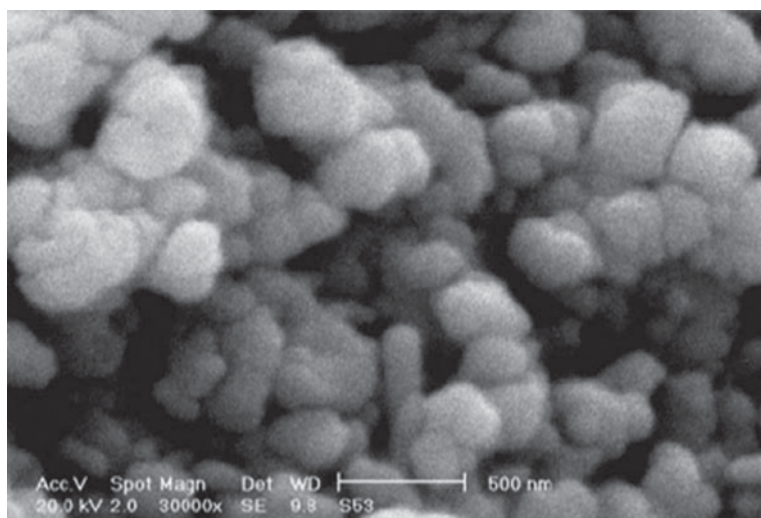


Figure 8.5 SEM photographs of $\{\text{Bi}_2(\mu\text{-}4,4'\text{-bipy})\text{Cl}_{10}\} \cdot 2(4,4'\text{-Hbipy}) \cdot (4,4'\text{-H}_2\text{bipy})$ nano-particles.

decomposition of the nano-sized particles of $\{\text{Bi}_2(\mu\text{-}4,4'\text{-bipy})\text{Cl}_{10}\} \cdot 2(4,4'\text{-Hbipy}) \cdot (4,4'\text{-H}_2\text{bipy}) \cdot 2\text{H}_2\text{O}\}$ in air produced Bi_2O_3 . Figure 4.12 shows the SEM images of nanostructured Bi_2O_3 obtained from calcinations of compound $\{\text{Bi}_2(\mu\text{-}4,4'\text{-bipy})\text{Cl}_{10}\} \cdot 2(4,4'\text{-Hbipy}) \cdot (4,4'\text{-H}_2\text{bipy}) \cdot 2\text{H}_2\text{O}\}$ under air atmosphere. It is interesting that the

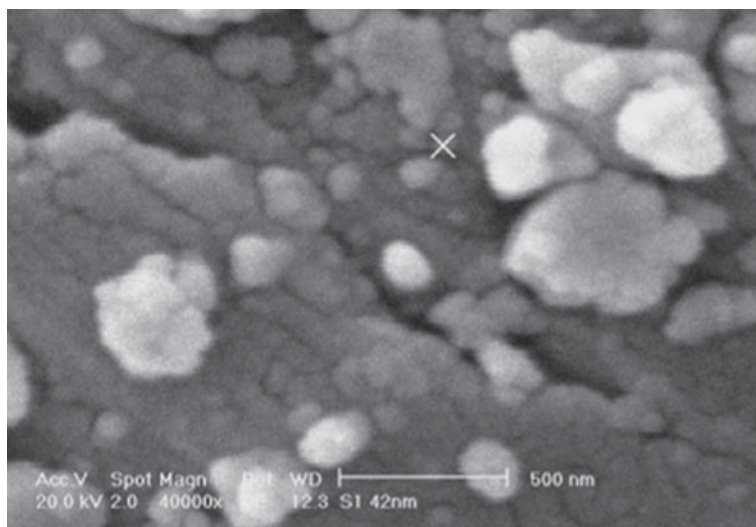


Figure 8.6 SEM photographs of Bi_2O_3 nano-particles.

calcination of the normal-sized crystals of compound $\{\text{Bi}_2(\mu\text{-}4,4'\text{-bipy})\text{Cl}_{10}\} \cdot 2(4,4'\text{-Hbipy}) \cdot (4,4'\text{-H}_2\text{bipy}) \cdot 2\text{H}_2\text{O}\}$ produces Bi_2O_3 but the particle sizes were not at nano-scale (Figure 8.6) [59].

8.7 Conclusion

Bi(III) is a borderline metal ion with a preferential interaction with ligands bearing soft donor groups [60, 61]. Nevertheless, APC and P APC ligands bearing both hard carboxylate groups and soft amine groups, form thermodynamically very stable complexes with this metal ion. Thus, despite the strong hydrolysis undergone by Bi(III) in aqueous media, multidentate APC and P APC ligands efficiently stabilize it under physiological and even higher pH conditions. This allows the use of some of these ligands as carrier molecules for $^{212/213}\text{Bi}$ isotopes for radiotherapy [61]. In spite of the large interest shown in the coordination properties of these ligands and the attention paid in recent years to the possible involvement of Bi(III) complexes in anti-cancer radiotherapies, studies dealing with formation equilibria of Bi(III) PAC and

PAPC complexes are still rare. A greater deal of research directed towards the formation equilibria of similar complexes with higher stability *in vivo* and lower cytotoxicity would be greatly desirable. The next step would probably be the optimization of the biocompatibility through the design of new ligands. APC and PAPC ligands show a high affinity to Bi(III), usually exhibiting the maximum denticity. A range of different arrangements have been found, from monomeric to polymeric, the presence of bridging carboxylate groups being a common structural feature. There is a great potential for bismuth(III) heterometallic APC and PAPC complexes as single-source molecular precursors in the preparation of mixed-oxide materials. Their remarkable air and moisture stability makes these systems particularly attractive from the technological point of view. On the other hand, it would be of great interest to attempt to introduce other metals and to produce other stoichiometries in Bi(III) APC and PAPC heterometallic complexes. By virtue of their high versatility, some of them may find a place in developing new materials, especially with regard to nanoscale applications. By varying the stability and the structure of the precursors, one may expect to influence the quality of the final materials. In conclusion, Bi(III) APC and PAPC complexes are essential for $^{212/213}\text{Bi}$ use in nuclear medicine, but much is to be done to improve the biocompatibility and *in vivo* stability of the complexes. Heterometallic Bi(III) APC and PAPC complexes are promising precursors for a range of bulk oxide materials, however little work has been reported on their use in nanomaterial synthesis. Due to their high stability and diversity of the coordination architectures, the potential of Bi(III) APC and PAPC complexes is yet to be realized.

References

1. Luckay, R., *et al.*, Synthesis, stability and structure of the complex of bismuth(III) with the nitrogen-donor macrocycle 1,4,7,10-tetraazacyclododecane. The role of the lone pair on bismuth(III) and lead(II) in determining co-ordination geometry. *Journal of the Chemical Society, Dalton Transactions*, 1997(5), p. 901–908.

2. Stavila, V. Davidovich, R. L. Gulea, A. Whitmire, K. H. Bismuth(III) complexes with animopolycarboxylate and polyaminopolycarboxylate ligands: Chemistry and structure. *Coordination Chemistry Review*, 250, 2782–2810, 2006.
3. Sadler, P.J., Sun, H. and Li, H. Bismuth(III) Complexes of the Tripeptide Glutathione (γ -L-Glu-L-Cys-Gly). *Chemistry – A European Journal*, 2(6), p. 701–708, 1996.
4. Burford, N., *et al.*, Definitive identification of cysteine and glutathione complexes of bismuth by mass spectrometry: assessing the biochemical fate of bismuth pharmaceutical agents. *Chemical Communications*, 2003(1), p. 146–147.
5. Burford, N., M.D. Eelman, and K. Groom, Identification of complexes containing glutathione with As(III), Sb(III), Cd(II), Hg(II), Tl(I), Pb(II) or Bi(III) by electrospray ionization mass spectrometry. *Journal of Inorganic Biochemistry*, 99(10), p. 1992–1997, 2005.
6. Cotton, F.A. Wilkinson, G. Murillo, C.A. Bochmann, M. *Advanced Inorganic Chemistry*, 6th ed., John Wiley & Sons Inc., USA, 1999.
7. Levason, W. Reid, G. in: Lever, A.B.P. (Ed.), *Comprehensive Coordination Chemistry II: Coordination Chemistry of the S, P, and F Metals*, vol. 3, Elsevier Pergamon, Amsterdam, p. 465, 2004.
8. Lazarini, F. *Crystal Structure Communications* 1979, Università degli studi di Parma.
9. Summers, S.P., *et al.*, Syntheses and structures of bismuth(III) complexes with nitrilotriacetic acid, ethylenediaminetetraacetic acid, and diethylenetriaminepentaacetic acid. *Inorganic Chemistry*, 33(1), p. 88–92, 1994.
10. Michaudet, L., P. Richard, and B. Boitrel, *Synthesis and crystal structure of an unprecedented bismuth porphyrin containing ester pendant arms*. *Chemical Communications*, 2000(17), p. 1589–1590.
11. Hassfjell, S., Kongshaug, K.O. and Romming, C. Synthesis, crystal structure and chemical stability of bismuth(iii) complexed with 1,4,7,10-tetraazacyclododecane-1,4,7,10-tetramethylene phosphonic acid (H8DOTMP). *Dalton Transactions*, 2003(7), p. 1433–1437.
12. Näslund, J., Persson, I. and Sandström, M. Solvation of the bismuth (III) ion by water, dimethylsulfoxide, N,N'-dimethylpropyleneurea, and N, N-dimethylthioformamide. An EXAFS, large-angle X-ray scattering, and crystallographic structural study. *Inorganic Chemistry*, 39(18), p. 4012–4021, 2000.
13. Hassan, A. and Wang, S. Organobismuth(V) complexes containing bifunctional ligands: hydrogen-bonded extended structures

- and stereoselectivity. *Journal of the Chemical Society, Dalton Transactions*, 1997(12), p. 2009–2018.
14. Suzuki, H., *et al.*, Unexpected formation of triarylbi-smuth diformates in the oxidation of triarylbi-smuthines with ozone at low temperatures. *Journal of the Chemical Society, Perkin Transactions 1*, 1993(20), p. 2411–2415.
 15. Dittes, U., B.K. Keppler, and B. Nuber, Synthesis and Structure of Seven-Coordinate Bismuth(V) Complexes with Benzenoid and Non-Benzenoid Arene Ligands: Tri(aryl)tropolonatobismuth(V) Complexes. *Angewandte Chemie International Edition in English*, 35(1), p. 67–68, 1996.
 16. Karadakov, B.P. Ivanova, Khr.R. Bismuth complexes with polyaminopolycarboxylate ligands, *Koord. Khim.*, 4 p. 1365, 1978.
 17. Ivanova, Khr.R. Karadakov, B.P. Ivanov, N.A. *Neorg. Zh. Khim.* 32, p. 354, 1987.
 18. Ershova, S.D. Fridman, A.Ya. Dyatlova, N.M. *Koord. Khim.* 6, p. 734, 1980.
 19. Ershova, S.D. Zhadanov, B.V. Polyakova, I.A. Baranova, N.F. *Neorg. Zh. Khim.* 33, p. 2245, 1988.
 20. Davidovich, R.L. *et al.*, Bismuth(III) complexes with β -hydroxyethyliminodiacetic acid, *Koord. Khim.* 22, p. 163–170, 1996.
 21. Davidovich, R.L. *et al.*, Crystal-structure of bismuth(iii) (oxyethyl)iminodiacetate dihydrate, *Koord. Khim.* 22, p. 916–920, 1996.
 22. Zevaco, T. Postel, M. Nourredine, B.-C. *Main Group Metal Chemistry*. 15, 217–224, 1992.
 23. Ranjbar, M., *et al.*, Crystal Structure of Bi(III) Complex of a Pyridine Containing Self-Assembling System, *Analytical Sciences*. 17, p. 1469, 2001.
 24. Bhat, T. and Iyer, R.K. *Studies on EDTA Complexes. V. Antimony (III) and Bismuth(III) EDTA System. Zeitschrift für anorganische und allgemeine Chemie*, 335(5–6), p. 331–336, 1965.
 25. Karadakov, B.P. Ivanova, Khr.R. *Zh. Anal. Khim.* 28, p. 525, 1973.
 26. Sochevanov, V.G. Volkova, G.A. *Neorg. Zh. Khim.* 14, p. 118, 1969.
 27. Stavila, V., *et al.*, Bismuth(III) complexes with aminopolycarboxylate and polyaminopolycarboxylate ligands: Chemistry and structure. *Coordination Chemistry Reviews*, 250(21), p. 2782–2810, 2006.
 28. Brintzenger, H. and Munkelt, S. Komplexverbindungen und Salze der Äthylendiamintetraessigsäure. III. Mitteilung. *Zeitschrift für anorganische Chemie*, 256(1–3), p. 65–74, 1948.

29. Bhat, T.R. and Krishna Iyer, R. Studies on EDTA complexes—VIII. *Journal of Inorganic and Nuclear Chemistry*, 29(1), p. 179–185, 1967.
30. Krishna Iyer, R. Shankar, J., *Indian Journal of Chemistry*. 10, p. 97, 1972.
31. Davidovich, R.L. Logvinova, V.B. Gerasimenko, A.V. *Proceedings of the 20th International Chugaev Conference on Coordination Chemistry*, Abstracts of Papers, 2001, p. 199.
32. Davidovich, R.L. Gerasimenko, A.V. Logvinova, V.B. Crystal Structure of Lithium Di(thiourea)ethylenediaminetetraacetatobismuthate(III) Hydrate $\text{LiBi}(\text{Edta})(\text{Tu})_2 \cdot 5.5\text{H}_2\text{O}$, *Russian Journal of Inorganic Chemistry*, 46, p. 1146, 2001.
33. Starikova, et al., *Koord. Khim.* 17, p. 317, 1991.
34. Davidovich, R.L. Gerasimenko, A.V. Logvinova, V.B. Crystal structure of a mixed-ligand bismuth(III) complexonate with HIda(-) and HIda(2-), *Russian Journal of Inorganic Chemistry*, 46 p. 1178–1183, 2001.
35. Davidovich, R.L. Gerasimenko, A.V. Logvinova, V.B. Synthesis and crystal structure of cesium ethylenediaminetetraacetatobismuthate(III) monohydrate, *Russian Journal of Inorganic Chemistry*, 46, p. 1518–1523, 2001.
36. Davidovich, R.L. Gerasimenko, A.V. Kovaleva, E.V., *Crystal Structure of Potassium Ethylenediaminetetraacetatobis(thiourea)bismutate(III)*, *Zh. Neorg. Khim.* 46, p. 623, 2001.
37. Davidovich, R.L. Gerasimenko, A.V. Logvinova, V.B. Discrete Complex Anion $[\text{Bi}(\text{Edta})(\text{H}_2\text{O})]^-$ of Seven-Coordinate Bismuth: Synthesis and Crystal Structure of Thiosemicarbazidium Ethylene diaminetetraacetatobismuthate(III) Monohydrate, *Russian Journal of Inorganic Chemistry*, 47, p. 967–972, 2001.
38. Davidovich, R.L. Gerasimenko, A.V. Logvinova, V.B. Synthesis and crystal structure of aminoguanidinium (Thiourea) ethylenediaminetetraacetatobismuthates(III) $(\text{CH}_7\text{N}_4)[\text{Bi}(\text{Edta})(\text{Tu})_2] \cdot 2.5\text{H}_2\text{O}$ and $(\text{CH}_7\text{N}_4)[\text{Bi}(\text{Edta})(\text{Tu})(\text{H}_2\text{O})] \cdot 2\text{H}_2\text{O}$, *Russian Journal of Inorganic Chemistry*, 48, p. 55–61, 2003.
39. Davidovich, R.L. et al., Synthesis and Crystal Structure of Aminoguanidinium Chloro(ethylenediaminetetraacetato)bismuthate(III), *Russian Journal of Inorganic Chemistry*, 46, p. 1172–1177, 2001.
40. Stavila, V., et al., Synthesis and Study of Heterometallic Co–Bi Compounds Based on Ethylenediaminetetraacetic Acid. Crystal and Molecular Structures of $[\text{Co}(\text{DH})_2(\text{o-NH}_2\text{C}_6\text{H}_4\text{CH}_3)_2][\text{Bi}_2(\mu\text{-Edta})_2(\text{H}_2\text{O})_2] \cdot 10\text{H}_2\text{O}$ (DH₂ is dimethylglyoxime). *Russian Journal of Coordination Chemistry*, 28(8), p. 565–572, 2002.

41. Stavila, V., *et al.*, A novel 3D Nd(III)–Bi(III) coordination polymer generated from EDTA ligand. *Inorganic Chemistry Communications*, 7(5), p. 634–637, 2004.
42. Wenkin, M., Touillaux, R. and Devillers, M. *Bismuth derivatives of 2,3-dicarboxypyrazine and 3,5-dicarboxypyrazole as precursors for bismuth oxide based materials*. *New Journal of Chemistry*, 22(9), p. 973–976, 1998.
43. Brechbiel, M.W., *et al.*, Preparation of the Novel Chelating Agent N-(2-Aminoethyl)-trans-1,2-diaminocyclohexane- N,N',N''-pentaacetic Acid ($H_5CyDTPA$), a Preorganized Analogue of Diethylenetriaminepentaacetic Acid (H_5DTPA), and the Structures of $BiIII(CyDTPA)_2^-$ and $BiIII(H_2DTPA)$ Complexes. *Inorganic Chemistry*, 35(21), p. 6343–6348, 1996.
44. Shkol'nikova, *et al.*, Crystalline and molecular-Structure Of (E,N',N'-Tetraacetato) Di(Thiocarbamide)Bismuth(III), *Koordinacionnaa khimia*, 19, p. 633–636, 1993.
45. Yingst, A. and A.E. Martell, New multidentate ligands. IX. Metal chelates of triethylenetetraminehexaacetic acid with trivalent metal ions. *Journal of the American Chemical Society*, 91(25), p. 6927–6930, 1969.
46. Wullens, H., Leroy, D. and Devillers, M. Preparation of ternary Bi–La and Bi–Pr oxides from polyaminocarboxylate complexes. *International Journal of Inorganic Materials*, 3(4–5), p. 309–321, 2001.
47. Wullens, H., *et al.*, Synthesis, characterization and crystal structures of bismuth(III) complexes with triethylenetetraaminehexaacetic acid and trans-cyclohexane-1,2-diaminetetraacetic acid. *Journal of the Chemical Society, Dalton Transactions*, 1996(10), p. 2023–2029.
48. Wullens, H., *et al.*, Bis(guanidinium) (Hydrogen triethylenetetraminehexaacetato)bismuthate(III) Tetrahydrate, *Acta Crystallography, C* 54 p. 770–773, 1998.
49. Kumar, K., Magerstadt, M. and Gansow, O.A. Lead(II) and bismuth(III) complexes of the polyazacycloalkane-N-acetic acids nota, dota, and teta. *Journal of the Chemical Society, Chemical Communications*, 1989(3), p. 145–146.
50. Couturier, O., *et al.*, Cancer radioimmunotherapy with alpha-emitting nuclides. *European journal of nuclear medicine and molecular imaging*, 32(5), p. 601–614, 2005.
51. Tiekink, E.R.T., Gold derivatives for the treatment of cancer, *Crit. Rev. Oncol. Hematol*, 42 p. 225–248, 2002.

52. Nikula, T.K. *et al.*, Alpha-emitting bismuth cyclohexylbenzyl DTPA constructs of recombinant humanized anti-CD33 antibodies: pharmacokinetics, bioactivity, toxicity and chemistry. *J. Nucl. Med.*, 40 p.166–176, 1999.
53. McDevitt, M.R. *et al.*, Preparation of alpha-emitting ^{213}Bi -labeled antibody constructs for clinical use, *J. Nucl. Med.*, 40 p. 1722–1727, 1999.
54. Milenic, D.E., Brady, E.D. and Brechbiel, M.W. Antibody-targeted radiation cancer therapy. *Nature Reviews Drug Discovery*, 3(6), p. 488–499, 2004.
55. P.J. Sadler, H. Sun, H. Li, *Chem. Eur. J.* 2 (1996) 701.
56. Sadler, P.J., Sun, H. and Li, H. Bismuth(III) Complexes of the Tripeptide Glutathione (γ -L-Glu-L-Cys-Gly). *Chemistry – A European Journal*, 2(6), p. 701–708, 1996.
57. Hanifehpour, Y., *et al.*, Synthesis and structural characterization of new bismuth(III) nano coordination polymer: A precursor to produce pure phase nano-sized bismuth(III) oxide. *Journal of Molecular Structure*, 1091: p. 43–48, 2015.
58. Soltanzadeh, N. and Morsali, A. Sonochemical synthesis of a new nano-structures bismuth(III) supramolecular compound: new precursor for the preparation of bismuth(III) oxide nano-rods and bismuth(III) iodide nano-wires. *Ultrasonics sonochemistry*, 17(1), p. 139–144, 2010.
59. Soltanzadeh, N. and Morsali, A. Syntheses and characterization nano-structured bismuth(III) oxide from a new nano-sized bismuth(III) supramolecular compound. *Polyhedron*, 28(7), p. 1343–1347, 2009.
60. Yao, Z., *et al.*, Pretargeted α emitting radioimmunotherapy using ^{213}Bi 1, 4, 7, 10-tetraazacyclododecane-N, N', N'', N'''-tetraacetic acid-biotin. *Clinical cancer research*, 10(9), p. 3137–3146, 2004.
61. Ruegg, C.L., *et al.*, Improved in vivo stability and tumor targeting of bismuth-labeled antibody. *Cancer research*, 50(14), p. 4221–4226, 1990.

9

Main Group Metal Coordination Chemistry

9.1 Introduction

Porous compounds have attracted the attention of chemists, physicists and materials scientists due to scientific interest in the creation of nanometer-sized spaces and the observation of novel phenomena therein. Commercial interest includes their application in separation, storage, and heterogeneous catalysis. Until the mid-1990s, there were basically two types of porous materials, namely, inorganic and carbon-based materials. In the case of microporous inorganic solids, the largest two subclasses are the aluminosilicates and aluminophosphates. Zeolites are 3D crystalline, hydrated alkaline or alkaline earth aluminosilicates with the general formula $M_{x/n}^{n+}[(AlO_2)_x(SiO_2)_y]^{x-} \cdot wH_2O$ [1, 2]. The activated carbons have a high open porosity and high specific surface area, but have a disordered structure, the essential feature of which

is a twisted network of defective hexagonal carbon layers, cross-linked by aliphatic bridging groups. On the other hand, porous coordination polymers (PCPs), beyond the scope of the former two porous materials have recently appeared. These porous coordination polymers have an infinite network with backbones constructed by metal ions as connectors and ligands as linkers, and form a family of “inorganic and organic hybrid polymers” [3–9], which are also called porous metal-organic frameworks (MOFs). The structural integrity of the building units, which can be maintained throughout the reactions, allows for their use as modules in the assembly of extended structures.

The definition of coordination chemistry in this chapter is the formation of a discrete new entity (complex, adduct) formed as a result of a Lewis acid–base (acceptor–donor, charge transfer) interaction between two species, with the formation of a new dative bond. This chapter will focus on the complexes of main group compounds with donor and acceptor atoms from Groups 13 to 18. Whilst it might be thought that “the only difference between a covalent bond and a dative bond is where you think the electrons come from”. Haaland has presented an elegant distinction between covalent and dative bonding based on the nature of the fragments formed when the relevant bond is broken either heterolytically or homolytically [10]. Rupture of a dative bond (such as in the ammonia borane complex) yields either two species without net charge or spin (H_3N and BH_3), or two species with both net charge and net spin (H_3N^{++} and $\text{BH}_3^{\bullet-}$). In contrast, rupture of the covalent bond in the isoelectronic H_3CCH_3 yields either species with net spin ($\text{H}_3\text{C}^\bullet$) or species with net charge (H_3C^+ and H_3C^-). As the minimum energy rupture in either dative or covalent bonding will yield neutral species, this indicates that dative bond rupture proceeds heterolytically, whilst covalent bond rupture proceeds homolytically. Main group coordination chemistry involving dative bond formation is commonly carried out in solution or the gas phase, and this approach has resulted in the spectroscopic and structural characterization of many different types and examples of coordination complexes [11].

9.2 Group 12

Mercury(II) and cadmium(II) and have been known for many years, although the development of the chemistry of corresponding zinc complexes is more recent. Their chemistry was often included in reviews on transition metal. However, since the M(II) complexes contain d^{10} metal centers they also fit within the main group coordination polymers that they are discussed in former chapters.

9.3 Group 13

There has been a recent renaissance of interest in Group 13 chemistry, of which cryochemistry, and in particular matrix isolation has played an important role. This includes the identification of gallane [12, 13], alane [14, 15], indane [16], thallium hydrides [17], as well as boranes [18]. There is a substantial body of work on Group 13 chemistry, much of it has been reviewed, with some containing more matrix work [19] than others [20–23]. As outlined in the introduction the emphasis of this chapter is on the complexes/adducts formed between two molecules via a coordinate/dative bond rather than compound formation following reaction or elimination. The first examples will involve halides, before considering hydride and methyl complexes of the Group 13 elements. Boron and aluminium halides are textbook examples of Lewis acids, much studied and widely used industrially. Gallium(III) and indium(III) halides function similarly, although their uses are much less widespread, whilst the Lewis acidity of thallium(III) is very limited.

9.3.1 Boron

Phosphine–borane adducts were the subject of two comprehensive reviews in 2010 [24, 25], and hence we restrict discussion to adducts of the boron halides BX_3 ($X = F, Cl, Br$ or I). The synthesis of X_3B-PR_3 adducts dates back over 100 years, with much experimental work carried out in the 1960–1980 period. In the process of adduct formation, the trigonal planar BX_3

unitis converted into a pyramidal fragment (an endothermic process variously described as the deformation or reorganisation energy) and the Lewis acid–Lewis base bond forms (an exothermic process). Boron halide adducts made in the gas phase or isolated in low temperature matrices have been reviewed, along with the relevant computational modelling [26]. Boron trihalides form 1:1 complexes with phosphine and arsine ligands, usually made by combination of the constituents in an inert solvent; hexane, benzene or toluene are the most commonly used, or sometimes in the absence of a solvent [27–34]. The PR_3 or AsR_3 (where R is a simple alkyl or aryl group) complexes are stable molecular monomers that have attracted a good deal of spectroscopic study, especially by IR/Raman and multinuclear NMR (^1H , ^{13}C , ^{11}B , $^{31}\text{P}\{^1\text{H}\}$) methods in general the data are unexceptional and the trends with changing X or ER_3 are systematic [35, 36]. Adducts with PX_3 (X = Cl, Br or I) are also known; these are less stable than PR_3 complexes and have markedly longer P–B bonds. Trivinylphosphine forms $[\text{BX}_3\{\text{P}(\text{CH}=\text{CH}_2)_3\}]$ (X = Cl, Br or I) by direct reaction with BX_3 at low temperatures, but the corresponding reaction of $[\text{BF}_3(\text{OEt}_2)]$ and $\text{P}(\text{CH}=\text{CH}_2)_3$ gave polymeric materials. The only structurally characterised BF_3 –phosphine complex is $[\text{BF}_3(\text{PEt}_3)]$, which is stable at room temperature, but which has a long B–P bond. The secondary phosphine adducts $[\text{BX}_3(\text{PHtBu}_2)]$ (X = Cl or Br) are unstable in air and convert to the phosphine oxides $[\text{BX}_3(\text{OPHtBu}_2)]$, whilst $\text{LiN}(\text{SiMe}_3)_2$ caused deprotonation to form $[\{\text{BX}_2(\text{PtBu}_2)\}_2]$. The silyl-phosphine and -arsine complexes $[\text{BX}_3\{\text{E}(\text{SiMe}_3)_3\}]$ (X = Cl, Br or I; E = P or As) were made by combination of the constituents at low temperatures, but at higher temperatures Si–E cleavage occurs to give $[\{\text{BX}_2(\text{E}(\text{SiMe}_3)_2)\}_2]$ which can be made directly from the appropriate boron halide and $\text{Li}[\text{E}(\text{SiMe}_3)_2]$.

9.3.2 Aluminium

There are considerable similarities between adducts formed by AlX_3 (X = Cl, Br or I) and those of BX_3 already discussed, but also some notable differences. Whilst tetrahedral four coordination

is still the norm, five- or six-coordination is found in some aluminium complexes. Very few complexes (none with soft donors) are known for AlF_3 , which unlike the molecular BF_3 is an inert fluorine-bridged polymer [37]. Monodentate ER_3 adducts of AlR_3 ($\text{R}' = \text{alkyl}$) have been thoroughly investigated, but detailed studies of complexes of AlX_3 are surprisingly rare and complexes with bi- and poly-dentates have received very limited study. Anionic mixed-donor polydentates containing— PR_2 groups are better known. Stibine and even bismuthine complexes have been obtained with tri-alkyl aluminiums. In addition to their inherent interest, several series of adducts have been explored as precursors for MOCVD (metal organic chemical vapour deposition) of the III–V materials AlE ($\text{E} = \text{P} - \text{Bi}$), which are direct band gap semi-conductors, whilst other aluminium-phosphine adducts have been isolated (sometimes serendipitously) from catalytic systems that have been activated with alkyl aluminiums. There is also a large amount of chemistry on aluminium dimers with ER_2^- bridges which fall out-side the scope of the present article; again the driving force for much of this work was reagents for the production of III–V semiconductors. The various energy contributions to the formation of $\text{X}_3\text{Al}-\text{ER}_3$ adducts follow closely from those discussed under boron above. The theoretical investigations have shown that whilst bond dissociation energies may be larger for aluminium than for the corresponding boron complex, this is a result of less energy needed to convert the planar AlX_3 fragment to the pyramidal shape, rather than to inherently stronger donor-acceptor bonds. An overview of the data indicates that despite some anomalies, the conclusion of decreasing Lewis acid strength is in the order $\text{AlCl}_3 > \text{AlBr}_3 > \text{AlI}_3$, and also an order $\text{AlCl}_3 > \text{AlBr}_3 > \text{GaCl}_3 > \text{GaBr}_3$ [38]. Note these are the reverse of that observed for boron halides, although more structural data on series of boron halide phosphine/arsine adducts are desirable to support the conclusions. The calculations are performed for gas phase molecules and do not take into account other (usually small) energy terms such as solvation or lattice energies. However, such small terms can result in significant effects, which may complicate or even obscure the underlying trends. For example, it has been proposed that some apparently

anomalous results in the experimental data from some solid aluminium adducts could be ascribed to solidstate effects such as H-bonding or intermolecular packing [38]. A large number of adducts of aluminium alkyls with phosphine ligands have been prepared; all appear to contain four-coordinate aluminium and are usually very moisture- and air-sensitive, although much less pyrophoric than the parent aluminium alkyls. In contrast to the aluminium halide complexes, there are di-, tri- and tetra-phosphine adducts of aluminium alkyls, although again all contain only one phosphorus bound to each aluminium [39–41]. Usually the AlR'_3 and the phosphine are simply mixed in an inert solvent, but other routes have been described, for example, $\text{Al}(\text{Bu})_2\text{H}$ and the diphosphine dioxide, $\text{Ph}_2\text{P}(\text{O})\text{CH}_2\text{CH}_2\text{P}(\text{O})\text{Ph}_2$, produced $[(\text{Al}(\text{Bu})_2)(\mu\text{-Ph}_2\text{PCH}_2\text{CH}_2\text{PPh}_2)]$ by a sequence of reduction and rearrangement reactions. $[\text{Al}_2\text{Me}_3\text{Cl}_3]$ and $\text{Ph}_2\text{PCH}_2\text{PPh}_2$ gave the scrambled product $[(\text{AlCl}_2\text{Me})(\text{AlCl}_2)(\mu\text{-Ph}_2\text{PCH}_2\text{PPh}_2)]$. For $[\text{AlMe}_3(\text{PR}_3)]$ ($\text{R}_3 = \text{Me}_3, \text{Et}_3, \text{Ph}_3, \text{Me}_2\text{Ph}, \text{MePh}_2, (\text{CH}_2\text{CH}_2\text{CN})_3, \text{Cy}_3, \text{tBu}_3, (\text{o-tolyl})_3$ etc.) the coordination shifts (Δ) in the ^{31}P NMR spectra are positive for small phosphines, but become negative as the steric bulk increases, attributed to an increase in the repulsive interaction of the phosphine substituents with the methyl groups on the small aluminium centre.

9.3.3 Gallium

Currently the complexes of gallium(I) and gallium(II) are limited to a few examples, but a large number of gallium(III) complexes have been reported. Gallium(III) halide and alkyl complexes show close resemblance to those of aluminium, but significant differences to the indium complexes. Gallium(III) has essentially the same covalent radius as aluminium(III) (1.25 Å), although the gallium compounds are often rather weaker Lewis acids. There is limited modelling work on the Lewis acidity of gallium systems, but it is likely that the key factors identified for boron and aluminium are also operating in the gallium systems. As discussed for aluminium, other factors sometimes complicate interpretation of Lewis acidity based upon bond length data, but it seems

clear in the case of gallium(III) that, apart from a few anomalies, the data indicate an order with halide $\text{Cl} > \text{Br} > \text{I}$. Analogous to the aluminium system, GaF_3 is an inert polymer and no soft donor complexes are known. For neutral phosphines and arsines, the gallium(III) overwhelmingly favours distorted tetrahedral four-coordination, and six-coordination is achieved only in some chelating diphosphine adducts. Five- and six-coordination does occur in some complexes of anionic hybrid ligands. A fair number of $[\text{GaX}_3(\text{ER}_3)]$ complexes were obtained pre-1975, although X-ray structural data were not obtained in that period.

Gallium(I) and gallium(II) complexes are very rare, but recent results have demonstrated possible entry routes into this area. The first example, $[\text{Ga}_8\text{I}_8(\text{PET}_3)_6]$ was obtained by condensing "GaI", PET_3 and toluene vapour at 77 K and cautiously allowing the mixture to thaw. The structure reveals a planar Ga_8 ring with two galliums bridged by iodides, and the remaining six gallium centres coordinated to terminal iodide and PET_3 groups. The formation of a Ga_8 ring contrasts with the Al_4 ring discussed above; although the reasons for the difference are not completely clear, both steric and electronic factors seem to be involved. More conventional syntheses from $[\text{Ga}(\text{PhMe})_2][\text{Al}\{\text{OC}(\text{CF}_3)_3\}_4]$ and PPh_3 or PtBu_3 in $\text{C}_6\text{H}_4\text{F}_2$ gave $[\text{Ga}(\text{PPh}_3)_3][\text{Al}\{\text{OC}(\text{CF}_3)_3\}_4]$ and $[\text{Ga}(\text{PtBu}_3)_2][\text{Al}\{\text{OC}(\text{CF}_3)_3\}_4]$, respectively. Several examples of formally Ga(II) compounds with unbridged Ga–Ga bonds have been prepared. Ultrasonication of Ga and I_2 in toluene, followed by addition of PET_3 at -78°C gave two compounds, $[\text{Ga}_2\text{I}_4(\text{PET}_3)_2]$ and $[\text{Ga}_3\text{I}_5(\text{PET}_3)_3]$. Complexes of halogallanes are also known [42, 43]. Synthesis routes involve redistribution between $[\text{GaCl}_3(\text{PCy}_3)]$ and $[\text{GaH}_3(\text{PCy}_3)]$, which gives $[\text{GaHCl}_2(\text{PCy}_3)]$ and $[\text{GaH}_2\text{Cl}(\text{PCy}_3)]$, and reaction of $[\text{GaH}_3(\text{PR}_3)]$ or $\text{Li}[\text{GaH}_4]$ and PR_3 with HCl . Direct substitution of the phosphine into $[\text{Ga}_2\text{H}_2\text{Cl}_4]$ is also possible. Trialkylgallium adducts are known for all ER_3 ($\text{E} = \text{P}, \text{As}, \text{Sb}$ or Bi) donor types and as expected generally resemble the aluminium analogues. The syntheses are straight forward involving combining the GaR_3 with ER_3 either in a hydrocarbon or without a solvent. Triaryl gallium examples are fewer but generally similar]. Di- and poly-phosphine adducts are also

known and all contain only a single phosphorus donor bonded to each gallium centre. The adducts with involatile phosphines have been used to store the GaR_3 , and since the GaR_3 is liberated on heating in vacuo, this also affords a means of purifying the GaR_3 for electronic materials applications [44].

9.3.4 Indium

The main similarity between the pnictogen complexes of indium and its lighter analogues, aluminium and gallium, is that the vast majority of the complexes contain the M(III) oxidation state, with very few examples of In(I) and In(II) complexes. For In(III), complexes with halide and alkyl co-ligands are common, in addition to some mixed donor bi- and multidentate ligands. The major differences are that In(III) has a significantly larger covalent radius of 1.50 Å, compared to 1.25 Å for Al and Ga, and that four-coordination is no longer dominant, with many examples of five- and six-coordinate complexes established. Indium is also a weaker Lewis acid. Studies showed that with monodentate phosphines, complexes of the type $[\text{InX}_3(\text{PR}_3)_2]$ were readily formed, and there were some reports of $[\text{InX}_3(\text{PR}_3)]$ and $[\text{InX}_3(\text{PR}_3)_3]$. There were also some complexes with diphosphines and diarsines whose structures were unclear, and in contrast to the lighter Group 13 metals, complexes of oxoanions such as $[\text{In}(\text{PR}_3)_4][\text{ClO}_4]_3$. For indium(III) halides there are well established examples of four-coordinate $[\text{InX}_3(\text{PR}_3)]$ [45–47] and five-coordinate trigonal bipyramidal $\text{trans-}[\text{InX}_3(\text{PR}_3)_2]$ [45, 47] complexes. There are also reports of some six-coordinate $[\text{InX}_3(\text{PR}_3)_3]$ species, but these lose PR_3 very easily and there seem to be no crystallographically authenticated cases with monodentate phosphines, although six-coordination is well established with diphosphines. Indium(III) complexes with various anionic chelating ligands incorporating alkoxide, thiolate or amido donor groups in addition to neutral Group 15 donor ligands are generally similar to the gallium analogues. These include $\text{Ph}_2\text{ECH}_2\text{CHRO}^-$ and $\text{Ph}_2\text{ECH}_2\text{CHRS}^-$ (E = P, Sb or Bi), which form adducts with In^iPr_2 groups, and

$\text{PPh}_2(\text{o-C}_6\text{H}_3\text{R}(\text{OH}))$ and $\text{PPh}(\text{o-C}_6\text{H}_3\text{R}(\text{OH}))_2$ which coordinate in various modes via the phosphino groups and phenolate anions [48]. Adducts of tertiary phosphines with indium(III) thiolates are formed from $[\text{In}(\text{p-R}'\text{C}_6\text{H}_4\text{S})_3]$ and the phosphine, and are of type $[\text{In}(\text{p-R}'\text{C}_6\text{H}_4\text{S})_3(\text{PR}_3)]$ ($\text{R}' = \text{H, Me, F}$; $\text{R} = \text{Cy, Et, Ph}$), being monomeric (distorted tetrahedral) in both solution and the solid state [49]. Similar complexes made from $[\text{InH}_3(\text{PCy}_3)]$ and R_2S_2 were described above. Electrochemical dissolution of an indium anode in MeCN solutions of phosphinothiols including $\text{o-Ph}_2\text{PC}_6\text{H}_4\text{SH}$ and $2\text{-Ph}_2\text{P-6-Me}_3\text{Si-C}_6\text{H}_3\text{SH}$, gave six-coordinate (P_3S_3 -coordinated) complexes containing the corresponding phos-phinothiolate [50].

9.3.5 Thallium

The Thallium coordination polymers have been discussed in former chapters.

9.4 Group 14

9.4.1 Silicon

Silicon studies in the 1960s reported $[\text{SiX}_4(\text{PMe}_3)_2]$ ($\text{X} = \text{Cl}$ or Br), believed to be trans isomers from their vibrational spectra and from a low precision X-ray determination of the geometry of the chloride complex. Recent attempts to isolate phosphine or diphosphine complexes of SiF_4 have been unsuccessful, and ^{19}F and $^{31}\text{P}\{1\text{H}\}$ NMR studies showed no evidence for complex formation between the constituents in CH_2Cl_2 solution down to 190 K [51]. Old reports of $[\text{SiF}_4(\text{PMe}_3)_n]$ ($n = 1$ or 2) formed at low temperatures in the absence of solvent, and identified by their Raman spectra, are not necessarily contradicted by the NMR results, since the experimental conditions are different, and these would merit reinvestigation. Very recently the trans- $[\text{SiX}_4(\text{PMe}_3)_2]$ ($\text{X} = \text{Cl}$ or Br) have been re-examined. They are readily isolated by combination of the constituents in CH_2Cl_2 , and although very sensitive to

water, are otherwise stable complexes. The structures show both to be trans isomers with little difference in the Si–P distances ($X = \text{Cl}$: 2.3483(3) Å, $X = \text{Br}$: 2.359(2) Å) and the NMR data show no significant dissociation in solution in CH_2Cl_2 at ambient temperatures. Attempts to prepare complexes with PPh_3 were unsuccessful, probably due to the weaker donor power, and significantly, no reaction was observed with bulky but very strong σ -donor phosphines like PBz_3 , PCy_3 or PtBu_3 ; the latter cases are consistent with the instability predicted for five-coordinate $[\text{SiX}_4(\text{PR}_3)]$, and these phosphines are too large to achieve six-coordination on the small silicon centre. No reaction occurred with AsMe_3 , which is only slightly larger than PMe_3 , suggesting that here the (assumed) weaker Si–As bond does not compensate for the deformation energy. A range of diphosphine complexes $\text{cis-}[\text{SiX}_4(\text{L-L})]$ ($X = \text{Cl}$ or Br ; $\text{L-L} = \text{Me}_2\text{P}(\text{CH}_2)_2\text{PMe}_2$, $\text{Et}_2\text{P}(\text{CH}_2)_2\text{PEt}_2$ or $\text{o-C}_6\text{H}_4(\text{PMe}_2)_2$) was isolated and all characterised by X-ray structure determinations and multinuclear NMR spectroscopy.

9.4.2 Germanium

Germanium Work reported pre-1975 described a series of $[\text{GeI}_2(\text{PR}_3)]$ complexes and two examples with GeCl_4 , $[\text{GeCl}_4(\text{PMe}_3)_n]$ ($n = 1$ or 2). In marked contrast to the failure of SiF_4 to form phosphine complexes, gaseous GeF_4 , or more conveniently, $[\text{GeF}_4(\text{MeCN})_2]$, react readily with PPh_3 or PMe_3 to form white solids, $\text{trans-}[\text{GeF}_4(\text{PR}_3)_2]$, whilst the diphosphines $\text{R}_2\text{P}(\text{CH}_2)_2\text{PR}_2$ ($\text{R} = \text{Me}$, Et , Cy or Ph) and $\text{o-C}_6\text{H}_4(\text{PR}_2)_2$ ($\text{R} = \text{Me}$ or Ph) afford $\text{cis-}[\text{GeF}_4(\text{diphosphine})]$. X-Ray crystal structures of two examples $[\text{GeF}_4\{\text{Ph}_2\text{P}(\text{CH}_2)_2\text{PPh}_2\}]$ (Figure 9.1) and $[\text{GeF}_4\{\text{o-C}_6\text{H}_4(\text{PMe}_2)_2\}]$ were determined, and detailed NMR and vibrational spectroscopic data reported. The coordination shifts in the $^{31}\text{P}\{^1\text{H}\}$ NMR spectra are again erratic, with both high and low frequency shifts being observed in different systems.

Attempts to characterise arsine complexes of GeF_4 were unsuccessful; although white solids were isolated with AsMe_3 or $\text{o-C}_6\text{H}_4(\text{AsMe}_2)_2$, these were very unstable and not identified. The reactions of GeCl_4 and GeBr_4 with phosphine ligands proved to

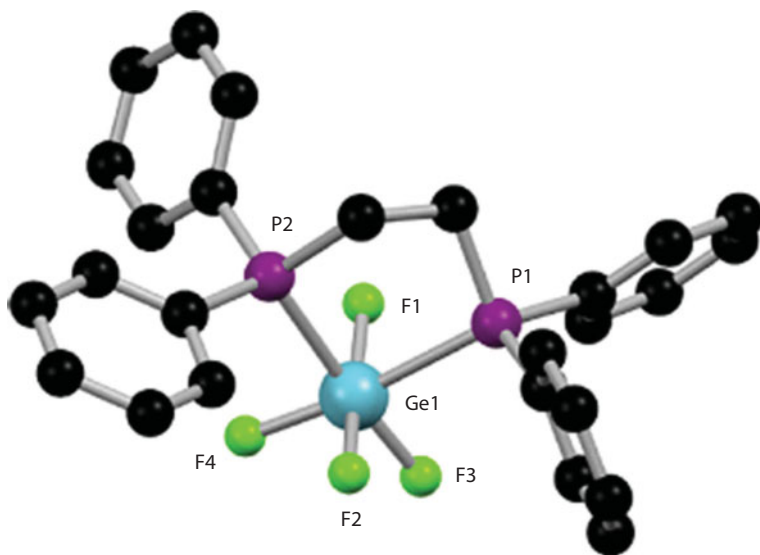


Figure 9.1 View of the structure of $[\text{GeF}_4\{\text{Ph}_2\text{P}(\text{CH}_2)_2\text{PPh}_2\}]$.

be very sensitive to the reaction conditions, and a clear picture of the chemistry has emerged only recently. The reaction of GeCl_4 with PMe_3 in the absence of a solvent was reported to give $\text{trans}[\text{GeCl}_4(\text{PMe}_3)_2]$ identified by vibrational spectroscopy, which on reaction with excess GeCl_4 gave five-coordinate $[\text{GeCl}_4(\text{PMe}_3)]$. However, reaction of PtBu_3 or PiPr_3 with GeX_4 ($\text{X} = \text{Cl}$ or Br) formed $[\text{PR}_3\text{X}][\text{GeX}_3]$ (which have the elemental composition “ $\text{GeX}_4(\text{PR}_3)$ ”), and this was confirmed by a structure determination of $[\text{PiPr}_3\text{Br}][\text{GeBr}_3]$. Reactions of AsMe_3 or AsEt_3 with GeCl_4 produced $\text{trans-GeCl}_4(\text{AsR}_3)_2$, both confirmed by X-ray crystal structures; in solution over several days these decompose forming AsR_3Cl_2 . No reaction was found between GeCl_4 and $\text{o-C}_6\text{H}_4(\text{AsMe}_2)_2$. The successful isolation of $[\text{GeCl}_4(\text{AsR}_3)_2]$, in contrast to the transient formation of the corresponding phosphines, is readily attributed to the much greater reducing power of the phosphines. Comparison of the chemistry of SiX_4 and GeX_4 with tertiary phosphines and arsines reveals unexpectedly great differences.

9.4.3 Tin

The tin(IV) coordination chemistry of halides and organometallic species is well developed, and the main types of pnictogen ligand complexes, based upon six-coordination, such as $[\text{SnX}_4(\text{PR}_3)_2]$, $[\text{SnR}'_2\text{X}_2(\text{PR}_3)_2]$ or their diphosphine analogues, were discussed in previous articles. Early work mostly used microanalysis and vibrational spectroscopy as the characterisation techniques and there were also several studies using ^{119}Sn Mössbauer spectroscopy. In recent work, multinuclear NMR and X-ray crystallography have taken over as the major characterisation techniques. In contrast, tin(II) chemistry of neutral Group 15 ligands has received surprisingly little effort, given the extensive work on tin chemistry in general. SnF_4 is an inert polymer, but by reacting $[\text{SnF}_4(\text{MeCN})_2]$ with the appropriate phosphine in CH_2Cl_2 , trans- $[\text{SnF}_4(\text{PR}_3)_2]$ ($\text{R} = \text{Me}$ or Cy) and cis- $[\text{SnF}_4(\text{diphosphine})]$ (diphosphine = $\text{R}_2\text{P}(\text{CH}_2)_2\text{PR}_2$, $\text{R} = \text{Me}$, Et , Ph or Cy ; o- $\text{C}_6\text{H}_4(\text{PR}_2)_2$, $\text{R} = \text{Me}$ or Ph) were obtained. The products are white, moisture sensitive solids, which are also dioxygen sensitive in solution. The other three tin(IV) halides, SnX_4 ($\text{X} = \text{Cl}$, Br or I), are tetrahedral monomers, and synthesis of their phosphine or arsine complexes (there are no reports of stibines) mostly involve mixing the SnX_4 with the ligand under anhydrous conditions and an inert atmosphere in CH_2Cl_2 , hexane, benzene etc. For tertiary phosphines the six-coordinate trans- $[\text{SnX}_4(\text{PR}_3)_2]$ are the usual solid products, exemplified by those of PMe_3 , PEt_3 , PPh_3 , PMe_2Ph and PnBu_3 . AsPh_3 complexes of both 1:1 and 2:1 stoichiometry have been reported. Interestingly, Mahon *et al.* determined the X-ray structures of $[\text{SnX}_4(\text{AsPh}_3)_2]$, finding that the chloride was the expected six-coordinate trans isomer, but the bromide was trigonal bipyramidal $[\text{SnBr}_4(\text{AsPh}_3)]$ with a second uncoordinated AsPh_3 group in the lattice interacting with the axial Br group (Figure 9.2). A different synthetic approach involved the reaction of tin powder with PR_3X_2 ($\text{R} = \text{nPr}$, $\text{X} = \text{I}$; $\text{R}_3 = \text{Ph}$, Ph_2Me or PhMe_2 , $\text{X} = \text{Br}$ or I) in diethyl ether, which produced the first structurally authenticated phosphine adduct of tin(IV) iodide, trans- $[\text{SnI}_4(\text{PnPr}_3)_2]$, and cis/trans mixtures for $[\text{SnBr}_4(\text{PR}_3)_2]$ identified by a combination of vibrational and Mössbauer spectroscopy.

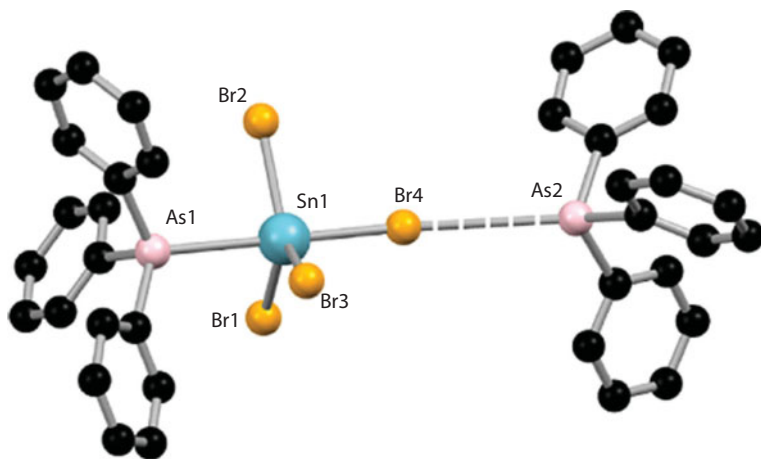


Figure 9.2 View of the structure of $[\text{SnBr}_4(\text{AsPh}_3)].\text{AsPh}_3$.

9.4.4 Lead

The lead coordination polymers have been discussed in former chapters.

9.5 Group 15

9.5.1 Phosphorus

Phosphorus Apart from the work on phosphonium compounds referred to above; there has been little new work on phosphorus halide complexes. The structure of the 1:1 adduct between PBr_3 and PMe_3 consists two square pyramidal units linked in to a dimer by very asymmetric bromine bridges $[(\text{PMe}_3)\text{PBr}_2(\mu\text{-Br})_2\text{PBr}_2(\text{PMe}_3)]$ with $\text{P} - \text{Br}_{\text{terminal}} = 2.424(2), 2.250(2) \text{ \AA}$ and $\text{P} - \text{Br}_{\text{bridge}} = 2.677(2), 3.327(2) \text{ \AA}$.

9.5.2 Arsenic

Both AsMe_3 and AsEt_3 form only 1:1 adducts with AsCl_3 , which are dimeric, but without any evidence for longer contacts.

Diphosphines or diarsines also form 1:1 adducts with arsenic(III) halides, including $[\text{AsX}_3\{\text{o-C}_6\text{H}_4(\text{AsMe}_2)_2\}]$ ($\text{X} = \text{Cl}, \text{Br}$ or I) and $[\text{AsCl}_3\{\text{o-C}_6\text{H}_4(\text{PR}_2)_2\}]$ ($\text{R} = \text{Ph}$ or Me). The $[\text{AsX}_3\{\text{o-C}_6\text{H}_4(\text{AsMe}_2)_2\}]$ ($\text{X} = \text{Br}$ or I) have dimeric structures based upon edge-shared bi-octahedra, with distorted environments about the central arsenics; there is no vacant vertex which could be occupied by the arsenic (on AsX_3) lone pair, but distortions in the bond lengths and angles suggest the lone pair may be localised in the direction of one AsX_3 triangular face. The $[\text{AsCl}_3\{\text{o-C}_6\text{H}_4(\text{PPh}_2)_2\}]$ decomposes in CDCl_3 solution to give a mixture of species including the chlorinated diphosphine (based on $^{31}\text{P}\{1\text{H}\}$ NMR evidence). Arsenic(III) iodide is reduced by $\text{Ph}_2\text{P}(\text{CH}_2)_2\text{PPh}_2$ to the arsenium cation $[\text{As}\{\text{Ph}_2\text{P}(\text{CH}_2)_2\text{PPh}_2\}]\text{I}$ and the cation has been structurally authenticated in $[\text{As}\{\text{Ph}_2\text{P}(\text{CH}_2)_2\text{PPh}_2\}][\text{As}_2\text{I}_7\{\text{Ph}_2\text{P}(\text{CH}_2)_2\text{PPh}_2\}]$ [52]. The triarsine $\text{MeC}(\text{CH}_2\text{AsMe}_2)_3$ forms 1:1 adducts with AsX_3 of unknown structure.

9.5.3 Antimony

Complexes of antimony(III) halides are mostly six-coordinate, with distorted octahedral antimony. An exception is the dimeric $[\text{Sb}_2\text{I}_4(\mu\text{-I})_2(\text{PMe}_3)_2]\cdot\text{thf}$ which has five-coordinate antimony centres with anti-disposed PMe_3 groups axial, weakly associated into polymer chains via long Sb-I contacts [53]. In $[\text{SbCl}_3(\text{AsEt}_3)]$ the antimony has a disphenoidal shape with equatorial AsEt_3 (alternatively described as trigonal bipyramidal with a vacant equatorial vertex) with these units linked via long Sb-Cl bonds into zig-zag chains [54]. In contrast, the yellow crystals formed from SbBr_3 and PEt_3 in thf solution, seemingly the product of adventitious hydrolysis, were found to be the anionic $[\text{PEt}_3\text{H}][\text{Sb}_2\text{Br}_7(\text{PEt}_3)_2]$ with discrete confacial bioctahedral anions [55]. The reactions of SbX_3 and SbR_3 typically result in scrambling to give $\text{SbR}_{3-n}\text{X}_n$, but stibine adducts of antimony halides include the structurally characterised $[\text{SbI}_3(\text{SbMe}_3)(\text{thf})]$, which is a centrosymmetric dimer with two iodide bridges [56], and $[\text{SbI}_2\text{Me}(\text{SbMe}_3)]$ [57], which has a trans-trigonal bipyramidal shape with a vacant equatorial vertex for the $(\text{Sb})\text{SbI}_2\text{Me}$ unit.

9.5.4 Bismuth

The complexes of bismuth(III) halides generally follow the pattern established for antimony, although they are rather more stable and the structures less distorted. BiBr_3 reacts with neat PMe_3 to form $[\text{BiBr}_3(\text{PMe}_3)_2]$; crystals obtained from CH_2Cl_2 solution show that the structure is dimeric $[\text{Br}_2(\text{PMe}_3)_2\text{Bi}(\mu\text{-Br})_2\text{BiBr}_2(\text{PMe}_3)_2]$ [58]. The corresponding reaction with PMe_2Ph in thf gave crystals of the mixed phosphine-phosphine oxide complex $[\{\text{BiBr}_3(\text{PMe}_2\text{Ph})(\text{OPMe}_2\text{Ph})\}_2]$, presumably due to air-oxidation. The structure is similar to that of the PMe_3 complex, with the phosphine oxides occupying axial positions on each bismuth [58]. The complexes formed in these systems are very sensitive to small changes in the reaction conditions. Thus reaction of BiBr_3 and PMe_3 in thf solution, followed by crystallisation of the product from $\text{MeCN}/\text{Et}_2\text{O}$ gave $[\text{PMe}_3\text{H}][\text{Bi}_2\text{Br}_7(\text{PMe}_3)_2]$ [59]. The anion has a planar Bi_2Br_6 core with one PMe_3 group on each bismuth arranged anti, the anions being assembled into zig-zag chains by single bromide bridges trans to PMe_3 . The iodide complex $[\text{PMe}_3\text{H}][\text{Bi}_2\text{I}_7(\text{PMe}_3)_2]$ (although not structurally characterised) appears to be similar, but the corresponding reaction between BiI_3 and PEt_3 in thf solution gave crystals of $[\text{PEt}_4]_4[\text{Bi}_6\text{I}_{22}]$ [59]. It is unclear how the $[\text{PEt}_4]^+$ cation is formed. The product from BiBr_3 and PEt_3 in thf is different again, forming a cubane tetramer $[\text{Bi}_4\text{Br}_{12}(\text{PEt}_3)_4]$ (Figure 9.3) [53] which is clearly related to the $[\text{Bi}_4\text{Br}_{16}]^{4-}$ anion, with one terminal bromide on each bismuth replaced by a phosphine.

The geometry about the bismuth centres is close to octahedral and the Bi–Br and Bi–P bond lengths are unexceptional, apart from $\text{Bi-Br}_{\text{transP}}$ which are significantly longer ($\sim 0.2 \text{ \AA}$) than $\text{Bi-Br}_{\text{transBr}}$. A mononuclear cis-octahedral anion is present in $[\text{PPh}_4][\text{BiI}_4(\text{PMe}_2\text{Ph})_2]$, formed from $[\text{PPh}_4]\text{I}$, BiI_3 and PMe_2Ph in MeNO_2 solution [55]. The d(Bi–I) are little different whether cis or trans to P (with an average length of 3.048 \AA), but d(Bi–P) are long at $2.981(2)$ and $3.005(2) \text{ \AA}$, and there are significant angle distortions—the axial $\angle \text{I-Bi-I}$ is 157.1° (bent towards the phosphines) and the $\angle \text{P-Bi-P}$ is 112.3° , which was discussed in terms of lone-pair activity.

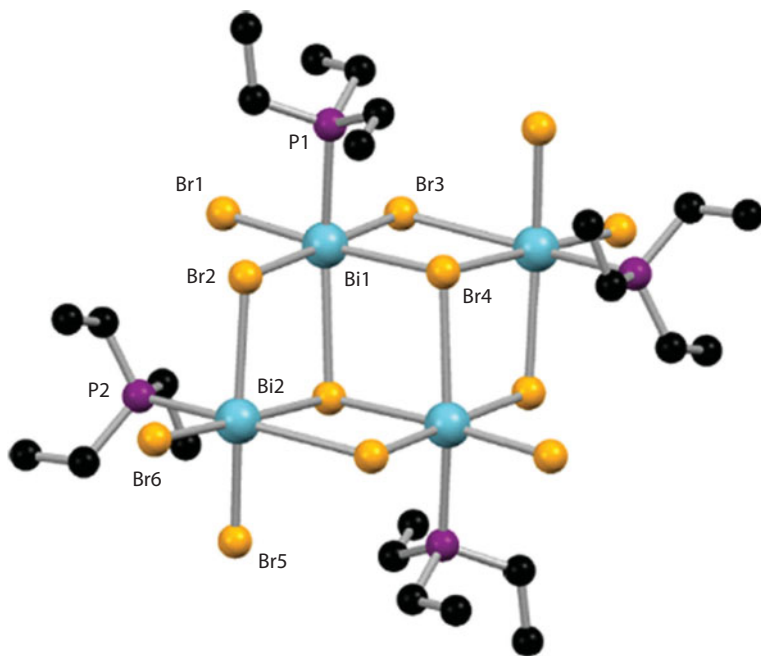


Figure 9.3 View of the structure of $[\text{Bi}_4\text{Br}_{12}(\text{PEt}_3)_4]$ redrawn from Ref. [53].

9.6 Group 16

Selenium(IV) and tellurium(IV) halides are reduced by phosphines; the complex mixture of products formed depends upon the reaction conditions, but the primary reaction is the formation of halo phosphorus(V) cations $[\text{PR}_3\text{X}]^+$ and selenium or tellurium anions, sometimes along with elemental Se or Te [60]. In the presence of air and moisture, the major products with TeX_4 are protonated phosphine oxide salts of halo tellurates(IV) [61]. Careful bromination of phosphine selenides affords $[(\text{R}_3\text{P})\text{SeBr}_2]$ $\text{R} = \text{NMe}_2, \text{NEt}_2, \text{Cy}, \text{iPr}, \text{tBu}$ which have T-shaped geometries at Se ($10e^-$ systems) and are formally phosphine complexes of SeBr_2 [62, 63]. However, iodination of R_3PSe produces the charge transfer complexes $\text{R}_3\text{PSe-I-I}$ [64, 65]. There are similar complexes of both types derived from diphosphine diselenides, but the initial products of reaction of R_3PSe with Cl_2 or SO_2Cl_2 eliminate elemental selenium below room temperature forming R_3PCl_2 .

Et_3PTe reacts with SO_2Cl_2 or I_2 to form $[(\text{Et}_3\text{P})\text{TeX}_2]$ ($\text{X} = \text{Cl}$ or I), and $[(\text{Et}_3\text{P})\text{TeBr}_2]$ was formed from $[(\text{Et}_3\text{P})\text{TeCl}_2]$ and Me_3SiBr [66]. All have T-shaped structures at Te with weak halogen bridges giving centrosymmetric dimer units. Although they cannot be made directly from selenium or tellurium halides, complexes of $\text{Ph}_2\text{E}(\text{CH}_2)_2$ ($\text{E} = \text{P}$ or As) of the type $[\text{M}\{\text{Ph}_2\text{E}(\text{CH}_2)_2\text{EPh}_2\}][\text{O}_3\text{SCF}_3]_2$, which are Group 16 analogues of triphosphenium complexes, can be made by ligand exchange from the diazabutadiene complexes $[\text{ML}_2][\text{O}_3\text{SCF}_3]_2$ ($\text{L} = \text{R}_2\text{diazabutadiene}$, where $\text{R} = \text{cyclohexyl}$ or $2,6\text{-diisopropylphenyl}$) [67].

References

1. Weitkamp, J., Sing, K.S.W. and Schüth, F. *Handbook of porous solids*, Wiley-Vch Weinheim, 2002.
2. Breck, D.W. *Zeolite Molecular Sieves*, Wiley & Sons, New York, 1984.
3. Bradshaw, D., *et al.*, Design, Chirality, and Flexibility in Nanoporous Molecule-Based Materials. *Accounts of Chemical Research*, 38(4), p. 273–282, 2005.
4. Férey, G., *et al.*, Crystallized Frameworks with Giant Pores: Are There Limits to the Possible? *Accounts of Chemical Research*, 38(4), p. 217–225, 2005.
5. Bruce, D.W., O'Hare, D. and Walton, R.I. *Porous Materials*, Wiley, 2011.
6. Yaghi, O.M., *et al.*, Reticular synthesis and the design of new materials. *Nature*, 423(6941), p. 705–714, 2003.
7. Bradshaw, D., *et al.*, Permanent Microporosity and Enantioselective Sorption in a Chiral Open Framework. *Journal of the American Chemical Society*, 126(19), p. 6106–6114, 2004.
8. Eddaoudi, M., *et al.*, Modular chemistry: secondary building units as a basis for the design of highly porous and robust metal-organic carboxylate frameworks. *Accounts of Chemical Research*, 34(4), p. 319–330, 2001.
9. Kitagawa, S. Kitaura, R. Noro, S.-I, Functional porous coordination polymers, *Angew. Chem., Int. Ed.* Engl, 43 p. 2334–2375, 2004.
10. Haaland, A., Covalent versus dative bonds to main group metals, a useful distinction. *Angewandte Chemie International Edition in English*, 28(8), p. 992–1007, 1989.

11. Davydova, E., *et al.*, Molecular complexes formed by halides of group 4, 5, 13–15 elements and the thermodynamic characteristics of their vaporization and dissociation found by the static tensimetric method. *Coordination Chemistry Reviews*, 254(17), p. 2031–2077, 2010.
12. Downs, A.J., Goode, M.J. and Pulham, C.R. Gallane at last! Synthesis and properties of binary gallium hydride. *Journal of the American Chemical Society*, 111(5), p. 1936–1937, 1989.
13. Pulham, C.R., *et al.*, Gallane: synthesis, physical and chemical properties, and structure of the gaseous molecule Ga_2H_6 as determined by electron diffraction. *Journal of the American Chemical Society*, 113(14), p. 5149–5162, 1991.
14. Andrews, L. Wang, X. The infrared spectrum of Al_2H_6 in solid hydrogen, *Science*, 299, p. 2049–2052, 2003.
15. Wang, X., *et al.*, Infrared Spectra of Aluminum Hydrides in Solid Hydrogen: Al_2H_4 and Al_2H_6 . *Journal of the American Chemical Society*, 125(30), p. 9218–9228, 2003.
16. Andrews, L. Wang, X. Infrared spectra of indium hydrides in solid hydrogen and of solid indane, *Angew. Chem. Int. Ed.* 43, 1706–1709, 2004.
17. Wang, X. and Andrews, L. Infrared spectra of thallium hydrides in solid neon, hydrogen, and argon. *The Journal of Physical Chemistry A*, 108(16), p. 3396–3402, 2004.
18. Tague, T.J. and Andrews, L. Reactions of Pulsed-Laser Evaporated Boron Atoms with Hydrogen. Infrared Spectra of Boron Hydride Intermediate Species in Solid Argon. *Journal of the American Chemical Society*, 116(11), p. 4970–4976, 1994.
19. Downs, A.J., Himmel, H.-J. and Manceron, L. Low valent and would-be multiply bonded derivatives of the Group 13 metals Al, Ga and In revealed through matrix isolation. *Polyhedron*, 21(5–6), p. 473–488, 2002.
20. Downs, A.J. and Pulham, C.R. The hydrides of aluminium, gallium, indium, and thallium: a re-evaluation. *Chemical Society Reviews*, 23(3), p. 175–184, 1994.
21. Downs, A.J., Recent advances in the chemistry of the Group 13 metals: hydride derivatives and compounds involving multiply bonded Group 13 metal atoms. *Coordination Chemistry Reviews*, 189(1), p. 59–100, 1999.
22. Pardoe, J.A. and A.J. Downs, Development of the chemistry of indium in formal oxidation states lower than + 3. *Chemical Reviews*, 107(1), p. 2–45, 2007.

23. Aldridge, S. Downs, A.J. *The Group 13 Metals Aluminium, Gallium, Indium and Thallium: Chemical Patterns and Peculiarities*, John Wiley & Sons, Chichester, U.K., 2011.
24. Staubitz, A., *et al.*, Amine- and Phosphine-Borane Adducts: New Interest in Old Molecules. *Chemical Reviews*, 110(7), p. 4023–4078, 2010.
25. Bouhadir, G., Amgoune, A. and Bourissou, D. *Chapter 1 - Phosphine-Boranes and Related Ambiphilic Compounds: Synthesis, Structure, and Coordination to Transition Metals*, in *Advances in Organometallic Chemistry*, F.H. Anthony and J.F. Mark, Editors. Academic Press. p. 1–107, 2010.
26. Young, N.A., Main group coordination chemistry at low temperatures: A review of matrix isolated Group 12 to Group 18 complexes. *Coordination Chemistry Reviews*, 257(5–6), p. 956–1010, 2013.
27. Monkowius, U., Nogai, S. and Schmidbaur, H. Trivinylphosphineborane (CH₂[double bond, length as m-dash]CH)₃PBH₃ and related compounds. *Dalton Transactions*, (5), p. 987–991, 2003.
28. Black, D. and Taylor, R. The crystal and molecular structures of the trimethylphosphine-boron trihalide complexes: (CH₃)₃PBCl₃, (CH₃)₃PBBr₃ and (CH₃)₃PBI₃. *Acta Crystallographica Section B: Structural Crystallography and Crystal Chemistry*, 31(4), p. 1116–1120, 1975.
29. Charmant, J.P.H., *et al.*, Synthesis and reactivity of dichloroboryl complexes of platinum(ii). *Dalton Transactions*, (1), p. 114–123, 2007.
30. Aubauer, C., *et al.*, Crystal Structures of the Phosphorus-Boron Adducts n-Pr₃P·BBr₃ and I₃P·BBr₃. *Zeitschrift für anorganische und allgemeine Chemie*, 626(11), p. 2373–2378, 2000.
31. Aubauer, C., Klapötke, T. and Schulz, A. On the bonding, structure and thermodynamics of phosphorus halide boron halide complexes X₃P·BY₃ (X, Y = Cl, Br, I). *Journal of Molecular Structure: THEOCHEM*, 543(1), p. 285–297, 2001.
32. Weller, F. Möhlen, M. Dehnicke, K. Crystal structure of tribromo-(triphenylphosphane)boron, (C₆H₅)₃P·BBr₃. *Z. Kristallogr, New Crystal Structure*, 212, p. 159–160, 1997.
33. Braunschweig, H., K. Radacki, and K. Uttinger, Syntheses of Mono- and Dinuclear Diiodoboryl Complexes of Platinum. *Inorganic Chemistry*, 46(21), p. 8796–8800, 2007.
34. Dornhaus, *et al.*, Phosphanylborohydrides: First Assessment of the Relative Lewis, *European Journal of Inorganic Chemistry*, p. 1777–1785, 2006.

35. Gushikem, Y. and Watari, F. Vibrational spectroscopic study of trimethylarsine-boron trihalide adducts. *Journal of the Chemical Society, Dalton Transactions*, (10), p. 2016–2019, 1980.
36. Drake, J.E., Khasrou, L.N. and Majid, A. A spectroscopic investigation of trimethyl- and triphenyl-arsine adducts of boron trihalides. *Canadian journal of chemistry*, 59(15), p. 2417–2428, 1981.
37. Benjamin, S.L., W. Levason, and G. Reid, Medium and high oxidation state metal/non-metal fluoride and oxide-fluoride complexes with neutral donor ligands. *Chemical Society Reviews*, 42(4), p. 1460–1499, 2013.
38. Timoshkin, A.Y., *et al.*, Do Solid-State Structures Reflect Lewis Acidity Trends of Heavier Group 13 Trihalides? *Experimental and Theoretical Case Study. Inorganic Chemistry*, 51(21), p. 11602–11611, 2012.
39. Barron, A.R., Adducts of trimethylaluminium with phosphine ligands; electronic and steric effects. *Journal of the Chemical Society, Dalton Transactions*, (12), p. 3047–3050, 1988.
40. Wierda, D.A. and A.R. Barron, Adducts of trimethylaluminium with phosphine ligands: X-ray crystal structures of $\text{Me}_3\text{AlPPh}_3$ and $\text{Me}_3\text{AlP(o-tolyl)}_3$. *Polyhedron*, 8(6), p. 831–834, 1989.
41. Shatunov, V.V., *et al.*, The synthesis and deep purification of GaEt_3 . Reversible complexation of adducts MAlk_3 ($\text{M} = \text{Al, Ga, In}$; $\text{Alk} = \text{Me, Et}$) with phenylphosphines. *Journal of Organometallic Chemistry*, 696(10), p. 2238–2251, 2011.
42. Tang, C.Y., *et al.*, Decomposition of monochlorogallane, $[\text{H}_2\text{GaCl}]_n$, and adducts with amine and phosphine bases: Formation of cationic gallane derivatives. *Inorganic Chemistry*, 44(20), p. 7143–7150, 2005.
43. Schmidbaur, H. and Nogai, S.D. From gallium hydride halides to molecular gallium sulfides. *Zeitschrift für anorganische und allgemeine Chemie*, 630(13–14), p. 2218–2225, 2004.
44. Bradley, D.C., *et al.*, The reversible adduct formation of group III trialkyls with relatively involatile phosphines; X-ray crystal structures of $(\text{Me}_3\text{M})_2 \cdot (\text{Ph}_2\text{PCH}_2)_2$ ($\text{M} = \text{Al, Ga, In}$) and $(\text{Me}_3\text{Al})_3 \cdot (\text{Ph}_2\text{PCH}_2\text{CH}_2)_2$ PPh. *Polyhedron*, 7(14), p. 1289–1298, 1988.
45. Brown, M.A., Tuck, D.G. and Wells, E.J. Spectroscopic and crystallographic studies of phosphino adducts of indium(III) iodide. *Canadian journal of chemistry*, 74(8), p. 1535–1549, 1996.
46. Alcock, N.W., *et al.*, Synthetic, spectroscopic and X-ray crystallographic studies on complexes formed between indium(III) iodide

- and phosphine ligands. *Journal of the Chemical Society, Dalton Transactions*, (19), p. 2775–2780, 1992.
47. Chen, F., *et al.*, Solid-state ^{115}In NMR study of indium coordination complexes. *Chemical Communications*, (45), p. 5933–5935, 2008.
 48. Saatchi, K., Patrick, B.O. and Orvig, C. Coordination chemistry of P, O-bidentate phosphinophenolates with Ga^{3+} and In^{3+} . *Dalton Transactions*, (13), p. 2268–2274, 2005.
 49. Briand, G.G., Davidson, R.J. and Decken, A. Substituent Effects on Indium-Phosphorus Bonding in $(4\text{-RC}_6\text{H}_4\text{S})_3\text{In PR}'_3$ Adducts ($\text{R} = \text{H, Me, F}$; $\text{R}' = \text{Et, Cy, Ph}$): A Spectroscopic, Structural, and Thermal Decomposition Study. *Inorganic Chemistry*, 44(26), p. 9914–9920, 2005.
 50. Pérez-Lourido, P., *et al.*, Synthesis and Characterization of Indium Compounds with Phosphinothiol Ligands. The Crystal and Molecular Structures of $[\text{In}\{2\text{-(Ph}_2\text{P)}\text{C}_6\text{H}_4\text{S}\}_3]$, $[\text{In}\{2\text{-(Ph}_2\text{P)}\text{-6-(Me}_3\text{Si)}\text{C}_6\text{H}_3\text{S}\}_2\{2\text{-(Ph}_2\text{PO)}\text{-6-(Me}_3\text{Si)}\text{C}_6\text{H}_3\text{S}\}]$, and $[\text{NMe}_4][\text{In}\{\text{PhP}(\text{C}_6\text{H}_4\text{S-2})_2\}]\text{CH}_3\text{CN}$. *Inorganic Chemistry*, 38(6), p. 1293–1298, 1999.
 51. George, K., *et al.*, Hypervalent neutral O-donor ligand complexes of silicon tetrafluoride, comparisons with other group 14 tetrafluorides and a search for soft donor ligand complexes. *Dalton Transactions*, 40(7), p. 1584–1593, 2011.
 52. Ellis, B.D. and Macdonald, C.L. Stabilized arsenic(I) iodide: A ready source of arsenic iodide fragments and a useful reagent for the generation of clusters. *Inorganic Chemistry*, 43(19), p. 5981–5986, 2004.
 53. Clegg, W., *et al.*, Neutral phosphine complexes of antimony(III) and bismuth(III) halides. *Journal of the Chemical Society, Dalton Transactions*, (12), p. 1743–1751, 1994.
 54. Conrad, E., *et al.*, Coordination of Arsine Ligands as a General Synthetic Approach to Rare Examples of Arsenic–Antimony and Arsenic–Bismuth Bonds. *Journal of the American Chemical Society*, 131(14), p. 5066–5067, 2009.
 55. Clegg, W., *et al.*, Anionic phosphine complexes of antimony(III) and bismuth(III) halogenoanions. *Journal of the Chemical Society, Dalton Transactions*, (12), p. 1753–1757, 1994.
 56. Breunig, H., *et al.*, Synthesen und Kristallstrukturanalysen von $[\text{SbI}_3(\text{SbMe}_3)(\text{THF})]_2$ und $[\text{Li}(\text{THF})_4][\text{Bi}_2\text{Cl}_8(\text{THF})_2]$. *Zeitschrift für anorganische und allgemeine Chemie*, 624(1), p. 81–84, 1998.

57. Breunig, H.J., M. Denker, and K.H. Ebert, Crystal structure of $\text{Me}_3\text{Sb}[\text{middle dot}]\text{SbI}_2\text{Me}$, an adduct with a short dative Sb-Sb bond. *Journal of the Chemical Society, Chemical Communications*, (7), p. 875–876, 1994.
58. Clegg, W., *et al.*, Edge-shared, bioctahedral, bismuth phosphine complexes. *Journal of the Chemical Society, Dalton Transactions*, (10), p. 1753–1754, 1992.
59. Clegg, W., *et al.*, A Phosphine Complex of Bismuth (III): X-Ray Crystal Structure of $[\text{PMe}_3\text{H}][\text{Bi}_2\text{Br}_7(\text{PMe}_3)_2]$. *Chemische Berichte*, 124(11), p. 2457–2459, 1991.
60. Dutton, J.L., *et al.*, Redox Reactions between Phosphines (R_3P ; $\text{R} = \text{nBu}$, Ph) or Carbene (iPr_2IM) and Chalcogen Tetrahalides ChX_4 ($\text{iPr}_2\text{IM} = 2,5\text{-diisopropylimidazole-2-ylidene}$; $\text{Ch} = \text{Se}$, Te ; $\text{X} = \text{Cl}$, Br). *Inorganic Chemistry*, 46(21), p. 8594–8602, 2007.
61. Närhi, S.M., *et al.*, The reactions of tellurium tetrahalides with triphenylphosphine under ambient conditions, *Inorganic Chemistry*, 43, p. 3742–3750, 2004.
62. Godfrey, M.S., *et al.*, Reaction of tertiary phosphine selenides, R_3PSe ($\text{R}[\text{space}]=[\text{space}]\text{Me}_2\text{N}$, Et_2N or C_6H_{11}), with dibromine. The first reported examples of 1[*ratio*]1 addition. *Journal of the Chemical Society, Dalton Transactions*, (24), p. 4201–4204, 1998.
63. Hrib, C.G. *et al.*, *European Journal of Inorganic Chemistry*, P. 88, 2006.
64. M. Godfrey, S., *et al.*, Reaction of R_3PSe with I_2 ; crystal structures of Ph_3PSeI_2 , $(\text{Me}_2\text{N})_3\text{PSeI}_2$ and $(\text{Et}_2\text{N})_3\text{PSeI}_2$, the first crystallographically characterised charge-transfer complexes of tertiary phosphine selenides with diiodine. *Journal of the Chemical Society, Dalton Transactions*, (23), p. 4499–4502, 1997.
65. Boyle, P.D. and S.M. Godfrey, The reactions of sulfur and selenium donor molecules with dihalogens and interhalogens. *Coordination Chemistry Reviews*, 223(1), p. 265–299, 2001.
66. Konu, J. and Chivers, T. Synthesis, spectroscopic and structural characterization of tertiary phosphine tellurium dihalides Et_3PTeX_2 ($\text{X} = \text{Cl}$, Br , I). *Dalton Transactions*, (32), p. 3941–3946, 2006.
67. Dube, J.W., *et al.*, Homoleptic Pnictogen–Chalcogen Coordination Complexes. *Inorganic Chemistry*, 51(16), p. 8897–8903, 2012.

10

S-block Coordination Polymers (Group 1)

10.1 Introduction

The coordination chemistry of groups 1 and 2 metal compounds with organic ligands in the widest sense has been, until relatively recently, largely unknown compared to transition metal coordination networks. This is true despite the fact that many s-block metal–organic compounds are already of commercial important. Thus, pharmaceuticals, dyes, and pigments typically use alkali and/or alkaline earth metal cations in preference to transition or lanthanide metal ions because most of them have the advantage of being non-toxic, cheap and soluble in aqueous media.

While systematic studies to construct transition metal–organic frameworks (MOFs) are frequent in the current literature, due to the often well-defined coordination numbers of the metal ions, they are still sparse for s-block elements. Due to the span of

coordination numbers possible for alkali and alkaline earth metal ions, control over the final structure is a challenge, and many results are obtained by serendipity. In this chapter, classified for the group 1 metal ions as well as for donor atoms in the organic ligands, mainly focusing on the classical O-, N, and S-donors, but also including aromatic rings as donor ligands. Thus, will be dedicated to alkali metal compounds with polymeric structures, starting with organic O-donor ligands, followed by examples with N-donor, C-donor, and S-donor ligands.

10.2 Group 1(Alkali) Metal Coordination Polymers

10.2.1 Neutral Oxygen Donor Ligands

Ethers in general (THF, Et₂O, etc.) are among the most frequently used solvents for alkali metal compounds. They are usually polar enough to dissolve group 1 compounds with ionic character because they are able to coordinate to the metal ions.

By acting as “chemical scissors” on alkali metal salts, they are able to stabilize structural fragments of these compounds by acting as neutral donor ligands where coordination is needed. Such solvent adducts are frequent at the molecular level, but not always identified when of polymer character due to the poorer solubility of the latter. One example is LiBH₄, forming different one-dimensional ether adducts which can be isolated and characterized as 1D structures in the solid state, i.e. LiBH₄(OEt₂) and LiBH₄(OMe_tBu) [1].

Instead of monodentate ethers, cyclic polyethers can also be used to stabilize low-dimensional structures of alkali metal salts. Since the pioneering discovery of crown ethers and cryptands by Pedersen, Cram and Lehn, coordination compounds based on these ligands have been studied in considerable detail. Crown ethers with four to six oxygen atoms are in principle predestined for building one-dimensional channel structures. Much effort has been made to obtain such structures for ion conductivity.

However, most syntheses lead to structures in which the alkali metal ions are (i) coordinated by the crown ether and (ii) bridged by water molecules to yield a one-dimensional (1D) zig-zag structure without alignment of the crown ether molecules. Only few examples are known from the literature, in which the crown ether ligands are also perfectly stacked to form a channel system. One of these is $[\text{Na}(\text{DB}_{18}\text{C}_6)(\mu\text{-OH})][\text{Na}(\text{DB}_{18}\text{C}_6)(\mu\text{-H}_2\text{O})]\text{I}_3$ (Figure 10.1) [2]. These systems do show transport properties for ions as well as water molecules [2], and could therefore be interesting for solid-state batteries.

Going from molecular ligands such as these crown ethers to 1D polyether such as PEO (polyethylene oxide), polymer electrolytes of group 1 metal ions are obtained, finding applications in ion rechargeable (lithium ion for instance) batteries. Their exact solid-state structure is not well known, but some studies on lithium, sodium and potassium reveal the coordination of the PEO ligand to the metal ions. Almost independently from the anions, the polyether oxygen atoms wrap around the alkali cations to form single or double helical structures with the metal ions in the center of a channel-like feature [3]. The mobility of lithium ions was studied by molecular dynamics simulations, where experimental and calculated X-ray diffractograms are compared for a good fit [4]. Other polyelectrolytes

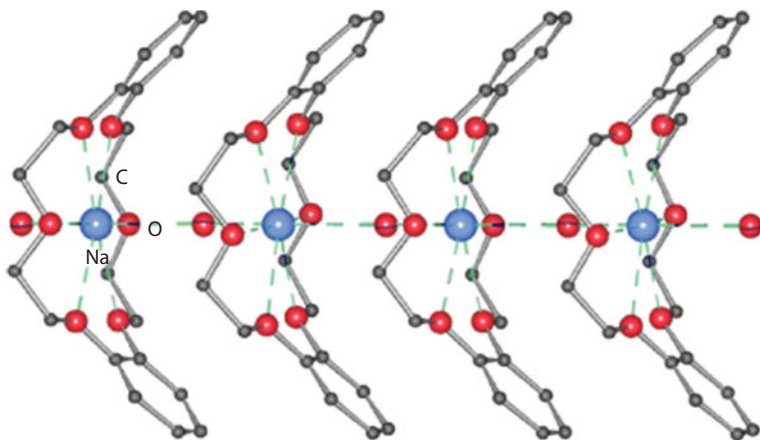


Figure 10.1 1D structure obtained within crown ether ligands.

derived from PEO, such as polyether poly(urethane)urea have been studied in a similar context [5].

10.2.2 Anionic Oxygen Donor Ligands

So far, we have looked at inorganic salts or clusters of alkali metal ions to which neutral oxygen donor ligands are coordinated, and which possess 1D, 2D or 3D structures. This chapter will now deal with organic, anionic ligands with a negative charge on the oxygen atom. The first examples to cite here are alkoxides, aryloxides and carboxylates.

10.2.2.1 Alkoxides and Aryloxides

One of the best known polymers of alkali alk- and aryloxides, MOR, are of course the methoxides and simple phenoxides which form insoluble compounds based on chain or sheet structures [6–12]. Structures can be tuned as a function of the steric demand of R, and thus, the larger R, the more aggregates (0-dimensional) are obtained [13].

Aryloxides can form coordination polymer compounds as well, and, additionally to the metal–oxygen interaction, the aromatic group can participate in the coordination to the metal ion. This is especially the case for the heavier and thus softer alkali metals, such as Rb or Cs [14]. Alkali metal salts of organic acids are numerous, and very often not well characterized in the solid state. The presence of two oxygen atoms in the acid function leads to a stronger bridging function than for alkoxides, resulting more typically in the formation of layered structures [15–18]. The use of cyclic polyphenols, like calixarenes, allows isolating one-dimensional coordination polymer compounds in which the cations can even be mobile similar to biological ion channels. One such example is given in $[\text{K}(\text{calix}[8]\text{arene-H})(\text{THF})_4(\text{H}_2\text{O})_7]$ [19].

10.2.2.2 Carboxylates

Combining the anionic carboxylate groups with neutral N-donor sites within one ligand, such as the 3,5-pyridinedicarboxylate

(3,5-pdc), the dimensionality of such polymers can be increased into a 3D-network, as exemplified in $[\text{Na}_2(3,5\text{-pdc})(\text{H}_2\text{O})_4]$, in which additional H-bonding occurs [20].

Upon addition of a further coordinating anion, the layers of Na-acetate for instance can be cross-linked into a three dimensional porous network with channels in which the solvent molecules can be found [21].

10.2.2.3 *Sulfonates and Nitro-derivatives*

Apart from aryl-, alkoxides and acid derivatives, sulfonates are an important class of oxygen donor ligands to alkali metal ions. A ligand combining sulfonate groups and aryloxy groups is Orange G, a synthetic azo dye used in histology in many staining formulations. One difficulty in examining sulfonated dyes is that they exhibit generally poor crystal growth properties, making single-crystal diffraction studies difficult. An exception is the disulfonated naphthalene-based dye Orange G, 7-hydroxy-8-(phenylazo)-1,3-naphthalenedisulfonic acid, the salts of which are found to grow as robust crystals [22]. The s-block metal salts of the Orange G dianion (Og) can be categorized into three structural classes related to those previously proposed for simple monosulfonated azo dyes. All of the structures feature alternate organic/inorganic layering, but whereas the Mg, Ca, and Li complexes are solvent-separated ion-pair species, the Sr and Ba complexes form simple discrete molecules based on metal sulfonate binding bonding, and the heavy alkali metal complexes utilize a variety of MO interactions to form two- and three dimensional coordination networks. These structural differences are rationalized in terms of simple properties of the metals (charge, size, and electronegativity) and the steric demands of the arylsulfonate groups. This is summarised by saying that the most electronegative metals favor $\text{M}-\text{OH}_2$ bond formation and hence solvent-separated ion-pair structures, whereas the most electropositive metals form higher-connectivity complexes with more $\text{M}-\text{O}_3\text{S}$ bond formation. Thus, the sodium derivative forms a two-dimensional extended structure, involving the sulfonate groups as well as the keto

O-atom in the coordination of the metal ions as well as bridging water molecules.

10.2.2.4 *Amino Acids*

Alkali metal derivatives of amino acids, which would combine the acid donor group with the amine function. Derivatives, such as the total-kill herbicide glyphosate [*N*-(phosphonomethyl)glycine = H_3L], possess low mammalian toxicity, are relatively quickly degraded in the soil and are usually dealt with in form of alkali metal salts. For the sodium salts, three different solvates of the monosodium compounds have been isolated, namely $\text{Na}(\text{H}_2\text{L}) \cdot 0.5\text{H}_2\text{O}$, sodium glyphosate monohydrate $\text{Na}(\text{H}_2\text{L}) \cdot \text{H}_2\text{O}$, sodium glyphosate dihydrate $\text{Na}(\text{H}_2\text{L}) \cdot 2\text{H}_2\text{O}$, together with a disodium glyphosate nonahydrate $\text{Na}_2(\text{HL}) \cdot 9\text{H}_2\text{O}$ [23]. The first two compounds are both polymeric and based on dimeric repeating units with six coordinate sodium ions, while the disodium salt is based on both discrete octahedral $[\text{Na}(\text{HL})(\text{H}_2\text{O})_5]^-$ anionic complex units with the unidentate glyphosate ligand bonded *via* a carboxylate oxygen, together with a cationic $[\text{Na}_2(\text{H}_2\text{O})_8]^+$ ribbon polymer. For the larger cations potassium and rubidium of the alkali metal series, the same ligand is used, but with an increased coordination number of seven to yield water-free three-dimensional compounds with a more regular structure than the sodium compound [24]. In contrast, the Cs-compound features anion monolayers that intercalate planar zig-zag chains of cations (Cs...Cs alternatingly 422.5 and 487.5 pm, Cs...Cs...Cs 135.7°), whereby each chain is surrounded and coordinated by four anion stacks and each anion stack connects two cation chains. All structures exhibit close C–H...A inter-anion contacts consistent with weak hydrogen bonding [24].

10.2.2.5 *Mixed O- and N-donors*

Polydentate ligands with anionic O-donors and neutral N-donors can be obtained by integration of a cyano-function in an appropriate position into anionic O-donors. Thus, 4-cyanosubstituted aryloxides, such as (4-NC-2,6-*t*Bu₂-C₆H₂OLi), lead to the formation of 1D chains *via* single metal ions stabilized by THF or pyridine

ligands [25]. Instead of using single metal ions as nodes, small cluster or aggregate units can also be interconnected into chains, sheets or three dimensional motifs. As an example, lithium derivatives with α -cyanophosphonates, $[(RO)_2P(O)CHCNLi]$ ($R = Et, iPr$), and (organo)sulfonyl-acetonitriles, $(RSO_2CHCNLi)$, as quasi linear bidentate ligands, tend to form 2D-layered structures by linking Li_2O_2 -units, respectively eight-membered ring dimmers $(SO_2Li)_2$, into sheets [26].

10.2.3 N-donor Ligands

Given the fact that alkali metal ions are generally considered as rather hard cations, they interact preferably with oxygen donor atoms rather than nitrogen atoms. However, when oxygen donors are not available in sufficient quantity to satisfy the coordination of the metal ions, nitrogen atoms are also involved in metal ion coordination. This is the case in the tripodal, pyridyl-substituted tris(pyrazolyl)borate ligands [27]. Whereas the water-rich potassium derivative of this ligand type yields a dimeric structure, the compound with only one water molecule in the potassium coordination sphere leads to a one-dimensional coordination polymer network, in which two of the three arms of the tripodal ligand act as bridging ligands towards two neighbor metal ions. Pure nitrogen donation is rare, as shown in the example of the toluene-soluble potassium salt of the $[(2,6-iPr_2C_6H_3)NC(Me)C(H)C(Me)N(2,6-iPr_2C_6H_3)]$ -ion, in which the aromatic rings complete the coordination sphere of the potassium ion by metal–aromatic interactions. This kind of interaction is finally responsible for the 1D-extension of the structure in the solid state (Figure 10.2) [28]. Similarly, cyano-cyclopentadienyl ($CpCN$) anions are ideal to combine nitrogen and aromatic ring interactions with alkali metal ions, such as in $CpCNM$, $M=K, Cs$ [29].

10.2.4 Carbon Donor Ligands

The larger alkali metal ions are softer than the smaller ones, and accept more easily aromatic coordination. This has been

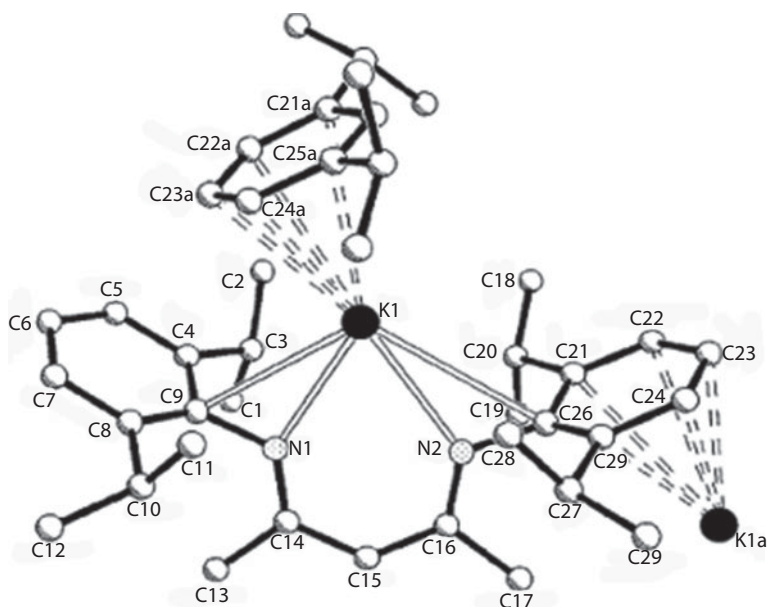


Figure 10.2 1D structure of $\text{K}[(2,6\text{-}i\text{Pr}_2\text{C}_6\text{H}_3)\text{NC}(\text{Me})\text{C}(\text{H})\text{C}(\text{Me})\text{N}(2,6\text{-}i\text{Pr}_2\text{C}_6\text{H}_3)]$

shown in the zig-zag-arranged structures of the solid state structures of CpM -compounds for the heavier alkali metal ions [30, 31]. Substituted phenyl rings with small and noncoordinating side-groups maintain such a chain-structure in the solid state [32].

The derived calcium compound is a THF adduct and by the way a monomer. In combination with phosphor donor atoms which are linked to a cyclopentadienyl-ligand and additional THF, a new 1D structure can be stabilized, as for instance in the solid-state compound $[(\text{THF})\text{K}(\text{C}_5\text{H}_4\text{CH}_2\text{CH}_2\text{PPh}_2)]$ [33].

Single metal–carbon bonds with more σ -character can be enforced with carbanions carrying large substituents like phosphine and borane rests [34]. The related potassium compound yields then a complicated sheet structure in which additional K–H bonds seem to stabilize the structure.

10.2.5 Sulfur Donor Ligands

Alkali metal coordination polymers with solely sulfur atoms as donors, have not been reported in the literature so far. However, as shown in some of the previous examples, the combination of different donor types allows the selective coordination of different metal ions to different donor sites, as anticipated from Pearson's hard-soft acid-base theory. Thus, the Janus scorpiate ligand $[\text{HB}(\text{mtda})_3]^-$ (mtda = mercaptothiadiazolyl) contains both sulfur and nitrogen atoms. This feature can be exploited for the controlled construction of homo- and heterometallic (hard-soft) alkali metal coordination polymers [35]. Remarkably, in the case of sodium, coordination polymers with both acentric (with $\text{NaS}_3\text{N}_3\text{H}$ kernels) and centric (with alternating NaN_6 and NaS_6H_2 kernels) chains are found in the same crystal (where the centricity is defined by the relative orientations of the BH-bonds of the ligands along the lattice). For the homometallic potassium congener, the larger cation size, compared to sodium, induced significant distortions and favored a polar arrangement of ligands in the resulting coordination polymer chain. An examination of the solid-state structure of the mixed alkali metal salt system revealed that synergistic binding of smaller sodium cations to the nitrogen portion and of the larger potassium cations to the sulfur portion of the ligand minimizes the ligand distortions relative to the homometallic coordination polymer counterparts, a design feature of the ligand that likely assists in thermodynamically driving the self-assembly of the heterometallic chains. The similarity of the solution analytical data regardless of the cation indicates that the salts are likely dissociated in solution rather than maintaining their solid-state polymeric structures. Thiophosphonates combine the coordination of sulfur atoms with the one of oxygen donors, within the same ligand. Thus, the ligand $[\text{ArP}(\text{OtBu})\text{S}_2]^-$ (Ar = 4-anisyl) may coordinate with both donor atoms to alkali metal ions in ethereal solvents to yield mostly one-dimensional coordination polymer compounds [36].

10.3 Conclusion

Summarizing the situation for alkali metal ions containing coordination polymer structures, even though a large number of materials are used as their group 1 metal salts, the structures of the latter are often not investigated in detail, ignoring the cations as simple “spectator” ions. However, this is an issue worth investigating in order to better understand the properties of these solid-state compounds. Few of the examples mentioned above have been investigated in this respect, and first recent results show that a certain design in the construction of alkali metal coordination polymer structures can be achieved by a) using (rigid) bridging ligands with two or more coordination sites, and/or b) template molecules to generate voids in the solid state structures, and/or c) the use of alkali metal aggregates as nodes of a low-dimensional network to yield porous materials with large cavities.

Synthesis or autoclave techniques for groups 1 coordination polymers are employed, microwave and solid-state synthesis are still scarce for these kinds of networks. Applications in many, very different fields are possible, and therefore such investigations should be continued.

References

1. Giese, H.-H., *et al.*, Structural Chemistry of Lithium Tetrahydroborate Ether Solvates. *European Journal of Inorganic Chemistry*, 1998(7), p. 941–949, 1998.
2. Fromm, K.M. and R.D. Bergougnant, Transport properties of solid state crown ether channel systems. *Solid State Sciences*, 9(7), p. 580–587, 2007.
3. Bruce, P.G., Ion-polyether coordination complexes: crystalline ionic conductors for clean energy storage. *Dalton Transactions*, (11), p. 1365–1369, 2006.
4. Brandell, D., *et al.*, Molecular dynamics simulation of the crystalline short-chain polymer system $\text{LiPF}_6 \cdot \text{PEO}_6$ (Mw [similar] 1000). *Journal of Materials Chemistry*, 15(40), p. 4338–4345, 2005.

5. Wang, H.-L., *et al.*, FTIR and Solid State ^{13}C NMR Studies on the Interaction of Lithium Cations with Polyether Poly(urethane urea). *Macromolecules*, 34(3), p. 529–537, 2001.
6. Wheatley, P.J., 835. A physicochemical investigation of the methoxides of lithium, sodium, and potassium. *Journal of the Chemical Society* (Resumed), (0), p. 4270–4274, 1960.
7. Weiss, V.E., Die Kristallstruktur des Natriummethylats. *Zeitschrift für anorganische und allgemeine Chemie*, 332(3–4), p. 197–203, 1964.
8. Weiss, E. B^üchner, W., Strukturuntersuchungen an Alkalicarbid- und-disulfiden. *Angew. Chem. Int. Ed. Engl.* 3, p.152, 1964.
9. Dinnebier, R., *et al.*, Powder Structure Solutions of the Compounds Potassium Phenoxide-Phenol: $\text{C}_6\text{H}_5\text{OK} \cdot x \text{ C}_6\text{H}_5\text{OH}$ ($x = 2, 3$). *Inorganic Chemistry*, 37(19), p. 4996–5000, 1998.
10. Weiss, v.E. and H. Alsdorf, Die Kristallstrukturen des Kalium-, Rubidium- und Cäsiummethylats. *Zeitschrift für anorganische und allgemeine Chemie*, 372(2), p. 206–213, 1970.
11. Dinnebier, R.E., *et al.*, Novel Alkali-Metal Coordination in Phenoxides: Powder Diffraction Results on $\text{C}_6\text{H}_5\text{OM}$ ($\text{M} = \text{Li}, \text{Na}, \text{K}, \text{Rb}, \text{Cs}$). *Inorganic Chemistry*, 36(16), p. 3398–3401, 1997.
12. Berny, M.F. Perrin, R. *Comput. Rend.* 260, 395, 1965.
13. Fromm, K.M. and E.D. Gueneau, Structures of alkali and alkaline earth metal clusters with oxygen donor ligands. *Polyhedron*, 23(9), p. 1479–1504, 2004.
14. Westerhausen, M., *et al.*, Influence of the Steric Demand of the 2,4,6-Trialkylphenyl Substituents on the Structures and Reactivity of Diarylzinc. *Zeitschrift für anorganische und allgemeine Chemie*, 631(13–14), p. 2836–2841, 2005.
15. Hsu, L.-Y. Nordman, C.E. Structures of two forms of sodium acetate, $\text{Na}^+ \cdot \text{C}_2\text{H}_3\text{O}_2^-$, *Acta Crystallography*, Sect. C 39, p. 690–694, 1983.
16. Lossin, A. and Meyer, G. Kristallstruktur von Caesiumacetat, $\text{Cs}(\text{CH}_3\text{COO})$. *Zeitschrift für anorganische und allgemeine Chemie*, 619(8), p. 1462–1464, 1993.
17. Hatibarua, J. Parry, G.S., A crystallographic study of the acetates of potassium, rubidium and caesium. *Acta Crystallography*. B 28, p. 3099–3100, 1972.
18. Wei, K.-T. Ward, D.L., Sodium acetate trihydrate: a redetermination. *Acta Crystallography*. B 33, p. 522–526, 1977.
19. Bergougnant, R.D., Robin, A.Y. and Fromm, K.M. “Hooked-on” Calix[8]arenes: A $(\text{H}_2\text{O})_{10}$ Cluster with an Unprecedented Structure. *Crystal Growth & Design*, 5(5), p. 1691–1694, 2005.

20. Huang, W., *et al.*, Sodium ions directed self-assembly with 3,5-pyridinedicarboxylate (3,5-pdc) and 4-pyridinecarboxylate (4-pc). *Inorganica Chimica Acta*, 358(4), p. 875–884, 2005.
21. Lavalette, A., *et al.*, Channel Structures in a Simple Inorganic Salt – An Open Framework Formed through Structural Integration of Distinct Sodium Acetate and Sodium Perchlorate Domains. *European Journal of Inorganic Chemistry*, 2004(20), p. 3981–3983, 2004.
22. Kennedy, A.R., Kirkhouse, J.B. and Whyte, L. Supramolecular motifs in s-block metal-bound sulfonated monoazo dyes: The case of orange G. *Inorganic Chemistry*, 45(7), p. 2965–2971, 2006.
23. Sagatys, D.S., *et al.*, The complex chemistry of N-(phosphonomethyl)glycine (glyphosate): preparation and characterization of the ammonium, lithium, sodium (4 polymorphs) and silver(I) complexes. *Journal of the Chemical Society, Dalton Transactions*, (19), p. 3404–3410, 2000.
24. Moers, O., *et al.*, Polysulfonylamine. CLX [1] Kristallstrukturen von Metall-di (methansulfonyl) amidien. 10 [2] Die dreidimensionalen Koordinationspolymere $M[(CH_3SO_2)_2N]$ mit $M =$ Kalium, Rubidium, Caesium (isotype Strukturen für $M = K, Rb$). *Zeitschrift für anorganische und allgemeine Chemie*, 629(1), p. 83–90, 2003.
25. MacDougall, D.J., *et al.*, 4-Methoxy- and 4-cyano-substituted lithium aryloxides: electronic effects of substituents on aggregation. *Dalton Transactions*, (15), p. 1875–1884, 2006.
26. Harder, S. and Prosenc, M.H. The Heaviest Alkali Metallocene: Structure of an Anionic Cesocene Triple-Decker. *Angewandte Chemie International Edition in English*, 35(1), p. 97–99, 1996.
27. Weis, K. and Vahrenkamp, H. Two New Pyridyl-Substituted Tris(pyrazolyl)borate Ligands and Their Potassium Salts. *Inorganic Chemistry*, 36(24), p. 5589–5591, 1997.
28. Clegg, W., *et al.*, Structural Characterization of $[(2, 6-Pri_2C_6H_3)NC(Me)C(H)C(Me)N(2, 6-Pri_2C_6H_3)KPhCH_3]$: A Heavy Alkali Metal Diazapentadienyl Complex. *Inorganic Chemistry*, 37(9), p. 2317–2319, 1998.
29. Herdtweck, E., Köhler, F.H. and Mölle, R. (Cyanocyclopentadienyl) potassium and -cesium. *European Journal of Inorganic Chemistry*, (5), p. 952–958, 2005.
30. Seewald, P.A., White, G.S. and Stephan, D.W. Cationic complexes of titanium(III); phosphine substitution reactions. *Canadian journal of chemistry*, 66(5), p. 1147–1152, 1988.

31. Harder, S. and Prosenc, M.H. Das schwerste Alkalimetallocen: Struktur eines anionischen Caesocen-Tripeldeckers. *Angewandte Chemie*, 108(1), p. 101–103, 1996.
32. Feil, F. and Harder, S. α,α -Bis(trimethylsilyl)-Substituted Benzyl Complexes of Potassium and Calcium. *Organometallics*, 19(24), p. 5010–5015, 2000.
33. H. Karsch, H., Graf, V. W. and Reisky, M. Synthesis and X-ray structure of $[(\text{THF})\text{K}(\text{C}_5\text{H}_4\text{CH}_2\text{CH}_2\text{PPh}_2)]_{\text{infinity}}$: a structurally characterized heavier alkali metal phosphane complex. *Chemical Communications*, (17), p. 1695–1696, 1999.
34. Izod, K., *et al.*, Heavier Alkali Metal Complexes of a Silicon- and Phosphine-Borane-Stabilized Carbanion. *Organometallics*, 25(22), p. 5326–5332, 2006.
35. Silva, R.M., *et al.*, Ligand-Promoted Solvent-Dependent Ionization and Conformational Equilibria of $\text{Re}(\text{CO})_3\text{Br}[\text{CH}_2(\text{S-tim})_2]$ (tim = 1-methylthioimidazolyl). Crystal Structures of $\text{Re}(\text{CO})_3\text{Br}[\text{CH}_2(\text{S-tim})_2]$ and $\{\text{Re}(\text{CO})_3(\text{CH}_3\text{CN})[\text{CH}_2(\text{S-tim})_2]\}(\text{PF}_6)$. *Inorganic Chemistry*, 45(17), p. 6794–6802, 2006.
36. Shi, W., *et al.*, Metal thiophosphonates and related compounds: an emerging area of supramolecular coordination chemistry. *Dalton Transactions*, 2006(26): p. 3257–3262.

11

S-block Coordination Polymers (Group 2)

11.1 Introduction

S-block cations should not be ignored as simple “spectator” ions when it comes to properties which depend on the solid-state structure and the intermolecular interactions. This is especially relevant in pharmaceutical industry where one salt might be preferred over others for practical as well as commercial purposes. Therefore, understanding the changes of material properties caused by changing the s-block metal ion is based on consideration of the fundamental properties such as charge, size, and electronegativity of these cations and their influence on the nature of the resultant solid-state structure. Furthermore, the chemistry of group 1/2 metal ions is not limited to the classical ionic behavior as known from aqueous media, but may exhibit a more covalent character similar to transition metal compounds when polar organic solvents are used.

With the aid of modern X-ray diffraction techniques, a variety of molecular and polymeric structures can be elucidated. Coordination polymer networks are made mainly from neutral or anionic ligands (linkers) with at least two donor sites which coordinate to metal ions or aggregates (nodes) also with at least two acceptor sites, so that at least a one-dimensional arrangement is possible. Depending on the number of donor atoms and their orientation in the linker, and on the coordination number of the node, different one (1D)-, two (2D)- and three (3D)-dimensional constructs are accessible.

In this chapter, classified for the group 2 metal ions well as for donor atoms in the organic ligands, mainly focusing on the classical O-, N, and S-donors, but also including aromatic rings as donor ligands. Thus, will be dedicated to alkali metal compounds with polymeric structures, starting with organic O-donor ligands, followed by examples with N-donor, C-donor, and S-donor ligands.

11.2 Group 2(Alkaline Earth) Metal Coordination Polymers

Passing from groups 1 to 2 metal ions, the charge density of the cations increases. Also, many alkaline earth metal compounds are hygroscopic. For these reasons, many of the species studies have focused on the use of aspartate, glutamate, orontate, or pyroglutamate ligands as careful investigation of the calcium or magnesium binding sites on proteins has shown that the acidic groups of l-aspartic acid and l-glutamic acid are the key anchoring positions for these ions. On the other hand, barium and strontium are considered as *trace elements* in the body.

Strontium is rated nontoxic, and traces of it appear to be essential, though the reason for this is not yet known. Barium causes typical heavy metal poisoning even at low concentrations if soluble compounds are applied. Barium and strontium metals have been known as antagonists for potassium and calcium, respectively.

In the process of binding to various sites, the ions compete with other common metal ions, some of which are antagonists through a different specificity. This specificity is predominantly governed by the charge and size of the cation, as well as by the resulting effective coordination number and geometry. An improved understanding of the function of biological cations is thus to be expected from a detailed study of the coordinating properties of the metals competing with various ligating groups.

11.2.1 Neutral Oxygen Donor Ligands

Similar to alkali metal ions, group 2 metal compounds can be treated with for instance neutral oxygen donor ligands to “cut out” fragments from the three-dimensional salt structure. This has been exemplified in the studies on alkaline earth metal iodides, which are still quite soluble in organic solvents which may act also as coordinating ligands. In these cases, it is important to control the quantity of water present, as water is a solventable to dissociate the mainly ionic bonds in alkaline earth metal salts [1–6]. Thus, it has been shown that one-dimensional coordination polymer compounds can be obtained with low concentrations of THF, used as chemical scissors to yield $[\text{BaI}_2(\text{thf})_3]$ (Figure 11.1) [7].

Other neutral solvents are however able to cleave the cation–anion contacts and to coordinate the cations completely, leaving the

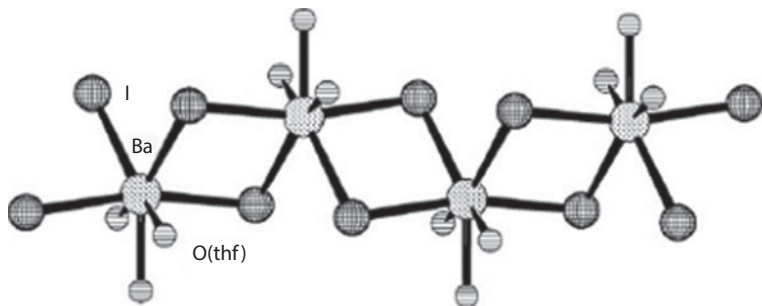


Figure 11.1 1D structure of $[\text{BaI}_2(\text{thf})_3]$.

anions out of the first coordination sphere of the cation. Water is such a solvent, and thus, can replace one or both anions from the first coordination of the cation. As cation-coordinated water is a hydrogen bond donor ligand, low-dimensional polymer structures can be designed as a function of the number of coordinating water molecules [8]. As an example, the H-bonded one-dimensional polymer $[\text{Ca}(\text{H}_2\text{O})_2(\text{diglyme})_2](\mu\text{-I})_2$ is cited [8–12].

11.2.2 Anionic Oxygen Donor Ligands

11.2.2.1 *Beta-diketonates*

Beta-diketonates of alkaline earth metal ions received prominent attention when High- T_c superconductors were discovered. One synthesis of such oxide materials is *via* metal organic chemical vapor deposition (MOCVD) or the sol-gel technique. For the first technique, volatile species are necessary. It turned out that beta-alkoxides are well suited, because they form cluster-like compounds in which the alkaline earth metal ions are surrounded by the organic ligands and turn out to be volatile at relatively low temperatures. From this property, the reader may deduce that these compounds do not form coordination polymer network. However, some cases are known, for which polymer structures are obtained. Thus, beryllium, the smallest of the alkaline earth metal ions, has a low coordination number of four, which in the case of bis-beta-diketones leads to a one-dimensional chain structure [13].

11.2.2.2 *Alkoxides*

Another group of alkaline earth metal compounds studied in the same context are the alkoxides. Unless multifunctional alcohols' and sterically crowded alkyl or aryl groups are employed these compounds are generally polymeric insoluble solids, which are poorly characterized from a structural point of view. The reactions of these compounds with small molecules such as CO_2 and SO_2 have been relatively neglected although organo-magnesium compounds are known to react with SO_2 to give

sulfinic acids after hydrolysis, while calcium oxide is used to scrub flue gases and for the desulfurisation of iron ores. In contrast, the corresponding reactions of the class 'b' or soft metal alkoxides of palladium, platinum and rhodium with SO_2 have been investigated in more detail. Structural studies of these complexes reveal, as expected, S-coordinated SO_2 moieties. Thus, the reaction of $\text{SO}_2(\text{g})$ with a suspension of $[\text{M}(\text{OMe})_2]$, ($\text{M} = \text{Mg}$ and Ca) in methanol yields the crystalline compounds, $[\text{M}(\text{O}_2\text{SOMe})_2(\text{MeOH})_2]$, ($\text{M} = \text{Mg}$, Ca). The insertion reaction is of high yield and the X-ray crystal structure of the second complex reveals that it is a chain polymer with eight-coordinated Ca-ions and the methylsulfito anions acting as both chelating and bridging ligands.

11.2.2.3 Carboxylates

Carboxylates were also among the species investigated as precursors for oxide materials, using sol-gel techniques. However, many of these precursors may lead to the formation of mixed alkaline earth metal carboxylates and oxides. Dicarboxylates have found a large field of application in the construction of coordination polymer arrays, especially the more rigid ligands, as they are useful building blocks for porous networks with metal ions throughout the periodic system [14]. A semi-rigid ligand, benzene-1,4-dioxyacetate, L, leads to the three-dimensional coordination polymer networks $[\text{M}(\text{L})\text{H}_2\text{O}]$, $\text{M} = \text{Ca}$, Sr , Ba [15]. Both $\text{Ca}(\text{L})\text{H}_2\text{O}$ and $\text{Sr}(\text{L})\text{H}_2\text{O}$ crystallize in the monoclinic space group $P2_1/c$ while $\text{Ba}(\text{L})\text{H}_2\text{O}$ in the monoclinic space group $P2_1$. As determined by X-ray single-crystal analysis, in these compounds each metal ion is coordinated by eight O atoms: four from different carboxylate groups, two from one carboxylate group, one from the ether oxygen and one from one water molecule. Each ligand coordinates to five alkaline earth metal ions through one of its ether oxygen atoms and two carboxylate groups adopting novel bridging coordination modes to give rise to a 3D network. The luminescence analysis shows that the Ca- and Sr-compounds exhibit fluorescence in the solid state at room temperature.

The slightly more rigid zwitterionic 1,3-bis(carboxymethyl)-imidazolium forms with SrCO_3 in water a two-dimensional structure between the layers of which are found sheets of water molecules intercalated [16].

The very rigid 2,6-naphthalenedicarboxylate (ndc) reacts in a solvothermal process with magnesium nitrate in either water or DMF [17]. Whereas in the presence of water molecules preferred coordination of H_2O and dmf in $[\text{Mg}(\text{dmf})_2(\text{H}_2\text{O})_4]\text{ndc}$ hinders the formation of extended three-dimensional networks, a porous network structure is obtained in the absence of water to yield the three-dimensional metal–organic framework of $[\text{Mg}_3(\text{ndc})_3(\text{dmf})_4]$. A systematic study of larger flat aromatic ligands with two carboxylic groups and beryllium and magnesium ions lead to a large number of different metal organic frameworks with good hydrogen absorption properties [18].

11.2.2.4 Phosphonates

Polyphosphonates are also used extensively in an array of industrial applications such as chemical water treatment, oilfield drilling, minerals processing, corrosion control, and metal complexation and sequestration. Metal phosphonates commonly form pillaredlayered inorganic–organic hybrid materials and microporous solids. Their properties can be useful for intercalation, catalysis, sorption, and ion exchange. One example is the aminotris(methylenephosphonic) acid (H_6AMP). At low pH, this ligand loses two protons, with all phosphonate groups being deprotonated while the amino function carries a proton. This ligand can react easily with the alkaline earth metal cations Mg, Ca, Sr, and Ba. $\text{Mg}[\text{HN}(\text{CH}_2\text{PO}_3\text{H})_3(\text{H}_2\text{O})_3]$ forms zig-zag chains in which the Mg-ions are bridged by two of the three phosphonate groups. The third phosphonate group is non-coordinated and involved in hydrogen bonding. A three-dimensional (3D) polymer is obtained with strontium, having the composition $[\text{Sr}(\text{H}_4\text{AMP})]$. The Sr-atoms are seven-coordinate, with five monohapto and one chelating AMP ligands. In the 3D barium polymer, $[\text{Ba}(\text{H}_4\text{AMP})(\text{H}_2\text{O})]$, the two crystallographically independent Ba-ions are 9- and 10-coordinated by phosphonate and H_2O oxygen atoms.

11.2.2.5 Sulfonates

In terms of anionic oxygen donor ligands to alkaline earth metal ions in polymeric scaffolds, the sulfonates have been quite well studied. Thus, a family of organosulfonates has been reported by Cote *et al.* [19]. They have developed new solids, which, in contrast to more typical crystal engineering approaches, are sustained by the assembly of building blocks that are coordinatively adaptable rather than rigid in their bonding preferences. The ligand, 4,5-dihydroxybenzene-1,3-disulfonate, L, progressively evolves from a 0D, 1D, 2D, to a 3D microporous network with the Group 2 cations Mg^{2+} , Ca^{2+} , Sr^{2+} , and Ba^{2+} .

11.2.3 Mixed N- and O-donors

Self-assembly is an increasingly viable method for the quick and efficient construction of large molecular architectures. Porphyrins are particularly suitable building blocks for non-covalent synthesis due to their attractive photophysical, spectroscopic, geometrical, catalytic, and synthetic properties [20]. Furthermore, the magnesium complex of porphyrin is responsible for photosynthesis. Thus, a mixture of 1:1 magnesium dicatechol porphyrin MgL and pyridine-3-boronic acid self-assembles into a one-dimensional coordination polymer. The boronic acid acts as N- and O-donor in a bridging function towards two magnesium cations. Another group of simultaneous N- and O-donating ligands of biological importance are the amino acids. A series of calcium α -aminocarboxylates was prepared by refluxing aqueous solutions/suspensions of calcium hydroxide and the respective α -amino acid [21]. The colorless, crystalline hydrates $\text{Ca}(\text{gly})_2 \cdot \text{H}_2\text{O}$, $\text{Ca}(\text{ala})_2 \cdot 3\text{H}_2\text{O}$, $\text{Ca}(\text{val})_2 \cdot \text{H}_2\text{O}$, $\text{Ca}(\text{leu})_2 \cdot 3\text{H}_2\text{O}$, $\text{Ca}(\text{met})_2 \cdot n\text{H}_2\text{O}$ ($n = 2$), and $\text{Ca}(\text{pro})_2 \cdot \text{H}_2\text{O}$ have been isolated in yields between 29 and 67% (gly = glycinate, ala = rac-alaninate, val = rac-valinate, leu = rac-leucinate, met = rac-methioninate, pro = rac-prolinate).

11.2.4 N-donor Ligands

Neutral N-donor ligands are, just as neutral O-donors, able to stabilize low-dimensional coordination polymers of alkaline earth

metal salts. The polymer structures are generated in most cases by bridging halides, while the N-donor molecules step in as terminal ligands to reduce dimensionality of the initial polymer structure [22]. Even though that 4,4'-bipyridine is a widely used ligand in transition metal ion coordination, examples with alkali and alkaline earth metal ions are rather scarce due to the general preference of block s elements towards oxygen. Complete elimination of oxygen donors leads however to alkaline earth metal compounds, in which the metal ions are entirely coordinated by N-atoms. This is especially true for the larger metal ions, as they have a lower charge density and are softer than their smaller homologues. However, steric bulk of the ligand needs to be sufficient to stabilize the coordination. Monoanionic heteroallylic ligand systems $[R-N-E-N-R]^-$ ($E = Si(R_2)$, $S(R_2)$ or $S(R)$, $C(R)$, and $P(R_2)$) are versatile chelating substituents both in main group and transition metal chemistry as they provide sufficient steric demand and solubility to the products [23]. Their application is only limited by the rigid bite of the ligands as the N–N distance cannot be tuned to the various radii of different metals. The $NP(R_2)N^-$ chelate in classical amino iminophosphoranates is extended by additional coordination sites in the organic substituents (e.g., 2-pyridyl (Py) instead of phenyl (Ph)). $Py_2P\{N(H)SiMe_3\}(NSiMe_3)$ is the starting material for a new class of complexes as the deprotonated ligand contains along with the NPN-chelate the pyridyl ring nitrogen atoms to generate a side selective Janus face ligand. In $[(THF)Sr\{Py_2P(NSiMe_3)_2\}_2]$ and $[(4,4'-bipy)Ba\{Py_2P(NSiMe_3)_2\}_2]$ both pyridyl rings are involved in metal coordination but only one imido nitrogen atom. Hence, the classical $NP(Ph)_2N^-$ chelating ligand is converted into a $NP(Py)_2N^-$ tripodal ligand. Whereas the strontium compound is a zero-dimensional compound due to its smaller radius and terminal THF-coordination, the bridging bipyridine ligand in the barium compound allows the formation of a one-dimensional coordination polymer.

11.2.5 Carbon Donor Ligands

As discussed for the alkali metal ions, the larger alkaline earth metal ions also have an increased tendency to interact with

aromatic π -systems when available. A general reaction pathway to such metal-organic compounds is the use of the alkali-organic compound and its reaction with alkaline earth metal halides under elimination of alkali halide in an organic solvent. Thus, indenyl (Ind) and its derivative, bis isopropylindenyl (Ind2i) react as potassium salts with alkaline earth metal iodides to yield $[(\text{Ind})_2\text{M}(\text{thf})_n]$ ($\text{M} = \text{Ca}, \text{Sr}, \text{Ba}$; $n = 1$ for Sr and Ba; $n = 2$ for Ca) and $[(\text{Ind2i})_2\text{M}(\text{thf})_n]$ ($n = 1$ for Ca; $n = 2$ for Sr and Ba) under KI elimination [24]. All complexes are air-sensitive solids, and while the calcium and barium compounds are monomeric, the strontium complex is an infinite coordination polymer, $[(\text{Ind})_2\text{Sr}(\text{thf})]$, with both terminal (Sr-C) 2.94 Å (av)) and bridging (Sr-C) 3.07 Å (av)) indenyl ligands.

Such a *trans*-metallation, using alkali reagents and alkaline earth metal halides in order to eliminate alkali iodide seems however not always successful [25]. Thus, the generation of [1,2,4-tris(trimethylsilyl)-cyclopentadienyl]metal iodides $(\text{Cp}_3\text{Si})\text{MI}(\text{thf})_n$ ($\text{M} = \text{Ca}$, $n = 1$; $\text{M} = \text{Sr}, \text{Ba}$, $n = 2$) are isolated from the 1:1 reaction of $\text{K}[\text{Cp}_3\text{Si}]$ and MI_2 in THF, but the yields range from very good (79%) when $\text{M} = \text{Ca}$ to poor (26%) when $\text{M} = \text{Ba}$. In the case of $\text{M} = \text{Sr}, \text{Ba}$, substantial amounts of $\text{K}[\text{Cp}_3\text{Si}]$ are recoverable at the end of the reaction. No redistribution of $(\text{Cp}_3\text{Si})\text{MI}(\text{thf})_n$ into $(\text{Cp}_3\text{Si})_2\text{M}$ and $\text{MI}_2(\text{thf})_n$ is observed in either THF or aromatic solvents at room temperature. Both $(\text{Cp}_3\text{Si})\text{CaI}(\text{thf})$ and $(\text{Cp}_3\text{Si})\text{SrI}(\text{thf})_2$ crystallize from THF/toluene as iodide-bridged dimers, while the organobarium complex $(\text{Cp}_3\text{Si})\text{BaI}(\text{thf})_2$ crystallizes from THF/toluene as a coordination polymer containing both linear and near-linear (177.8°) Ba-I-Ba links in a zig-zag motif; this is an unprecedented arrangement for bridging iodide ligands.

11.2.6 Sulfur Donor Ligands

Combination of carboxylate groups with sulfur donor groups such as thiols, additional coordination of sulfur to the cations may be observed in the case of the correct design of the ligand. Treating alkaline earth metal chlorides with the ligand 2-mercaptobenzoic acid, extended polymer structures $[\text{Ca}(\text{DTBB})(\text{H}_2\text{O})_2 \cdot 0.5(\text{C}_2\text{H}_5\text{OH})]$,

[Sr(DTBB)(H₂O)₂·0.5(C₂H₅OH)], and [Ba₂(DTBB)₂(H₂O)₂·0.5H₂O] are obtained, in which the ligand under thiol oxidation to form 2,2'-dithiobis(benzoic acid) (H₂DTBB) as a bridging ligand [26]. The calcium and strontium coordination polymers are isomorphous with the DTBB ligands acting as hexadentate ligands.

Both compounds have a channel structure in which solvent ethanol molecules are included. In the barium compound, a complex three-dimensional coordination polymer where both the carboxylate and the sulfur groups of the DTBB ligands (which are hepta- and octadentate) coordinate to the metal is observed.

11.3 Conclusion

The alkaline earth metal ions have received more attention, probably due to the research on group 2 metal containing precursors for oxide as well as biomimetic materials. In terms of networks and nodes, moving from group 1 to 2 metals halves the number of nodes and so decreases connectivity for the same ligand types.

For both, alkali and alkaline earth metal MOFs, the presence of water molecules in the coordination sphere of the metal ions strongly influences the final structures. Water molecules are highly attracted to s-block ions, and are small enough to coordinate easily to any of the metal ions. This is due to the fact that groups 1 and 2 metal ions usually are able to rapidly exchange their neutral ligands in solution, and that, if water is present, the latter may then often bind to the metal ions in a stronger fashion than another neutral ligand.

All in all, the formation of metal–organic frameworks (MOFs) with alkali and alkaline earth metal ions has not been exhaustively investigated. Whereas mostly solution synthesis or autoclave techniques for groups 1 and 2 coordination polymers are employed, microwave and solid-state synthesis are still scarce for these kinds of networks. Additionally, applications in many, very different fields are possible, and therefore such investigations should be continued.

References

1. Fromm, K.M., Ionic or covalent? Can some first hints be derived from the solid state structures of alkaline earth metal halide adducts? *CrystEngComm*, 4(57), p. 318–322, 2002.
2. Fromm, K.M., Recent Advances in the Chemistry of Clusters and Inorganic Polymers of Alkali and Alkaline Earth Metal Compounds. *CHIMIA International Journal for Chemistry*, 56(12), p. 676–680, 2002.
3. Fromm, K.M., *et al.*, Understanding the formation of new clusters of alkali and alkaline earth metals: A new synthetic approach, single-crystal structures, and theoretical calculations. *Journal of the American Chemical Society*, 125(12), p. 3593–3604, 2003.
4. Fromm, K.M., Oxygen Donor Stabilized Alkaline Earth Metal Iodides. *CHIMIA International Journal for Chemistry*, 57(4), p. 175–178, 2003.
5. Fromm, Katharina M. and Maudez, W. Polar Molecular Precursors for Alkali and Alkaline Earth Metal Clusters and Low-Dimensional Polymer Structures: the Solid-State Structures of $[\text{CaI}(\text{dme})_3]$ I, and *cis*- $[\text{SrI}_2(\text{diglyme})_2]$ ($\text{dme} = \text{CH}_3\text{OC}_2\text{H}_4\text{OCH}_3$; *diglyme* = $\text{CH}_3(\text{OC}_2\text{H}_4)_2\text{OCH}_3$). *European Journal of Inorganic Chemistry*, (18), p. 3440–3444, 2003.
6. Fromm, K.M., *et al.*, Recent Advances in the Chemistry of “Clusters” and Coordination Polymers of Alkali, Alkaline Earth Metal and Group 11 Compounds. *Zeitschrift für anorganische und allgemeine Chemie*, 631(10), p. 1725–1740, 2005.
7. Fromm, K.M., Strukturelle Evolution vom Festkörper zum Molekül für BaI_2 : Synthese und Kristallstrukturanalyse von $[\text{BaI}_2(\mu_2\text{-OH}_2)_2]_{3/\infty}$, $[\text{BaI}_2(\mu_2\text{-OH}_2)(\text{OC}_3\text{H}_6)_{2/\infty}]$, $[\text{BaI}_2(\text{THF})_3]_{1/\infty}$ und $[\text{BaI}_2(\text{THF})_5]_n$. *Angewandte Chemie*, 109(24), p. 2876–2878, 1997.
8. Fromm, K.M., A Logical Concept of Structure Prediction Derived from Supramolecular Polymers of Alkaline Earth Metal Halides Formed by Hydrogen Bonding and Complexation of the Metal Ion. *Chemistry – A European Journal*, 7(10), p. 2236–2244, 2001.
9. Fromm, K.M., Goesmann, H. On the way to sol–gels: an analysis of the intra- and intermolecular hydrogen bonding in $[\text{Ba}(\text{OH})(\text{H}_2\text{O})_4]$. *Acta Cryst., Sect. C* 56, p.1179–1180, 2000.
10. Fromm, K.M., Goesmann, H. and Bernardinelli, G. H-bonded polymer structures of different dimensionality: syntheses and crystal structures of $[\text{Ca}(\text{DME})_n(\text{H}_2\text{O})_m]\text{I}_2 \cdot (\text{DME})_x$ (1: $n=3$, $m=3$,

- x=1; 2: n=2, m=4, x=0) and $[\text{Ca}\{\text{CH}_3(\text{OCH}_2)_3\text{OCH}_3\}(\text{H}_2\text{O})_4]\text{I}_2$. *Polyhedron*, 19(15), p. 1783–1789, 2000.
11. Fromm, K.M., *et al.*, Similar Coordination – Different Dimensionality: Synthesis, Single Crystal Structures, and Theoretical Studies of Hydrogen-bonded $\{[\text{Ca}(\text{H}_2\text{O})_2\text{L}_4]\text{I}_2\}_{n/\infty}$ (1: L=CH₃COOC₂H₅, n=1; 2: L=OC₄H₈, n=2). *Zeitschrift für anorganische und allgemeine Chemie*, 626(7), p. 1685–1691, 2000.
 12. Fromm, K.M., Recent advances in tailoring the aggregation of heavier alkaline earth metal halides, alkoxides and aryloxides from non-aqueous solvents. *Dalton Transactions*, (43), p. 5103–5112, 2006.
 13. Klein, R.M. and Bailar, J.C. Reactions of Coordination Compounds. Polymers from 3-Substituted Bis-(β-diketone)-beryllium Complexes. *Inorganic Chemistry*, 2(6), p. 1190–1194, 1963.
 14. Rowsell, J.L.C. Yaghi, O.M. Strategies for hydrogen storage in metal-organic frameworks. *Angew. Chem. Int. Ed.* 44, p. 4670–4679, 2005.
 15. Yang, Y., *et al.*, Synthesis, structures and properties of alkaline earth metal benzene-1,4-dioxyacetates with three-dimensional hybrid networks. *Inorganica Chimica Acta*, 359(10), p. 3257–3263, 2006.
 16. Fei, Z., *et al.*, A Nearly Planar Water Sheet Sandwiched between Strontium–Imidazolium Carboxylate Coordination Polymers. *Inorganic Chemistry*, 44(15), p. 5200–5202, 2005.
 17. Senkovska, I. and Kaskel, S. Solvent-Induced Pore-Size Adjustment in the Metal-Organic Framework $[\text{Mg}_3(\text{ndc})_3(\text{dmf})_4]$ (ndc = naphthalenedicarboxylate). *European Journal of Inorganic Chemistry*, (22), p. 4564–4569, 2006.
 18. Han, S.S., *et al.*, Improved designs of metal-organic frameworks for hydrogen storage. *Angew. Chem. Int. Ed.* 46, p. 6289–6292, 2007.
 19. Côté, A.P. and G.K. Shimizu, Coordination solids via assembly of adaptable components: Systematic structural variation in alkaline earth organosulfonate networks. *Chemistry–A European Journal*, 9(21), p. 5361–5370, 2003.
 20. Sarson, L.D., *et al.*, Porphyrin self-assembly using a boronic acid template. *Chemical Communications*, (5), p. 619–620, 1996.
 21. Fox, S., *et al.*, Coordination of Biologically Important α-Amino Acids to Calcium(II) at High pH: Insights from Crystal Structures of Calcium α-Aminocarboxylates. *Inorganic Chemistry*, 46(3), p. 818–824, 2007.
 22. Waters, A. and White, A. Synthesis and Structural Systematics of Nitrogen Base Adducts of Group 2 Salts. I. Some Adducts of Group

- 2 Halides With Acetonitrile. *Australian Journal of Chemistry*, 49(1), p. 27–34, 1996.
23. Wingerter, S., *et al.*, Phosphorus-Based Ambidentate Chelating Ligands: Pyridyl-N- and Imido-N-Metal Coordination in the $\text{Py}_2\text{P}(\text{NSiMe}_3)_2$ Anion. *Journal of the American Chemical Society*, 123(7), p. 1381–1388, 2001.
 24. Overby, J.S. and Hanusa, T.P. Synthesis and Crystallographic Study of Indenyl and Isopropylated Indenyl Complexes of Calcium, Strontium, and Barium. *Organometallics*, 15(9), p. 2205–2212, 1996.
 25. Harvey, M.J. and Hanusa, T.P. Mono(cyclopentadienyl) Complexes of Calcium, Strontium, and Barium, $\{[\text{C}_5(\text{SiMe}_3)_3\text{H}_2](\text{Ca}, \text{Sr}, \text{Ba})\text{I}(\text{thf})_n\}_x$. Influence of Alkali-Metal Cations on Ligand Exchange Reactions. *Organometallics*, 19(8), p. 1556–1566, 2000.
 26. Murugavel, R., Baheti, K. and Anantharaman, G. Reactions of 2-Mercaptobenzoic Acid with Divalent Alkaline Earth Metal Ions: Synthesis, Spectral Studies, and Single-Crystal X-ray Structures of Calcium, Strontium, and Barium Complexes of 2,2'-Dithiobis(benzoic acid). *Inorganic Chemistry*, 40(27), p. 6870–6878, 2001.

Glossary

Coordination number: the number of atoms or ions immediately surrounding a central atom in a complex or crystal.

Coordinate covalent bond: A coordinate covalent bond, also known as a dative bond or coordinate bond is a kind of 2-center, 2-electron covalent bond in which the two electrons derive from the same atom. The bonding of metal ions to ligands involves this kind of interaction.

π - π stacking interactions: In chemistry, pi stacking (also called π - π stacking) refers to attractive, noncovalent interactions between aromatic rings, since they contain pi bonds.

Crystal engineering: Crystal engineering is the design and synthesis of molecular solid state structures with desired properties, based on an understanding and use of intermolecular interactions. The two main strategies currently in use for crystal engineering are based on hydrogen bonding and coordination bonding. These may be understood with key concepts such as the supramolecular synthon and the secondary building unit.

SBU: Secondary Building Blocks, Subunits of a MOF

Metal-organic frameworks: (MOFs) are compounds consisting of metal ions or clusters coordinated to organic ligands to form one-, two-, or three-dimensional structures. They are a subclass

of coordination polymers, with the special feature that they are often porous.

Chelating agent: A chelating agent is a substance whose molecules can form several bonds to a single metal ion. In other words, a chelating agent is a multidentate ligand. An example of a simple chelating agent is ethylenediamine.

Photo excitation: is the photoelectrochemical process of electron excitation by photon absorption, when the energy of the photon is too low to cause photoionization. The absorption of the photon takes place in accordance with Planck's quantum theory.

Luminescence: Luminescence is emission of light by a substance not resulting from heat; it is thus a form of cold-body radiation. It can be caused by chemical reactions, electrical energy, subatomic motions, or stress on a crystal.

Fluorescence: is the emission of light by a substance that has absorbed light or other electromagnetic radiation. It is a form of luminescence. In most cases, the emitted light has a longer wavelength, and therefore lower energy, than the absorbed radiation.

Spin crossover: (SCO), sometimes referred to as spin transition or spin equilibrium behavior, is a phenomenon that occurs in some metal complexes wherein the spin state of the complex changes due to external stimuli such as a variation of temperature, pressure, light irradiation or an influence of a magnetic field.

Magnetic susceptibility: (χ_M), is the degree of magnetization of a material in response to an applied magnetic field. If magnetic susceptibility is positive then the material can be paramagnetic, ferromagnetic, ferrimagnetic, or antiferromagnetic.

Critical temperature: (T_c), the critical temperature of a substance is the temperature at and above which vapor of the substance cannot be liquefied, no matter how much pressure is applied.

SCM: Single chain magnets, Single-chain magnets are molecular spin chains displaying slow relaxation of the magnetisation on a macroscopic time scale.

Non-linear optical: (NLO), is the branch of optics that describes the behaviour of light in nonlinear media, that is, media in which the polarization P responds nonlinearly to the electric field E of the light. This nonlinearity is typically only observed at very high light intensities such as provided by pulsed lasers.

Second-harmonic generation: (also called frequency doubling or abbreviated SHG) is a nonlinear optical process, in which photons with the same frequency interacting with a nonlinear material are effectively «combined» to generate new photons with twice the energy, and therefore twice the frequency and half the wavelength of the initial photons. Second harmonic generation, as an even-order nonlinear optical effect, is only allowed in media without inversion symmetry. It is a special case of sum frequency generation and is the inverse of half-harmonic generation.

Conformational isomers: is a form of stereoisomerism in which the isomers can be interconverted exclusively by rotations about formally single bonds (refer to figure on single bond rotation). Such isomers are generally referred to as conformational isomers or conformers and, specifically, as rotamers.

Stereochemistry: a subdiscipline of chemistry, involves the study of the relative spatial arrangement of atoms that form the structure of molecules and their manipulation. An important branch of stereochemistry is the study of chiral molecules. The study of stereochemistry focuses on stereoisomers and spans the entire spectrum of organic, inorganic, biological, physical and especially supramolecular chemistry.

Nanostructure: is a structure of intermediate size between microscopic and molecular structures. Nanostructural detail is microstructure at nanoscale.

Sonochemistry: In chemistry, the study of sonochemistry is concerned with understanding the effect of ultrasound in forming acoustic cavitation in liquids, resulting in the initiation or enhancement of the chemical activity in the solution. Therefore, the chemical effects of ultrasound do not come from a direct interaction of the ultrasonic sound wave with the molecules in the solution. The simplest explanation for this is that sound waves propagating through a liquid at ultrasonic frequencies do so with a wavelength that is significantly longer than that of the bond length between atoms in the molecule. Therefore, the sound wave cannot affect that vibrational energy of the bond, and can therefore not directly increase the internal energy of a molecule. Instead, sonochemistry arises from acoustic cavitation: the formation, growth, and implosive collapse of bubbles in a liquid. The collapse of these bubbles is an almost adiabatic process, thereby resulting in the massive build-up of energy inside the bubble, resulting in extremely high temperatures and pressures in a microscopic region of the sonicated liquid.

Scanning electron microscopy: (SEM) is a type of electron microscope that produces images of a sample by scanning it with a focused beam of electrons. The electrons interact with atoms in the sample, producing various signals that contain information about the sample's surface topography and composition. The electron beam is generally scanned in a raster scan pattern, and the beam's position is combined with the detected signal to produce an image. SEM can achieve resolution better than 1 nanometer. Specimens can be observed in high vacuum, in low vacuum, in wet conditions (in environmental SEM), and at a wide range of cryogenic or elevated temperatures.

Metal-to-ligand charge transfer (MLCT) and Ligand to metal charge transfer (LMCT): In inorganic chemistry, most charge-transfer complexes involve electron transfer between metal atoms and ligands. The charge-transfer bands of transition metal complexes result from shift of charge density between molecular orbitals (MO) that are predominantly metal in character and those that are predominantly ligand in character. If the transfer

occurs from the MO with ligand-like character to the metal-like one, the complex is called a ligand-to-metal charge-transfer (LMCT) complex. If the electronic charge shifts from the MO with metal-like character to the ligand-like one, the complex is called a metal-to-ligand charge-transfer (MLCT) complex. Thus, a MLCT results in oxidation of the metal center, whereas a LMCT results in the reduction of the metal center. Resonance Raman spectroscopy is also a powerful technique to assign and characterize charge-transfer bands in these complexes.

Cambridge Structural Database: (CSD) is both a repository and a validated and curated resource for the three-dimensional structural data of molecules generally containing at least carbon and hydrogen, comprising a wide range of organic, metal-organic and organometallic molecules. The specific entries are complementary to the other crystallographic databases such as the PDB, ICSD and PDF. The data, typically obtained by X-ray crystallography and less frequently by neutron diffraction, and submitted by crystallographers and chemists from around the world, are freely accessible (as deposited by authors) on the Internet via the CSD's parent organization's website (CCDC, Repository). The CSD is overseen by the not-for-profit incorporated company called the Cambridge Crystallographic Data Centre, CCDC.

Bridging ligand: In coordination chemistry, a bridging ligand is a ligand that connects two or more atoms, usually metal ions. ^[1] The ligand may be atomic or polyatomic. Virtually all complex organic compounds can serve as bridging ligands, so the term is usually restricted to small ligands such as pseudohalides or to ligands that are specifically designed to link two metals. In naming a complex wherein a single atom bridges two metals, the bridging ligand is preceded by the Greek character <mu>, μ , with a subscript number denoting the number of metals bound to the bridging ligand. μ_2 is often denoted simply as μ . When describing coordination complexes care should be taken not to confuse μ with η (<eta>), which relates to hapticity. Ligands that are not bridging, are called terminal ligands

Organic light emitting diodes: (OLED) is a light-emitting diode (LED) in which the emissive electroluminescent layer is a film of organic compound that emits light in response to an electric current. This layer of organic semiconductor is situated between two electrodes; typically, at least one of these electrodes is transparent. OLEDs are used to create digital displays in devices such as television screens, computer monitors, portable systems such as mobile phones, handheld game consoles and PDAs. A major area of research is the development of white OLED devices for use in solid-state lighting applications.

Chemical vapor deposition: (CVD) is a chemical process used to produce high quality, high-performance, solid materials. The process is often used in the semiconductor industry to produce thin films. In typical CVD, the wafer (substrate) is exposed to one or more volatile precursors, which react and/or decompose on the substrate surface to produce the desired deposit. Frequently, volatile by-products are also produced, which are removed by gas flow through the reaction chamber. Microfabrication processes widely use CVD to deposit materials in various forms, including: monocrystalline, polycrystalline, amorphous, and epitaxial. These materials include: silicon (SiO_2 , germanium, carbide, nitride, oxynitride), carbon (fiber, nanofibers, nanotubes, diamond and graphene), fluorocarbons, filaments, tungsten, titanium nitride and various high-k dielectrics.

Index

- Adducts 98, 123, 185–191, 195,
196, 201–203, 206, 229, 231
- Building blocks 3, 6, 14, 24, 36, 38,
39, 41–43, 52, 55, 92, 116,
223, 225
- Catalysis 3, 5, 17, 19, 20, 28, 31, 64,
129, 154, 183, 224
- Coordination number 4, 48, 62, 83,
84, 88, 91, 94, 95, 97, 102,
103, 105, 114, 116, 120,
132, 140–142, 153, 171,
205, 206, 210, 220–222
- Coordination bonds 2, 3, 5, 6, 12,
26, 32, 59, 64, 132, 164
- Crystal engineering 3, 5, 6,
10, 14, 15, 29, 52, 98,
100, 127, 150, 225
- Covalent bonds 2, 18
- Dimension 3, 4, 9, 14–16, 23,
28, 29, 33, 43, 47–50,
52–58, 60, 63, 64, 67–71,
75, 76, 78–80, 83, 84,
88–98, 103–117,
136–152, 171, 174,
206–214, 216
- Framework 1–3, 13, 15, 18, 21, 30,
32, 33, 35, 37–43, 46,
52–55, 60, 61, 63, 64, 66,
68, 73, 76–79, 92, 94, 105,
110–112, 123, 126–128, 149,
165, 171, 184, 205, 214, 216,
224, 228, 230
- Gas Storage 5, 17–19
- Hydrogen bonds 2, 3, 6, 13, 50, 88,
137, 139, 141, 165
- Magnetism 3, 17, 21, 22, 79
- MOF 60, 68, 133, 184, 205, 228
- Motifs 2, 30, 77, 84, 89, 91,
141, 163, 211
- Networks 4, 10, 14, 17, 25, 27, 29,
31, 32, 34, 38, 40, 46, 50,
54–56, 59, 62, 64, 65, 66,
78, 85, 89, 98, 136, 151,
205, 209, 214, 220, 223,
224, 228, 230
- Organic ligands 2–5, 52, 61,
80, 84, 94, 205, 206, 220,
222

- Self-assembly 2, 3, 14, 29, 31, 33,
35, 38, 40, 52, 53, 56, 61, 78,
100, 128, 213, 216, 225, 230
- Sonochemistry 47, 58, 81, 113,
127, 129, 130, 181
- Supramolecular 1, 2, 5, 6, 13, 15,
28, 49, 52, 55, 59, 69, 71, 72,
73, 75–78, 81, 84, 86, 87, 94,
97, 98, 103, 105, 107, 110,
120, 125, 127, 132, 137, 139,
143, 144, 147, 148, 152, 171,
173, 174, 181, 217, 229
- Zeolites 18, 19, 28, 183
- π - π stacking 5, 50, 51, 62, 70,
103, 104, 107, 120, 122,
141, 171